

University of Louisville

ThinkIR: The University of Louisville's Institutional Repository

Electronic Theses and Dissertations

5-2014

The anti-obesogenic effects of nitric oxide.

Brian Edward Sansbury 1985-
University of Louisville

Follow this and additional works at: <https://ir.library.louisville.edu/etd>



Part of the [Biophysics Commons](#), and the [Physiology Commons](#)

Recommended Citation

Sansbury, Brian Edward 1985-, "The anti-obesogenic effects of nitric oxide." (2014). *Electronic Theses and Dissertations*. Paper 1262.
<https://doi.org/10.18297/etd/1262>

This Doctoral Dissertation is brought to you for free and open access by ThinkIR: The University of Louisville's Institutional Repository. It has been accepted for inclusion in Electronic Theses and Dissertations by an authorized administrator of ThinkIR: The University of Louisville's Institutional Repository. This title appears here courtesy of the author, who has retained all other copyrights. For more information, please contact thinkir@louisville.edu.

THE ANTI.OBESOGENIC EFFECTS OF NITRIC OXIDE

By

Brian Edward Sansbury

B.A., Miami University, 2007
M.S., University of Louisville, 2008

A Dissertation
Submitted to the Faculty of the
University of Louisville School of Medicine
in Partial Fulfillment of the Requirements
for the Degree of

Doctor of Philosophy

Department of Physiology and Biophysics
University of Louisville,
Louisville, Kentucky

May 2014

THE ANTI.OBESOGENIC EFFECTS OF NITRIC OXIDE

By

Brian Edward Sansbury

B.A., Miami University, 2007

M.S., University of Louisville, 2008

A Dissertation Approved on

April 22, 2014

By the following Dissertation Committee:

Aruni Bhatnagar, Ph.D.

Bradford G. Hill, Ph.D.

Gary L. Anderson, Ph.D.

Steven P. Jones, Ph.D.

Dale A. Schuschke, Ph.D.

William B. Wead, Ph.D.

ACKNOWLEDGEMENTS

Completion of my graduate career could not have been achieved without significant contributions from many people. Most importantly, I thank my beautiful wife, Lauren. Her unwavering support, understanding, and encouragement are the source from which I draw so much strength. Without her, none of this would be possible. I also thank my parents, John and Anne, who instilled in me the belief that anything is possible through hard work and persistence. They will never know how deeply I admire and appreciate them or how proud I am to be their son. To my brothers, John, Mark and Kevin, I thank you all for always being there for me and for being able to brighten my day and lift my spirits no matter the circumstances. I would also like to thank my co-mentors, Drs. Bhatnagar and Hill. They have served as an effective yin and yang throughout my scientific and personal development. While very different in their personalities, styles and approaches to science, together they create a complementary and dynamic environment where the whole is truly greater than its parts. Additionally, I acknowledge the members of my advisory committee. Their input and advice has been greatly appreciated, respected and valued. Finally, I would like to thank all the members of the lab, both current and former, that have been invaluable to my work. I have cherished my time working with all of them and look forward to continuing collaborations and friendships for years to come.

ABSTRACT

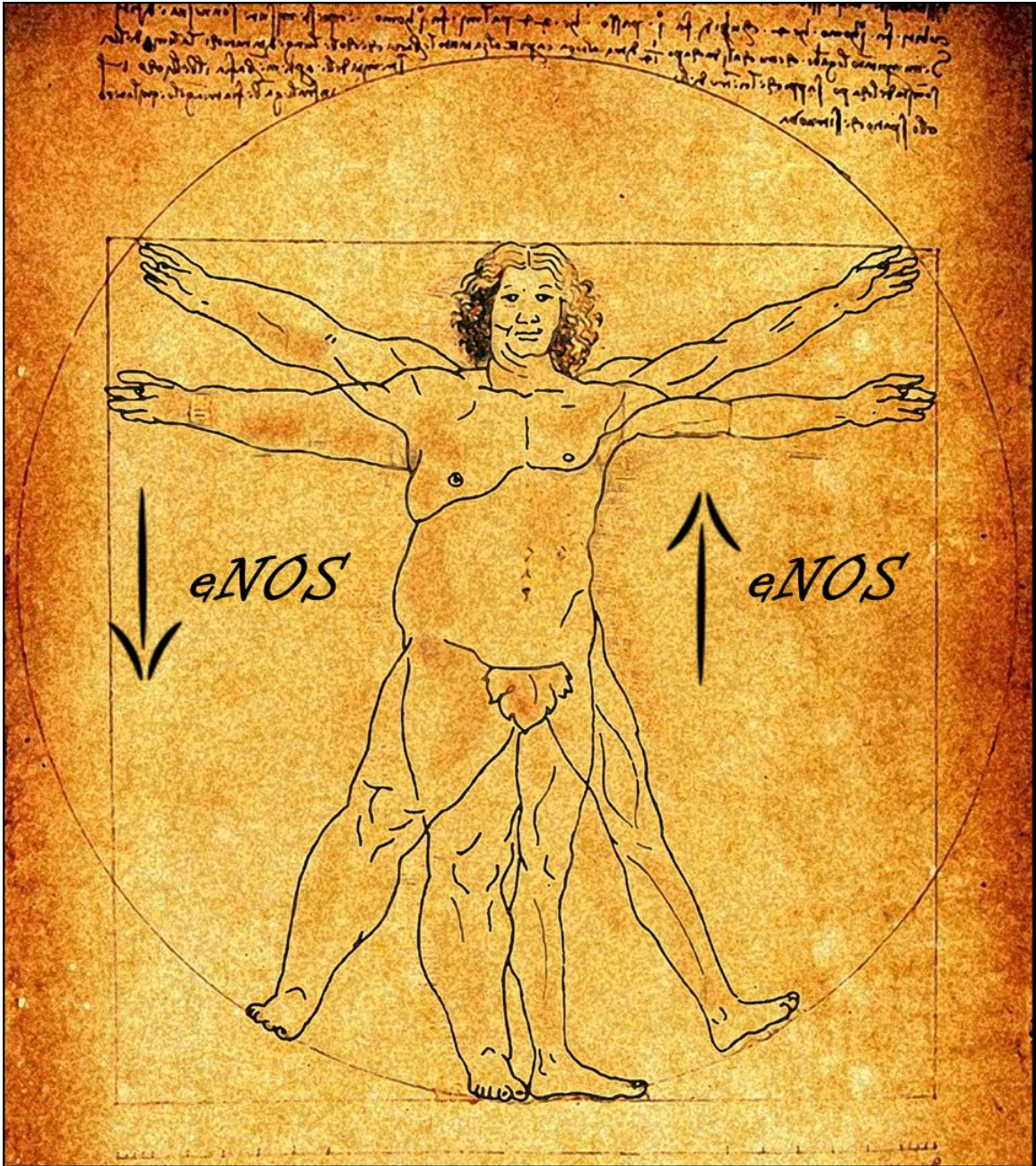
THE ANTI.OBESOGENIC EFFECTS OF NITRIC OXIDE

Brian E. Sansbury

April 22, 2014

Obesity is a strong risk factor for developing type 2 diabetes and cardiovascular disease and has quickly reached epidemic proportions with few tangible and safe treatment options. While it is generally accepted that the primary cause of obesity is energy imbalance, i.e., more calories are consumed than are utilized, understanding how caloric balance is regulated has proven a challenge. Molecular processes and pathways that directly regulate energy metabolism represent promising targets for therapy. In particular, nitric oxide (NO) is emerging as a central regulator of energy metabolism and body composition. NO bioavailability is decreased in animal models of obesity and in obese and insulin resistant patients, and increasing NO output has remarkable effects on obesity and insulin resistance. Additionally, deletion of eNOS (the source of NO in the vasculature) is associated with adiposity, insulin resistance and impaired fatty acid oxidation. The role of eNOS in regulating metabolism, however, is not well understood. We propose that decreased vascular-derived NO bioavailability during nutrient excess is a critical development that leads to metabolic dysregulation. The studies presented here show that obesity induces severe

GRAPHICAL ABSTRACT



Modified from: Leonardo DaVinci's *Vitruvian Man*, courtesy of Thomas P. Gorton

metabolic changes in adipose tissue including profound decreases in eNOS abundance. Overexpression of eNOS prevents obesity and its related metabolic alterations while causing significant changes in energy expenditure and systemic metabolism. Our findings reveal potent anti-obesogenic effects of NO and demonstrate a significant role for NO in regulating metabolism.

TABLE OF CONTENTS

	PAGE
ACKNOWLEDGEMENTS	iii
ABSTRACT	iv
GRAPHICAL ABSTRACT	v
CHAPTER I	
<i>GENERAL INTRODUCTION</i>	
The Obesity Epidemic.....	1
Obesity, Insulin Resistance and Type 2 Diabetes.....	5
Nitric oxide – endogenous formation and general modes of biological action	16
NO bioavailability is diminished in obesity	20
Project Objective.....	31
CHAPTER II	
<i>METABOLIC REMODELING OF WHITE ADIPOSE TISSUE IN OBESITY</i>	
Introduction.....	33

Experimental Procedures	36
Results.....	41
Discussion	65

CHAPTER III

*OVEREXPRESSION OF ENDOTHELIAL NITRIC OXIDE SYNTHASE
PREVENTS DIET-INDUCED OBESITY AND REGULATES ADIPOCYTE
PHENOTYPE*

Introduction	77
Experimental Procedures	79
Results.....	87
Discussion.....	124

CHAPTER IV

REGULATION OF SYSTEMIC METABOLISM BY NITRIC OXIDE

Introduction.....	146
Experimental Procedures	150
Results.....	152
Discussion	182

CHAPTER V

<i>CONCLUDING DISCUSSION.....</i>	191
Regulation of obesity and insulin resistance by NO	193

REFERENCES	209
CURRICULUM VITAE.....	240

LIST OF FIGURES

FIGURE	PAGE
1. Distal and proximal causes of obesity.	3
2. Mechanisms for decreased endothelial-derived NO in obesity and diabetes. 21	
3. Effects of high fat diet on weight gain, adiposity and systemic metabolism....	42
4. Glucose and insulin tolerance in mice fed low fat or high fat diets.....	44
5. Effect of HFD on adipose tissue expansion and inflammation.....	47
6. Metabolomic analyses of adipose tissue.	50
7. Z-score plot analysis of metabolite changes in adipose tissue from high fat fed mice.....	55
8. Obesity-related energetic changes in white adipose tissue.	58
9. Obesity-related changes in mitochondrial protein abundance in white adipose tissue.	60
10. Ultrastructure of white adipose tissues from lean and obese mice.....	63
11. Evidence for activation of mitophagy in WAT of obese mice.	66
12. Nutrient excess alters tissue eNOS levels.....	90

13. Effects of nutrient excess on eNOS levels, and body weight gain of mice expressing different levels of eNOS.	92
14. The eNOS transgene localizes to the vasculature in adipose tissue.	94
15. Measurements of eNOS and NO metabolites in plasma and adipose tissue.	96
16. eNOS prevents diet-induced obesity.	100
17. Diet and genotype do not affect circulating free T3 or T4 levels.	102
18. Effect of eNOS overexpression on indices of insulin resistance.	106
19. Measures of insulin resistance and gluconeogenesis in WT and eNOS-TG mice fed a high fat diet for 12 weeks.	108
20. eNOS overexpression decreases diet-induced adipocyte hypertrophy.	111
21. Effects of high fat diet on macrophage subtypes in WT and eNOS-TG mice.	113
22. Flow chart illustrating procedure for metabolomic profiling of adipose tissues.	115
23. Metabolomic analyses of adipose tissues from high fat-fed mice.	120
24. Overexpression of eNOS regulates intermediary metabolism in adipose tissue.	122
25. Mitochondria are increased in the adipose tissue of eNOS-TG mice.	125
26. eNOS overexpression increases adipose tissue mitochondrial energetics.	127
27. Western blot analysis of AMPK activation status.	131

28. Overexpression of eNOS does not affect capillary density in adipose tissue.	134
29. Hematoxylin and eosin-stained images of pancreas from WT and eNOS-TG mice.....	138
30. Analysis of eNOS expression and modification.	141
31. High fat feeding increases protein-nitrotyrosine adducts in adipose tissue.	143
32. Overexpression of eNOS prevents diet-induced obesity.	154
33. Changes in the plasma metabolome due to high fat feeding or eNOS overexpression.	157
34. Plasma metabolic changes due to diet.	160
35. Z-score plot analysis of metabolite changes in plasma from low and high fat-fed mice.....	162
36. Plasma metabolic changes due to genotype.	165
37. Z-score plot analysis of metabolite changes in plasma from low fat-fed WT and eNOS-TG mice.	167
38. Plasma metabolic changes due to genotype in obesity.	169
39. Z-score plot analysis of metabolite changes in plasma from high fat-fed WT and eNOS-TG mice.	172
40. Modified Z-score plot analysis of metabolite changes in plasma from low fat-fed WT and both high fat-fed WT and eNOS-TG mice.	174
41. Changes in bile acid and fatty acid levels induced by diet and eNOS overexpression.....	177

42. Preventing bile acid synthesis does not prevent diet-induced obesity. 180

43. Working model of the systemic effects of NO on obesity and metabolism. 207

LIST OF TABLES

TABLE	PAGE
1. List of adipose tissue metabolites that changed significantly in high fat-fed mice.....	52
2. Parameters measured from plasma of low fat-fed and high fat-fed WT and eNOS-TG mice.....	104
3. List of adipose tissue metabolites that were significantly different between high fat-fed WT and eNOS-TG mice.....	117

CHAPTER I

GENERAL INTRODUCTION

The Obesity Epidemic

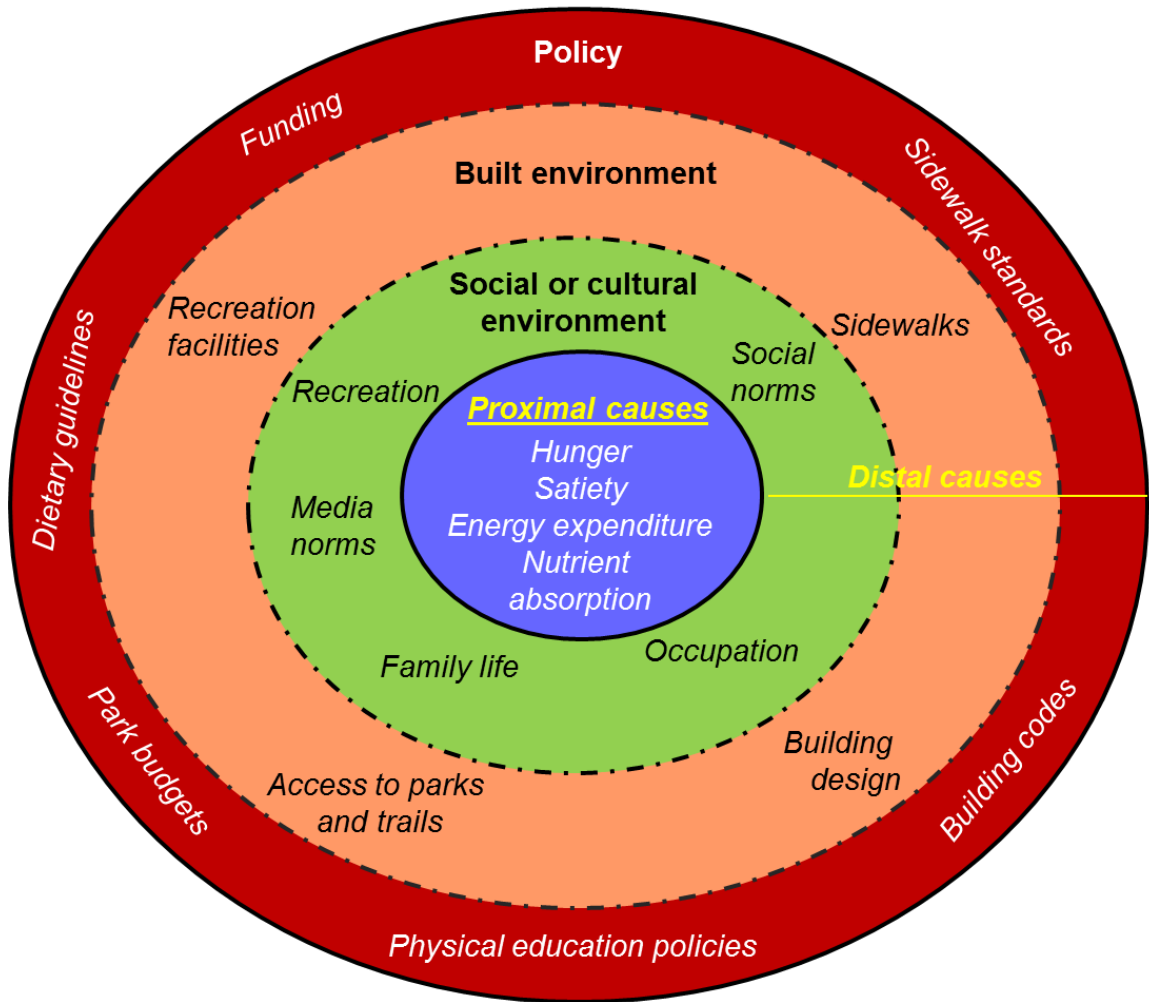
The recent increase in the prevalence of obesity is alarming. The Centers for Disease Control and Prevention (CDC) estimate that from 1962 to 2010 prevalence of obesity has increased from 13% to 36%. In 2008, approximately 1.5 billion adults aged 20 years or older were overweight, and 10% were obese ¹; more recent data from the United States indicate that >33% of adults and 17% of children are obese ². This has led to a dramatic increase in individuals with pre-diabetes. For example, current estimates indicate that one-third of the population in the US meets the criteria for pre-diabetes ^{3, 4}, and, in addition to type 2 diabetes (T2D), obesity is closely associated with co-morbidities such as coronary artery disease, hypertension, atherosclerosis, stroke, and cancer ⁵. Hence, the current high prevalence of obesity is likely to have a considerable impact on worldwide health. In the US, the economic burden of obesity is substantial and accounts for an estimated \$147 billion per year ⁶. The problem has become so severe that, in 2013, the American Medical Association House of Delegates declared obesity a *disease*.

The principal cause of obesity is energy imbalance: the calories consumed are greater than that utilized by bodily processes, e.g., breathing, digestion, thermogenesis and mechanical work ⁷. Indeed, the average consumption of calories in the US increased by >200 kcal/d per person from 1971-2000, which is partly attributable to the abundance of affordable, widely marketed, energy-dense foods ⁸⁻¹¹. Nevertheless, evidence suggests that the balance between calorie intake and energy expenditure is complex and regulated by many factors. Exposure to increasingly obesogenic environments has been suggested to promote not only overeating, but inactivity as well. For example, the human environment is fraught with both chemical and structural “obesogens.” These include but are not limited to: pollutants that promote adiposity and insulin resistance ¹²⁻²¹; lack of structural features of the built environment that promote an active lifestyle, such as easy access to parks, sidewalks, and bike paths ²²⁻²⁴; and the night/day cycles in the natural environment of the individual, which can be altered in those having certain occupations ²⁵⁻²⁷. Moreover, the genetic makeup of individuals shows strong associations with the predisposition to become obese ²⁸⁻³⁰.

Many of these factors influence body composition in an indirect or distal manner, and thus could be considered “distal causes” of obesity (Fig. 1). Interventions to mitigate the effects of these distal causes are exceedingly difficult to test and implement. For example, changing the structural environment would likely entail departing from particular types of communities or neighborhoods. Similarly, living under favorable day-night cycles is difficult for workers in some occupations, and

Figure 1. Distal and proximal causes of obesity. Influencing factors distal to the disease, such as policy as well as structural and chemical “obesogens” of the built and social (cultural) environment, may contribute to the prevalence of obesity. Funding for obesity research, dietary guidelines, physical education policies, and sidewalk standards are examples of potential influences related to *Policy*, which is most distal to the actual disease. The *Built environment*, which comprises places created or modified by people—i.e., where individuals work, their transportation systems, and life outside their homes—is another cause distal to obesity. The *Social or cultural environment* includes those family or cultural influences that affect behavioral activity, occupation (which may involve shift work), and social and media norms, all of which could affect eating habits and physical activity. Lastly, direct mechanisms that control hunger, satiety, energy expenditure, and nutrient absorption are *Proximal causes* of obesity. Commonly, these proximal causes are more tangible targets for anti-obesity/diabetes therapies compared with distal causes.

Figure 1



changing genetic makeup is currently not an option. Even weight loss via caloric restriction faces difficulties, including an evolution-engendered guard against low fat mass ^{7, 31} and the propensity of the body to increase caloric efficiency during dieting ^{32, 33}. The intransigency of these problems has led to a search for causes more proximal to obesity, which may be tangible targets for anti-obesity therapies.

Obesity, Insulin Resistance and Type 2 Diabetes

The World Health Organization (WHO) defines obesity as abnormal or excessive fat accumulation that may impair health and is characterized by a body mass index (BMI) equal to or greater than 30 kg/m². Evidence from numerous studies has demonstrated that obesity and increased weight gain are strongly associated with an increased risk of T2D ³⁴⁻³⁶ and that intentional weight loss decreases that risk ³⁷. T2D is characterized by chronic hyperglycemia with disturbances of carbohydrate, protein and fat metabolism resulting from defects in insulin secretion, action or both ³⁸. While a causal link between obesity and diabetes remains to be fully clarified, their association is undeniable. Development of effective treatments, therefore, depends on greater understanding of the metabolic dysregulation that accompanies the onset of obesity and its progression to insulin resistance and diabetes.

Metabolic pathways known to regulate obesity

Understanding the mechanisms that promote adiposity and insulin resistance are critical to stem the growing tide of metabolic disease. In particular, the development of therapies for obesity and T2D requires a better understanding of the biochemical pathways that regulate metabolism and body composition. As a first principle, energy balance must be considered to understand how changes in body composition could occur. Any effective obesity treatment must decrease energy intake, increase energy expenditure or both. Systems that regulate energy balance include:

- 1) *Hunger and satiety*: The central nervous system regulates caloric intake and the feeling of satisfaction or fullness after a meal, i.e., satiety. This regulation is dependent on neural and endocrine inputs that can be divided into short- and long-term control systems. Release of cholecystokinin (CCK) in combination with neural signaling in response to gut distension are potent signals of satiety and trigger an end to feeding ³⁹. The adipose tissue-derived hormone, leptin, is crucial to integrate the melanocortin neuronal circuit of the hypothalamus with the energy stores of the body ³⁹⁻⁴¹. In addition to leptin, neuropeptide Y (NPY) directly affects feeding behavior, metabolism and body composition ^{42, 43}, and corticotropin-releasing hormone, growth-hormone-releasing hormone, galanin and ghrelin, some of which are expressed in both the stomach and the brain, function in hunger and satiety signaling ⁴⁴. The

neurotransmitters norepinephrine, dopamine and serotonin are also important in central energy balance ^{39, 41} and inhibiting their reuptake by drugs such as sibutramine, has proven anti-obesogenic effects but leads to side effects such as increased blood pressure and heart rate ⁴⁵. Other drugs that have been shown to be effective in decreasing energy intake by suppressing appetite ^{7, 46, 47}.

- 2) *Nutrient absorption*: Targeting nutrient absorption in the gut may be an effective obesity therapy. Signals from the gut released post-prandially are important not only in regulating food intake, but also in digestion and nutrient absorption. Ghrelin and CCK, as well as, peptide YY, glucagon-like peptides 1 and 2, gastric inhibitory peptide and corticotropin-releasing factor function to regulate both signaling and digestion [39, 43, 44]. Inhibition of gastric and pancreatic lipases via orlistat treatment decreases triglyceride hydrolysis and is able to inhibit absorption of ingested fat by ~30% and contributes to a caloric deficit of approximately 200 calories per day [45]. As with neurotransmitter reuptake inhibitors, orlistat promotes weight loss; however, because of side effects the drug is poorly tolerated by many patients [40].
- 3) *Energy expenditure*: The largest contributor to obligatory energy expenditure is the basal metabolic rate (BMR), which is defined as the resting energy expenditure at thermoneutrality in the unfed state ⁴⁸. BMR includes cellular turnover, repair and basic functions (e.g., maintenance of ion gradients, transmembrane metabolite transfer), basal synthetic

reactions (e.g., RNA, DNA and protein synthesis) and mitochondrial proton leak. It also includes obligatory thermogenesis (e.g., digestion and absorption)⁴⁸.

Mitochondria are central to the regulation of energy expenditure, and targeting their activity has been a prospect for obesity therapies for decades. Perhaps most infamous is the work by Cutting and Tainter^{49, 50}, which showed that 2,4-dinitrophenol (DNP)—a compound found to be responsible for weight loss in workers of French munitions factories during World War I—could be used to increase the metabolic rate of patients. Although the use of DNP led to weight loss as well as improvements in glucose tolerance in some diabetic patients, results were largely disastrous: people were “literally cooked to death” due to overdose, as the systemic uncoupling of mitochondria by DNP resulted in overheating. Other side effects included rashes, cataracts, and agranulocytosis. Hence, although the drug was effective for weight loss, it was not deemed safe by the FDA and was withdrawn from the market in 1938⁵¹.

In recent years, a more in-depth understanding of how mitochondrial metabolism could be regulated has been sought. Unlike rudimentary approaches using pharmacological mitochondrial uncouplers, which have systemic effects, targeting mitochondrial metabolism in specific tissues may prove more beneficial. Therapies that mimic physiological anti-obesogenic effects are likely to prove most effective. Mitochondria in organs with high energetic need (e.g., the heart) are likely

to maintain relatively well-coupled mitochondria, while other organs such as adipose tissue could afford to be less economical. Overexpression of uncoupling protein 1 (UCP1), which generates an increase in substrate utilization and electron transport chain activity, in adipose tissue⁵² or skeletal muscle⁵³ can prevent diet-induced obesity in mice, suggesting that uncoupling of oxidative phosphorylation in these two organs is sufficient to regulate body composition. Interestingly, oxidative phosphorylation in skeletal muscle is less well-coupled in endurance athletes compared with sedentary subjects⁵⁴, and this appears to result in an increase in fatty acid oxidation and a decrease in oxidative stress. Furthermore, genes encoding fatty acid oxidation are increased in the skeletal muscle of athletes compared with sedentary subjects⁵⁵, suggesting a gene profile in athletes that favors fat oxidation rather than storage⁵⁶.

Brown adipose tissue (BAT), which expresses relatively high levels of UCP1, is an exciting target for therapy. Despite the small amounts in humans, as little as 50 g of BAT has been estimated to be capable of utilizing up to 20% of basal caloric needs⁵⁷. Mice with genetically reduced BAT mass are prone to obesity⁵⁸. The recent discovery that adult humans maintain active depots of BAT^{59, 60} in conjunction with the identification of UCP2 and UCP3 in the skeletal muscle and other tissues^{61, 62} suggests that enhancement of mitochondrial activity may hold promise for combatting obesity.

Increasing energy expenditure by BAT activation is an anti-obesity strategy that has recently gained widespread attention and represents an intriguing new therapeutic approach. However, the finding that adipocytes in some white adipose tissue depots can be programmed to become similar to BAT has further invigorated research into understanding the role of adipose tissue in systemic metabolism.

White adipose tissue is an important regulator of whole-body metabolism

White adipose tissue (WAT) is a complex, essential and highly active metabolic and endocrine organ⁶³. Its utility as the main storage depot for excess energy from dietary intake has long been recognized⁶⁴, but only recently has its importance beyond energy storage been fully appreciated. WAT not only responds to afferent signals from traditional hormone systems and the central nervous system but it also expresses and secretes factors with important endocrine functions including cellular signaling, energy metabolism and inflammatory processes^{63, 65}. This network of secreted adipokines signal changes in the adipose tissue energy status to other metabolic organs that control fuel consumption and redistribution⁶⁶. In this way, adipose tissue is a critical regulator of whole-body metabolic homeostasis. The contribution of adipose tissue to regulating circulating levels of free fatty acids (FFAs), glucose and insulin is of particular importance⁶⁵ and will be discussed in detail in the following sections.

WAT dysfunction in the progression of obesity and diabetes

Chronic energy overload promotes systemic metabolic dysfunction, which appears to commence at the level of the adipose tissue. Though adipocytes have a large capacity to synthesize and store triglycerides (TGs) during feeding, after prolonged periods of nutrient excess their storage and endocrine functions become compromised^{67, 68}. Failure of WAT to store fat appropriately results in pathological adipocyte hypertrophy, hypoxia and secretion of macrophage chemoattractants, particularly monocyte chemoattractant protein-1 (MCP-1)^{65, 69}. Infiltrating macrophages secrete large amounts of tumor necrosis factor α (TNF α) and other inflammatory cytokines thereby creating a chronic proinflammatory state in the WAT associated with impaired TG deposition and increased lipolysis⁶⁵. The result is increased circulating TGs and FFAs which can be deposited in skeletal muscle, liver and β -cells of the pancreas^{70, 71}. Elevated FFAs and ectopic lipid deposition are associated with metabolic dysregulation in peripheral tissues of both humans and rodents⁷²⁻⁷⁸. In the liver, infusion of FFAs increases glucose output and causes insulin resistance⁷⁹. Similarly, skeletal muscle insulin resistance has been shown to be associated with elevated circulating FFAs and intramyocellular triglyceride accumulation^{80, 81}. Increased hepatic glucose production and decreased glucose uptake by skeletal muscle (which accounts for approximately 80% of glucose disposal in the post-prandial state) contributes to elevated systemic glucose levels⁶⁶. In response, the pancreas releases more insulin and after prolonged periods of positive energy balance, this leads to

hyperinsulinemia⁸². Additionally, chronic exposure to elevated FFAs may result in β -cell dysfunction^{82,83} a key event in the development of frank T2D.

Proper lipid partitioning is critical in metabolic disease

A critical feature in this model of disease progression is the failure of the WAT to benignly accommodate excess lipid. When the WAT is unable to sequester fat, a malignant cascade of events ensues. Studies in rodent models underscore the importance of fat storage in the adipocyte. These studies show that increasing adipocyte cell number, and therefore overall adipose tissue mass, by overexpressing the adipokine adiponectin in severely obese *ob/ob* mice, decreased hepatic and muscle fat deposits and normalized metabolic parameters⁸⁴. Therefore, by providing additional adipose depots for fat storage, fat “spillover” or ectopic deposition in peripheral tissues can be prevented and insulin resistance and diabetes averted. This is further supported by the observation that mice almost totally devoid of adipose tissue due to the expression of A-ZIP/F-1 protein in adipocytes, are severely insulin resistant due to defects in insulin action, particularly insulin receptor substrate (IRS)-1/IRS-2–dependent activation of PI 3-kinase, in muscle and liver⁸⁵. These abnormalities were associated with a twofold increase in muscle and liver triglyceride content, and upon transplantation of fat tissue into these mice, triglyceride content in muscle and liver returned to normal, as did insulin signaling and action^{85,86}. While intensively studied, the mechanism by which increased lipid in peripheral tissues disrupts insulin signaling, remains to be fully elucidated⁸⁷. What is clear, however, is that

proper partitioning of fat in the WAT rather than in peripheral tissues is crucial for preserving insulin sensitivity.

WAT mitochondria as therapeutic targets in metabolic disease

While numerous studies have focused on modulating mitochondrial activity in skeletal muscle and liver to prevent lipid accumulation and maintain insulin sensitivity, only recently has significant attention been paid to metabolic intervention at the level of the adipose tissue. Despite adipocytes having a relatively low mitochondrial abundance, mitochondria are essential for many adipocyte functions. Previous work has demonstrated that mitochondria play an important role in the differentiation and the maturation of adipocytes, as evidenced by a synchronized initiation of adipogenesis and mitochondrial biogenesis⁸⁸ and the promotion of differentiation in response to enhanced mitochondrial metabolism, biogenesis and reactive oxygen species (ROS) production⁸⁹. Additionally, adipocyte mitochondria must generate sufficient ATP to support energy-consuming lipogenic processes, while still maintaining normal cellular activity⁹⁰. Further, to sustain lipogenesis, mitochondria provide key intermediates for the synthesis of TGs through the actions of pyruvate carboxylase⁹¹. Reacting to cues from its nutritional and hormonal microenvironment, the adipocyte coordinates the appropriate mitochondrial response to either oxidize incoming FAs and carbohydrates through the tricarboxylic acid (TCA) cycle and the respiratory chain, or store them as TGs⁹¹. In light of this, it has been proposed that 'FFA recycling in the adipocyte' (a TG-

to-FA cycle) is a crucial sequence of events that determines systemic FFA concentrations⁹².

During obesity and nutrient excess, mitochondrial function in adipocytes is compromised. Levels of ATP decrease while there is increased accumulation of NADH⁶⁶, thereby shifting the adipocyte toward lipid storage accompanied by reduced mitochondrial biogenesis and increased ATP synthesis from glycolysis⁹¹. Prolonged exposure to nutrient overload only further induces these mitochondrial alterations and leads to yet more lipid accumulation. Studies in diabetic mice have shown a decrease in both the number and the function (both oxidative phosphorylation and β -oxidation) of mitochondria in WAT⁹³. Further, several genes involved in mitochondrial function and oxidative phosphorylation, as well as PPAR α , ERR α , and PGC-1 α were downregulated in WAT from high fat diet-induced obese and *db/db* mice^{94, 95}. Similar changes have been observed in the WAT of obese, insulin resistant and diabetic patients. In human WAT, mitochondrial abundance is decreased and genes crucial for mitochondrial function are downregulated⁹⁶ as well. Adipocytes isolated from these patients had decreased oxygen consumption rates and ATP production^{91, 97}. These findings suggest a clear association between the activity of the mitochondria in adipose tissue and the pathological remodeling of the tissue that accompanies obesity.

Targeting the mitochondria of WAT to combat obesity has emerged as a promising new strategy and has been the subject of increasing scientific scrutiny. A general idea is to increase mitochondria in WAT, which could promote a higher

basal metabolic rate. Several molecular targets have been identified, with PGC-1 α being of critical importance⁹⁸. PGC-1 α is a known regulator of energy metabolism and of mitochondrial biogenesis⁹⁹ and may induce many of the characteristic brown fat traits in white adipocytes *in vitro*⁹⁸. Additionally, recent studies have identified secreted proteins that stimulate brown adipocyte thermogenesis and recruit brown (or beige) adipocytes to WAT¹⁰⁰. One such secreted protein is irisin—a skeletal muscle-derived myokine that enhances systemic energy expenditure and improves obesity and glucose homeostasis in mice—via a mechanism, which depends, at least in part, on PGC-1 α ¹⁰¹.

Interestingly, treatment with the gaseous signaling molecule, nitric oxide (NO), can induce PGC-1 α -dependent mitochondrial biogenesis in both mouse white fat 3T3-L1 adipocytes and brown adipocytes^{102, 103}. Importantly, NO-induced mitochondrial biogenesis leads to the formation of functionally active mitochondria capable of coupled respiration leading to the generation of ATP through oxidative phosphorylation¹⁰⁴. Furthermore, emerging evidence suggests that changes in vascular function could regulate metabolic homeostasis, and many studies have shown that NO may play a pivotal role in regulating systemic metabolism, body composition, and insulin sensitivity. In the sections that follow, the potential role of NO in regulating metabolism, obesity and insulin resistance is discussed.

Nitric oxide – endogenous formation and general modes of biological action

Nitric oxide and related nitrogen oxides have emerged as critical regulators of cell and tissue function ¹⁰⁵. The potency of NO was perhaps first realized when it was inhaled by Sir Humphrey Davy, who nearly died from the self-experiment, and after which he vowed to “never design again...so rash an experiment” ¹⁰⁶. Nearly two centuries later, identification of the cardiovascular processes controlled by NO led to the Nobel Prize in Physiology or Medicine in 1998. Nevertheless, the pleiotropy of NO continues to unfold, and we are only now beginning to appreciate the deeper aspects of its impact on metabolism.

Generation of NO

The most common route of NO production is through the action of the nitric oxide synthase (NOS) family of enzymes ^{105, 107}. These enzymes catalyze NADPH- and O₂-dependent oxidation of L-arginine to L-citrulline, producing NO in the process. Such synthesis of NO depends on the availability of cofactors such as FAD, FMN, tetrahydrobiopterin (BH₄), as well as the prosthetic group, heme ¹⁰⁸.

The three NOS isoforms generate NO at different rates ¹⁰⁵. Endothelial NOS (eNOS) is localized to the vascular endothelium, but has also been found in neurons, epithelial cells and cardiomyocytes ¹⁰⁹. It produces relatively low quantities of NO, and its activity is controlled by Ca²⁺ and calmodulin, post-translational modifications ^{110, 111}, and physical forces such as shear stress ^{112, 113}. Neuronal NOS (nNOS) is also a Ca²⁺/calmodulin-dependent isoform that is

activated by agonists of the N-methyl-D-aspartate (NMDA) receptor ¹¹³. It is expressed in neurons, skeletal muscle, and epithelial cells. Lastly, inducible NOS (iNOS), which has the highest capacity to generate NO, is expressed in multiple cell types in response to inflammatory stimuli ^{113, 114}. The results of some studies also suggest the presence of a mitochondria-localized isoform, which could be important in regulating mitochondrial function ^{115, 116}; however, the identity of this isoform remains to be fully established. In addition to post-translational modifications and substrate and cofactor availability, NOS activity is regulated by its localization within cells and by interactions with itself and other proteins ¹¹³.

NO could also be produced endogenously from its more oxidized nitrogen oxide precursor, nitrite. Reduction of nitrite to NO is increased under acidic and hypoxic conditions, with the reduction occurring enzymatically by heme proteins such as deoxyhemoglobin or deoxymyoglobin ¹¹⁷. The therapeutic potential of dietary or pharmacological nitrite is supported by multiple studies describing improvements in reperfusion injury following myocardial infarction, in pulmonary hypertension, and injury after organ transplantation ¹¹⁸.

Biochemical properties of NO

NO is a free radical of rather limited biological reactivity. The endogenous half-life of NO is in the range of 2 ms to > 2 s and appears to depend primarily on the availability of metals and oxygen ¹¹⁹. NO reacts avidly with ferrous (Fe²⁺) iron and with other radical species and such reactions form the basis for nearly all of the biological effects of NO. The highest affinity interactions of NO are with

metalloproteins such as soluble guanylate cyclase (sGC), cytochrome *c* oxidase, and hemoglobin; NO reacts also with non-heme iron. Reaction of NO with Fe²⁺ iron results in the formation of a coordinate bond, which is termed a nitrosyl adduct (i.e., nitrosylation). The presence of free radicals such as superoxide (O₂^{•-})¹²⁰⁻¹²³ changes the fate of NO because once NO reacts with O₂^{•-} it forms peroxynitrite^{120, 122, 123} and can no longer bind to ferrous heme¹²⁴. Peroxynitrite and other reactive species (e.g., NO₂) derived from the reaction of NO with O₂^{•-} are important in inflammatory responses¹²³ and can modulate cell signaling¹²⁵⁻¹²⁸, in part by promoting the oxidation and nitration of a broad range of biomolecules¹⁰⁵.

The NO molecule can also react directly with O₂, which itself is a free radical possessing two unpaired electrons in different π* antibonding orbitals¹²⁹. The reaction of NO with O₂ commonly underlies mechanisms by which S-nitrosation or S-oxidation of protein side chains occurs. In addition, NO can react directly with thiol radicals, forming a nitroso covalent bond between NO and the thiol (termed S-nitrosation or S-nitrosylation). Cysteinyll residues of glutathione and proteins are among the most recognized and studied targets of NO and its oxidized species [(such as N₂O₃; collectively called reactive nitrogen species (RNS)]; reaction of RNS with thiols results in the formation of S-nitrosothiols, S-glutathiolated species, and oxidized cysteinyl residues¹³⁰. Such modifications can lead to transient changes in enzyme activity, providing redox switches that can be modulated by addition or removal of the modifications¹³¹.

General physiological roles of NO

NO has multiple biological actions and this versatile molecule can regulate physiology acutely or lead to long-term changes in cell function. The pleiotropic roles of NO include the regulation of long-term synaptic transmission, learning, memory, platelet aggregation, leukocyte-endothelial interactions, immune function, and angiogenesis and arteriogenesis (for review, see ¹³²). However, NO is most well known as a potent regulator of blood flow and was originally termed endothelial-derived relaxing factor (EDRF). The story unfolded from Furchgott and Zawadzki's initial discovery that endothelial cells control acetylcholine-induced relaxation of smooth muscle ¹³³. A few years later, NO was identified as the key endothelium-derived molecule promoting vasodilation: NO synthesized by NOS in the endothelium diffuses into the vessel wall where it activates sGC in vascular smooth muscle. This leads to an increase in cyclic GMP (cGMP) levels in the tissue and elicits vessel relaxation ¹³⁴⁻¹⁴⁰. However, it readily became apparent that different isoforms of NOS have different physiological roles. For example, eNOS and nNOS were found to have distinct roles in regulating microvascular tone ¹⁴¹; nNOS activity in the medulla and hypothalamus is important for systemic regulation of blood pressure ¹⁴²⁻¹⁴⁵; and, the nitrenergic nerves containing nNOS are responsible for penile erection ^{137, 146}. Overall, NO derived from the integration of eNOS and nNOS activities play key roles in regulating systemic blood pressure and acutely regulating organ blood flow, whereas iNOS-derived NO species are most well recognized for their impact on pathogen killing and inflammatory processes ¹²⁰.

Another key function of NO is the regulation of mitochondrial respiration. Acutely, NO inhibits respiration by binding and inhibiting cytochrome *c* oxidase. Modulation of respiration by NO is dependent on both mitochondrial activity and the O₂ level^{147, 148}. In addition, NO directly regulates the binding and release of oxygen with hemoglobin¹⁴⁹ and is able to increase blood flow at sites of very low oxygen concentrations¹⁵⁰. Thus, a key function of NO is to modulate O₂ gradients in cells and tissues by regulating hemoglobin action and by inhibiting O₂ consumption in respiring mitochondria¹¹⁹. Chronic exposure to relatively high levels of NO results in mitochondrial biogenesis¹⁵¹⁻¹⁵³, which could reprogram a cell or tissue to have a higher metabolic capacity.

NO bioavailability is diminished in obesity

NO bioavailability is decreased in animal models of obesity^{154, 155} and in both adult and adolescent humans^{156, 157}. Because NO bioavailability is dependent upon the balance between its generation and degradation, diminished levels of NO in obese states may be due to decreased expression of NOS, impairments in NOS activity, decreased NOS substrates or by the reaction of NO with reactive species (e.g., superoxide) (Fig 2). These are discussed below.

NOS expression changes in obesity

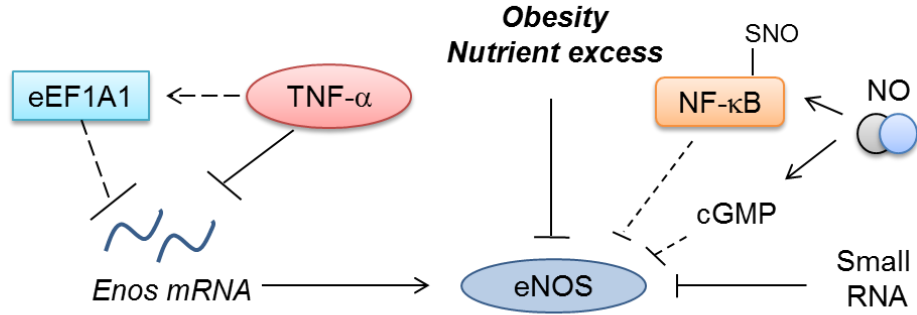
A primary mechanism by which NO bioavailability could be decreased is via diminished expression of NOS enzymes (Fig. 2A). In particular, lower eNOS abundance is found in both WAT and skeletal muscle of obese humans and

Figure 2. Mechanisms for decreased endothelial-derived NO in obesity and diabetes. Schematic of changes in NOS or NO: **(A)** Decreased eNOS expression commonly occurs in obese and diabetic states. Mechanisms proposed for diminished expression include TNF- α -mediated destabilization of eNOS mRNA, which may involve eEF1A1. High levels of NO may regulate eNOS abundance through cGMP-mediated or via NF- κ B-SNO feedback regulatory pathways. A small 27-nt RNA regulates eNOS expression also, although it is not known whether this mechanism is invoked in obesity or diabetes. **(B)** Decreased eNOS activity in obesity and diabetes is largely attributed to insulin resistance, which may be mediated by free fatty acid (FFA)-induced activation of TLR2, TLR4, and NF- κ B. In addition, activation of PKC β II may diminish Akt signaling, which causes phosphorylation of eNOS on Ser1177. Phosphorylation at this site increases NO output by the enzyme. Hyperglycemia may also lead to increased O-GlcNAcylation of eNOS, which decreases Ser1177 phosphorylation and inhibits its activity. In addition, conditions leading to obesity promote upregulation of Cav-1, which is a negative regulator of eNOS, and ceramide accumulation disrupts the eNOS-Akt-HSP90 complex, diminishing activity of the enzyme. **(C)** eNOS may also be uncoupled or NO quenched in obese and diabetic states. Diminished levels of substrates and cofactors, such as L-arginine or tetrahydrobiopterin (BH₄), lead to uncoupling of the enzyme, which is commonly associated with the presence of eNOS monomers rather than dimers and can produce superoxide instead of NO. Endogenous inhibitors of eNOS such as ADMA are also increased in obese conditions and can promote

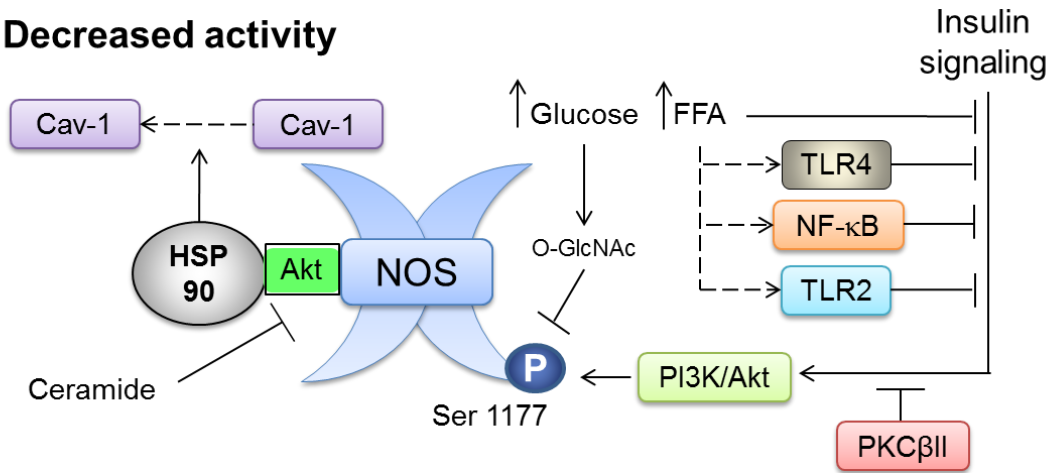
NOS uncoupling. Elevated production of reactive oxygen species such as superoxide can quench NO and result in its oxidation to highly reactive peroxynitrite, which damages biomolecules and can oxidize BH_4 to BH_2 . Increased levels of BH_2 exacerbate NOS uncoupling and superoxide production.

Figure 2

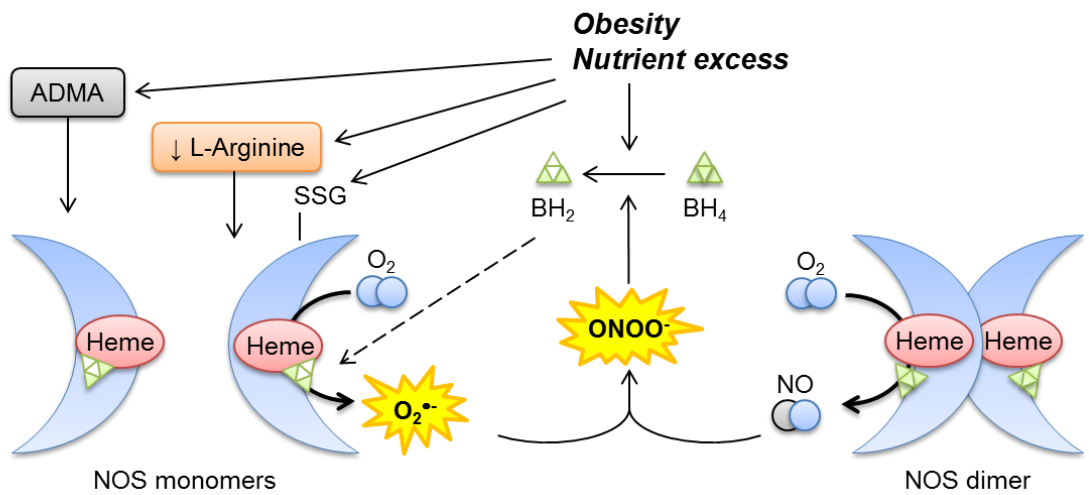
A. Decreased expression



B. Decreased activity



C. NOS uncoupling or NO quenching



rodents¹⁵⁸⁻¹⁶². Factors associated with obesity and diabetes including increased shear stress, lysophosphatidylcholine, oxidized LDL, insulin and decreased ability to exercise can also regulate eNOS expression¹⁶³⁻¹⁶⁷. TNF α , which is increased in obesity and implicated in the etiology of insulin resistance¹⁶⁸, has been found to downregulate eNOS expression and abundance^{161, 169-172} by decreasing the stability of eNOS mRNA^{173, 174}, effectively shortening its half-life¹⁷⁵. This destabilization of the eNOS message has been linked, at least in part, to upregulation of elongation factor 1- α ¹⁷⁶.

Acutely, TNF α increases eNOS activity¹⁷⁷, most likely via activation of the PI3K-Akt¹⁷⁸ and sphingomyelinase/sphingosine-1-phosphate pathways^{179, 180}. Such diametrically opposite acute versus chronic effects of TNF α would appear to suggest the potential existence of negative feedback loops that sense high levels of NO, leading to downregulation of eNOS. Indeed, NO donors downregulate eNOS expression both *in vitro* and *in vivo*, which may involve cGMP and/or S-nitros(yl)ation of NF- κ B^{181, 182}. A small, 27-nt RNA has also been shown to be an effective feedback regulator of eNOS¹⁸³. Whether such small RNAs or miRNAs that regulate NOS expression are induced with obesity is currently unclear.

Notable changes in the abundance of other NOS isoforms also occur in obesity. The iNOS enzyme increases in abundance in pancreatic β -cells¹⁸⁴, aorta¹⁸⁵, skeletal muscle¹⁸⁶, liver^{187, 188}, and adipose tissue¹⁸⁹⁻¹⁹¹ of obese rodents. In adipose tissue, the majority of iNOS is derived from infiltrating bone marrow-derived macrophages that display a proinflammatory phenotype¹⁸⁹⁻¹⁹¹. However, high levels of TNF α were shown to increase iNOS also in adipocytes,

which appears to downregulate UCP2¹⁹²; hence, this mechanism could contribute to decreases in WAT energy expenditure. In the ventromedial hypothalamus, which controls energy intake, diet-induced obesity was associated with lower numbers of nNOS-expressing cells¹⁹³. In the aorta, however, nNOS was increased in abundance in mice fed a high fat diet. The induction of nNOS was demonstrated to be due to leptin stimulation¹⁹⁴ and may partially compensate for the loss of eNOS-mediated vasodilatory action that typically occurs in obese, insulin-resistant states.

Changes in eNOS activity in obesity

Beyond changes in expression, the NO-producing activity of eNOS is diminished in metabolic disease (Fig. 2B). In addition to the required substrates, calcium, and cofactors, the activity of eNOS is regulated by protein-protein interactions and by several post-translational modifications^{132, 195, 196}. High fat feeding upregulates caveolin-1, a negative regulator of eNOS^{197, 198}, in the aorta of obese rats¹⁹⁹. Furthermore, ceramide (which is increased in obesity²⁰⁰) promotes disruption of the eNOS-Akt complex from HSP90²⁰¹, which increases eNOS activity by promoting displacement of caveolin-1 from eNOS²⁰².

Conditions of obesity have profound effects on eNOS phosphorylation. In particular, eNOS phosphorylation at serine 1177 (S1177; S1176 in mice), which is critical for increasing NO output from the enzyme²⁰³, is diminished in mice by nutrient excess²⁰⁴⁻²⁰⁷ or high fat feeding^{155, 160, 208, 209}; studies in obese rats²¹⁰⁻²¹² and pigs²¹³ have shown similar results. This eNOS phosphorylation site is

regulated by Akt ²¹⁴, which is activated by insulin ²¹⁵. Insulin stimulation of the Akt-eNOS pathway could thus be important for regulating post-prandial blood flow and nutrient disposition to peripheral tissues. Indeed, insulin resistance in the endothelium is sufficient to diminish NO bioavailability and promote endothelial dysfunction ²¹⁶, and impaired eNOS phosphorylation due to insulin resistance was shown to be responsible for diminished glucose uptake in the skeletal muscle of mice subjected to nutrient excess ²¹⁷.

Reasons for diminished phosphorylation of eNOS under conditions of nutrient excess and obesity could be due to fatty acid (e.g., palmitate)-mediated induction of insulin resistance ¹⁵⁵. Elevated free fatty acids lower NO bioavailability in cultured cells ²¹⁸, isolated arteries ²¹⁹, animal models ²²⁰ and humans ^{221, 222}. Insulin resistance due to FFAs may be engendered by activation of Toll-like receptor 4 (TLR4) and NF- κ B ^{208, 218} or Toll-like receptor 2 (TLR2) ²²³. Other nutrient conditions inherent to diabetes may also be responsible for loss of S1177-eNOS phosphorylation. For example, hyperglycemia causes O-linked N-acetylglucosamine (O-GlcNAc) modification of eNOS, which diminishes its activity ²²⁴. Additional mechanisms posited for diminished eNOS phosphorylation in the context of obesity include a fatty acid-mediated, yet Akt-independent impairment of eNOS phosphorylation ²⁰⁹, and PKC β II-mediated diminishment in Akt and eNOS responsiveness to insulin ^{210, 212}. How these signaling pathways integrate to regulate NO production in obesity and diabetes remains to be addressed.

Uncoupling of NOS and quenching of NO in metabolic disease

The ability of NOS to produce NO is also dependent on its proper coupling, which is regulated by multiple cofactors, the ability of the NOS enzyme to remain in the dimerized form^{225, 226}, and post-translational modifications^{132, 227-229} (Fig. 2C). In particular, the cofactor BH₄ is critical to NOS activity, and it has been termed a 'redox sensor' because elevations in reactive oxygen and nitrogen species can result in its depletion²³⁰. Furthermore, BH₄ may reflect the overall 'health' of the endothelium²³¹. Obese and diabetic states in rodents and human cells are associated with decreased BH₄ and elevated levels of its oxidized form, BH₂²³¹⁻²³⁵. This is important because deficiency in BH₄ or elevations in BH₂ can uncouple NOS, which results in superoxide production from the enzyme and increases peroxynitrite generation²²⁷. Hence, deficiency of BH₄ is thought to be a major regulator of vascular dysfunction that occurs during obesity and in diabetic states. Indeed, the ratio of BH₄ to BH₂ is critical in preventing glucose-induced eNOS uncoupling²³⁶ and replenishment of BH₄ pools has proven effective in multiple pathological scenarios^{227, 228, 237-239}. Uncoupling of NOS does not appear to be a factor unique to eNOS, however, as nNOS was shown to be uncoupled in penile arteries of obese rats, leading to nitrgergic dysfunction, which was restored by increasing BH₄ levels²⁴⁰.

Peroxyntirite may be especially critical in promoting NOS uncoupling. The 3-nitrotyrosine (3-NT) is a typical 'footprint' post-translational modification that helps identify sites at which eNOS uncoupling might have occurred, and it is worth noting that this modification is observed in abundance in the context of

obesity and diabetes (e.g., ^{160, 232, 241, 242}). Patients with diabetes had diminished flow-mediated dilation of coronary arterioles and increased 3-NT protein adducts that colocalized with caveolae, demonstrating a dysfunction of the endothelium associated with elevated peroxynitrite production ²⁴³. Interestingly, endothelial dysfunction in diabetic patients was rescued by sepiapterin supplementation ²⁴³, inferring that peroxynitrite may disrupt eNOS function not only by caveolar disruption, but by depleting BH₄. This would be consistent with multiple studies showing that elevated levels of reactive species (in addition to peroxynitrite, such as superoxide produced from NADPH oxidase) promote eNOS uncoupling ²⁴⁴⁻²⁴⁸. Nevertheless, the specific contribution of peroxynitrite and other reactive species to endothelial function is still unclear. Some studies suggest that rather than contributing to the uncoupling of eNOS, superoxide derived from NADPH oxidase activates the enzyme ²⁴⁹. Hence, inhibited eNOS function perceived under conditions of oxidative stress could be due in part to the quenching of NO and not to uncoupling of the enzyme *per se*. While this would be consistent with the near diffusion-limited reaction rate of NO with superoxide (which is reported to be as high as $1.9 \times 10^{10} \text{ M}^{-1} \text{ s}^{-1}$) ²⁵⁰, the evidence for a deleterious role of uncoupled NOS should not be underestimated, and multiple other factors beyond BH₄ depletion, such as asymmetric dimethyl arginine (ADMA) levels, insufficient L-arginine levels or glutathio(ny)lation of the eNOS enzyme, can promote eNOS uncoupling and endothelial dysfunction ^{132, 251-254}. That levels of ADMA are positively correlated with insulin resistance and diabetes, and that arginine supplementation overcomes this competitive inhibition ²⁵⁵ further suggests that

eNOS uncoupling or inhibition are major contributors to the development of metabolic diseases associated with obesity.

Despite these findings, it is unclear whether obesity itself decreases NO availability. The fact that obesity in humans is associated with decreased blood flow in response to methacholine²⁵⁶, bradykinin^{257, 258}, substance P and acetylcholine²⁵⁸, shear stress²⁵⁹, and insulin^{260, 261} appears to suggest that the obese condition is somehow linked causally with diminished vascular NO bioavailability. Several studies showing similar results lend credence to this hypothesis^{158, 262-273}. However, the question remains: Is loss of NO production somehow due to excess adiposity, or is its etiology derived from those conditions commonly associated with obesity? Interestingly, endothelial dysfunction was found to occur in morbidly obese humans only in the presence of insulin resistance²⁷⁴. And, severely obese humans, in the absence of insulin resistance, showed better flow-mediated dilation compared with normal and obese insulin-sensitive subjects²⁷⁵. Furthermore, capillary recruitment has been shown to be higher in overweight compared with lean individuals²⁷⁶. This suggests that the maintenance of a metabolically benign form of obesity is possible and that either insulin resistance or conditions directly linked with the insulin resistant phenotype (e.g., dyslipidemia, inflammation, hyperglycemia) are to blame for loss of NO bioavailability during obesity. Collectively, these findings raise multiple questions: What determines how the metabolically benign versus harmful forms of obesity develop?; How does NO affect obesity and insulin resistance?; What is the relevance of changes in NOS isoform abundance, (some of which go in

diametrically opposite directions (e.g., eNOS vs. iNOS)), in the development of metabolic disease?; and, how does NO regulate tissue-specific metabolic pathways?

Project Objective

Extensive evidence shows that obesity is a robust risk factor for the development of T2D, yet the mechanisms by which obesity increases the risk of T2D remain unclear. Recent studies suggest that endothelial dysfunction, characterized by a decrease in nitric oxide (NO) production, is pivotal in the progression of metabolic disease. The endothelium is a central regulator of insulin sensitivity and is the first tissue to become insulin resistant. In addition, it has been reported that deletion of eNOS is associated with adiposity, insulin resistance and impaired fatty acid oxidation. Nevertheless, the role of eNOS in regulating metabolism is not well understood. The overall goal of my work is to understand how NO regulates metabolism. We propose that during nutrient excess decreased vascular-derived NO bioavailability is a critical step that leads to the development of metabolic dysregulation. ***Specifically, we hypothesize that an increase in NO derived from eNOS prevents diet-induced obesity by promoting adipose tissue browning and increasing systemic metabolism.*** To determine effects of nutrient excess on tissues critical to obesity-related insulin resistance, we examined nutrient excess-induced metabolic changes occurring in adipose tissue. As discussed in Chapter II, we found changes consistent with mitochondrial remodeling and loss of mitochondrial bioenergetic capacity in adipose tissue. Further we show that obesity induces profound decreases in eNOS abundance. To assess the significance of eNOS downregulation, we investigated whether increasing eNOS expression was sufficient to prevent obesity-related metabolic consequences (Chapter III, Aim I). After studying the

anti-obesogenic effects of eNOS, we examined how overexpression of eNOS affects systemic metabolism (Chapter IV, Aim II). Our findings reveal an important role of NO in regulating metabolism and suggest that increasing NO could prevent diet-induced obesity. In addition, our findings support the view that, while obesity and insulin resistance are closely associated they remain distinctly separate consequences of nutrient excess.

CHAPTER II

METABOLIC REMODELING OF WHITE ADIPOSE TISSUE IN OBESIT.

Introduction

The increasing prevalence of obesity is a principal health concern worldwide. In 2008, approximately 1.5 billion adults aged 20 years or older were overweight, and 10% were obese ¹. In the US, more than one-third of the adult population is currently obese (BMI >30), and 68% have a BMI>25 ²⁷⁷; these numbers are expected to increase by more than 50% by the year 2025 ⁷. These statistics are cause for alarm. Obesity is a powerful predictor of insulin resistance ⁴ and a major risk factor for several common medical conditions, including type 2 diabetes (T2D), cardiovascular disease, non-alcoholic fatty liver and gallstones, Alzheimer's disease, and some cancers ²⁷⁸.

While lack of exercise is an undeniable risk factor for weight gain ²⁷⁸⁻²⁸⁰, excessive caloric intake appears to be one of the key factors fueling the obesity epidemic. In the past three decades, the average consumption of calories in the US has increased by at least 200 kcal/d per person, which is partly attributable to an increase in the intake of energy-dense foods ^{8-10, 281}. Such poor dietary habits negatively affect metabolic homeostasis, which could not only promote obesity, but the development of obesity-related co-morbidities as well. Despite the

simplicity of the apparent remedy (i.e., decreasing caloric intake), treatment of obesity remains a challenging crisis facing the health care system. Losing weight via caloric restriction faces multiple conceptual challenges: these include an evolutionarily engendered guard against starvation and low fat mass ^{7, 31} and a propensity to increase caloric efficiency during dieting ^{32, 33}. While several approaches to combat obesity have been approved for clinical use, including medications that reduce caloric intake or absorption and bariatric surgery, these approaches in many cases show marginal long-term efficacy or have unacceptable or overtly dangerous side effects ⁷. Thus, recent strategies to modulate obesity have begun to target tissues that naturally regulate energy metabolism.

Increasing energy expenditure by modulating adipose tissue activity has become an especially attractive target for therapy. Guided by the fact that adult humans maintain small depots of brown fat capable of burning significant amounts of calorific energy ⁵⁷, multiple studies focused on the physiological and molecular mechanisms regulating the thermogenic capacity of adipose tissue. These studies show that adaptive thermogenesis in brown fat can be a powerful regulator of systemic energy metabolism. However, the relatively small amount of brown adipose (less than 0.4% of body weight) compared with white adipose tissue (WAT; which can comprise 40% or more of the body weight of an obese human) suggests that WAT may be a more tangible target. Interestingly, white adipose depots, which typically function to esterify free fatty acids (FFA) and store excess lipids, have the capacity to develop brown adipose-like tissue

capable of modulating systemic metabolism and preventing obesity and insulin resistance²⁸².

While the phenomenon of adipose “browning” is an exciting area of research, there is also considerable interest in understanding the metabolic changes that occur in WAT with obesity. It has become increasingly clear that conditions of nutrient excess promote a “whitening” of adipose tissue characterized by decreases in mitochondrial abundance^{93, 283, 284}. Hence, while promoting “browning” is one way to positively modulate metabolism, decreasing adipose tissue “whitening” could in principle prevent the dysregulation of systemic metabolism caused by obesity. Indeed, the therapeutic actions of thiazolidinediones such as rosiglitazone and pioglitazone have been suggested to be due to their ability to prevent loss of mitochondria or increase mitochondrial function in WAT^{284, 285}. Nevertheless, the metabolic changes occurring during adipose tissue whitening have not been well-characterized, in part because these metabolic changes have been difficult to dissect from other sequelae of obesity such as adipose tissue inflammation.

In this study, we examined both the systemic and WAT-specific changes in metabolism in a common model of diet-induced obesity—the C57BL/6J mouse fed a high fat diet (60% kcal from fat). Our data indicate that mitochondrial remodeling, leading to decreases in mitochondrial oxidative phosphorylation and substrate oxidation, precedes the infiltration of inflammatory cells such as macrophages. The changes apparently precede overt loss of mitochondrial mass and coincide with decreases in PGC1 α and dysregulation of lipid and

amino acid metabolism. In addition, we find ultrastructural and biochemical changes consistent with autophagy and mitochondrial remodeling, the onset of which also appears to precede the infiltration of macrophages. These findings have important implications for our understanding of the effects of obesity on adipose tissue metabolism and suggest that inhibiting the metabolic changes that contribute to adipose whitening could form the basis for novel therapies to combat metabolic disease.

Experimental Procedures

Animal studies: All procedures were approved by the University of Louisville Institutional Animal Care and Use Committee. C57BL/6J (wild-type; WT) mice were purchased from The Jackson Laboratory (Bar Harbor, ME). At 8 weeks of age, male mice were placed on either a 10% low fat diet (LFD; Research Diets, Inc., #D12450B) or a 60% high fat diet (HFD; Research Diets Inc., #D12492) for 6 or 12 weeks. Water and diet were provided *ad libitum*. Body weights were recorded weekly.

Metabolic phenotyping: Body composition was measured by dual-energy X-ray absorptiometry using a mouse densitometer (PIXImus2; Lunar, Madison, WI), and whole body energy expenditure, respiratory exchange ratio, food consumption, and locomotion, ambulatory and fine movements were measured using a physiological/metabolic cage system (TSE PhenoMaster System, Bad

Homberg, Germany) ²⁸⁶. Glucose and insulin tolerance tests and plasma levels of insulin were measured as described in Sansbury et al ²⁸⁶.

Adipocyte size measurements: Adipose tissue was excised at the time of euthanasia, and wet weight was recorded. All adipose tissue was either snap-frozen at -80°C or fixed in 10% formalin (Leica), paraffin embedded, and sectioned. Sections were stained in hematoxylin and eosin. Adipocyte cross-sectional area and size distribution was determined using Nikon Elements. Adipose tissue sections were assessed for crown-like structures as described previously ²⁸⁷.

Adipose tissue metabolite profiling: WAT from the epididymal fat pads of mice fed a LFD or HFD for 6 weeks were used for these analyses. Prior to tissue collection, mice were fasted for 16 h. After euthanasia, the adipose tissue was removed and immediately snap-frozen in liquid nitrogen. Relative metabolite abundance was then measured by GC/MS or LC/MS as described before ²⁸⁶. Metabolites with missing values were imputed by replacing missing values with half of the minimum positive value in the original data. Metabolites with greater than 57% of values missing were omitted from the analysis. After a generalized logarithm transformation, data were autoscaled, i.e., mean-centered and divided by the standard deviation of each variable. This step was performed to transform the intensity values so that the distribution was more Gaussian. T-test statistical

comparisons were then performed. Univariate (e.g., volcano plots), multivariate (e.g., PLS-DA), and cluster (heatmap and dendrogram) analyses were then performed. Most analyses were performed using Metaboanalyst 2.0 software (<http://www.metaboanalyst.ca/>)²⁸⁸; z-score plots were constructed in GraphPad 5.0 software using data derived from volcano plot analysis.

Adipose tissue bioenergetic measurements: The oxygen consumption rate (OCR) of intact WAT explants was measured using a Seahorse XF24 analyzer (Seahorse Bioscience, Billerica, MA) as described previously²⁸⁶. At least two replicates from each animal were used for the assay. After baseline measurements, the maximal OCR was measured by exposing the explants to carbonyl cyanide-4-(trifluoromethoxy)phenylhydrazone (FCCP) (10 μ M). The non-mitochondrial OCR was measured following injection of antimycin A (25 μ M) and rotenone (5 μ M).

Citrate synthase activity assay: Citrate synthase activity was measured in 100 mM Tris-HCl, pH 8.0, containing 1 mM EDTA, 1 mM 5', 5'-Dithiobis 2-nitrobenzoic acid (DTNB), 10 mM acetyl-CoA. The reaction was initiated by addition of 10 mM oxaloacetate. Cuvettes were warmed to 37°C, and upon addition of 10 μ g of protein from WAT lysates, absorbance at 420 nm was measured for 10 min. Activity was expressed as nmoles/min/ μ g protein.

Expression analyses: For quantitative RT-PCR, RNA was extracted from tissues using the RNeasy lipid tissue kit (Qiagen), followed by cDNA synthesis. Real-time PCR amplification was performed with SYBR Green qPCR Master Mix (SA Biosciences) using a 7900HT Fast Real-Time PCR System (Applied Biosystems) and commercially available primers for *il1*, *tnfa*, *il6*, *arg1*, *il10*, *ym1*, *hif1a*, *emr1*, *pgc1a*, *cytc*, *sirt1*, *sirt3*, *pdk4*, *cpt1a*, *cpt1b*, *cox7a1*, *hpvt*, and *idh3a* (SA Biosciences). Relative expression was determined by the $2^{-\Delta\Delta CT}$ method. M1 macrophages in WAT were measured by flow cytometry using well-validated surface markers as shown previously²⁸⁷.

To measure protein abundance, WAT homogenates were prepared exactly as described in Horrillo et al²⁸⁹. Equal amounts of protein were separated by SDS-PAGE, electroblotted to PVDF membranes, and probed using primary antibodies according to the manufacturers' protocol. The antibodies used were: ALDH2 (Abcam), Sirt3 (Cell Signaling), MitoProfile[®] Total OXPHOS Rodent WB Antibody Cocktail (Mitosciences), COX4I1 (Cell Signaling), GAPDH (Cell Signaling), Parkin (Abcam), Pink1 (Cell Signaling), p62 (Cell Signaling), LC3 (Cell Signaling), protein-ubiquitin (Cell Signaling) and α -tubulin (Cell Signaling). Fluorescent or HRP-linked secondary antibodies (Invitrogen) were used for detection and visualized with a Typhoon 9400 variable mode imager (GE Healthcare). Band intensity was determined using Image Quant TL[®] software.

Relative mitochondrial DNA (mtDNA) measurements: Mitochondrial abundance in adipose tissue was estimated by measuring the mtDNA abundance relative to nDNA, essentially as described previously²⁹⁰. Total DNA

was isolated from WAT using a QIAamp DNA Mini Kit (Qiagen). Aliquots of 25 mg tissue were homogenized followed by overnight digestion in Proteinase K at 55°C. Following isolation, relative amounts of mtDNA and nuclear DNA (nDNA) were compared using quantitative RT PCR. In each assay 2 ng of DNA was used with specific primers for cytochrome b (mtDNA) and β -actin (nDNA). Sequences for the primer sets used were: cytochrome b, 5'-TTGGGTTGTTTGATCCTGTTTCG-3' and 5'-CTTCGCTTTCCACTTCATCTTACC-3'; β -actin, 5'-CAGGATGCCTCTCTTGCTCT-3' and 5'-CGTCTTCCCCTCCATCGT-3'.

Electron microscopy: Adipose tissues were fixed with 3% glutaraldehyde in 0.1 M sodium phosphate buffer (pH 7.4) for 4 h at room temperature (25 °C). Tissues were then post-fixed with 1% osmium tetroxide for 1 h, dehydrated, embedded in Embed-812 plastic (Electron Microscopy Sciences). Ultrathin (50-70 nm) sections were stained with uranyl acetate and Reynolds lead citrate, and electron micrographs were taken using a Philips CM10 transmission electron microscope operating at 80 kV.

Statistical analyses: Data are mean \pm SEM. Unpaired Student's *t* test was used for direct comparisons. Statistical analyses for metabolomic datasets were performed using Metaboanalyst 2.0 software. A *p* value <0.05 was considered significant.

Results

High fat diet leads to increased adiposity and altered systemic metabolism.

Wild-type C57BL/6J mice were placed on a LFD or HFD for 6 weeks. Significant weight gain occurred as early as 1 week on HFD, and the change in total body mass was nearly 10 g by 6 weeks on the diet (Fig. 3A). Food and water intake were not significantly different between groups (Fig. 3B,C). Dexascan analysis showed a 2-fold increase in fat mass and a concomitant decrease in lean mass in HF-fed mice (Fig. 3D,E). These results are typical of this commonly utilized model of diet-induced obesity, e.g., see ^{155, 286}.

To determine how diet affects systemic metabolism, mice fed either LFD or HFD for 6 weeks were placed in metabolic chambers, and their oxygen consumption (VO_2), carbon dioxide production (VCO_2), and physical activity were measured. As shown in Fig. 3F and G, average VO_2 and VCO_2 values decreased in HF-fed mice compared with mice fed a LFD. The respiratory exchange ratio (RER) was also decreased in mice fed a HFD compared with mice fed LFD (Fig. 3H). Physical activity, measured by total beam breaks (Fig. 3I), ambulatory counts (Fig. 3J), and fine movements (Fig. 3K), was not significantly different between groups, although the group fed a HFD appeared to show a trend toward decreased physical movement. Similar to previous studies ²⁸⁶, mice fed a HFD also demonstrated worsened glucose and insulin tolerance (Fig. 4) as well as a significant increase in plasma insulin levels (WT LFD, 151 ± 71 pg/ml vs. WT HFD, 2690 ± 593 pg/ml, $n = 3$ per group, $p < 0.05$).

Figure 3. Effects of high fat diet on weight gain, adiposity and systemic metabolism. Male WT C57BL/6J mice were fed a low fat diet (LFD, 10% kcal fat) or high fat diet (HFD, 60% kcal fat) for 6 weeks and the following measurements were recorded: **(A)** mouse weights during 6 weeks of feeding, n = 20 per group; **(B)** food intake, n = 7 per group; **(C)** water intake, n = 7 per group; **(D)** representative DEXA images; **(E)** percentages of lean mass and body fat, n = 10 per group; and **(F)** average oxygen consumption (VO_2); **(G)** average carbon dioxide production (VCO_2); **(H)** respiratory exchange ratio (RER); **(I)** total activity level; **(J)** ambulatory counts; and **(K)** fine movements. n = 7 per group; * $p < 0.05$ vs. LFD.

Figure 3

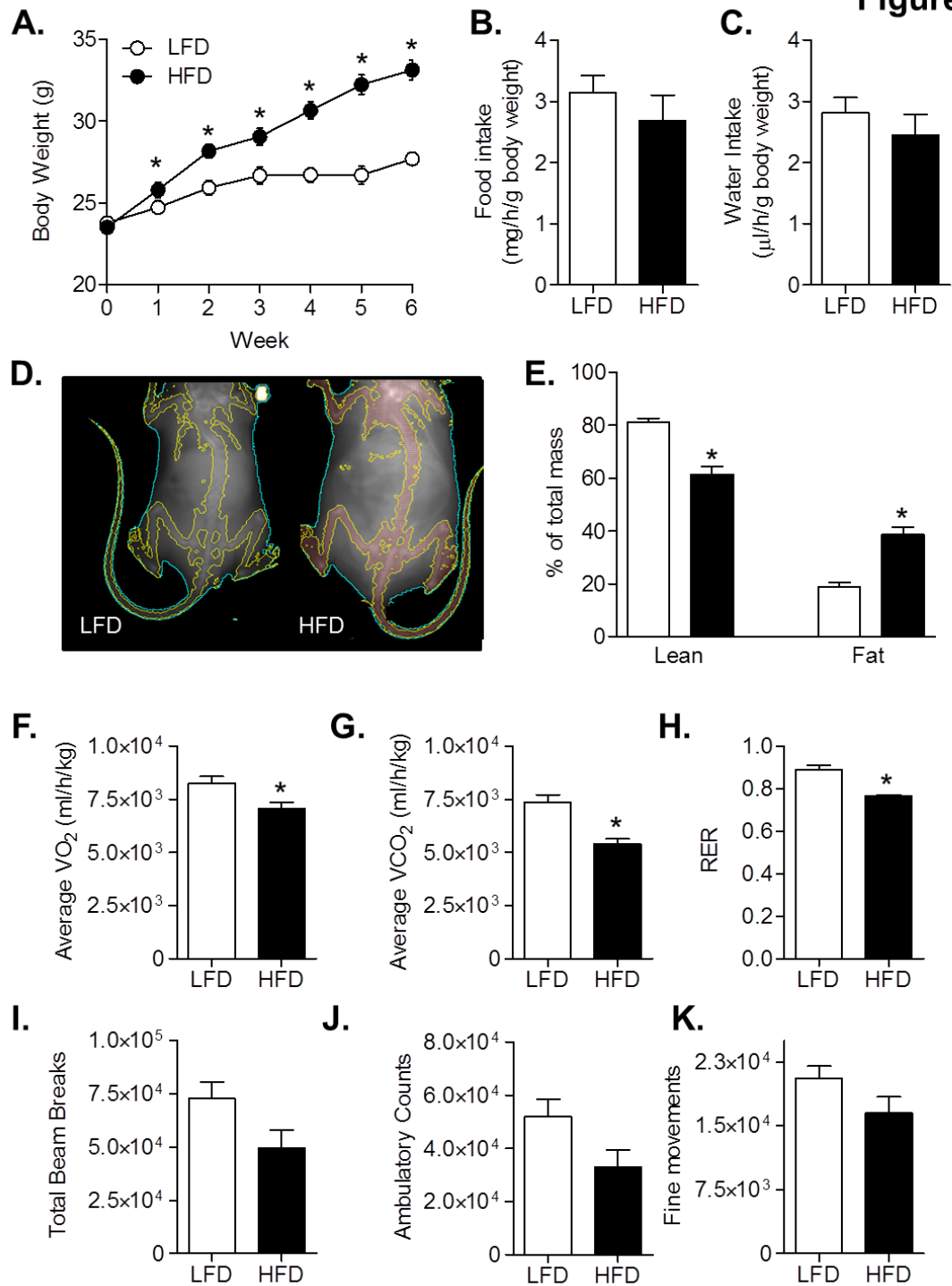
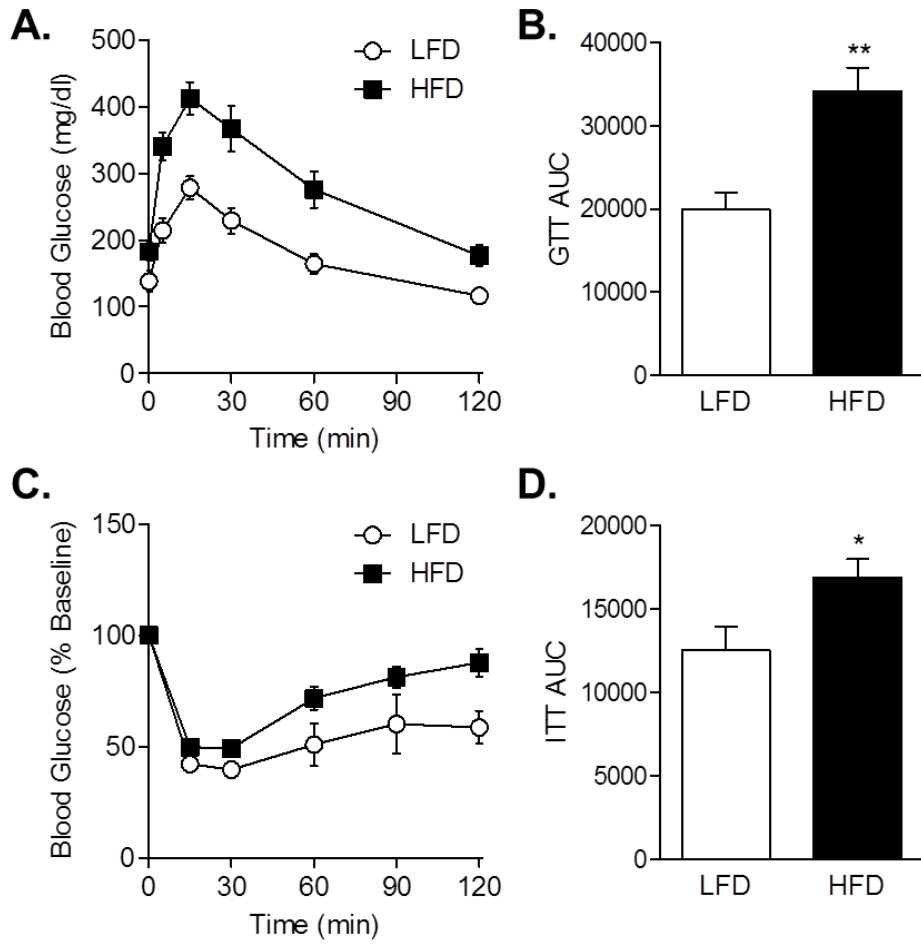


Figure 4. Glucose and insulin tolerance in mice fed low fat or high fat diets.

After 6 weeks of a low fat (LFD) or high fat diet (HFD), glucose tolerance and insulin sensitivity were examined: **(A)** Glucose tolerance test (GTT); **(B)** GTT area under the curve (AUC); **(C)** insulin tolerance test (ITT) shown as % of baseline; and **(D)** ITT AUC. n = 7 per group; * $p < 0.05$, ** $p < 0.01$ vs. LFD.

Figure 4

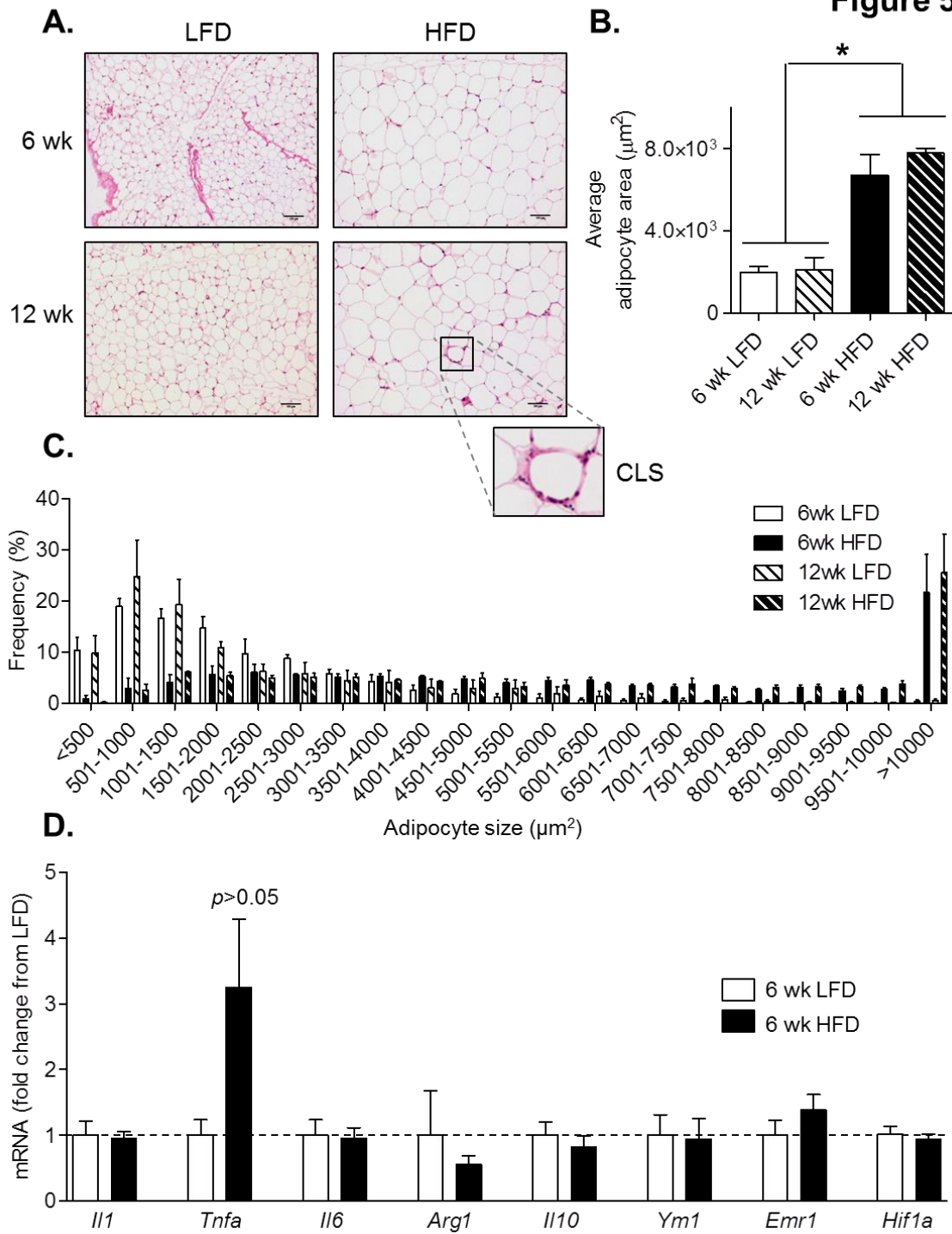


Macrophage infiltration does not occur until after 6 weeks of HFD. To measure the metabolic effects of obesity on adipocytes in the intact adipose organ, effects of inflammatory cells such as macrophages must first be ruled out or otherwise delineated. To examine effects of HFD on macrophage infiltration, we placed mice on LFD or HFD for 6 and 12 weeks and measured adipocyte size, crown-like structures indicative of macrophage infiltration, and the expression of inflammatory genes. As shown in Fig. 5A–C, mice fed a HFD for 6 and 12 weeks showed a 3–4-fold increase in adipocyte size when compared with LFD controls. While sections of WAT derived from mice fed a HFD for 12 weeks showed obvious increases in crown-like structures, WAT from mice fed HFD for 6 weeks showed minimal changes in such structures. This suggested that with 6 weeks of HFD, there was minimal macrophage accumulation. Indeed, the expression of *emr1*—a marker of macrophages—as well as that of other inflammatory genes was not changed with 6 weeks of HFD, and hypoxia was not evident as measured by expression of Hif1a (Fig. 5D). Moreover, the abundance of M1 macrophages in adipose tissue stromal vascular fractions was not different between mice fed the different diets (F4/80⁺/CD11c⁺/CD301⁻ cells as F4/80⁺ cells: LFD 37.4±3.5; HFD, 45.9±1.8; n = 9–10 per group, p>0.05.). Most likely, the modest, insignificant increase in *Tnfa* is due to adipocytes, which have been shown to produce TNF- α ^{291, 292}. Collectively, these data show that after 6 weeks of HFD, there is an increase in adipocyte size without significant changes in infiltrating inflammatory cells.

Figure 5. Effect of HFD on adipose tissue expansion and inflammation.

Morphological and molecular changes in adipose tissues: **(A)** Representative hematoxylin and eosin stains of epididymal adipose tissue of mice fed a LFD or HFD for 6 or 12 weeks; **(B)** average size of adipocytes; **(C)** adipocyte size distribution; and **(D)** qRT-PCR analyses of markers of inflammation in adipose tissues from mice fed a LFD or HFD for 6 weeks. CLS, crown-like structure; n = 4-5 per group; * $p < 0.05$ vs. indicated groups.

Figure 5



Obesity alters the metabolite profile of adipose tissue. To examine the effect of obesity on adipose tissue metabolism, epididymal WAT from mice fed a LFD or HFD for 6 weeks was subjected to unbiased metabolomic analysis. The relative concentrations of adipose metabolites were measured by mass spectrometry and queried against the Metabolon reference library. Partial least squares-discriminant analysis (PLS-DA) showed that the LFD samples clearly separate from HFD samples (Fig. 6A), and cluster analysis showed that the abundance of most metabolites was decreased in the HFD group compared with the LFD group (Fig. 6B). Out of the 191 metabolites measured, 82 were found to be significantly different ($p < 0.05$) in the WAT of mice fed a HFD compared with that of adipose from mice fed a LFD. Volcano plot analysis showed that the levels of 79 metabolites decreased significantly and only 3 metabolites increased significantly with HF feeding (Fig. 6C and Table 1). To examine and visualize the data in the biological context of metabolic pathways, metabolites that were statistically different in each group were analyzed using the MetPA tool of Metaboanalyst 2.0 software. Pathways were calculated as the sum of the importance measures of the matched metabolites normalized by the sum of the importance measures of all metabolites in each pathway²⁸⁸. As shown in Fig. 6D, the highest pathway impact values were related with branched chain amino acid (BCAA) metabolism (i.e., Val, Leu, and Ile metabolism) and Phe, Tyr and Trp metabolism. Significant changes were also observed in His metabolism as well as Gly and Ser metabolism. Glycerophospholipid metabolism showed the most significant change with HF feeding. To further delineate changes in

Figure 6. Metabolomic analyses of adipose tissue. Metabolomic analyses of epididymal adipose tissue metabolites from WT mice fed a LFD or HFD for 6 weeks: **(A)** Multivariate analysis: partial least squares-discriminant analysis (PLS-DA); **(B)** Hierarchical clustering: Heatmap and dendrogram; **(C)** Univariate analysis: Volcano plot of metabolites. Those metabolites that significantly increased are in the quadrant shaded red and those that significantly decreased are shaded green ($p < 0.05$, t-test). A list of these metabolites can be found in Table 1; **(D)** Metabolites found to be significantly different were subjected to pathway impact analysis using Metaboanalyst MetPA and the *Mus musculus* pathway library. Fisher's exact test was used for overrepresentation analysis, and relative betweenness centrality was used for pathway topology analysis. n = 14 animals: 7 WT LFD and 7 WT HFD

Figure 6

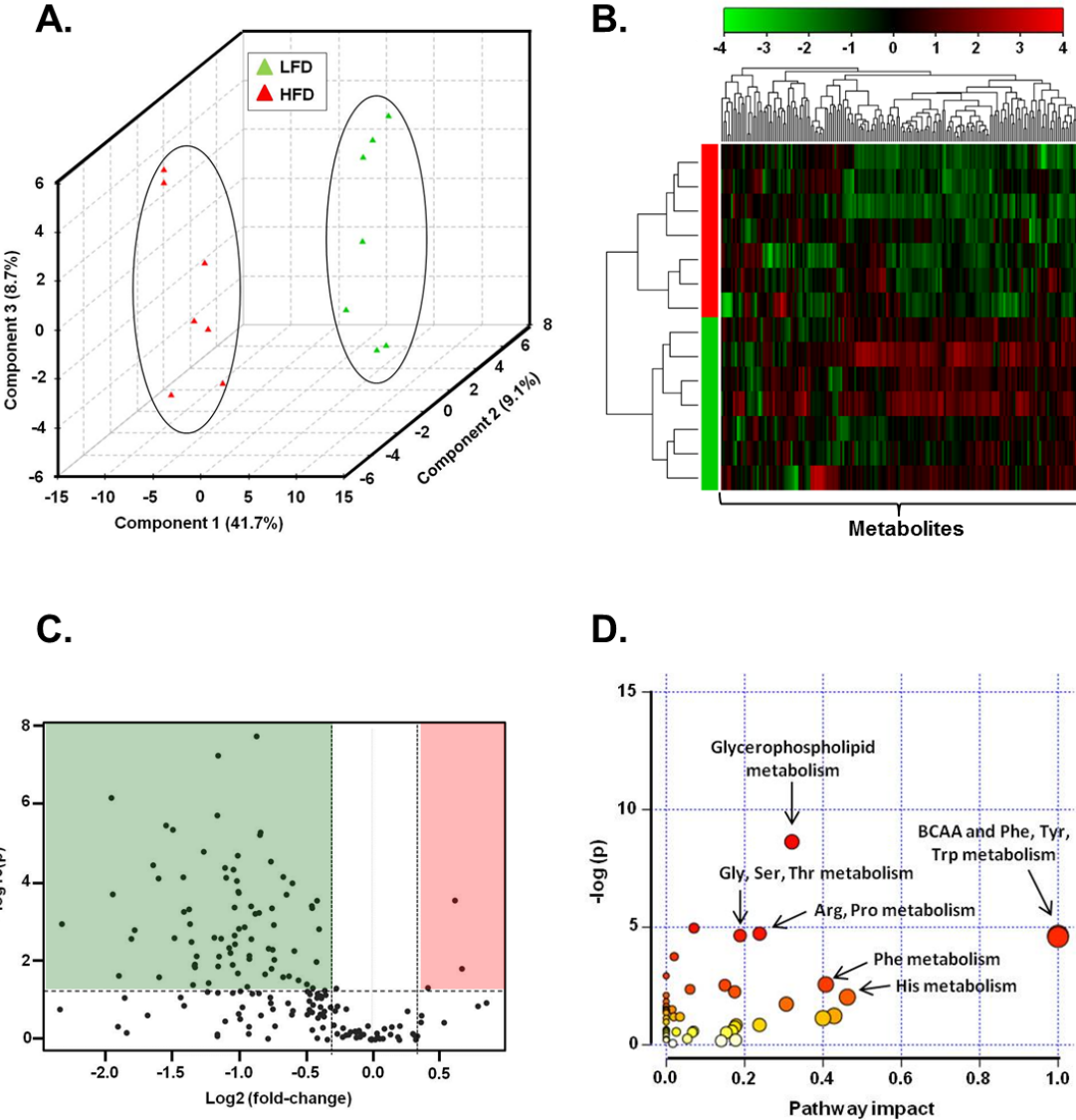


Table 1. List of adipose tissue metabolites that changed significantly in high fat-fed mice.

Metabolite	Fold change	p value	FDR
threonine	0.54948	2.03E-08	3.57E-06
leucine	0.45023	6.26E-08	5.51E-06
ergothioneine	0.25885	7.34E-07	4.31E-05
tyrosine	0.44838	2.05E-06	9.03E-05
valine	0.34372	3.68E-06	0.00013
phenylalanine	0.35614	4.73E-06	0.000139
phosphoethanolamine	0.56087	5.51E-06	0.000139
proline	0.55922	6.39E-06	0.000141
pantothenate	0.41779	1.70E-05	0.000333
lysine	0.49838	2.14E-05	0.000376
xanthine	0.5918	3.02E-05	0.000484
1,5-anhydroglucitol (1,5-AG)	0.32145	3.73E-05	0.000547
isoleucine	0.46664	4.36E-05	0.000591
betaine	0.48746	4.84E-05	0.000608
asparagine	0.63104	7.38E-05	0.000792
mead acid (20:3n9)	0.37579	7.54E-05	0.000792
flavin adenine dinucleotide (FAD)	0.46937	7.75E-05	0.000792
3-dehydrocarnitine	0.33055	8.10E-05	0.000792
tryptophan	0.49615	9.37E-05	0.000868
carnitine	0.66176	0.000107	0.00094
methionine	0.49975	0.000175	0.001466
serine	0.50099	0.000188	0.001502
histamine	0.26069	0.000204	0.001523
arginine	0.6417	0.000208	0.001523
glycerophosphoethanolamine	1.5377	0.000292	0.001997
glutamine	0.75187	0.000295	0.001997
cholesterol	0.7317	0.000403	0.002579
C-glycosyltryptophan	0.53405	0.00041	0.002579
cis-vaccenate (18:1n7)	0.49012	0.000438	0.002608
citrulline	0.73299	0.000454	0.002608
phosphate	0.59509	0.000459	0.002608
urea	0.38721	0.000489	0.002689
17-methylstearate	0.37705	0.000566	0.00302
nicotinamide	0.55648	0.000601	0.003114
hydroxyisovaleroyl carnitine	0.54575	0.000634	0.00319
mannose-6-phosphate	0.20024	0.001153	0.00549
histidine	0.38909	0.001154	0.00549
choline	0.60096	0.001218	0.005641
palmitoleate (16:1n7)	0.51634	0.001386	0.006253
glycerol	0.50143	0.001522	0.00668
taurine	0.75975	0.001556	0.00668

glucose-6-phosphate (G6P)	0.29197	0.001647	0.006899
1-stearoylglycerophosphoinositol	0.49031	0.002247	0.009195
uracil	0.44141	0.002558	0.010175
hypoxanthine	0.35895	0.002619	0.010175
isobutyrylcarnitine	0.4573	0.002703	0.010175
isopalmitic acid	0.28706	0.002733	0.010175
uridine	0.53462	0.002775	0.010175
scyllo-inositol	0.39204	0.00328	0.011781
S-adenosylhomocysteine (SAH)	0.49132	0.003745	0.013182
1-oleoylglycerophosphoethanolamine	0.47672	0.004631	0.015981
1-palmitoylglycerophosphoethanolamine	0.58479	0.004838	0.016374
glycerol 3-phosphate (G3P)	0.59732	0.005149	0.017099
1-palmitoylglycerophosphoinositol	0.66829	0.005556	0.01811
nonadecanoate (19:0)	0.47985	0.006228	0.01993
cysteine	0.5292	0.007339	0.023067
eicosenoate (20:1n9 or 11)	0.40267	0.00756	0.023275
10-nonadecenoate (19:1n9)	0.45235	0.00767	0.023275
cysteine-glutathione disulfide	0.5291	0.008825	0.026327
palmitoyl sphingomyelin	0.60227	0.009257	0.027153
choline phosphate	0.74957	0.010514	0.030335
N-acetylglucosamine 6-phosphate	0.39909	0.012184	0.034588
1-arachidonoylglycerophosphoinositol	0.48542	0.012459	0.034806
2-hydroxyglutarate	0.39816	0.013183	0.036253
inosine	0.45019	0.013616	0.036867
glycerol 2-phosphate	0.39934	0.014415	0.038439
cytidine	0.59371	0.015663	0.040621
stearoyl sphingomyelin	1.5942	0.015695	0.040621
urate	0.49862	0.020514	0.052327
1-arachidonoylglycerophosphoethanolamine	0.57421	0.021629	0.054382
1-palmitoleoylglycerophosphoethanolamine	0.26907	0.023675	0.058687
stearidonate (18:4n3)	0.65008	0.024231	0.05923
lactate	0.63047	0.025519	0.061036
alpha-tocopherol	0.33155	0.025663	0.061036
oleate (18:1n9)	0.6828	0.030736	0.072127
2-methylbutyrylcarnitine	0.42844	0.036105	0.083611
palmitate (16:0)	0.71324	0.03874	0.088549
isovalerylcarnitine	0.39518	0.040257	0.090836
guanosine	0.52357	0.044904	0.10004
succinate	1.3363	0.047935	0.10531
adenosine	0.73547	0.048468	0.10531

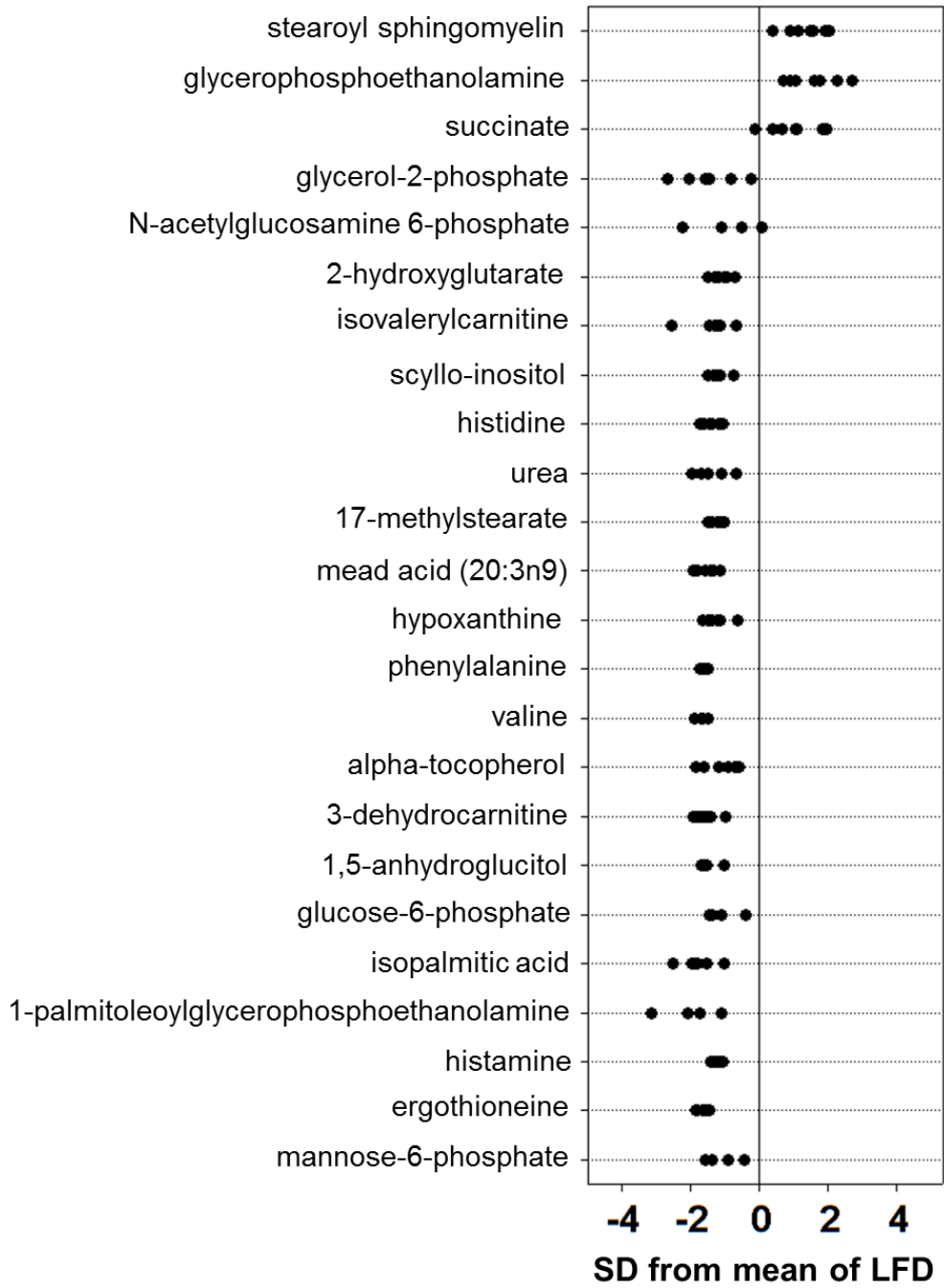
Wild-type (WT) mice were fed a low fat or high fat diet (LFD or HFD, respectively) for 6 weeks. Epididymal adipose tissue was then subjected to LC or GC mass spectrometric analysis. Those metabolites found to be significantly different by t-test are listed above. n = 7 mice per group.

metabolites, we examined those metabolites that were either significantly elevated or those that were decreased in abundance by more than 60%. As shown in Fig. 7, stearoyl sphingomyelin, glycerophosphoethanolamine, and succinate were the only metabolites that increased in abundance in WAT derived from HF-fed mice. The majority of metabolites that decreased by >60% belonged to the lipid and amino acid superfamilies.

The effect of obesity on mitochondrial oxygen consumption and mitochondrial remodeling in WAT explants. The increase in succinate found in our metabolomic analyses suggested that HFD may alter adipose tissue bioenergetics. Importantly, these changes occurred in the absence of inflammatory cell infiltration (see Fig. 5), which could otherwise confound adipocyte-specific changes in metabolism. To determine how obesity affects adipose tissue mitochondrial function, WAT explants from mice fed a LFD or HFD were subjected to extracellular flux analysis. As shown in Fig. 8A and B, the apparent basal mitochondrial oxygen consumption rate of adipose tissue derived from mice fed a LFD was >2-fold higher when compared with adipose explants derived from HF-fed mice ($p < 0.05$); however, statistical significance in OCR between groups was lost upon exposure of explants to FCCP (Fig. 8C). This appeared to be largely due to an enhanced FCCP response in WAT explants from obese mice. As shown in Fig. 8D, explants derived from mice fed a HFD responded more strongly to FCCP. No significant difference in the

Figure 7. Z-score plot analysis of metabolite changes in adipose tissue from high fat fed mice. Mice were fed a LFD or HFD for 6 weeks. Data are shown as standard deviations from the mean of LFD. Only the metabolites that increased significantly and those that decreased by >60% are shown. Each point represents one metabolite in one sample. n = 7 per group.

Figure 7



extracellular acidification rate (ECAR, a measure of the coupling between glycolysis and glucose oxidation) was observed.

Although citrate synthase activity was decreased by more than 50% in WAT derived from these mice (Fig. 8E), which suggested a decrease in mitochondrial abundance, relative abundance of mtDNA, as assessed by qPCR of mtDNA and nDNA, was not changed after 6 weeks of diet (Fig. 8F). From our protein determination measurements, we calculated that the yield of protein per wet weight is diminished by 43% in adipose tissue from high fat-fed mice (μg protein/mg wet weight: 6 wk LFD, 10.86 ± 1.70 ; 6 wk HFD, 6.21 ± 1.28 ; $n = 10\text{--}12$ per group). Applying this information to our data would then shift the OCR curves to levels near those observed in explants from low fat-fed mice; which suggested no overall change in oxygen consumption per mitochondrion. However, the expression of *cox7a1*, a subunit in the electron transport chain per mg protein, was increased more than 2-fold in adipose tissue from mice fed a HFD, whereas *pgc1a*, *sirt3*, and *pdk4* expression were decreased (Fig. 8G) which indicated mitochondrial remodeling with preserved function.

To examine how WAT mitochondria change with obesity, we assessed the relative abundance of several mitochondrial complex proteins as well as mitochondrial matrix proteins. Although no changes in mitochondrial protein abundance were observed at 6 weeks of HFD, the protein levels of NDUF8, SDHB, and COX4I1—subunits of complexes I, II, and IV, respectively—were diminished significantly by 12 weeks of HFD (Fig. 9A–D). The matrix proteins

Figure 8. Obesity-related energetic changes in white adipose tissue.

Metabolic analysis of adipose tissue from mice fed a LFD or HFD for 6 weeks: (A) Extracellular flux analysis: After three basal oxygen consumption rate (OCR) measurements, FCCP (10 μ M) was injected, followed by injection of antimycin A (AA, 25 μ M) and rotenone (Rot, 5 μ M). The apparent contribution of the non-mitochondrial OCR to the total OCR is indicated by the gray box. (B) Apparent basal mitochondrial OCR: The stabilized non-mitochondrial OCR achieved after AA+Rot treatment was subtracted from the basal OCR to calculate the rate of mitochondrial oxygen utilization in each explant; (C) FCCP-stimulated OCR: The FCCP-stimulated OCR was calculated by subtracting the non-mitochondrial OCR from maximal rate achieved after FCCP addition; (D) FCCP response: the FCCP response in each explant was calculated using the equation: $(OCR_{MAX}/OCR_{BASAL}) \times 100$; n = 10 mice per group; (E) citrate synthase activity, n = 3-6 mice per group; (F) Relative mtDNA content, n = 6 per group; and (G) expression of metabolic genes, n = 4 mice per group. *p<0.05 vs. LFD group.

Figure 8

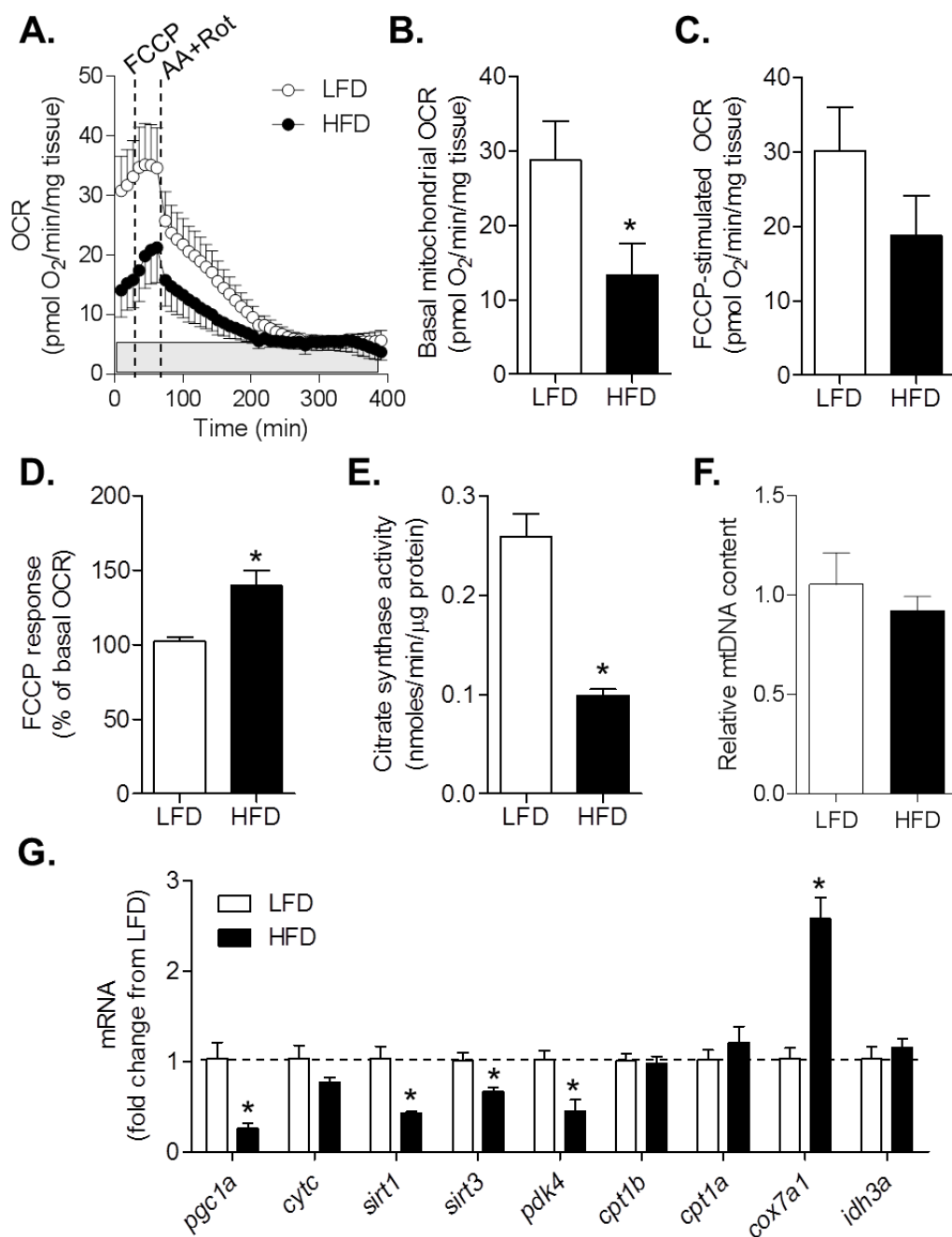
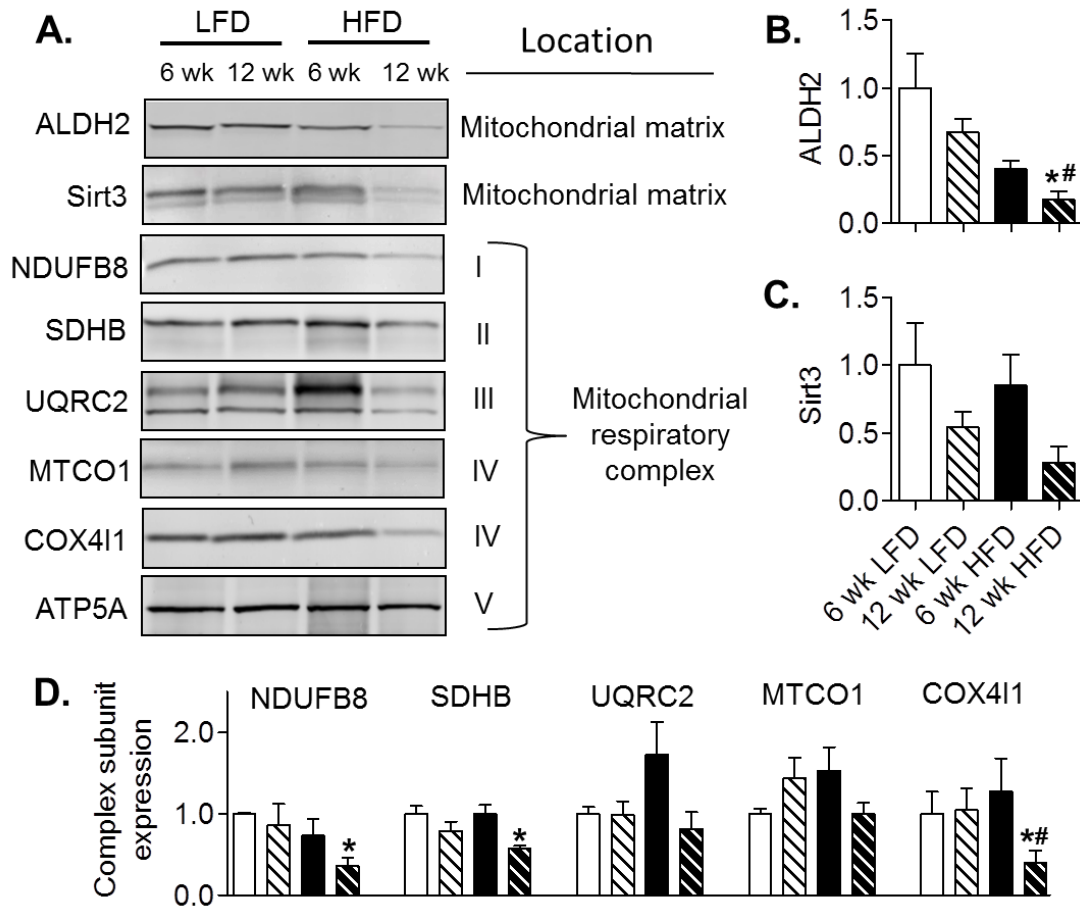


Figure 9. Obesity-related changes in mitochondrial protein abundance in white adipose tissue. Analysis of adipose tissue from mice fed a LFD or HFD for 6 or 12 weeks: **(A)** Representative Western blots of mitochondrial matrix proteins and respiratory chain subunits; **(B)** Quantification of ALDH2; **(C)** Quantification of Sirt3; **(D)** Quantification of respiratory subunit abundance. All blots were normalized to ATP5A, which showed no change in abundance in any group. n = 4 per group; *p<0.05 vs. 6 wk LFD, #p<0.05 vs 12 wk LFD.

Figure 9



ALDH2 and Sirt3 showed similar trends, with ALDH2 decreasing significantly by 12 weeks of HFD.

Assessment of adipose tissue ultrastructure. To examine in greater detail the subcellular changes that occur in adipose tissue of nutrient-stressed animals, we examined adipocyte ultrastructure using electron microscopy. As shown in Fig 8A, adipose tissue from mice fed a LFD showed mitochondria with three distinct morphologies: a round morphology of small size that was located near the nucleus (Fig. 10A-i,ii), a typical elongated shape up to $\sim 0.7 \mu\text{m}$ in length located in small protrusions along the adipocyte cell membrane (Fig. 10A-iii), and extremely long mitochondria (up to $5 \mu\text{m}$ and above) that were located in juxtaposition to the fat locule (Fig. 10A-iv). In adipocytes derived from HF-fed mice, autophagosomes—defined by a double-membrane and comprising cytoplasmic constituents—were found next to mitochondria (Fig. 10B-i), and large vacuoles of electron-dense material were present adjacent to autophagosomes (Fig. 10B-ii,iii). In addition, many mitochondria in adipose tissues from HF-fed mice appeared to be undergoing fission (Fig. 10B-iv,v).

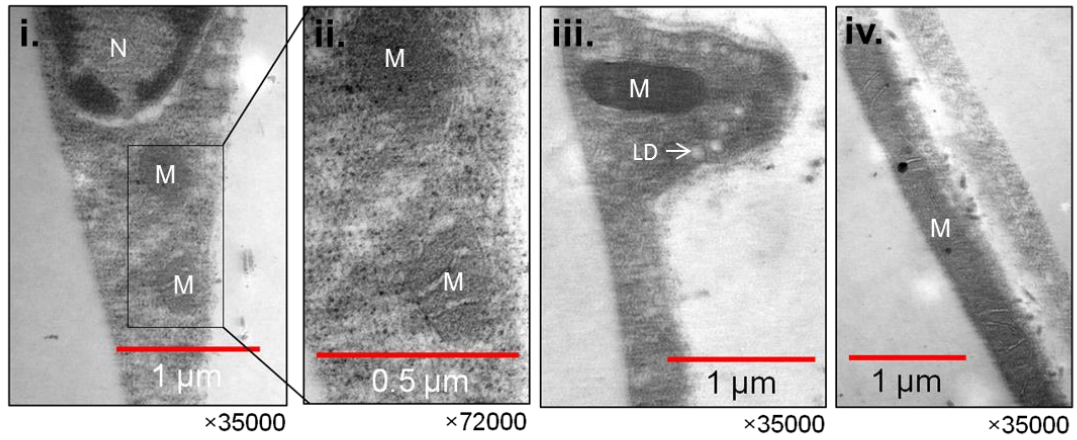
Effects of HFD on autophagy. Changes in citrate synthase and mitochondrial proteins combined with the ultrastructural alterations found in adipose tissue suggest that HFD may promote mitochondrial remodeling and activate mitophagy

Figure 10. Ultrastructure of white adipose tissues from lean and obese mice. Representative transmission electron micrographs of epididymal adipose tissues derived from mice fed a LFD or HFD for 6 weeks. **(A)** Ultrastructure of mitochondria in adipose tissues from LF-fed mice: **(i)** micrograph of adipocytes in areas close to the nucleus; **(ii)** higher magnification of panel i; **(iii)** a cytosolic compartment containing a mitochondrion found protruding into the fat locule; and **(iv)** an elongated mitochondrion in juxtaposition to the fat locule. **(B)** Ultrastructure of adipose tissue derived from HF-fed mice: **(i)** An elongated mitochondrion next to an autophagosome; **(ii)** an autophagosome in close proximity to a vacuole containing electron-dense material; **(iii)** magnified image of panel ii; **(iv)** protrusion of cytosolic compartment containing an atypical mitochondrion; and **(v)** mitochondrion that appears to be undergoing fission. Asterisks (*) indicate autophagosomes; small arrows indicate collagen; mitochondria (M), nucleus (N), vacuole lipid droplet (LD).

Figure 10

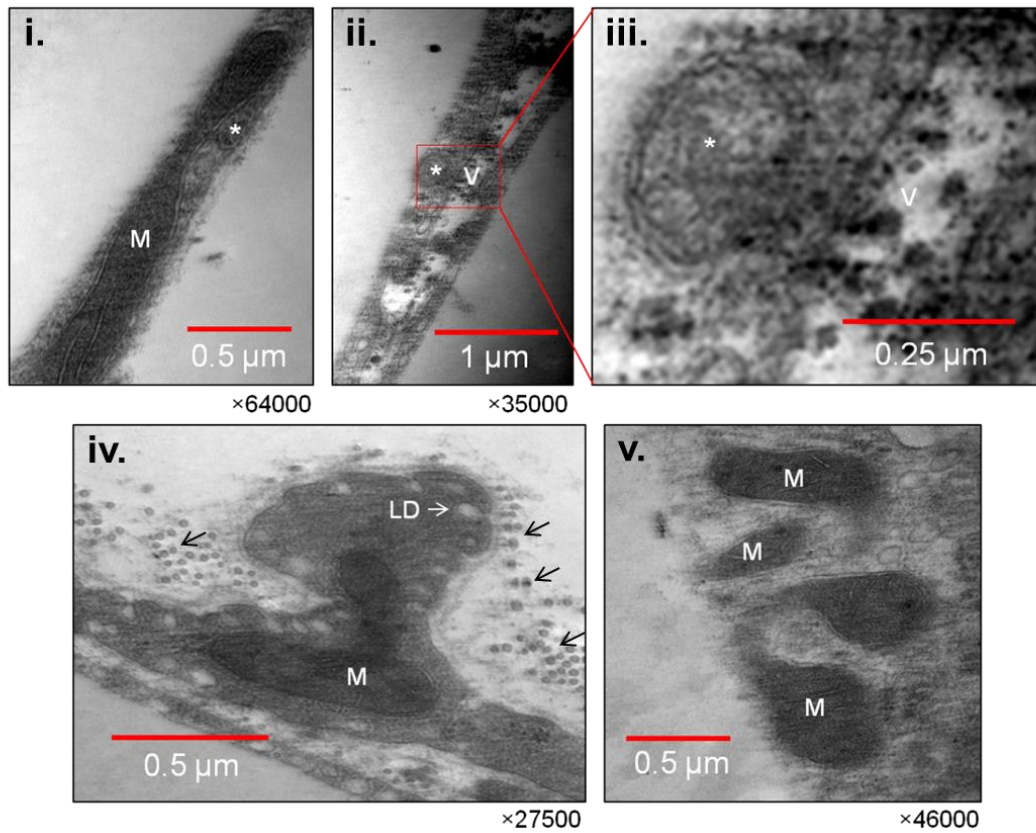
A.

LFD



B.

HFD



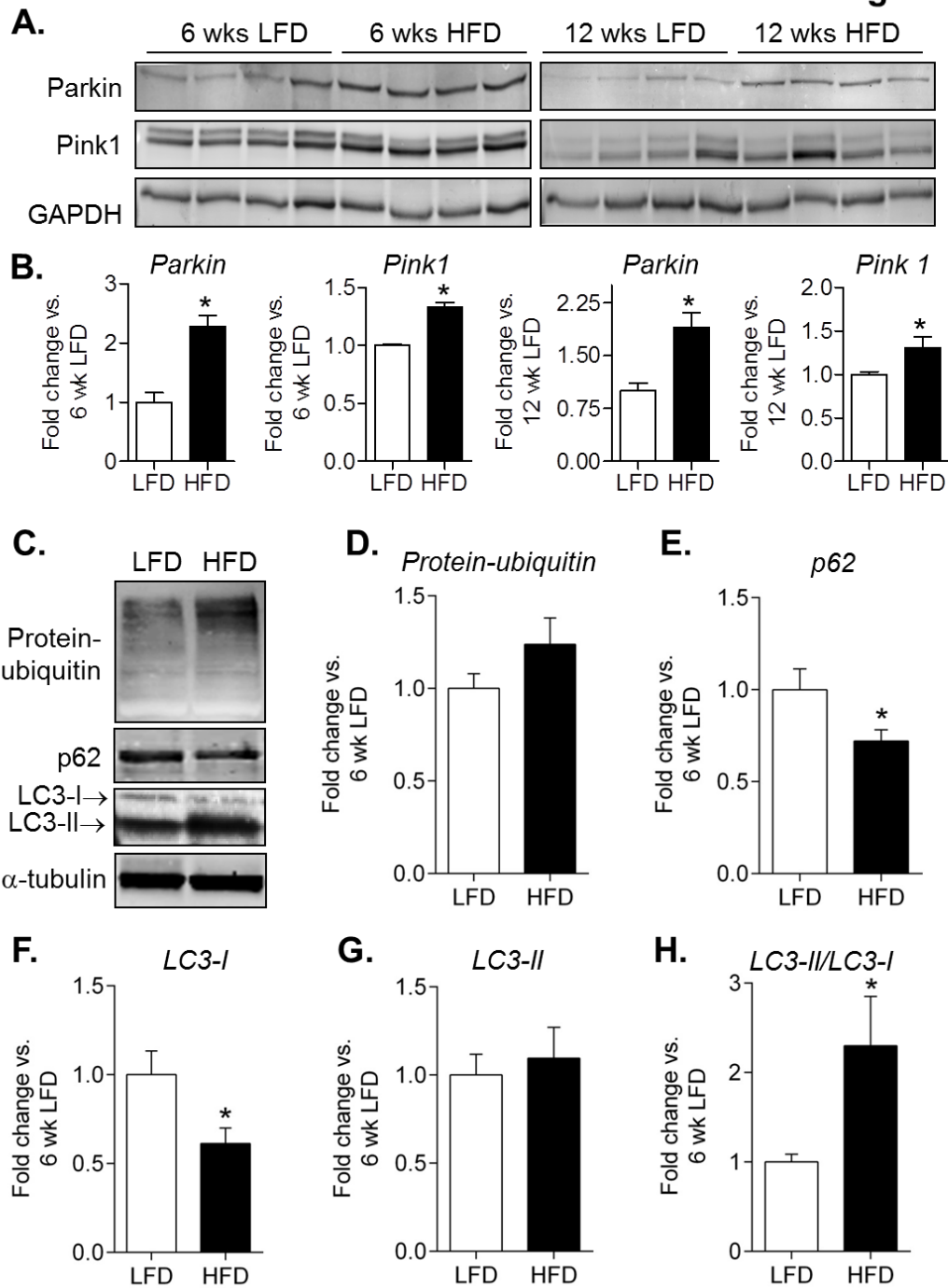
in WAT. To examine this possibility, we measured markers of mitophagy and autophagy in adipose tissues from mice fed a LFD or HFD. The E3 ubiquitin ligase Parkin, which has been shown to accumulate in mitochondria destined for degradation²⁹³, was increased 2.3-fold by 6 weeks of HFD and nearly 2-fold by 12 weeks of HFD (Fig. 11A,B). Furthermore, the kinase Pink1—critical for identifying mitochondria destined for autophagy²⁹³—was also increased by nearly 40% with HFD. Combined with the presence of autophagosomes and mitochondrial alterations observed by EM (Fig. 10), this suggests that autophagy may be involved in the metabolic remodeling of adipocytes in the expanding adipose organ and protein indicators of autophagy were examined. As shown in Fig. 11C–H, levels of p62 and LC3-I were diminished significantly and the LC3-II/LC3-I ratio was increased more than 2-fold in mice fed a HFD for 6 weeks in comparison with those placed on LFD. There was no significant difference in total protein abundance of protein-ubiquitin and LC3-II.

Discussion

This study demonstrates coordinated changes in adipose tissue metabolism that contribute to the “whitening” program during obesity. Using metabolomics analysis, we identified that lipid and amino acid metabolism was significantly significantly changed by HFD. Importantly, these analyses were independent of inflammatory cell infiltration and are therefore unlikely to be confounded by changes in cell composition of the fat depot. The metabolomics

Figure 11. Evidence for activation of mitophagy in WAT of obese mice.

Immunoblot analysis of markers of mitophagy and autophagy: **(A)** Western blots of Parkin and Pink 1 in adipose tissues from mice fed a LFD or HFD for 6 weeks (left panels) or 12 weeks (right panels); and **(B)** Quantification of Parkin and Pink1 abundance from panel E. n = 4 per group; *p<0.05 vs. LFD. n = 4 per group; *p<0.05 vs. 6 wk LFD, #p<0.05 vs 12 wk LFD. **(C)** Representative Western blots of ubiquitinated proteins, p62, and LC3 in mice fed a LFD or HFD for 6 weeks. **(D)** Quantification of protein-ubiquitin abundance. **(E)** Quantification of p62 abundance. **(F)** Quantification of LC3-I abundance. **(G)** Quantification of LC3-II abundance. **(H)** Quantification of the LC3-II/LC3-I ratio. n = 10 per group; *p<0.05 vs. LFD.

Figure 11

dataset also indicated possible changes in energy metabolism. The Krebs cycle intermediate, succinate, was significantly elevated in adipose tissue from obese mice. Further experiments identified early decreases in citrate synthase activity and explant oxygen consumption that coincided with decreased expression of *pgc1a*; yet diminishment in citrate synthase activity was independent of decreases in mitochondrial abundance, as indicated by mtDNA measurements and the abundance of electron transport chain subunits. Evidence of mitochondrial remodeling was found with 6 weeks of HFD, and elevation of the mitophagy markers Parkin and Pink1 persisted through 12 weeks of feeding. The decrease in p62 and LC3-I and elevation of the LC3-II/LC3-I ratio in WAT from obese mice support the notion that autophagic flux is increased in adipocytes of mice fed a high-fat diet. Collectively, these studies suggest a progressive remodeling of adipocyte metabolism under conditions of nutrient excess that involves downregulation of mediators of mitochondrial biogenesis, mitochondrial remodeling, and potential activation of the mitophagic program.

A major goal of this study was to understand changes in adipose tissue biology and metabolism that occur with obesity. This is important because such key metabolic features that change with obesity could become targets for anti-obesity or insulin-sensitizing therapies. By 6 weeks of HFD, mice demonstrate profoundly increased fat mass, decreased systemic VO_2 , VCO_2 and RER, and insulin resistance. Although adipose tissue inflammation is apparent by the 10th-12th week of HFD in this model ^{294, 295}, 6 weeks of HFD was insufficient to produce a robust inflammatory response in adipose tissue (e.g., see Fig. 5 and

^{155, 295}). In addition, no increase in plasma levels of sensitive markers of inflammation such as IL-6 were identified at 6 weeks of HFD (IL-6 (pg/ml): LFD, 23.6±7.5; HFD, 18.8±4.2). The absence of significant levels of inflammation therefore allowed us to examine how obesogenic changes due to HFD regulate adipose tissue metabolism without the confounding features of highly energetic infiltrating cells such as macrophages ²⁹⁶.

Metabolomic analyses showed several metabolic pathways affected in obesity. These include glycerolipid metabolism, amino acid metabolism, and energy and glucose metabolism. HFD decreased levels of long-chain fatty acids in adipose tissue, and, coupled with significant decreases in glycerol and 1-palmitoylglycerol, is consistent with an increase in lipogenesis. Glycerophosphoethanolamine (GPEA), one of the few metabolites that increased in adipose tissue from obese mice, could be elevated as a result of phosphatidylethanolamine (PE) breakdown. This is consistent with the decreased abundance of 1-palmitoleoylglycerophosphoethanolamine and lysoPE species in adipose tissue from HF-fed mice. Increased GPEA could also be due to limitations in the rate of its hydrolysis: GPEA can be hydrolyzed by enzymes such as glycerophosphodiester phosphodiesterase to form glycerol-3-phosphate (G3P) ²⁹⁷, which is required for the formation of triglycerides and thus would likely be in high demand in expanding adipocytes ²⁹⁸.

Demand for G3P may also be met by glycolysis and glyceroneogenesis, or, in some tissues, from the recycling of glycerol by glycerol kinase ²⁹⁸. In our

study, G3P was significantly decreased, suggesting that it might be used quickly to accommodate lipid storage. The glycolytic intermediate glucose-6-phosphate was decreased as well, which suggests perturbations in adipocyte glucose metabolism. Indeed, *pdk4* expression, which regulates pyruvate dehydrogenase activity, was decreased by HFD; it is then plausible that the decrease in *pdk4* may promote the glyceroneogenic formation of G3P²⁹⁹ via cataplerosis³⁰⁰. The possibility that systemic glucose metabolism was affected by HFD is supported by the lower abundance of 1,5-anhydroglucitol in samples from mice fed a HFD. Plasma 1,5-anhydroglucitol (1,5-AG), is distributed to all organs and tissues and is a validated marker of short-term glycemic control^{301, 302}. Hence, even though fasting glucose levels are not different after 6 weeks of HFD²⁸⁶, the decrease in this metabolite is in agreement with insulin resistance in skeletal muscle and liver occurring at 6 weeks of HFD¹⁵⁵.

The increase in stearoyl sphingomyelin in adipose tissue from mice fed a HFD may be particularly significant. Sphingomyelin (SM; d18:1/18:0)—which in humans is the only membrane phospholipid not derived from glycerol—is a type of sphingolipid found in cell membranes that consists of oleic acid attached to the C1 position and stearic acid attached to the C2 position. Deficiency of enzymes involved in sphingomyelin synthesis have been shown to protect against diet-induced obesity and insulin resistance^{303, 304}, and the breakdown of sphingomyelin could yield significant amounts of ceramide, which inhibits insulin signaling³⁰⁵. Hence, the elevated levels of sphingomyelin could poise adipocytes to release significant amounts of ceramide if acted upon by

sphingomyelinases. Although ceramides were not measured in these analyses, HFD has been shown to increase plasma and adipose ceramides in mice by more than 300% ³⁰⁶. Interestingly, depleting ceramides in mice fed a HFD increases oxygen consumption and citrate synthase activity as well as preserves PGC1 expression ^{307, 308}, all of which were decreased by HFD in the current study. Ceramide also alters membrane permeability, inhibits electron transport chain function and promotes oxidative stress ²⁰⁰, which is consistent with the evolving hypothesis that ceramide (and by proxy excess SM) induces mitochondrial stress ³⁰⁵.

In addition to changes in lipid and glucose metabolism, metabolites in the amino acid and energy metabolism pathways were also remarkably changed by HFD. Recent studies suggest that changes in amino acid metabolism may be critical to the development of obesity and insulin resistance. In particular, pathway impact analyses showed that BCAA and phenylalanine, tyrosine, and tryptophan metabolism were significantly impacted by diet. In obese and insulin-resistant humans, these amino acids are elevated systemically (reviewed in ³⁰⁹), and changes in several amino acid classes, including BCAAs and Phe, Tyr and Trp, are associated with metabolic risk factors in humans ³¹⁰. Although there is a clear relationship among amino acids, insulin resistance and obesity in animal models, the mechanistic interpretations are less clear. For example, increasing circulating BCAAs in mice by preventing BCAA catabolism prevents diet-induced obesity and insulin resistance in mice ³¹¹, whereas feeding BCAAs to high fat-fed rats increases insulin resistance ³¹². Levels of amino acids in adipose tissues

appear to be important because BCAA metabolism in adipose tissues modulates levels of circulating BCAAs³¹³. In our study, we found that several amino acids were decreased in abundance in adipose tissues from mice fed a HFD for 6 weeks. This could be due to changes in the catabolic flux of BCAAs, which occurs in the mitochondrial matrix.

While most studies show a decrease in BCAA catabolism in obesity³⁰⁹, our data are most consistent with an increase in BCAA catabolism. BCAA catabolism results in the formation of acetyl CoA and succinyl CoA, the latter of which can be converted to succinate by hydrolysis and release of CoA by succinate thiokinase. Interestingly, succinate was one of the few metabolites that were significantly increased in WAT from HF-fed mice. Other Krebs cycle intermediates, such as citrate and malate, were not changed in abundance. This would appear to suggest an influx of carbon from BCAA catabolism into the Krebs cycle, which might be sufficient to sustain concentrations of other citric acid cycle intermediates or impart energetic changes.

Interestingly, adipose explants derived from mice fed a HFD showed an apparent decrease in the rate of mitochondrial oxygen consumption; however, when the OCR rates were normalized to the wet weight of each explant the OCR was similar in adipose tissue from HF- and LF-fed mice. Given the fact that there was a 3-fold increase in adipocytes due to lipid accumulation, it is likely that the decreases in the apparent mitochondrial OCR are due simply to a decreased number of adipocytes in the explants due to an increased volume of triglycerides,

which comprises a large portion of the adipose tissue wet weight. Thus, despite extensive remodeling, mitochondrial function remains preserved. However, because the basal oxygen consumption in the explants was unaffected, it would suggest increased non-mitochondrial oxygen consumption potentially due to an increase in cytosolic oxidase activity^{314, 315} in WAT from high-fat fed mice. This possibility is consistent with previous work showing an increase in adipose tissue oxidative stress in obese mice, due to an increase in the expression of NADPH oxidase and downregulation of antioxidant enzymes³¹⁶⁻³²⁰.

Despite no changes in mitochondrial number or oxygen consumption, there was a remarkable decrease in citrate synthase activity by HFD. This was accompanied by an increase in the gene expression of some subunits (e.g., *cox7a1*) in the adipose tissue of obese mice. These observations suggest that HFD promotes an early remodeling of mitochondria to accommodate for shifting metabolic needs and substrate availability. Reasons for increased *cox7a1* gene expression and the augmented response of adipose explants from 6 week high fat-fed mice to FCCP are currently unclear. We speculate that the enhanced response to FCCP relative to the basal OCR could be due to increased substrate delivery to adipose tissue mitochondria in high fat-fed mice, which occurs only when the proton motive force is diminished with the uncoupler. *Cox7a1*, is a heart and muscle-specific subunit, which is also present in brown adipocytes. This subunit has been shown to be increased in the WAT of fattening cattle³²¹. While reasons for the increase in this subunit are not clear, it is possible that its increase may be an adaptive response to dissipate excess energy in the

adipocyte. Further studies are required to assess fully the role of this subunit in mediating energetic changes in WAT during obesity.

With prolonged high fat feeding (i.e., 12 weeks), decreases in mitochondrial mass do appear to occur, which is supported both by our results showing decreases in mitochondrial matrix and inner membrane proteins as well as by published studies showing decreased mitochondrial mass in WAT of severely obese mice^{161, 283} and humans³²². These data are consistent also with published data showing a decrease in adipocyte mitochondrial function in obese humans, independent of adipocyte size³²².

Electron micrographs showed mitochondria appearing to undergo fission in adipose tissue from HF-fed mice, and autophagosomes were found adjacent to vacuolated structures containing electron-dense material and to mitochondria. This suggested that both mitochondrial remodeling and autophagy may be induced by HFD. That Parkin and Pink1 were also increased in adipose tissues from obese mice would support the notion that mitophagy is induced by HFD. Previous studies show that Pink1 accumulating within mitochondria recruits Parkin, which ubiquitinates mitochondrial proteins that are then recognized by autophagy adaptor proteins such as p62. The p62 then binds to LC3 which sequesters mitochondria into autophagosomes for degradation²⁹³. Although LC3-II and ubiquitinated proteins were not significantly changed with HFD, the abundance of p62 was decreased, which is consistent with an increase in autophagic flux³²³. Moreover, when autophagy is inhibited, the abundance of

both LC3-I and p62 have been shown to increase^{324, 325}, and, in our study, both p62 and LC3-I were decreased and the LC3-II/LC3-I ratio was increased. These data would then be consistent with the notion that autophagy is increased in WAT of high fat-fed mice. However, a limitation of this study is that autophagic flux was not measured. Nevertheless, the aggregate of ultrastructural and immunological data, combined with published data showing that autophagy is increased in adipocytes from obese humans and mice³²⁶⁻³²⁸, suggest that HFD apparently increases autophagy and perhaps mitophagy in WAT.

The loss of mitochondria shown to occur by the 12th week of HFD would then appear to suggest a role for autophagic degradation of mitochondria in the “whitening” of adipose tissue. Deletion of essential autophagy genes such as *atg7* in mice results in resistance to obesity and promotion of a brown-like adipose tissue phenotype having more mitochondria and higher rates of substrate oxidation³²⁵. Furthermore, mouse embryonic fibroblasts (MEFs) isolated from *atg5*^{-/-} mice accumulate less lipid when stimulated to develop into adipocytes³²⁵, suggesting that autophagy is essential for lipogenesis and WAT expansion. Interestingly, systemic knock-out of Parkin prevents diet-induced obesity and insulin resistance; however, this was shown to be due to decreased uptake of fat from the diet³²⁹, indicating that functions of Parkin are not exclusive to mitophagy. Nevertheless, the Pink1-Parkin pathway has been shown to promote both mitophagy and selective respiratory chain turnover *in vivo*³³⁰, which is consistent with our findings in adipose tissues of obese mice. The use of genetic models with adipose tissue-selective overexpression or deletion of Parkin

would further help to understand how mitophagy regulates adipose tissue phenotype.

In summary, in this study we identified key metabolic changes that occur during WAT expansion. These coordinated changes occur before the infiltration of inflammatory cells and include: loss of mitochondrial biogenetic capacity; dysregulation of glycerolipid, sphingolipid and amino acid metabolism; mitochondrial remodeling; and changes suggestive of activation of mitophagy. Based on these observations, we posit that such metabolic remodeling contributes to the whitening of adipose tissue during obesity.

CHAPTER III

OVEREXPRESSION OF ENDOTHELIAL NITRIC OXIDE SYNTHASE
PREVENTS DIET-INDUCED OBESITY AND REGULATES
ADIPOGENIC PHENOTYPE

Introduction

Obesity and type 2 diabetes (T2D) have become major health challenges worldwide. Current data show that approximately 1.5 billion adults aged 20 years or older are overweight, and 10% are obese¹. In the US, one-third of the population meets the criteria for metabolic syndrome^{3, 4}. While lifestyle changes and lack of exercise are important risk factors for weight gain^{279, 331}, excessive caloric intake appears to be one key factor fueling the epidemic of obesity. Poor dietary habits negatively affect a broad range of cardiovascular functions and promote the onset of T2D⁴.

Although it is currently believed that obesity results from excessive nutrient consumption^{11, 332}, i.e., more calories are ingested than are utilized, recent evidence suggests that the balance between nutrient intake and energy expenditure is complex and is regulated by many inter-dependent mechanisms³³². Several studies indicate that obesity and insulin resistance may be distinct sequelae of nutrient excess³³³. Hence, to stem the tide of the epidemics of

T2D and obesity, it is important to understand the relationship between obesity and insulin resistance as well as the physiological processes that regulate their development.

Accumulating evidence suggests that the vascular endothelium regulates insulin action. In humans, states of obesity and insulin resistance are characterized by endothelial dysfunction, impaired vasodilation and insulin resistance³³⁴; and in rats, inhibition of endothelial nitric oxide synthase (eNOS) decreases insulin-stimulated uptake of glucose by skeletal muscle, suggesting that eNOS may be a key regulator of metabolic homeostasis. This role of eNOS is further corroborated by observations that deletion of the eNOS gene in mice induces insulin resistance^{335, 336} and impairs fatty acid oxidation³³⁷. Nevertheless, the role of eNOS in regulating metabolic changes that contribute to obesity under conditions of nutrient excess is not well understood. In particular, it is unclear whether eNOS could prevent or attenuate diet-induced adiposity and insulin resistance.

To understand the metabolic role of eNOS, we studied effects of high fat diet in mice overexpressing eNOS. Our hypothesis was that increasing eNOS levels mitigates effects of high fat feeding by regulating adipose tissue metabolism. We found that eNOS-transgenic (eNOS-TG) mice were resistant to diet-induced weight gain, but not glucose intolerance. These findings reveal a new anti-obesogenic role of eNOS and its favorable influence on adipose tissue metabolism.

Experimental Procedures

Animal studies: The B6.BKS(D)-*Lep^{db}/J* (*db/db*) mice and C57BL/6J (wild-type; WT) mice were purchased from The Jackson Laboratory (Bar Harbor, ME). The eNOS-TG mice, which express bovine eNOS under the control of the preproendothelin-1 promoter³³⁸, were maintained on the C57BL/6J background. At 8 weeks of age, male mice were placed on either a 10% low fat diet (LFD; Research Diets, Inc., #D12450B) or a 60% high fat diet (HFD; Research Diets Inc., #D12492) and maintained for 6–15 additional weeks. Water and diet were provided *ad libitum*. Body weights were recorded weekly. During the 7th and 13th weeks of feeding, glucose and insulin tolerance tests were performed. Pyruvate tolerance tests were performed only after the 13th week of feeding; all other variables were evaluated after euthanasia. All procedures were approved by the University of Louisville Institutional Animal Care and Use Committee.

Expression analyses: Tissue homogenates were prepared and used for Western blot protein expression analysis. For quantitative RT-PCR, RNA extracted from tissues was used to assess *pgc1a*, *cytb6*, *gapdh*, *ppara*, and *pparg* expression using commercially available primers (SABiosciences, Valencia, CA).

Glucose, insulin, and pyruvate tolerance tests: As described before³³⁹, glucose tolerance tests were performed following a 6 h fast by injection (i.p.) of

D-glucose (1 mg/g) in sterile saline. Insulin tolerance tests were performed on nonfasted animals by i.p. injection of 1.5 U/kg Humulin R (Eli Lilly, Indianapolis, IN). After a 6 h fast, pyruvate tolerance tests were performed as described ³⁴⁰.

Biochemical analyses: Plasma lipids, proteins, and metabolites were measured using a Cobas Mira Plus 5600 Autoanalyzer (Roche, Indianapolis, IN) or Luminex kits (Millipore, Billerica, MA, USA). Plasma levels of non-esterified free fatty acids and glycerol were measured by ELISA (Wako Chemicals, Richmond, VA and Cayman Chemical, Ann Arbor, MI, respectively). Nitrite and nitrate levels were measured as described ³⁴¹.

Adipocyte size measurements: Adipose tissue excised at the time of euthanasia was either snap-frozen at -80°C or fixed in 10% formalin (Leica), paraffin-embedded, and sectioned. Sections were stained in hematoxylin and eosin. Adipocyte cross-sectional area was measured using Nikon Elements software. To assess relative mitochondrial abundance, sections were stained with MitolD Red (Enzo Life Sciences, Farmingdale, NY). Crown-like structures and inflammatory cells indicative of adipose tissue inflammation were measured as described before ^{287, 294}.

Body composition and calorimetry: Body composition was measured by dual-energy X-ray absorptiometry using a mouse densitometer (PIXImus2; Lunar, Madison, WI). Whole body energy expenditure, respiratory exchange ratio, food consumption, and locomotion, ambulatory and fine movements were measured using a physiological/metabolic cage system (TSE PhenoMaster System, Bad Homburg, Germany).

Immunostaining of adipose tissue: Capillary density was quantified in paraffin-embedded sections using fluorescently labeled isolectin B4 as described ³⁴². Nitrotyrosine adducts were measured in paraffin-embedded tissues using anti-nitrotyrosine and goat-anti-rabbit IgG-Cy3 antibodies.

Adipose tissue bioenergetic measurements: The oxygen consumption rate (OCR) and extracellular acidification rate (ECAR) of intact adipose tissue explants were measured using a Seahorse XF24 analyzer (Seahorse Bioscience, Billerica, MA). Briefly, freshly isolated epididymal adipose tissue was rinsed with unbuffered DMEM (Dulbecco's modified Eagle's medium, pH 7.4). The adipose tissue was cut into sections, and 10 mg were placed in each well of an XF 24 Islet Capture Microplate (Seahorse Bioscience, Billerica, MA). The tissue was then covered with a screen, which allows free perfusion while minimizing tissue movement. Unbuffered DMEM (500 μ l) supplemented with 50 μ M BSA-conjugated palmitic acid, 200 μ M L-carnitine, and 2.5 mM D-glucose was then

added to each well. At least two replicates from each animal were used for the assay, and each tissue section was examined to ensure absence of large vessels (which can skew oxygen consumption measurements). The plate was incubated at 37°C in a non-CO₂ incubator for 1 h prior to extracellular flux analysis. After three baseline measurements, a mixture of antimycin A (10 µM) and rotenone (1 µM) was injected. Following injection, the OCR was closely monitored until the rates stabilized, and then the experiment was terminated.

Metabolomic analysis of adipose tissue: White adipose tissue from the epididymal fat pad of fasted mice (16 h fast) was collected and snap-frozen in liquid nitrogen. At the time of analysis, sample metabolites were extracted with methanol. A recovery standard was introduced at the beginning of the extraction process. The extracted samples were split into equal parts for analysis on the GC/MS and LC/MS/MS platforms. Also included were several technical replicate samples created from a homogeneous pool containing a small amount of all study samples. Samples were placed briefly on a TurboVap[®] (Zymark) to remove the organic solvent. Each sample was then frozen and dried under vacuum. Samples were then prepared for the appropriate instrument, either LC/MS or GC/MS

LC/MS, LC/MS²: The LC/MS portion of the platform was based on a Waters ACQUITY UPLC and a Thermo-Finnigan LTQ mass spectrometer, which

consisted of an electrospray ionization (ESI) source and linear ion-trap (LIT) mass analyzer. The sample extract was split into two aliquots, dried, then reconstituted in acidic or basic LC-compatible solvents, each of which contained 11 or more injection standards at fixed concentrations. One aliquot was analyzed using acidic positive ion optimized conditions and the other using basic negative ion optimized conditions in two independent injections using separate dedicated columns. Extracts reconstituted in acidic conditions were gradient eluted using water and methanol both containing 0.1% formic acid, while the basic extracts, which also used water/methanol, contained 6.5 mM ammonium bicarbonate. The MS analysis alternated between MS and data-dependent MS² scans using dynamic exclusion.

GC/MS: Samples destined for GC/MS analysis were re-dried under vacuum desiccation for a minimum of 24 hours prior to being derivatized under dried nitrogen using bistrimethyl-silyl-trifluoroacetamide. The GC column was 5% phenyl and the temperature ramp was from 40° to 300° C in a 16 minute period. Samples were analyzed on a Thermo-Finnigan Trace DSQ fast-scanning single-quadrupole mass spectrometer using electron impact ionization. The instrument was tuned and calibrated for mass resolution and mass accuracy on a daily basis. The information output from the raw data files was automatically extracted as discussed below.

Accurate mass determination and MS/MS fragmentation: In addition to the LIT front end, the LC/MS portion of the platform had a Fourier transform ion cyclotron resonance (FT-ICR) mass spectrometer backend. For ions with counts greater than 2 million, an accurate mass measurement could be performed. Accurate mass measurements could be made on the parent ion as well as fragments. The typical mass error was less than 5 ppm. Fragmentation spectra (MS/MS) were typically generated in data-dependent manner, but if necessary, targeted MS/MS could be employed, such as in the case of lower level signals.

QA/QC: Instrument variability was determined by calculating the median relative standard deviation (RSD) for the internal standards that were added to each sample prior to injection into the mass spectrometers. Overall process variability was determined by calculating the median RSD for all endogenous metabolites (i.e., non-instrument standards) present in 100% of the samples, which are technical replicates of pooled samples. Values for instrument and total process variability were 5% for internal standards and 15% for endogenous biochemicals, respectively. For QA/QC purposes, a number of additional samples are included with each day's analysis. Furthermore, a selection of QC compounds was added to every sample, including those under test. These compounds were carefully chosen to avoid interference with the measurement of the endogenous compounds.

Metabolite identification: Compounds were identified by comparison to library entries of purified standards or recurrent unknown entities. Identification of known chemical entities was based on comparison to metabolomic library entries of purified standards. More than 1000 commercially available purified standard compounds had been acquired registered into the Metabolon Laboratory Information Management System (LIMS) for distribution to both the LC and GC platforms for determination of their analytical characteristics. The combination of chromatographic properties and mass spectra gave an indication of a match to the specific compound or an isobaric entity.

Curation: A variety of curation procedures were carried out to ensure that a high quality data set was made available for statistical analysis and data interpretation. The QC and curation processes were designed to ensure accurate and consistent identification of true chemical entities, and to remove those representing system artifacts, mis-assignments, and background noise. Visualization and interpretation software were used to confirm the consistency of peak identification among the various samples. Library matches for each compound were checked for each sample and corrected if necessary.

Bioinformatics: The bioinformatics system consisted of four major components, the LIMS system, data extraction and peak-identification software, data processing tools for QC and compound identification, and a collection of

information interpretation and visualization tools. The purpose of the LIMS system was to enable fully auditable laboratory automation through a secure, easy to use, and highly specialized system. The scope of the LIMS system encompasses sample accessioning, sample preparation and instrumental analysis and reporting and advanced data analysis. Some of the subsequent software systems were grounded in the LIMS data structures, which have been modified to leverage and interface with the Metabolon information extraction and data visualization systems, as well as other data analysis software such as Metaboanalyst (<http://www.metaboanalyst.ca/>).

Metabolomic analysis: The general outline for how metabolomic data were analyzed is shown in Fig. 22. Metabolites with missing values were imputed by replacing missing values with half of the minimum positive value in the original data. Metabolites with greater than 57% of values missing were omitted from the analysis. Data were then quantile normalized within replicates after log transformation. This step was performed to transform the intensity values so that the distribution was more Gaussian. T-test statistical comparisons were then performed. Further univariate and multivariate analysis, such as correlation analysis, principal component analysis and partial least squares discriminant analysis was then performed using the Metaboanalyst 2.0 software (<http://www.metaboanalyst.ca/>)^{288, 343}.

Statistical analyses: Data are expressed as mean \pm SEM. Multiple groups were compared using one-way or two-way ANOVA, followed by Bonferroni post-tests. Unpaired Student's *t* test was used for direct comparisons. Statistical analyses were performed with the program "R" <http://cran.r-project.org/>, Metaboanalyst (<http://www.metaboanalyst.ca/>), and/or GraphPad 5.0. A *P* value less than 0.05 was considered significant.

Results

Nutrient excess alters eNOS abundance. To study effects of obesity and diabetes on eNOS protein levels, C57BL/6J mice were placed on a high fat diet¹⁵⁵, and *db/db* mice were used as a model of T2D³⁴⁴. High fat feeding for 6 and 12 weeks resulted in a profound decrease in eNOS levels in adipose tissue (Fig. 12A,B), with no statistically significant changes in the aorta (Fig. 12A,C) or skeletal muscle (Fig. 13A,B). Similar changes were observed in 20 week old *db/db* mice, in which eNOS in the adipose tissue was undetectable despite a lack of change in eNOS levels in most other tissues. Interestingly, eNOS expression was increased in hearts of *db/db* mice (Fig. 13A,C), which might be a compensatory change in response to an increase in NO demand. These data show that both obesity and diabetes result in tissue-specific changes in eNOS expression with a profound and selective decrease in eNOS levels in the adipose tissue. This decrease in eNOS in adipose tissue is consistent with previous reports in obese humans^{158, 159} and in mouse models of obesity¹⁶¹, indicating

that the expansion of adipose tissue establishes a state of chronic eNOS deficiency.

Overexpression of eNOS prevents diet-induced obesity. To examine the role of eNOS, we used eNOS-TG mice³³⁸. Previous studies have shown that these mice reproduce in a Mendelian fashion, maintain normal growth characteristics, and are protected from numerous pathologies including myocardial³⁴⁵, hepatic³⁴⁶, lung³⁴⁷, and vascular injury³⁴⁸ as well as sepsis³⁴⁹. In comparison with WT mice, hemizygous mice showed a 4-fold increase in eNOS levels in the aorta, with no significant change in eNOS levels in the adipose tissue (Fig. 12D,E). In contrast, in homozygous mice there was a 2-fold increase in eNOS in the adipose tissue and a 6-fold increase in the aorta. The eNOS in TG animals localized exclusively with isolectin staining (Fig. 14), indicating that the transgene was expressed only in the vasculature^{338, 350}. Plasma from eNOS-TG mice showed increased L-citrulline and nitrite levels when compared with WT mice (Fig. 15A,C), and adipose tissue from eNOS-TG mice demonstrated an increase in L-citrulline (Fig. 15B). Due to high variability, there were no significant differences in nitrate or nitrite in adipose tissue (Fig. 15D) perhaps due to other confounding factors, such as nitrite/nitrate found in the diet or reduction of nitrite to NO.

When placed on a high fat diet for 6 weeks, the homozygous eNOS-TG mice gained 50% less weight than WT mice, and this effect persisted for 12

weeks (Fig. 16B,C). Food intake was not different between WT and eNOS-TG mice (Fig. 16D). A more modest resistance to weight gain was also observed in hemizygous eNOS-TG mice (Fig. 13-D), perhaps due to lower adipose tissue eNOS levels in these mice compared with homozygous eNOS-TG mice. Hence, for all subsequent studies, only eNOS homozygous mice were used.

The transgenic mice maintained a higher percent of lean mass (Fig. 16G), although the tibia length in transgenic mice was only slightly smaller than in WT mice (Fig. 16H). These observations indicate that overexpression of eNOS decreases adiposity and prevents weight gain induced by high fat diet.

eNOS overexpression increases whole body metabolism. To determine how eNOS overexpression affected whole-body metabolism, we measured oxygen consumption (VO_2), carbon dioxide production (VCO_2), and activity in high fat-fed WT and eNOS-TG mice over the course of a 12 h dark period and a 4.5 h light period. The fact that food intake was not different between WT and TG mice (Fig. 16D), indicates that the lean phenotype of eNOS-TG mice is not due to a decrease in food consumption. This view is reinforced by the observation that high fat feeding increased plasma cholesterol and leptin to similar levels in WT and eNOS-TG mice (Table 2). In comparison with WT mice, eNOS-TG mice showed higher mean VO_2 and VCO_2 rates throughout the dark and light periods (Fig. 16I,J), with no change in the respiratory exchange ratio (RER; Fig. 16K).

Figure 12. Nutrient excess alters tissue eNOS levels. Tissue levels of eNOS from mice fed a low fat (LFD) or high fat diet (HFD) for 6 or 12 weeks; age-matched *db/db* mice were included as an additional model of T2D: (A) Representative Western blots of eNOS from epididymal adipose tissue and aorta. (B,C) Quantification of eNOS expression from panel A. n = 3–4 per group; ** $p < 0.01$ vs. 6 week LFD. (D,E) Levels of eNOS in adipose tissue and aorta from wild-type (WT), littermate eNOS-TG hemizygous, and eNOS-TG homozygous mice. n = 3 per group; ** $p < 0.01$ vs. indicated groups

Figure 12

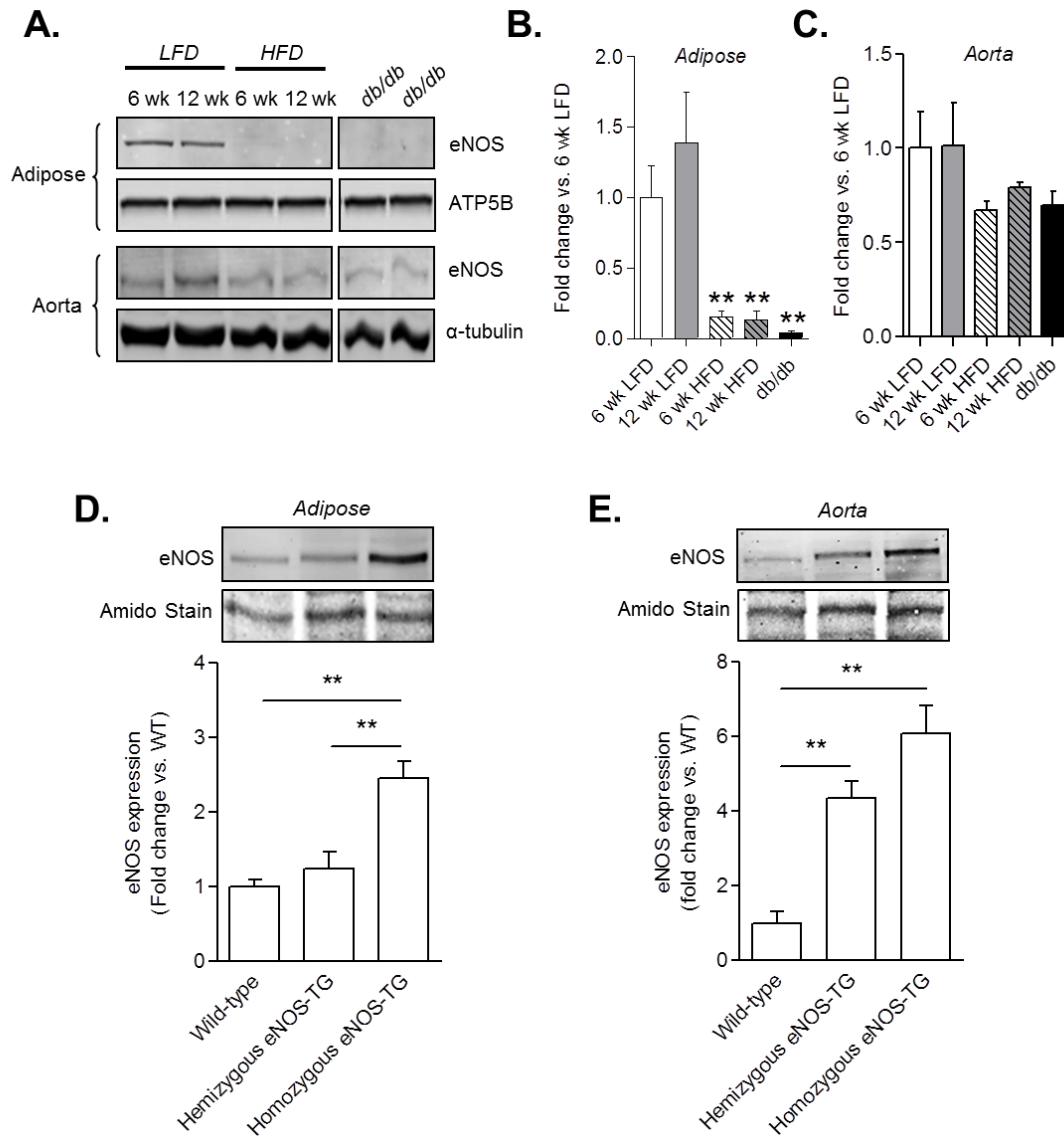


Figure 13. Effects of nutrient excess on eNOS levels, and body weight gain of mice expressing different levels of eNOS. Panels **A–C**: Immunoblot analysis of eNOS expression in skeletal muscle and heart in C57BL/6J mice fed a low fat diet (LFD) or high fat diet (HFD) for 6 or 12 weeks; *db/db* mice age-matched to the 12 week feeding group were included as an additional model of metabolic syndrome. **(A)** Representative Western blots of eNOS expression in skeletal muscle and heart; **(B)** Quantification of skeletal muscle eNOS expression; and **(C)** Quantification of heart eNOS expression. $n = 3–4$ per group;*** $p < 0.001$ vs. WT LFD. Panel **D**: Weight gain of wild-type, littermate eNOS hemizygous, and eNOS homozygous mice fed HFD over the course of 12 weeks. $n = 4–8$ per group.

Figure 13

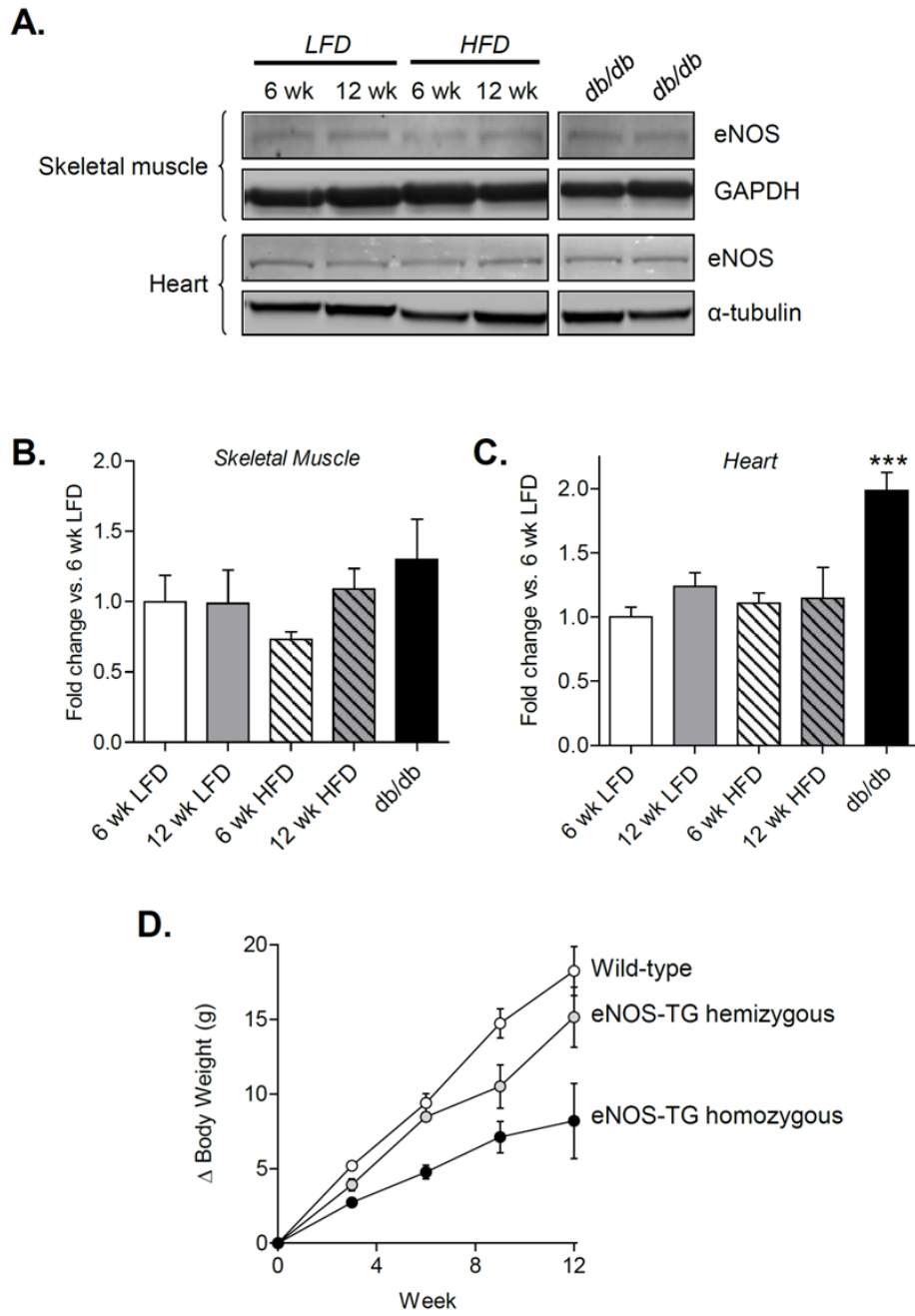


Figure 14. The eNOS transgene localizes to the vasculature in adipose tissue. Immunofluorescence images of epididymal adipose tissue from eNOS-TG mice: Adipose tissues were fixed, sectioned, and stained with DAPI (blue), isolectin (green), and eNOS antibody (red). The overlay shows the co-localization of the eNOS and isolectin signals.

Figure 14

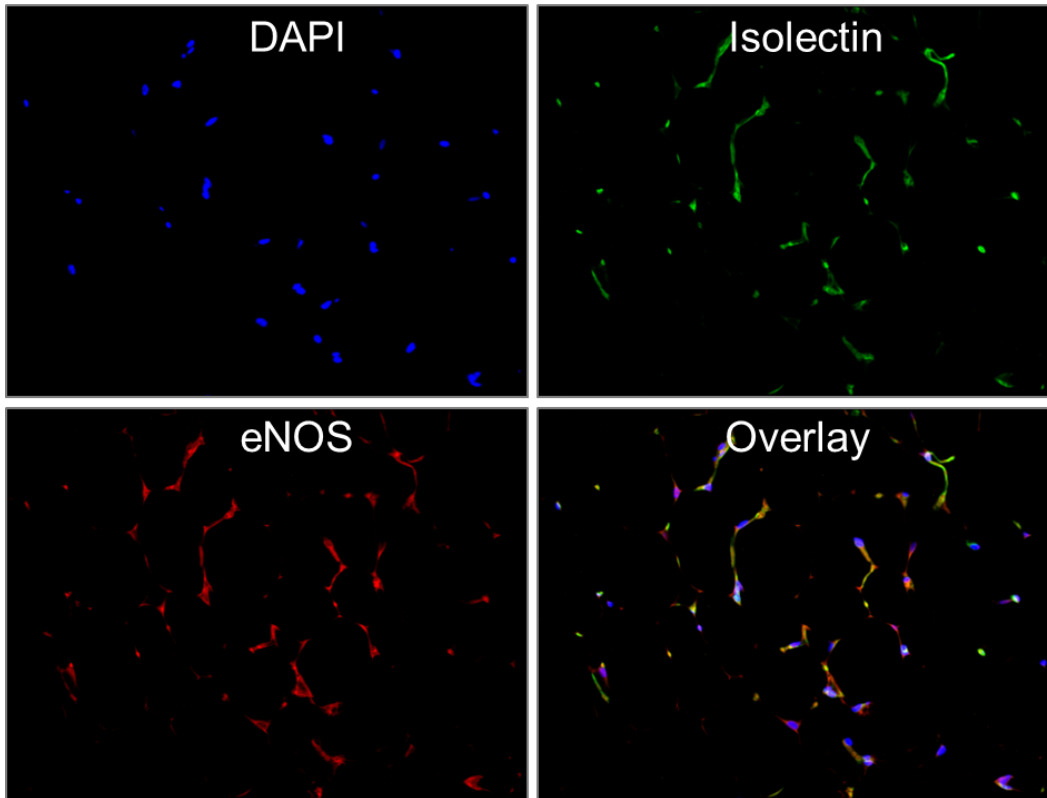
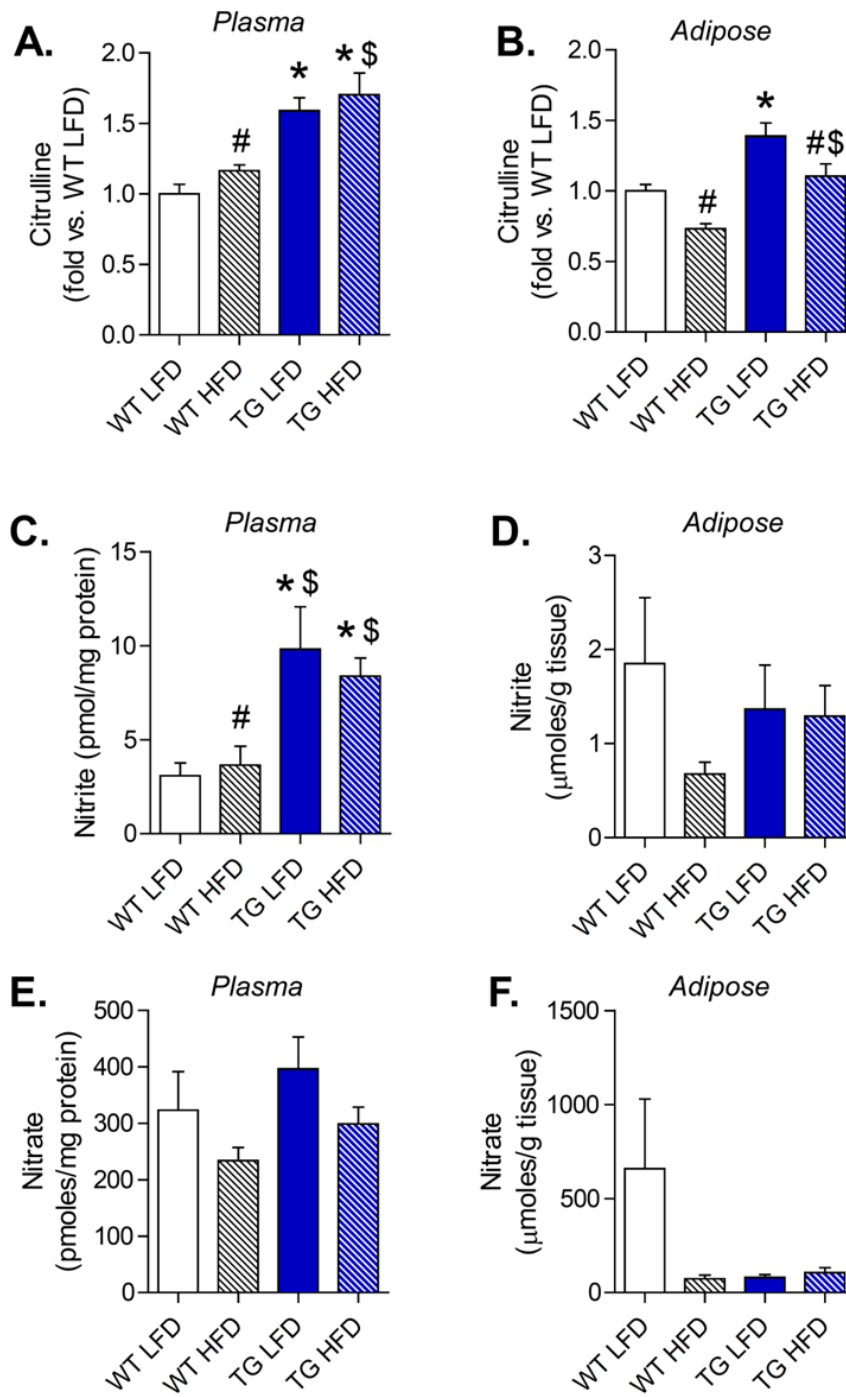


Figure 15. Measurements of eNOS and NO metabolites in plasma and adipose tissue. Mice were fed a LFD or HFD for 6 weeks and citrulline, nitrite, and nitrate levels in the plasma and adipose tissue were analyzed by LC/MS or HPLC. Panels A and B: Relative levels of L-citrulline from (A) plasma and (B) adipose tissue; Panels C and D: Measurements of nitrite from (C) plasma and (D) adipose tissue; Panels E and F: Measurements of nitrate from (E) plasma and (F) adipose tissue. n = 6–7 per group; *p<0.05 vs. WT LFD; #p<0.05 vs. TG LFD; \$p<0.05 vs. WT HFD.

Figure 15



Activity levels, assessed by horizontal activity count (beam breaks) showed similar patterns and levels of activity, and total ambulatory activity was not significantly different (Fig. 16L). Taken together, these observations suggest that on a high fat diet, eNOS-TG mice maintain a higher metabolic rate than WT mice. This increase in systemic metabolism, however, cannot be attributed to thyroid hormones, because plasma levels of triiodothyronine (T3) and thyroxine (T4) in WT and eNOS-TG mice were not significantly different (Fig. 17).

Measurements of body composition by dual-energy X-ray absorptiometry (Dexascan) showed that after 6 weeks of high fat feeding, the body fat content was much lower in eNOS-TG mice than in non-transgenic mice (Fig. 16E,F).

Effect of eNOS on diet-induced insulin resistance. Because we found that eNOS overexpression prevented diet-induced weight gain, we expected concurrent changes in insulin resistance. Indeed, we found that overexpression of eNOS completely prevented diet-induced hyperinsulinemia (Table 2), although plasma levels of adiponectin and resistin were not affected. This was associated with a remarkably lower HOMA-IR score (WT low fat, 1.45 ± 0.65 ; WT high fat, 34.4 ± 5.3 , $p < 0.05$ vs. WT low fat; TG low fat, 6.9 ± 3.1 ; TG high fat, 8.2 ± 2.9 , $p < 0.05$ vs. WT high fat). Moreover, even though 6 weeks of high fat feeding did not significantly increase triglycerides or plasma non-esterified free fatty acids (NEFA), both of these were decreased by 50% in the TG mice compared with WT mice (Table 2). We found no significant differences in plasma glycerol

between groups (Table 2), suggesting that adipose tissue lipolysis was not affected. Collectively, these data indicate that overexpression of eNOS prevents high fat diet-induced hyperinsulinemia and decreases plasma triglycerides and fatty acids.

To examine how eNOS overexpression affects systemic glucose disposal, WT and eNOS-TG mice were placed on a high fat diet for 6 weeks, and GTT and ITT were performed. There was no significant difference in the basal blood glucose levels in non-fasted WT and eNOS-TG mice (Fig. 18A). After a fast of 6 h, the plasma glucose levels of both high fat-fed groups were significantly increased compared with the WT low fat-fed group. Fasting for 16 h resulted in near normalization of blood glucose in WT mice; however, glucose levels in the eNOS-TG mice remained slightly, but significantly, elevated (Fig. 18A). There were no significant differences in plasma HbA1c in any group (Fig. 18B).

To test whether effects of the transgene would manifest after prolonged feeding, we placed WT and eNOS-TG mice on high fat diet for 12 weeks and assessed insulin resistance. At completion of the feeding protocol, the GTT and ITT curves were superimposable suggesting that eNOS overexpression does not affect diet-induced insulin resistance even after prolonged nutrient excess (Fig. 19A-D). Although, plasma glucose levels in non-fasted and 6 h-fasted mice were not statistically different, a 16 h fast led to a greater decrease in blood glucose in WT compared with TG mice (Fig. 19E), indicating that the TG mice were more resistant to fasting-induced hypoglycemia, which could be due to increased gluconeogenesis in the liver.

Figure 16. eNOS prevents diet-induced obesity. Weight gain, adiposity, and indirect calorimetry measurements from WT and eNOS-TG mice fed a low fat (LFD) or high fat diet (HFD): **(A)** Body weights during 6 weeks of LF feeding, n = 22–26 per group; **(B)** body weights during 6 weeks of HF feeding, n = 26 per group; **(C)** summarized weight gain over the course of 6 weeks and 12 weeks of HF feeding, n = 28–29 per group for 6 week group, n = 4–7 per group for 12 week group; **(D)** food intake, n = 4 per group; **(E)** representative DEXA images of mice fed a LFD or HFD for 6 weeks; **(F)** body fat percentage, n = 8–12 per group; **(G)** lean mass percentage, n = 8–12 per group; and **(H)** tibia length for mice fed a LFD or HFD for 6 weeks, n = 8–12 per group; **(I)** average oxygen consumption (VO_2); **(J)** average carbon dioxide production (VCO_2); **(K)** respiratory exchange ratio (RER); and **(L)** ambulatory counts. n = 4 per group; * $p < 0.05$, ** $p < 0.01$, and *** $p < 0.001$ vs. indicated groups; # $p < 0.05$ vs. WT HFD.

Figure 16

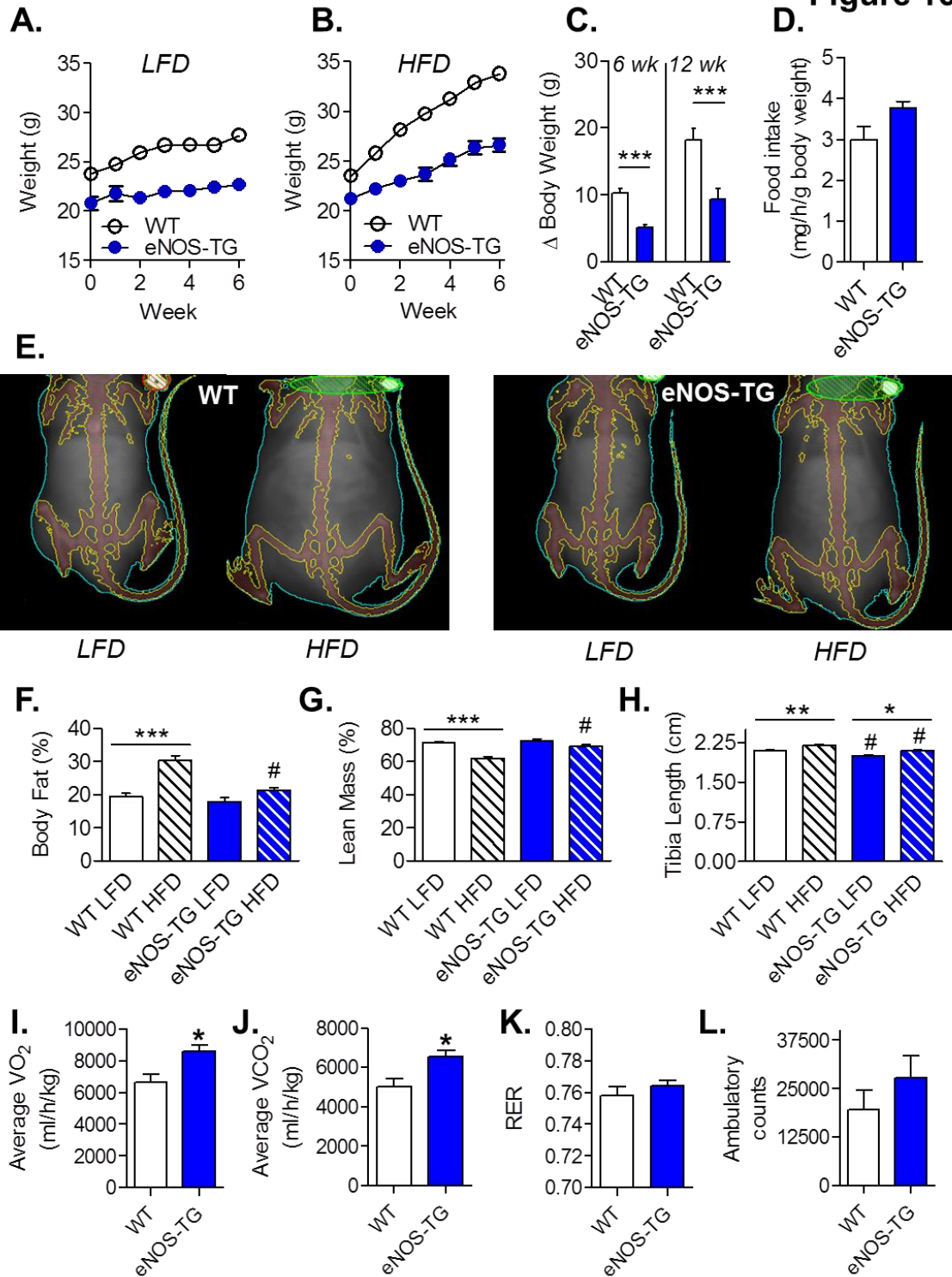


Figure 17. Diet and genotype do not affect circulating free T3 or T4 levels.

Free triiodothyronine (T3) and thyroxine (T4) were measured in plasma from WT and eNOS-TG mice that were fed LF or HF diets for 6 weeks. n = 4–6 per group.

Figure 17

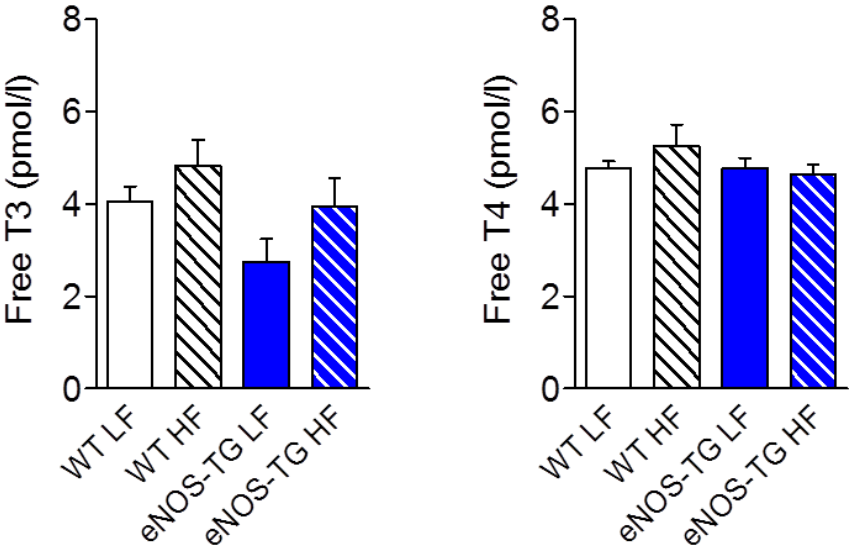


Table 2. Parameters measured from plasma of low fat-fed and high fat-fed WT and eNOS-TG mice.

<i>Parameter</i>	<i>WT LFD</i>	<i>WT HFD</i>	<i>eNOS-TG LFD</i>	<i>eNOS-TG HFD</i>
*Insulin (pg/ml)	116.2±40.7	3010.6±537.3 [†]	480.8±95.4 [‡]	568.1±175.6 [#]
Adiponectin (µg/ml)	22.0±3.8	25.7±4.0	27.8±3.0	30.1±3.8
Resistin (pg/ml)	2449.8±156.1	7894.0±1155.0 [†]	3547.3±387.2 [‡]	6251.3±497.9 ^{§,@}
Leptin (pg/ml)	209.0±38.3	5099.0±1265.0 [†]	997.4±203.4 [‡]	4874.4±783.1 ^{§,@}
Cholesterol (mg/dl)	96.4±2.7	117.8±5.9 [†]	92.1±4.4 [‡]	124.0±6.8 ^{§,@}
Triglycerides (mg/dl)	37.8±2.5	46.2±4.8	26.2±3.0 [‡]	23.8±2.8 ^{§,#}
NEFA (mEq/L)	0.39±0.05	0.38±0.06	0.19±0.04 ^{‡,‡}	0.16±0.02 ^{§,#}
HDL (mg/dl)	74.1±1.6	92.1±4.1 [†]	71.5±3.6 [‡]	99.6±4.9 ^{§,@}
LDL (mg/dl)	14.4±1.1	14.9±0.8	14.9±0.9	17.3±1.3
*Total protein (g/dl)	4.7±0.05	4.9±0.04	4.1±0.06 ^{‡,‡}	4.5±0.13 ^{#,@}
*Albumin (g/dl)	3.2±0.06	3.2±0.05	2.9±0.06 ^{‡,‡}	3.1±0.07
ALT (U/l)	34.1±3.5	38.7±1.2	31.5±1.1	30.7±0.8 [#]
AST (U/l)	66.0±6.1	71.8±4.7	73.1±2.9	66.4±3.4
CK (U/l)	124.9±19.0	100.0±28.8	236.5±25.9 ^{‡,‡}	176.1±12.9
*LDH (U/l)	225.9±20.3	190.6±6.3	191.1±49.2	166.4±11.5
Creatinine (mg/dl)	0.18±0.02	0.19±0.02	0.23±0.02	0.21±0.02

Wild-type (WT) and eNOS-TG mice were fed a low fat diet (LFD) or high fat diet (HFD) for 6 weeks. Plasma from the mice was used to measure the indicated parameters. *n = 6–7 mice per group; for all other parameters, the groups contained 13–14 mice per group.

[†]WT LFD vs. WT HFD

[‡]WT LFD vs. eNOS-TG LFD

[§]WT LFD vs. eNOS-TG HFD

[‡]WT HFD vs. eNOS-TG LFD

[#]WT HFD vs. eNOS-TG HFD

[@]eNOS-TG LFD vs. eNOS-TG HFD

To test this, we performed pyruvate tolerance tests, which did not show remarkable differences between WT and TG mice (Fig. 19F,G), indicating that resistance to hypoglycemia in TG mice may not be due to increased hepatic production of glucose. Collectively, these data suggest that eNOS overexpression does not significantly affect diet-induced insulin resistance or glucose intolerance, but maintains glucose homeostasis during starvation.

Effect of eNOS on adipose tissue. Given our observations that obesity and diabetes were associated with a selective decrease of eNOS levels in adipose tissue and that eNOS-TG mice were resistant to diet-induced weight gain, we measured changes in adipocyte area and size in epididymal fat pads. These measurements revealed that high fat diet induced adipocyte hypertrophy leading to a 3–4-fold increase in mean adipocyte area (Fig. 20A,B). Moreover, the high fat diet promoted size heterogeneity in WT, but not eNOS-TG mice (Fig. 20C), indicating that eNOS overexpression prevents diet-induced adipocyte hypertrophy and size dispersion.

In murine models of diet-induced obesity, adipocyte hypertrophy is associated with inflammation and accumulation of macrophages in adipose tissue³⁵¹. This is commonly recognized by the presence of crown-like structures that appear between adipocytes^{190, 287, 351}. In humans, obesity is similarly associated with adipose tissue inflammation, and weight loss interventions such as bariatric surgery improve endothelial function^{352, 353}.

Figure 18. Effect of eNOS overexpression on indices of insulin resistance.

After 6 weeks of a low fat (LFD) or high fat diet (HFD), glucose tolerance and insulin sensitivity were examined in WT and eNOS-TG mice: **(A)** Non-fasting and fasting glucose levels; white bars, WT LFD; blue bars, eNOS-TG LFD; white hatched bars, WT HFD; blue hatched bars, eNOS-TG HFD; **(B)** HbA1c; **(C–E)** glucose tolerance tests; and **(F–H)** insulin tolerance tests. n = 14 per group; * $p < 0.05$ vs WT LFD or otherwise indicated groups.

Figure 18

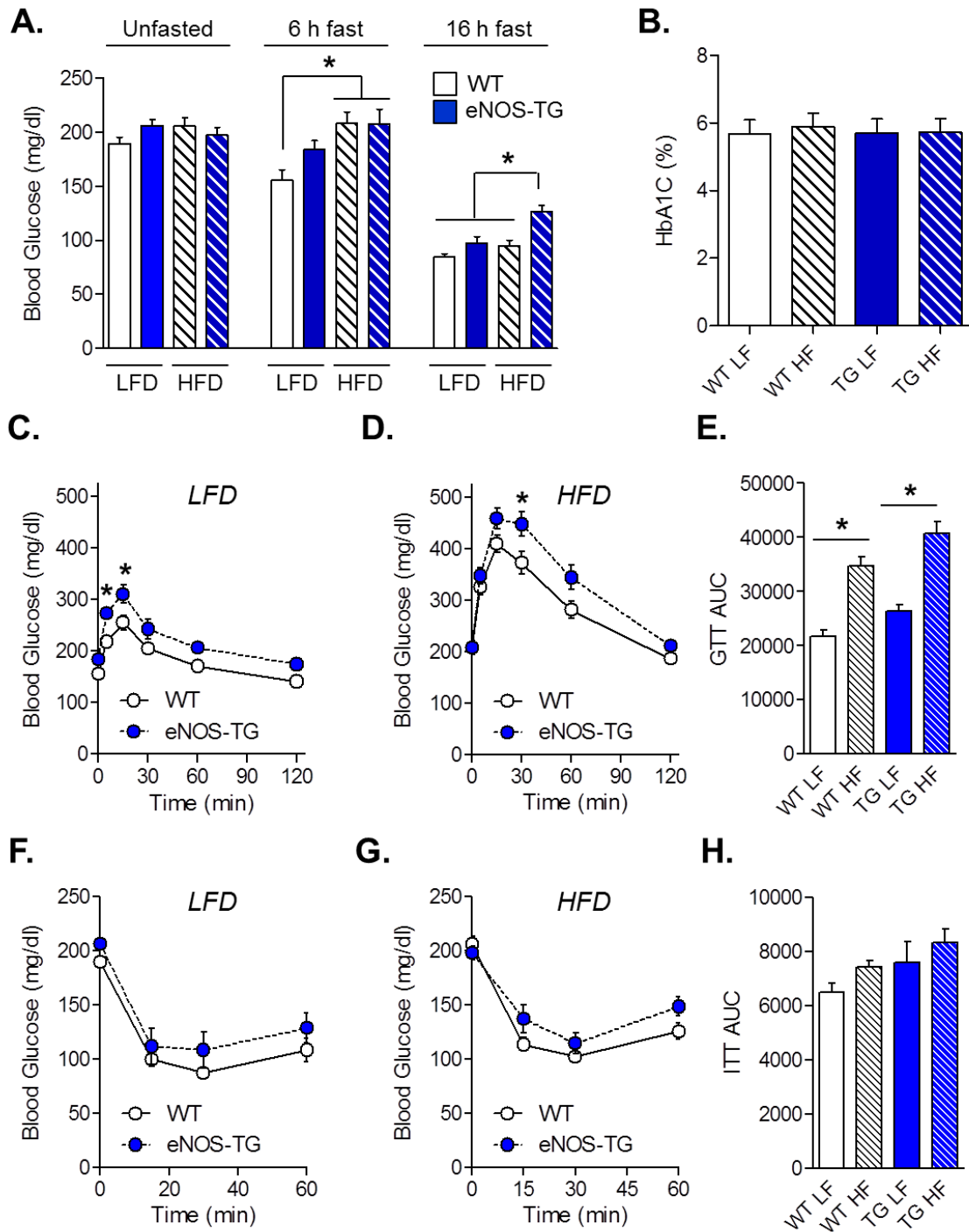
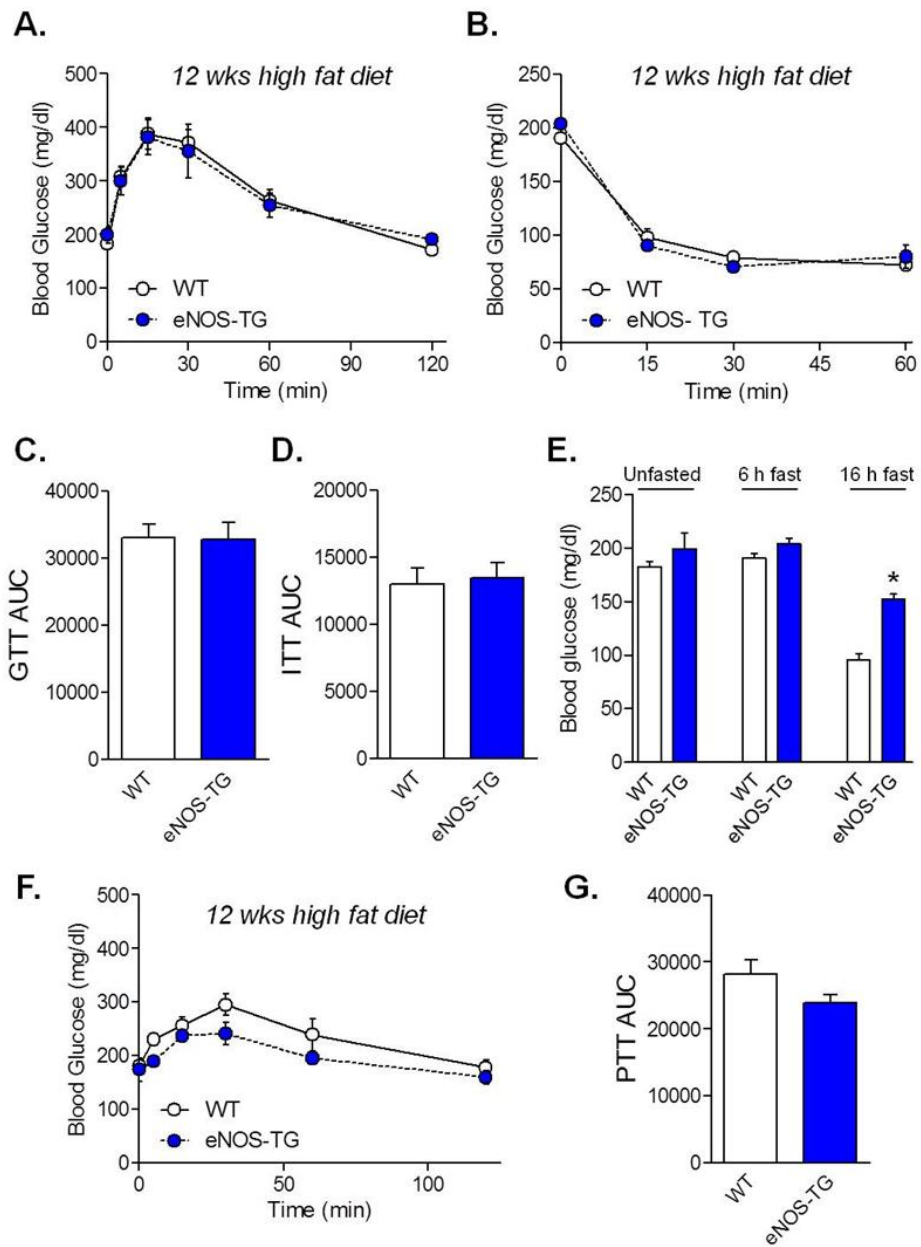


Figure 19. Measures of insulin resistance and gluconeogenesis in WT and eNOS-TG mice fed a high fat diet for 12 weeks. After 12 weeks of HFD, glucose tolerance and insulin sensitivity were examined in WT and eNOS-TG mice: **(A)** Glucose tolerance test (GTT); **(B)** Insulin tolerance test (ITT); **(C)** GTT area under the curve (AUC); **(D)** ITT AUC; **(E)** Blood glucose under non-fasted, 6-h-fasted and 16-h-fasted conditions; **(F)** Pyruvate tolerance test (PTT) was used to determine differences in gluconeogenesis between the mice; and **(G)** PTT AUC. n = 4 per group; * $p < 0.05$ vs. WT.

Figure 19



Therefore, we examined adipose tissue inflammation in WT and eNOS-TG mice after 6 weeks of high fat diet. Analysis of adipose tissue showed no significant difference in the abundance of crown-like structures between WT and TG mice (Fig. 20A), and analysis of the adipose tissue stromal vascular fractions showed no difference in total F480⁺ cells or changes in macrophage subtypes (Fig. 21). These results are in accordance with studies showing that macrophage accumulation and insulin resistance occur only with prolonged high fat feeding (>10 weeks)^{155, 295} and suggest that the anti-hypertrophic effects of eNOS are not associated with significant changes in adipose tissue inflammation, but are likely to be related to favorable changes in metabolism that prevent lipid accumulation and adipocyte expansion.

Metabolic changes in adipose tissues of eNOS-overexpressing mice. The lean phenotype of eNOS-TG mice and their resistance to diet-induced weight gain and adipocyte expansion clearly indicated that eNOS overexpression has a significant impact on adipocyte metabolism. Therefore, to assess this impact, we measured metabolite levels in epididymal adipose tissue of high fat-fed WT and eNOS-TG mice using UHPLC/MS/MS and GC/MS. Spectral data were identified, searched against a standard library, and quantified (Fig. 22). Internal standards, including injection standards, process standards, and alignment standards were used for quality control and to control for experimental and instrument variability. This analysis led to the identification of 192 metabolites of which 37 were significantly different between WT and eNOS-TG mice (Fig. 23A and Table 3).

Figure 20. eNOS overexpression decreases diet-induced adipocyte hypertrophy. Adipocyte size measurements from WT and eNOS-TG mice fed a LFD or HFD for 6 weeks: **(A)** Representative hematoxylin and eosin-stained images of adipose tissue from the epididymal fat pad ($\times 20$ magnification; scale bar = 100 μm); **(B)** Mean adipocyte area; **(C)** Distribution of adipocyte sizes from mice fed a LFD (upper panel) and a HFD (lower panel). $n = 5$ per group, $*p < 0.05$ vs. WT LFD; $\#p < 0.05$ vs. WT HFD.

Figure 20

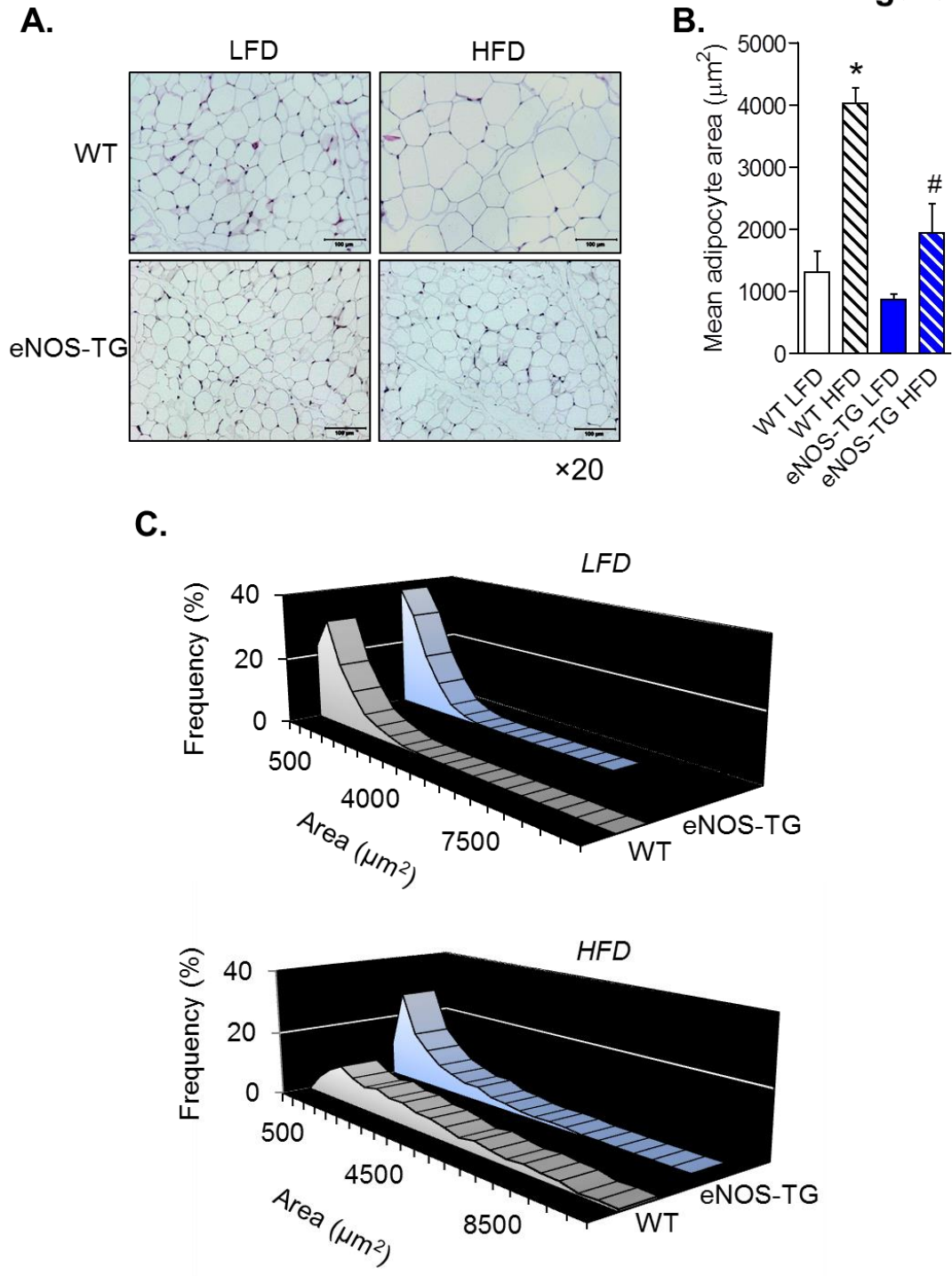


Figure 21. Effects of high fat diet on macrophage subtypes in WT and eNOS-TG mice. Macrophage subpopulations measured in epididymal adipose tissues after 6 weeks of LFD or HFD: **(A–D)** Representative flow cytometry dot plots of F4/80⁺ adipose tissue macrophages from WT and eNOS-TG mice. **(E)** Quantification of M1 macrophage subpopulations; **(F)** Quantification of M2 macrophage subpopulations; and **(G)** Quantification of macrophages doubly positive for M1 and M2 macrophage markers. n = 6 per group.

Figure 21

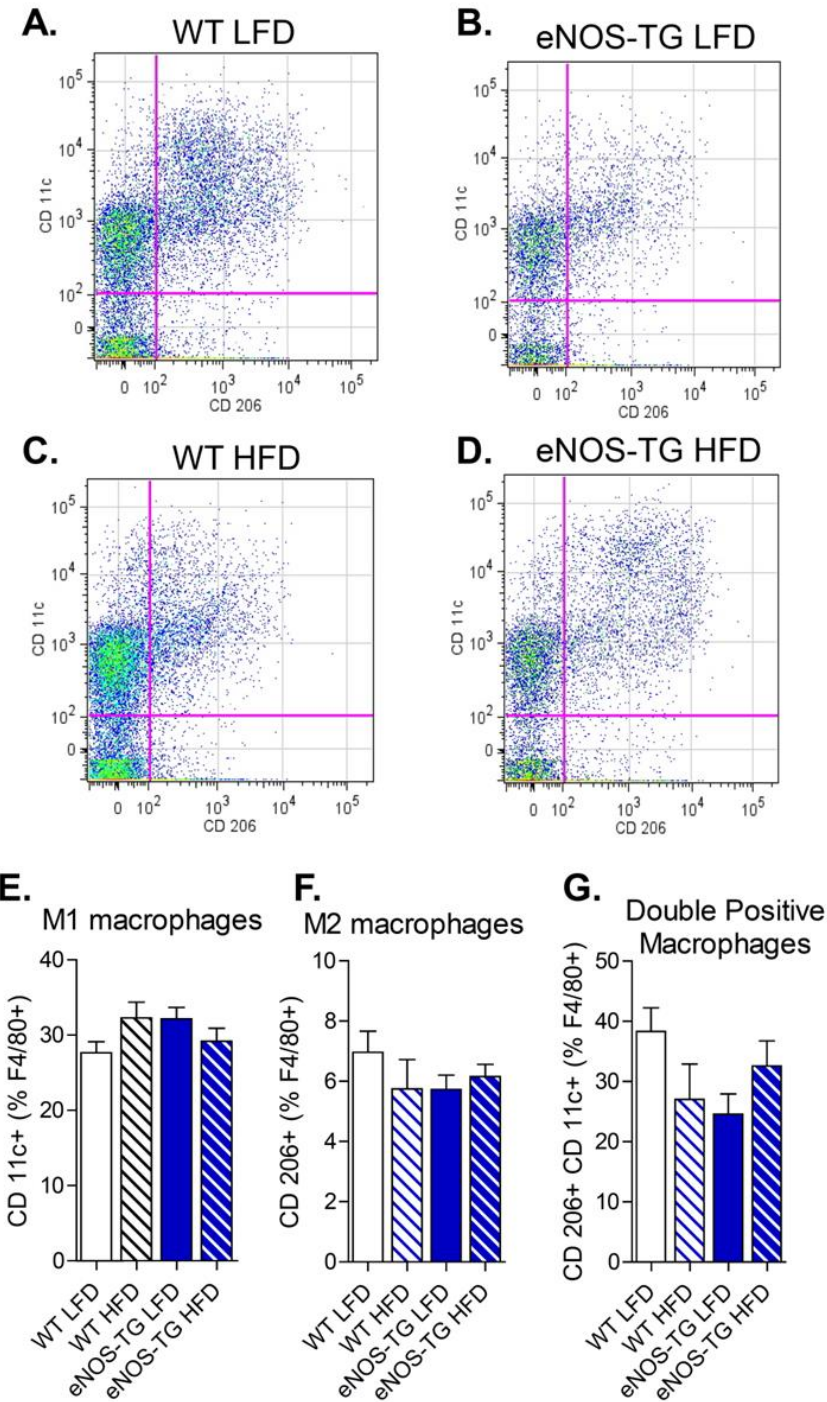


Figure 22. Flow chart illustrating procedure for metabolomic profiling of adipose tissues. Mice were fed a HFD for 6 weeks. The adipose tissue was then procured, and metabolites were extracted. The samples were divided for GC/MS or LC/MS analysis. Following spectral analysis, the data were imputed, normalized, and analyzed using Metaboanalyst 2.0 software.

Figure 22

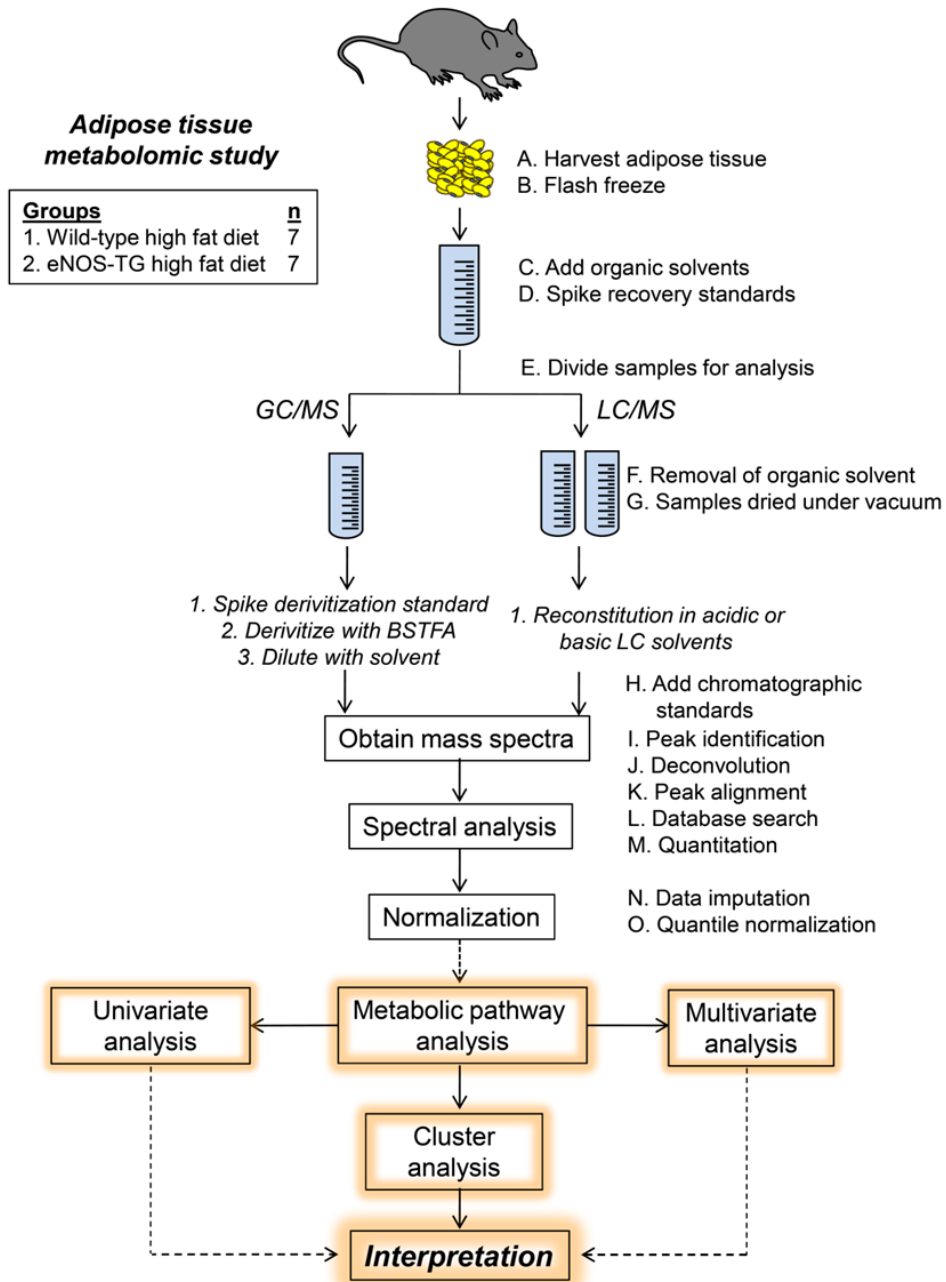


Table 3. List of adipose tissue metabolites that were significantly different between high fat-fed WT and eNOS-TG mice.

<i>Metabolite</i>	<i>KEGG</i>	<i>Super pathway</i>	<i>Sub-pathway metabolism</i>	<i>p-value</i>	<i>-log(10)p</i>	<i>FDR</i>
3-dehydrocarnitine	C02636	Lipid	Carnitine	1.0e-5	4.99	0.001
Phenylalanine	C00079	Amino acid	Phe/Tyr	1.2e-5	4.91	0.001
Histamine	C00388	Amino acid	His	2.3e-5	3.64	0.013
Citrulline	C00327	Amino acid	Urea/Arg/Pro	2.9e-5	3.53	0.013
Creatine	C00300	Amino acid	Creatine	4.8e-5	3.32	0.016
2-aminoadipate	C00956	Amino acid	Lys	5.7e-5	3.24	0.016
Serine	C00065	Amino acid	Gly/Ser/Thr	6.4e-5	3.19	0.016
Phosphoethanolamine	C00346	Lipid	Glycerolipid	8.6e-5	3.06	0.018
Pantothenate	C00864	Cofactors/Vitamins	Pantothenate/CoA	0.001	2.99	0.018
Leucine	C00123	Amino acid	Val/Leu/Ile	0.001	2.96	0.018
Proline	C00148	Amino acid	Urea/Arg/Pro	0.001	2.93	0.018
Threonine	C00188	Amino acid	Gly/Ser/Thr	0.001	2.90	0.018
1-stearoylglycerophosphoinositol	-	Lipid	Lysolipid	0.001	2.86	0.018
Tryptophan	C00078	Amino acid	Trp	0.001	2.85	0.018
Arginine	C00062	Amino acid	Urea/Arg/Pro	0.002	2.79	0.019
Isobutyrylcarnitine	-	Amino acid	Val/Leu/Ile	0.002	2.63	0.026
C-glycolysyltryptophan	-	Amino acid	Trp	0.002	2.60	0.026
Lysine	C00047	Amino acid	Lys	0.003	2.58	0.026
Methionine	C00073	Amino acid	Cys/Met/SAM	0.003	2.55	0.026
Valine	C00183	Amino acid	Val/Leu/Ile	0.004	2.45	0.031
Propionylcarnitine	C03017	Lipid	Fatty acid/BCAA	0.004	2.41	0.032
Urea	C00086	Amino acid	Urea/Arg/Pro	0.005	2.26	0.044
Tyrosine	C00082	Amino acid	Phe/Tyr	0.006	2.19	0.050
Isoleucine	C00407	Amino acid	Val/Leu/Ile	0.007	2.14	0.053
Adenosine	C00212	Nucleotide	Purine	0.012	1.92	0.075
Hypoxanthine	C00262	Nucleotide	Purine	0.014	1.84	0.098
Phosphate	C00009	Energy	Oxidative phosphorylation	0.020	1.70	0.124
Betaine	-	Amino acid	Gly/Ser/Thr	0.020	1.69	0.124
Stachydrine	C10172	Xenobiotics	Food component	0.020	1.69	0.124
Asparagine	C00152	Amino acid	Ala/Asp	0.022	1.66	0.129
Palmitate	C00249	Lipid	Long chain fatty acid	0.030	1.52	0.174
1-arachidonoylglycerophosphoethanolamine	-	Lipid	Lysolipid	0.037	1.44	0.192
Histidine	C00135	Amino acid	His	0.037	1.43	0.192
Acetylcarnitine	C02571	Lipid	Carnitine/BCAA	0.037	1.43	0.192
Glycerophosphoethanolamine	C01233	Lipid	Glycerolipid	0.038	1.42	0.192
2-hydroxyglutarate	C02630	Lipid	Fatty acid, dicarboxylate	0.041	1.39	0.200
Docosapentaenoate	C16513	Lipid	Essential fatty acid	0.04	1.37	0.206

Wild-type (WT) and eNOS-TG mice were fed a high fat diet (HFD) for 6 weeks. Epididymal adipose tissue was then subjected to LC or GC mass spectrometric analysis. Those metabolites found to be significantly different by t-test are listed above. The (-) indicates no KEGG identification number; FDR, false discovery rate. n = 7 mice per group.

Although intermediates in the glycolytic pathway and TCA cycle were not affected, there were significant increases in propionylcarnitine, acetylcarnitine, 3-dehydrocarnitine, and isobutyrylcarnitine, some of which have been shown to stimulate fatty acid oxidation^{354, 355}. Higher levels of amino acids such as threonine, methionine, valine, isoleucine, and leucine were also observed in TG mice (Table 3). Multivariate and cluster analyses showed that these changes were determining factors in the separation of the groups (Fig. 23B,C), and pathway impact analysis (Fig. 23D) suggested that changes in amino acid synthesis and degradation may be important features regulating the lean phenotype of eNOS-TG mice. Plotting of the z-scores of metabolites from adipose tissues of eNOS-TG and WT mice showed increases in short-chain acylcarnitines as well as amino acids and their degradation products (Fig. 24A). Metabolites correlating with citrulline levels showed a similar pattern of metabolites (Fig. 24B). The adipose tissue metabolites in eNOS-TG mice shown to be significantly different from WT mice equated to differences in urea cycle/arginine metabolism, branched chain amino acid (BCAA) metabolism, carnitine metabolism, purine metabolism, oxidative phosphorylation, and fatty acid metabolism subpathways (Fig. 24C). Taken together, changes in metabolite levels in the adipose tissue indicated that overexpression of eNOS stimulates amino acid and fatty acid metabolism in adipose tissue.

Adipose tissue mitochondria are increased in eNOS-TG mice. Favorable changes in BCAA and fatty acid metabolism are indicative of increased mitochondrial activity. Previous studies have shown that BCAA increases

mitochondrial biogenesis and that this is attenuated in eNOS-null mice ³⁵⁶. In addition, it has been reported that NO triggers mitochondrial biogenesis in adipocytes and that deletion of eNOS decreases mitochondrial content in adipose tissue ³⁵⁷. Based on this evidence, we hypothesized that the change in BCAA and fatty acid metabolism in the adipose tissue of eNOS-TG mice may be related to greater mitochondrial content. Indeed, adipose tissue, but not skeletal muscle, from eNOS-TG mice showed significant increases in key mitochondrial proteins such as COX4I1 and ALDH2 (Fig. 25A,C). The increase in mitochondrial proteins in TG adipose tissue could be due to remodeling of the mitochondria or an increase in mitochondrial abundance. To distinguish between these possibilities, sections of adipose tissue were stained with a non-membrane potential-dependent mitochondrial stain, mitID-Red. As shown in Fig. 25E, adipose tissue isolated from high-fat-fed eNOS-TG mice stained more strongly than WT mice, indicating that the adipose tissue mitochondrial content was higher in TG than WT mice. Indeed, adipocytes isolated from high fat-fed eNOS-TG mice were more brown in color than those isolated from WT mice (Fig. 25F), suggesting an increase in mitochondrial cytochromes. Indeed, in addition to increased abundance of COX4I1 (Fig. 25A,C), the expression of the mitochondrial gene cytochrome b6 (*cytb6*), was elevated 2-fold in eNOS-TG mice (*cytb6:gapdh* ratios, fold change: WT, 1.0±0.1; eNOS-TG, 2.0±0.3; n=4–7/group, p<0.05). That this increase in mitochondrial content may be due to increased biogenesis is supported by our observation that in comparison with WT mice, TG mice had higher adipose levels of PGC1α and Sirt3, as well as an increase in

Figure 23. Metabolomic analyses of adipose tissues from high fat-fed mice.

Metabolomic analyses of epididymal adipose tissue metabolites from WT and eNOS-TG mice fed HFD for 6 weeks: **(A)** Univariate analysis: *t*-tests of compounds from adipose tissues. All metabolites above the dotted line were found to be significantly different between WT and eNOS-TG mice ($p < 0.05$). Each of these metabolites is listed in Table 4; **(B)** Multivariate analysis: partial least squares-discriminant analysis (PLS-DA); **(C)** Hierarchical clustering: Heatmap and dendrogram using the the most significantly different metabolites. **(D)** The significant metabolites were subjected to pathway impact analysis using Metaboanalyst MetPA and the *Mus musculus* pathway library. Fisher's exact test was used for overrepresentation analysis, and relative betweenness centrality was used for pathway topology analysis. n = 14 animals: 7 WT HFD, 7 eNOS-TG HFD.

Figure 23

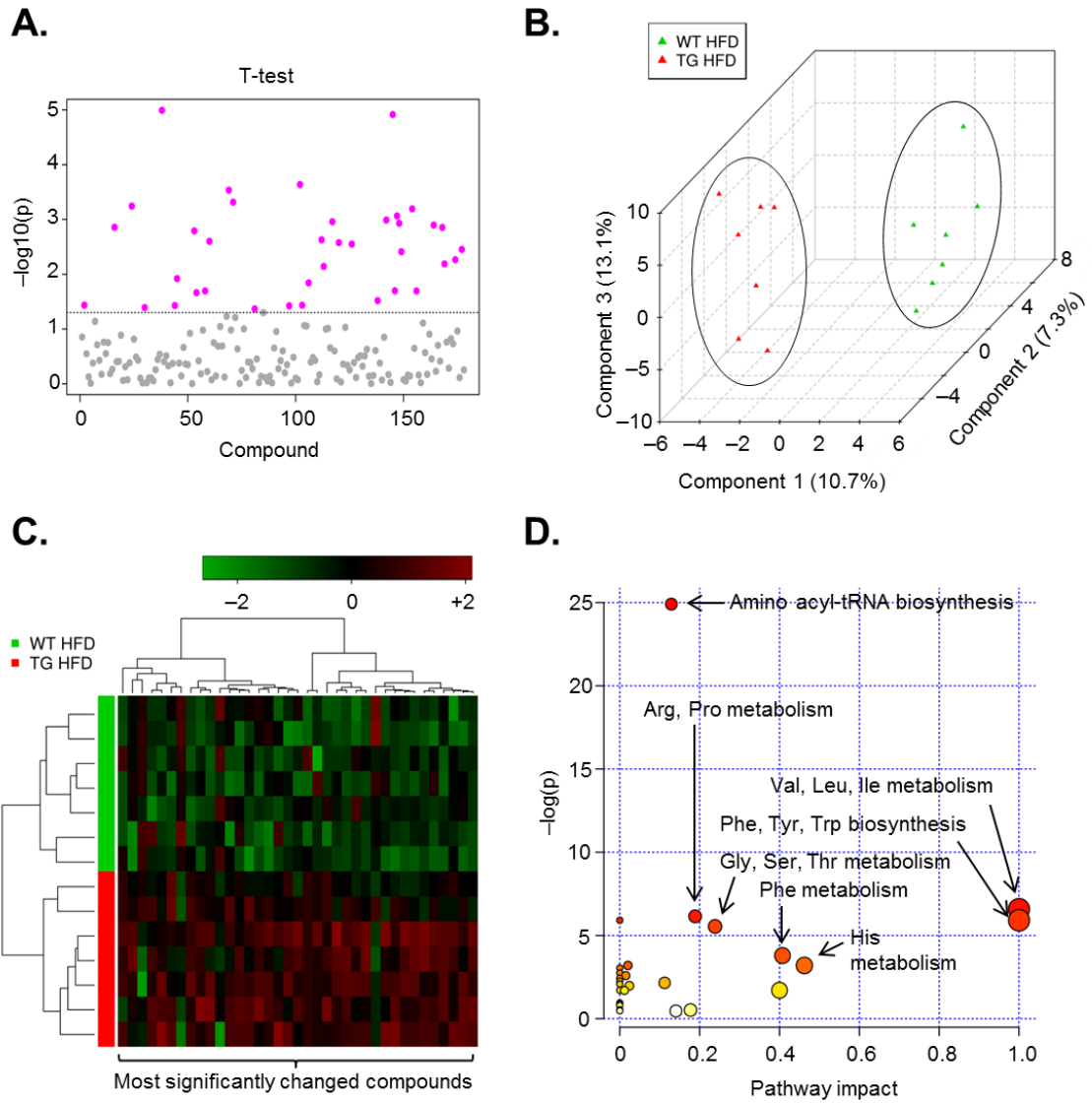
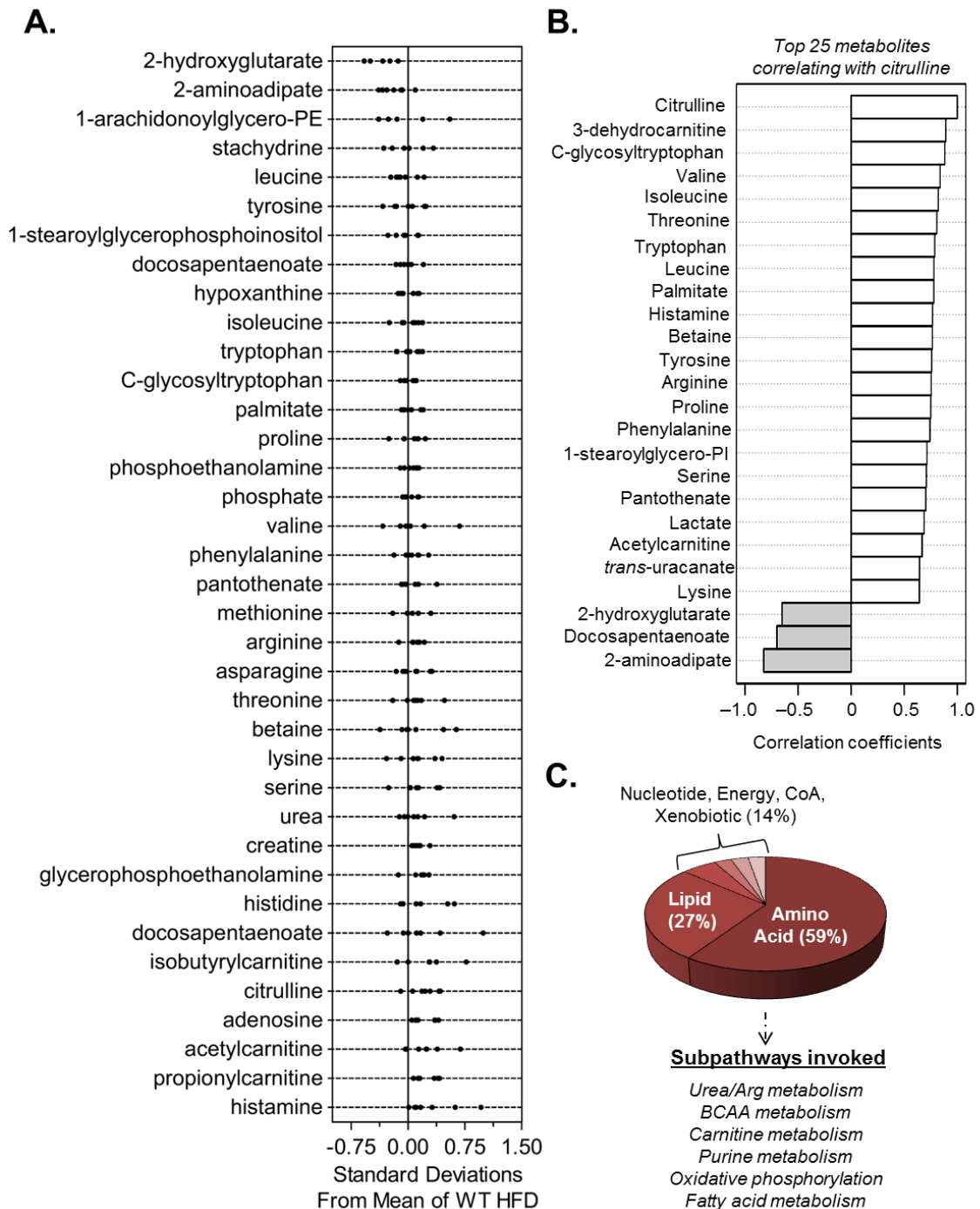


Figure 24. Overexpression of eNOS regulates intermediary metabolism in adipose tissue. Metabolite analysis from adipose tissues of WT and eNOS-TG mice fed HFD for 6 weeks: **(A)** z-score plots of significantly changed metabolites; **(B)** Correlation analysis was assessed using the Spearman rank correlation test, and metabolites that correlated with citrulline were then examined. **(C)** Super- and sub-pathway distribution of adipose tissue metabolites found to be significantly different between WT and eNOS-TG mice. n=14 animals: 7 WT HFD and 7 eNOS-TG HFD.

Figure 24



ppar α and γ (Fig. 25G); factors that are important activators of mitochondrial biogenesis^{284, 358-362}.

Effect of eNOS on adipose tissue metabolic flux. To assess the functional implications of our observations, we measured oxygen consumption in adipose tissue explants using extracellular flux technology. As shown in Fig. 26B, adipose tissue from eNOS-TG mice showed a significantly higher oxygen consumption rate (OCR) compared with adipose tissue from WT mice. To determine the contribution of mitochondria to the OCR, we treated explants with the electron transport chain inhibitors antimycin A and rotenone. The stabilized rate measured thereafter was used to calculate the mitochondria-derived OCR, which was 2-fold higher in eNOS-TG compared with WT adipose tissue (Fig. 26C). No statistically significant difference was observed in the extracellular acidification rate (ECAR), a surrogate index of glycolysis (Fig. 26D). Collectively, these observations corroborate our metabolic, biochemical, and anatomical measurements by demonstrating directly that the adipose tissue of eNOS-TG mice maintains a hypermetabolic state that could at least partially account for their increase in whole-body oxygen consumption and resistance to obesity.

Discussion

The major findings of this study are that high fat diet results in the downregulation of eNOS in adipose tissue and that overexpression of eNOS

Figure 25. Mitochondria are increased in the adipose tissue of eNOS-TG mice. Measurements of mitochondria in epididymal adipose tissue and skeletal muscle from WT and eNOS-TG mice: **(A)** Representative Western blots of adipose tissue eNOS, PGC1 α , ALDH2, COX4I1, and Sirt3; GAPDH was used as a loading control. **(B)** Representative Western blots of skeletal muscle eNOS, PGC1 α , VDAC, COX4I1, and Sirt3. GAPDH was used as a loading control. **(C)** Quantification of protein expression from panel A. **(D)** Quantification of protein expression from panel B. n = 3 per group; * p <0.05 vs. WT; White bars, WT; blue bars, TG. **(E)** Immunofluorescence images of adipose tissue sections from HF-fed WT (panel i) and eNOS-TG (panel ii) mice; the sections were stained with MitolD-Red as a qualitative index of mitochondrial mass. Scale bar=200 μ M **(F)** Representative photomicrograph of adipocytes isolated from HF-fed WT and eNOS-TG mice (600,000 adipocytes per well). **(G)** mRNA analysis of *Ppara* and *Pparg*. White bars, WT LFD; blue bars, eNOS-TG LFD; white hatched bars, WT HFD; blue hatched bars, eNOS-TG HFD; n=6 per group; * p <0.05 vs. indicated groups.

Figure 25

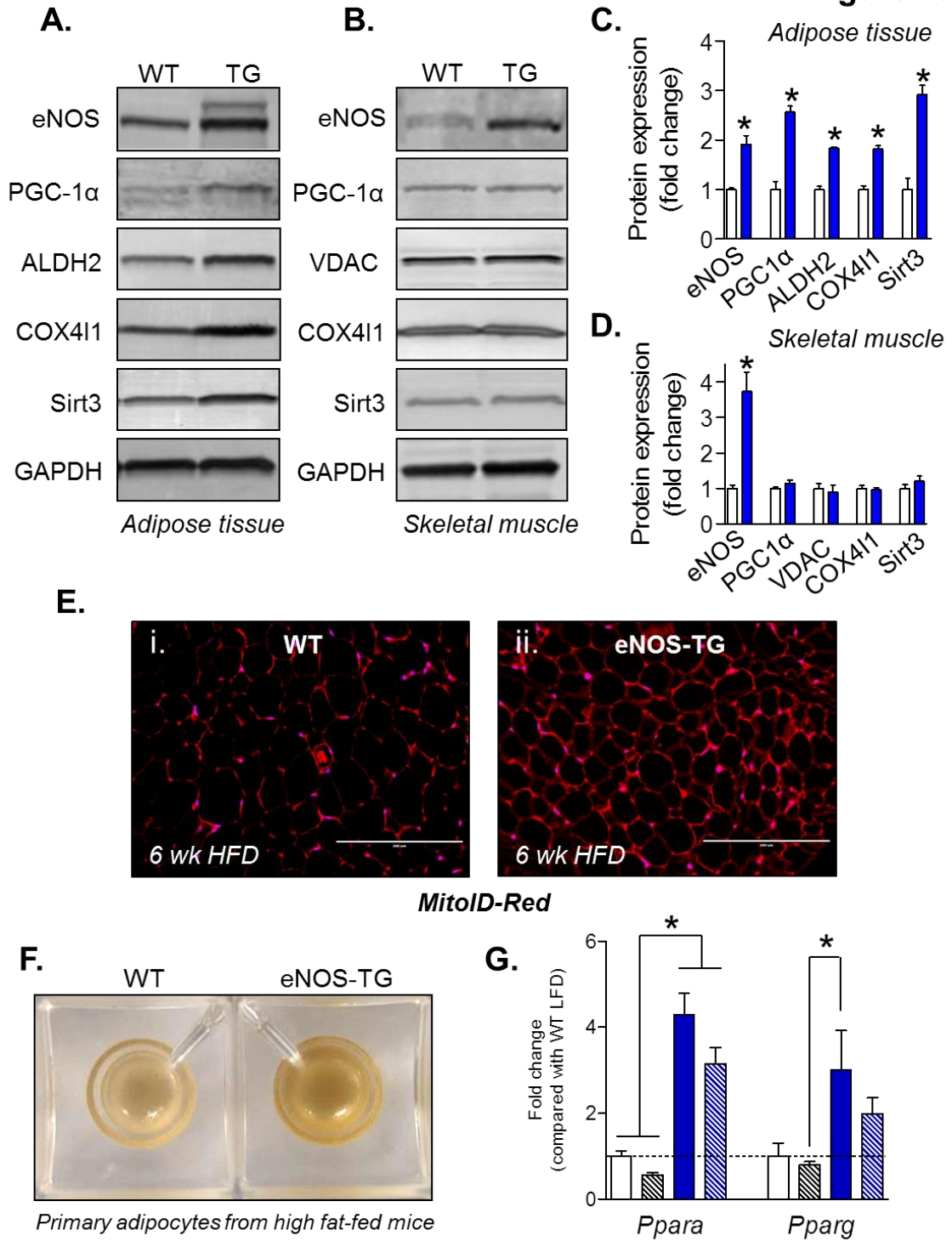
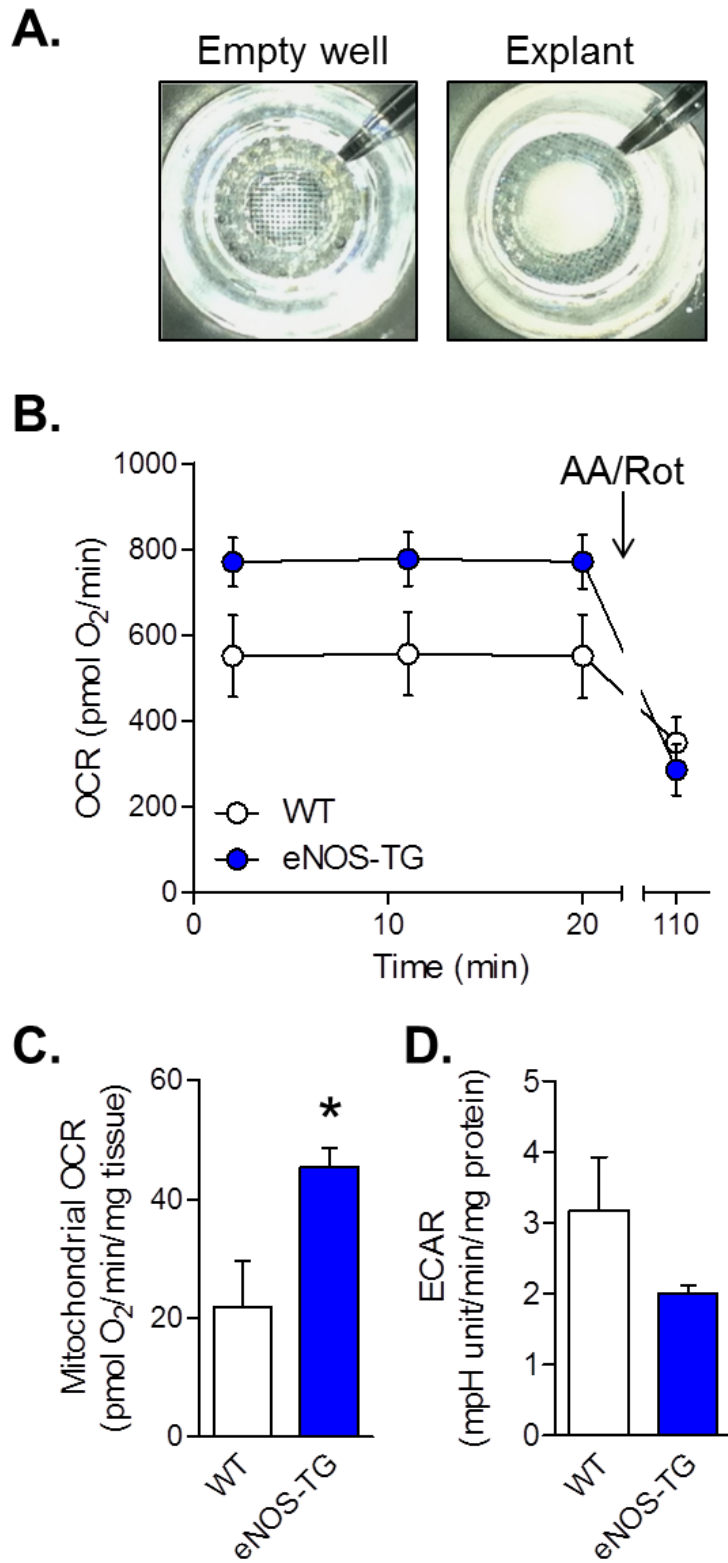


Figure 26. eNOS overexpression increases adipose tissue mitochondrial energetics. Extracellular flux (XF) analysis of adipose tissue explants from WT and eNOS-TG mice fed a HFD for 14 wks: **(A)** Representative photomicrographs of adipose tissue explants used for XF analysis; **(B)** Oxygen consumption rates (OCR) of adipose tissue explants: After three baseline measurements, antimycin A and rotenone (AA/Rot) were injected to identify the mitochondria-dependent OCR. **(C)** Mitochondrial OCR calculated from measurements in panel B. **(D)** Extracellular acidification rate (ECAR) measured from adipose explants; ECAR is a surrogate measure of glycolytic rate. n = 3–4 per group, * $p < 0.05$ vs WT.

Figure 26



prevents diet-induced obesity. These findings support a causal role of eNOS in regulating obesity and whole-body metabolism. Our results suggest that the mechanism of this anti-obesogenic effect of eNOS is related to an increase in whole-body oxygen consumption associated with increased mitochondrial abundance and activity in the adipose tissue. Collectively, these observations support the notion that NO is an important regulator of adipocyte metabolism and thereby weight gain due to a high fat diet. While it has been shown before that deletion of eNOS gives rise to features of metabolic syndrome³³⁶, the rescue of the obese phenotype by increasing eNOS indicates that enhancing eNOS expression can overcome the metabolic changes caused by consumption of high fat diet.

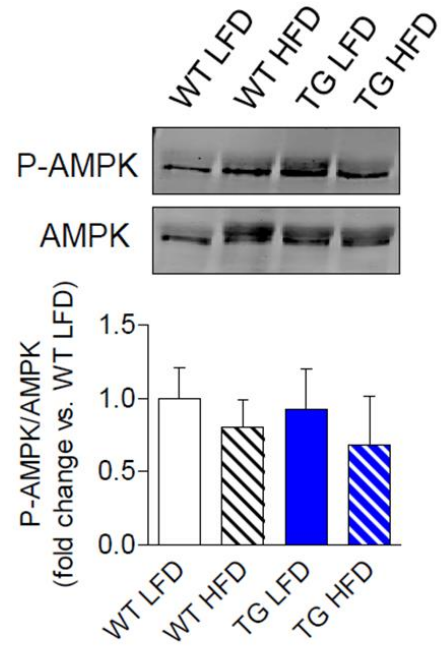
Several lines of evidence gathered during this study support the view that the anti-obesogenic effects of eNOS are due to favorable changes in adipocyte metabolism. Although on the basis of current results we cannot rule out, or even fully assess all potential systemic effects, our observations that food consumption, activity, plasma levels of cholesterol, leptin and thyroid hormones were not different between WT and TG mice argue against a global, systemic change that could completely account for the lean phenotype of the TG mice. Both insulin resistance and obesity are complex phenotypes that are regulated by multiple interactions between several tissues, some or all of which might be affected in a manner not captured by our current analysis. Nevertheless, in regulating obesity, the adipose tissue appears to be a major target of eNOS. Our gene-dosage studies show that despite a 4-fold increase in eNOS in the aorta,

diet-induced obesity was only marginally affected in eNOS hemizygous mice, in which there was no increase in eNOS in adipose tissue. Only in homozygous mice, in which eNOS was increased both in adipose tissue and aorta, did the anti-obesogenic effects of eNOS become apparent. This association of the lean phenotype with eNOS expression in adipose tissue supports the view that an increase in NO in adipose depots may be required for the manifestation of the anti-obesogenic effects of eNOS.

How does eNOS regulate adipose tissue metabolism? Our results suggest that eNOS supports both mitochondrial biogenesis and metabolic activity. Previous observations showing that β -oxidation is impaired in eNOS-null mice³³⁷ and that dietary supplementation with the NO precursor nitrite reverses features of metabolic syndrome in eNOS-null mice³⁶³ are supportive of this concept. Although AMP kinase (AMPK) has been shown to relate with NO levels^{364, 365}, we did not find an increase in the phosphorylation state of AMPK in adipose tissue (Fig. 27). However, we did find elevated levels of several metabolites such as BCAAs and short-chain acylcarnitines (e.g., acetylcarnitine, propionylcarnitine) in the adipose tissue of TG mice that were indicative of high metabolic activity. Interestingly, oral supplementation with propionylcarnitine reduces obesity and hyperinsulinemia in obese rats³⁶⁶, which at least partially recapitulates the phenotype of eNOS-TG mice. We also found in the adipose tissue of TG mice elevated levels of proteins such PGC-1 α and Sirt3 and increased expression of *ppara* and *pparg* that regulate mitochondrial activity, fatty acid oxidation, and biogenesis^{284, 358-362, 367, 368}. That the increase in these

Figure 27. Western blot analysis of AMPK activation status. Mice were fed a LFD or HFD for 6 weeks and P-AMPK and total AMPK abundance were measured by western blotting. n = 3–4 per group

Figure 27



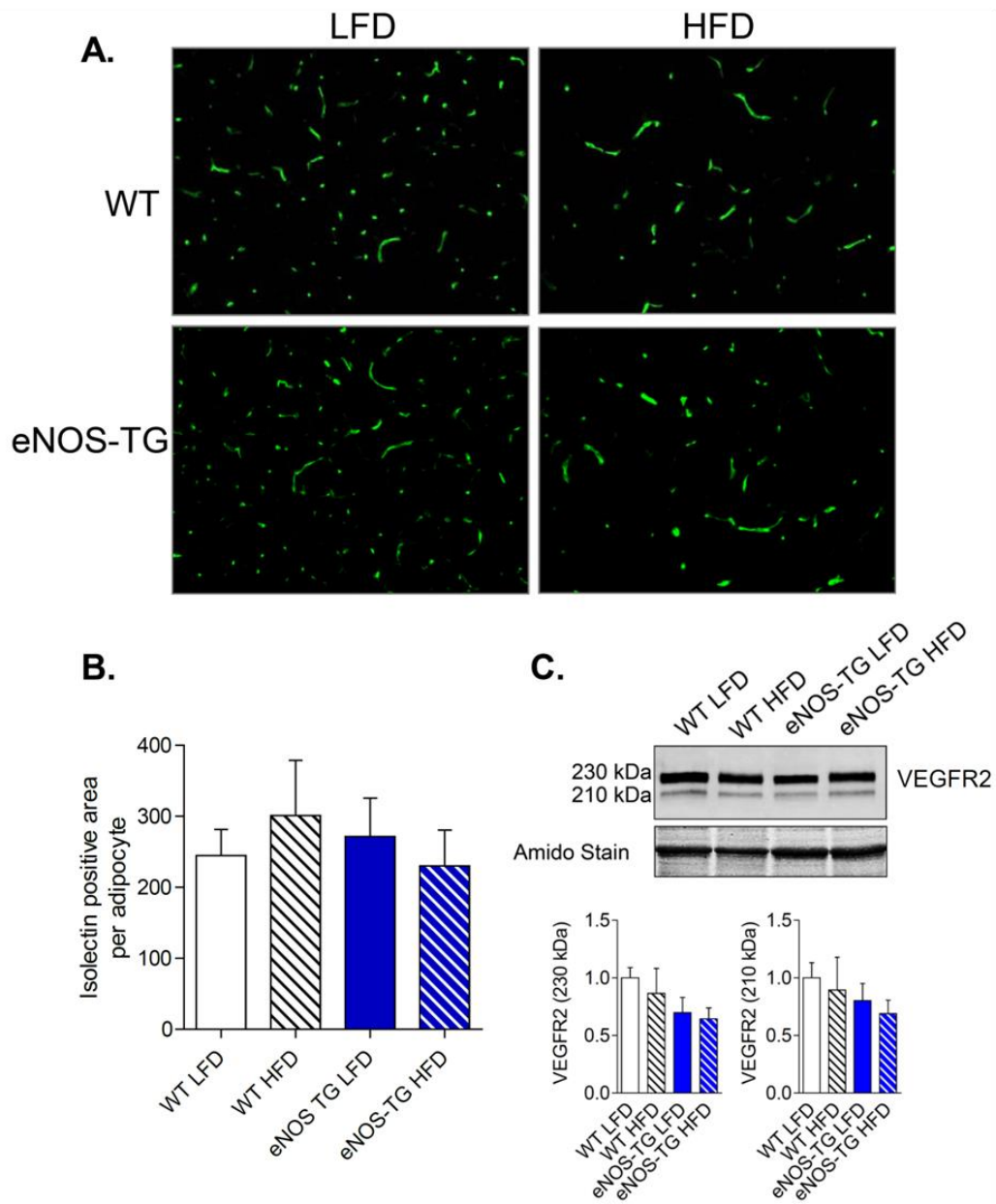
proteins was functionally significant is reflected by our observations that mitochondrial abundance and rates of fatty acid oxidation were higher in the adipose tissue from eNOS-TG mice. On the basis of these observations, we propose that high levels of eNOS lead to an increase in mitochondrial biogenesis and stimulation of fatty acid oxidation. This establishes a state of heightened metabolism that attenuates the obesogenic effects of high fat consumption.

Although our results show that eNOS overexpression increases adipose tissue metabolism by increasing mitochondrial content and activity, metabolic activity could also be affected by eNOS-dependent changes in oxygen distribution. Hence, it is possible that adipocytes of eNOS-TG mice are better perfused than those of WT mice. Such an increase in tissue perfusion could be due to either regulatory effects on vascular tone³⁶⁹ and O₂ consumption³⁷⁰ or an increase in angiogenesis³⁷¹. Nevertheless, we found that capillary density was unaffected by eNOS overexpression, as isolectin B4 staining per adipocyte and VEGFR2 expression were similar between the groups (Fig. 28), suggesting that an increase in angiogenesis is unlikely explain the lean phenotype of eNOS-TG mice.

The metabolic role of eNOS, however, appears to be tissue-specific. We found that high fat feeding decreased eNOS in the adipose tissue but not in the heart or the skeletal muscle. Hence, we expected that overexpression of eNOS would ameliorate adipose tissue hypertrophy without affecting high fat-induced changes in other peripheral tissues. Data from eNOS-TG mice substantiated this expectation. These results showed that high fat-induced changes in glucose

Figure 28. Overexpression of eNOS does not affect capillary density in adipose tissue. Fluorescence images and markers of capillary density in sections of epididymal adipose tissue isolated from WT or eNOS-TG mice fed a LFD or HFD for 6 weeks: **(A)** Representative images of isolectin B4 (green) staining. **(B)** Isolectin B4 staining quantified per adipocyte. n = 9 per group. **(C)** VEGFR2 expression in adipose tissue. Density of the VEGFR2 bands were normalized to amido black stain. n = 6 per group. Note: the apparent decrease in isolectin staining in HFD groups from panel A relates to an increase in adipocyte size relative to the LFD group.

Figure 28



disposal were not different between WT and eNOS-TG mice indicating that whole body glucose metabolism, which is regulated primarily by glucose uptake by the skeletal muscle³⁷², was not related to changes in eNOS levels. Nevertheless, the observation that despite their lean phenotype the TG mice develop insulin resistance is significant because a lean phenotype characterized by the browning of fat is usually associated with improved glucose tolerance^{325, 373-375}. It is likely that a decrease in eNOS is a critical event in adipose tissue but not skeletal muscle, and therefore, elevated levels of eNOS in the adipose tissue prevent obesity without affecting systemic insulin resistance.

Results showing that overexpression of eNOS prevents obesity without affecting insulin resistance also suggest that the two symptoms of metabolic syndrome could be dissociated from one another. Similar segregation between obesity and insulin resistance has been described previously. For instance, it has been shown that overexpression of adiponectin completely rescues the diabetic phenotype of *ob/ob* mice while promoting morbid obesity³⁷⁶. Moreover, the observations that decreasing inflammation³⁷⁷⁻³⁷⁹ does not result in lower adiposity but improves insulin sensitivity, and that PPAR γ agonists decrease insulin resistance but increase weight gain³³³ provide additional support that obesity and diabetes are disconnected and, in some cases, even conflicting events in the etiology of metabolic disease. However, it remains to be established how eNOS prevents hyperinsulinemia as well as impacts other processes that are associated with insulin resistance, such as inflammation. It is currently believed that, due to excessive adipocyte expansion, hypoxia and

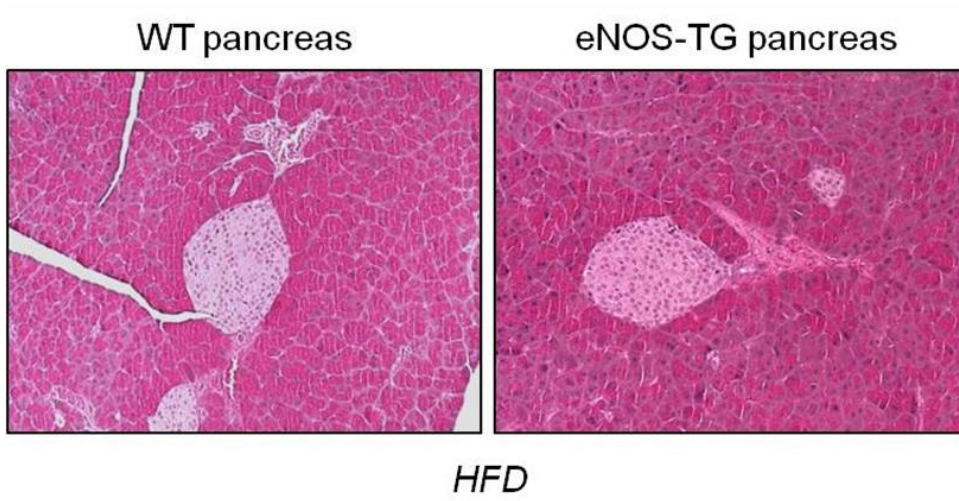
necrosis occur in adipose tissue, which in turn leads to the recruitment of inflammatory cells^{380, 381}. The resultant low-grade chronic inflammation is proposed to establish a state of insulin resistance^{382, 383}. However, the eNOS-TG mice develop the anti-obesogenic phenotype far before macrophage infiltration, inflammation, and insulin resistance in adipose tissue occur^{155, 295}.

It is important to note that the eNOS-TG mice did not display a lipodystrophic phenotype. Lipodystrophy in humans and animal models generally results in severe hypertriglyceridemia, hyperinsulinemia, and insulin resistance³⁸⁴⁻³⁸⁶. The eNOS-TG mice, however, show decreased triglycerides and were protected from hyperinsulinemia despite developing diet-induced glucose intolerance. The prevention of hyperinsulinemia does not appear to be due to a pancreatic defect: baseline insulin levels were not significantly different from WT mice (Table 2), the glucose tolerance test showed a normal profile (Fig. 18 and 19), and the pancreatic islets from eNOS-TG mice appeared unremarkable (Fig. 29). These observations raise the interesting possibility that hyperinsulinemia in response to systemic insulin resistance may be in part regulated by the adipose tissue, although additional work is required to fully understand this relationship.

Additional investigations will also be required to assess how high fat diet affects eNOS activity and expression. Although it has been shown that eNOS levels are suppressed in high fat diet in part due to TNF- α -dependent mechanisms¹⁶¹, the effects of diet on eNOS protein and activity are less clear. The eNOS protein is subject to several post-translational modifications including

Figure 29. Hematoxylin and eosin-stained images of pancreas from WT and eNOS-TG mice. Representative photomicrographs of pancreas isolated from WT and eNOS-TG mice fed a HFD for 6 weeks; ×20 magnification.

Figure 29



phosphorylation³⁸⁷, O-GlcNAcylation³⁸⁸, S-glutathiolation²⁵³, and acylation^{389, 390}. In addition, the enzyme could also be uncoupled and therefore generate superoxide instead of synthesizing NO. Interestingly, we found that while eNOS monomer abundance was maintained in eNOS-TG mice (Fig. 30), the phosphorylation of eNOS at Ser¹¹⁷⁷ and abundance of the eNOS dimer were significantly decreased in both WT and TG mice fed a high fat diet (Fig. 30). Although these changes in the eNOS-TG mice might be compensated by continually elevated levels of eNOS protein, as evidenced by persistently elevated citrulline levels (Fig. 15A,B), such changes in WT mice might result in a chronic state of NO deficiency. Moreover, uncoupling of the enzyme could lead to increased superoxide production and the formation of the toxic metabolite peroxynitrite. Indeed, we found increased nitrotyrosine formation in adipose tissue of high fat-fed mice (Fig. 31), although this was not significantly affected by eNOS overexpression. Hence, in future studies it will be important to identify the processes that regulate eNOS activity and how they might be involved in the development of diet-induced obesity and insulin resistance.

In conclusion, the present study shows that preventing eNOS depletion by forced expression of the eNOS transgene attenuates diet-induced obesity in mice, without ameliorating systemic insulin resistance. These findings reveal a novel anti-obesogenic role of eNOS and are consistent with the notion that eNOS prevents weight gain in high fat-fed mice by stimulating mitochondrial biogenesis and activity in adipose tissues. Further understanding of this role of eNOS could

Figure 30. Analysis of eNOS expression and modification. Immunoblotting of eNOS enzyme states that reflect eNOS activity state: WT and eNOS-TG (TG) mice were fed a LFD or HFD for 6 weeks and eNOS abundance and phosphorylation status were examined by immunoblotting. **(A)** Representative Western blots of eNOS dimer, Ser¹¹⁷⁷ phosphorylation of eNOS (P-eNOS), and the eNOS monomer; **(B)** Quantification of P-eNOS; **(C)** Quantification of the eNOS dimer; n = 3–4 per group; *p<0.05 vs WT LFD; # p<0.05 vs. TG LFD.

Figure 30

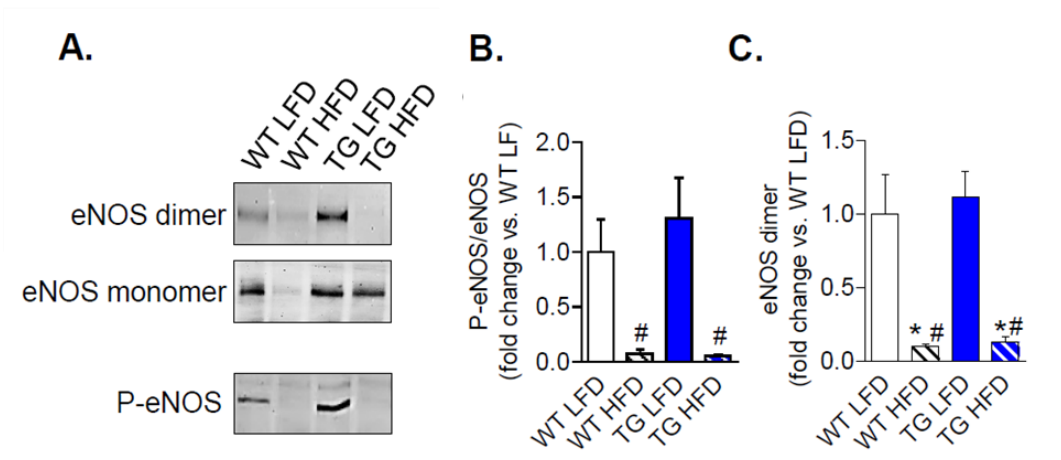
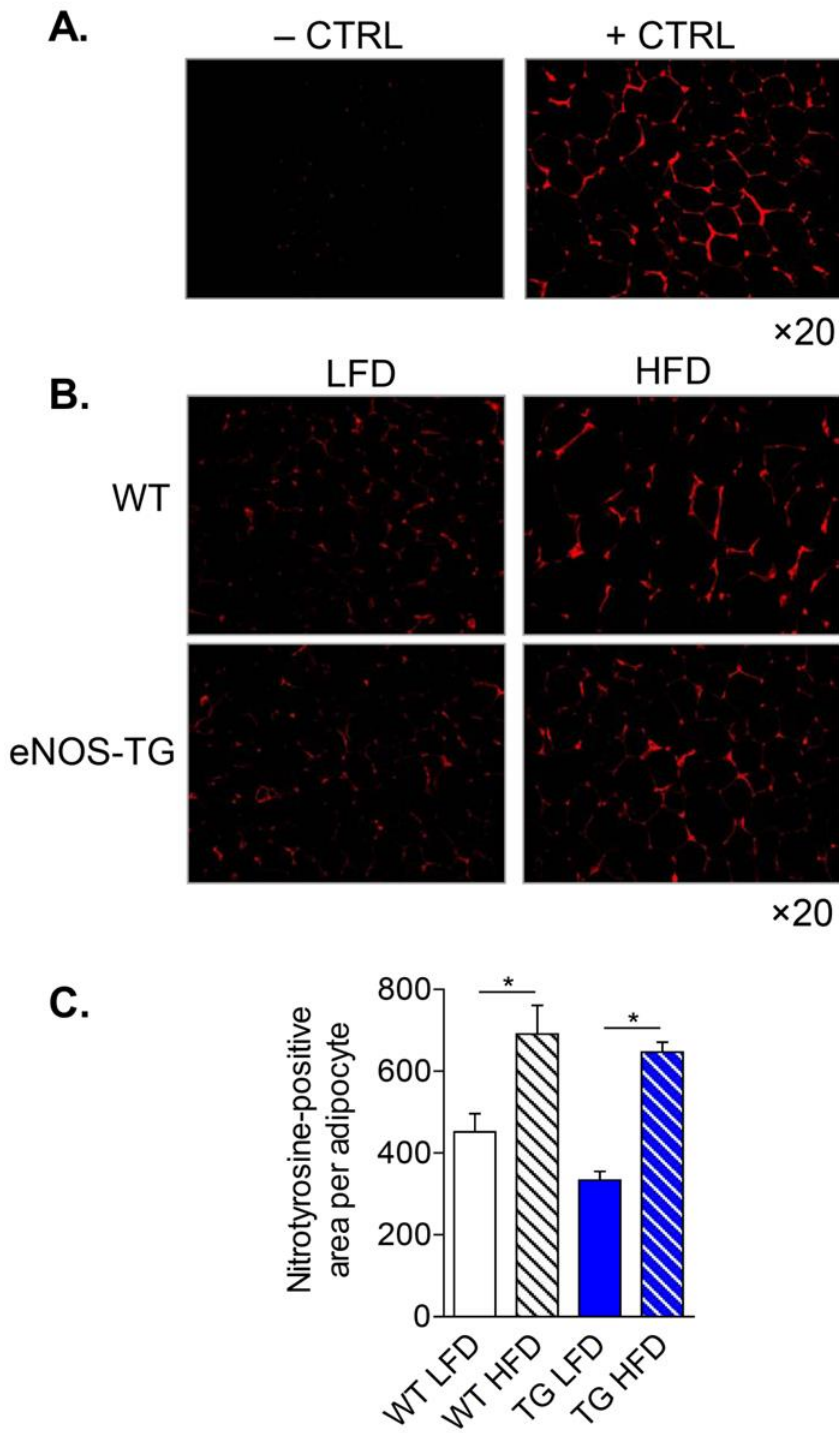


Figure 31. High fat feeding increases protein-nitrotyrosine adducts in adipose tissue. Immunofluorescence images and quantification of nitrotyrosine adducts in adipose tissue: WT and eNOS-TG mice were fed a LFD or HFD for 6 weeks. The adipose tissue was stained for nitrotyrosine adducts, and the adducts were visualized by fluorescence microscopy. **(A)** Negative (–) and positive (+) controls for nitrotyrosine staining. **(B)** Representative images of nitrotyrosine staining in WT and eNOS-TG mice fed a LFD or HFD. **(C)** Quantification of nitrotyrosine adducts from adipose tissues. n = 3 per group; *p<0.05 vs. indicated group.

Figure 31



lead to the development of new therapeutic modalities for preventing obesity and weight gain in human populations.

CHAPTER IV

REGULATION OF SYSTEMIC METABOLISM BY NITRIC OXIDE

Introduction

Our previous work shows that overexpression of eNOS in mice regulates diet-induced obesity, in part by increasing total body energy expenditure. This resistance to obesity in eNOS transgenic mice is associated with the presence of a more “brown-like” adipocyte in white adipose tissue depots, suggesting that eNOS-induced changes in adipose tissue could underlie the anti-obesogenic effects of eNOS. However, in rodents, adipocytes utilize less energy compared to other peripheral tissues such as liver and skeletal muscle, which have estimated metabolic rates 50 and 3 times that of adipose tissue, respectively³⁹¹, and they collectively account for at least 50% of the overall oxygen use³⁹². To understand the role of eNOS in regulating adipose tissue energy consumption and systemic energy expenditure, we estimated the proportion of whole body oxygen consumption that could be ascribed to adipose tissue.

To estimate the contribution of adipose tissue consumption, whole body VO_2 values and adipose tissue oxygen consumption rates were measured. Using the Ideal Gas Law: ($pV = nRT$), where p is pressure of the gas, V is volume of the

gas, n is number of moles of the gas, R is the universal gas constant, and T is temperature in Kelvin, the number of moles of O_2 consumed was calculated. The VO_2 in wild type (WT) mice was 6.622 L O_2 /h/kg (Chapter III, Fig. 16I). Assuming an average body weight of ~40 g per mouse, this corresponds to 0.26 L O_2 /h/mouse, which is equivalent to $\cong 250$ mmols O_2 /day/mouse. Body fat percentage, as measured by dual X-ray absorptiometry, was approximately 30% (12.03 g fat) in the high fat-fed WT mice (Chapter III, Fig 16F). From adipose tissue explant respirometry, we calculated the mitochondrial oxygen consumption rate of adipose tissue explants from WT high fat-fed mice to be 21.94 pmols O_2 /min/mg tissue (Chapter III, Fig 26C). Therefore, 12,030 mg of adipose tissue consuming oxygen at a rate of 21.94 pmol/min/mg tissue is approximately equal to 263,938.2 pmols O_2 /min and 0.380 mmols O_2 /day. Thus, dividing the adipose explant value (0.380 mmols O_2 /day) by the whole body value (250 mmols O_2 /day/mouse) suggests that approximately 0.15% of the total O_2 consumption per day is accounted for by adipose tissue in a WT mouse. When the same calculation was applied to eNOS-TG mice, 0.18% of oxygen consumption is attributed to adipose tissue; a difference of only 0.03% compared with WT mice.

These estimates suggest that an increase in adipose tissue mitochondrial activity is unlikely to account for the anti-obesogenic phenotype of eNOS-TG mice. The differences in standard metabolic rate between animals of different body mass have been assessed to be due to proportional changes in the whole of energy metabolism³⁹³. It has been estimated that ~90% of mammalian oxygen consumption in the standard state is due to mitochondrial activity of which ~80%

is coupled to ATP synthesis ³⁹³. Therefore, to assess the source of increased energy expenditure in eNOS-TG mice a wider metabolic analysis is necessary.

The metabolic effects of nutrient excess extend beyond adipose tissue. Indeed, the skeletal muscle of obese diabetic patients is characterized by fewer and smaller-sized mitochondria ^{394, 395}, with decreased oxidative capacity ³⁹⁶. Moreover, high fat diet decreases the expression of genes involved in oxidative phosphorylation and mitochondrial biogenesis of humans and mice ³⁹⁷. In the liver, it is associated with increased intracellular lipid accumulation ³⁹⁸⁻⁴⁰⁰. Mitochondrial abnormalities including ultrastructural lesions, depletion of mtDNA, decreased activity of respiratory chain complexes ⁴⁰¹ and impaired mitochondrial β -oxidation have been found in patients with elevated hepatic lipid deposition ^{395, 402}, while increased expression or activity of hepatic fatty acid oxidation enzymes reduces fat accumulation ⁴⁰³⁻⁴⁰⁶.

Metabolic dysfunction in peripheral tissue is likely to be reflected in the plasma. Dysregulated fatty acid oxidation is characterized by increased plasma levels of acylcarnitines in both obese and diabetic individuals ⁴⁰⁷ as well as in animal models of obesity and diabetes ⁴⁰⁸. Similarly, plasma lactate levels are increased in individuals with severe diabetes ⁴⁰⁹ and levels of circulating FFAs have been shown to be correlated with obesity and diabetes ⁴¹⁰⁻⁴¹². As a result, metabolic changes in tissues other than the adipose depots could strongly influence adiposity and thereby contribute to the metabolic phenotype of eNOS-TG mice. Hence, identifying the specific metabolic pathways affected is therefore important understanding the mechanism(s) by which eNOS prevents obesity.

Recent advances in metabolomics have been critical for understanding the systemic effects of metabolic diseases like obesity and diabetes ⁴¹³. By measuring and, in some cases, mathematically modelling, changes in metabolites found in biological fluids and tissues, metabolomic data can provide key information on metabolic changes required to link phenotype to genetics ⁴¹⁴, ⁴¹⁵. In particular, biological fluids such as plasma and urine can be used to identify metabolic pathways that are perturbed by disease or impacted by drug treatment or experimental intervention ⁴¹⁶⁻⁴¹⁹. Interestingly, the idea of quantifying changes in biological fluids as markers of disease is not a new one. Indeed, there is evidence of such endeavors occurring as early as ancient Greece and diagnostic 'urine charts' that linked the colors, smells and tastes of urine to various medical conditions were widely used from the Middle Ages onwards ⁴¹⁴. Metabonomics, and the related field of metabolomics, uses modern techniques to analyse samples, but the basic principle of relating chemical patterns to biology is the same. More recently, highly sensitive analytical techniques (i.e., mass spectrometry, nuclear magnetic resonance spectroscopy) applied to metabolomics and systems biology have emerged at the forefront of drug discovery and understanding disease processes ⁴²⁰.

Using a metabolomics approach, we examined plasma from WT and eNOS-TG mice fed low or high fat diets to identify changes in systemic metabolism caused by nutrient excess or eNOS overexpression. Our analysis, was driven by three main questions: **1) How are plasma metabolites affected by a high fat diet?; 2) What are the metabolic changes induced eNOS**

overexpression?; and 3) Which plasma metabolites are sensitive to both high fat diet and eNOS? To address these questions we compared the metabolite profiles of each group of animals and identified the metabolic pathways most affected by diet and/or genotype.

Experimental Procedures

Animal studies: The C57BL/6J (wild-type; WT) mice were purchased from The Jackson Laboratory (Bar Harbor, ME). The eNOS-TG mice, which express bovine eNOS under the control of the preproendothelin-1 promoter³³⁸, were maintained on the C57BL/6J background. At 8 weeks of age, male mice were placed on a 10% low fat diet (LFD; Research Diets, Inc., #D12450B), a 60% high fat diet (HFD; Research Diets Inc., #D12492) or a custom formulated 60% high fat diet containing GW4064 and maintained for 6 additional weeks. The custom GW4064 diet was produced by Research Diets Inc. and was formulated by adding GW4064 (Sigma, #G5172) to the HFD (#D12492) at a concentration of 180 mg of compound/kg of diet. Water and diet were provided *ad libitum*. Body weights were recorded weekly. During the 7th week of feeding, body composition analysis and glucose and insulin tolerance tests were performed. All other variables were evaluated after euthanasia. All procedures were approved by the University of Louisville Institutional Animal Care and Use Committee.

Glucose and insulin tolerance tests: As described previously³³⁹, glucose tolerance tests were performed following a 6 h fast by injection (i.p.) of D-glucose (1 mg/g) in sterile saline. Insulin tolerance tests were performed on nonfasted animals by i.p. injection of 1.5 U/kg Humulin R (Eli Lilly, Indianapolis, IN).

Body composition: Body composition was measured by dual-energy X-ray absorptiometry (Dexascan) using a mouse densitometer (PIXImus2; Lunar, Madison, WI).

Metabolomic analysis of plasma: Whole blood was collected from WT and eNOS-TG mice fed a LFD or HFD for 6 weeks by cardiac ventricular puncture following a 16 hour fast. EDTA was added to whole blood samples to prevent coagulation and plasma was separated from red blood cells by centrifugation. Samples were shipped to Metabolon, Inc. (Durham, NC) for analysis. Metabolites were extracted with methanol and relative metabolite abundance was measured by GC/MS or LC/MS/MS exactly as described before²⁸⁶. Metabolites with missing values were imputed by replacing missing values with half of the minimum positive value in the original data. Metabolites with greater than 57% of the values missing were omitted from the analysis. After a generalized logarithm transformation, the data were autoscaled, i.e., mean-centered and divided by the standard deviation of each variable. This step was performed to transform the intensity values so that the distribution was more Gaussian. Values between

groups were then compared using t-tests. Univariate (e.g., volcano plots), multivariate (e.g., PLS-DA), cluster (heatmap and dendrogram), and Z-score analyses were then performed. Z-scores were calculated using the equation: $= \frac{x - \mu}{\sigma}$; where x is the raw score, μ is the mean of the population and σ is the standard deviation of the entire population. Most analyses were performed using Metaboanalyst 2.0 software (<http://www.metaboanalyst.ca/>)²⁸⁸; Z-score plots were constructed in GraphPad 5.0 software using data derived from volcano plot analysis.

Statistical analyses: Data are presented as mean \pm SEM. Multiple groups were compared using one-way or two-way ANOVA, followed by Bonferroni post-tests. Unpaired Student's t test was used for direct comparisons. Statistical analyses were performed with the program "R" <http://cran.r-project.org/>, Metaboanalyst (<http://www.metaboanalyst.ca/>), and/or GraphPad 5.0. A P value less than 0.05 was considered significant.

Plasma bile acid measurements: Total bile acids were measured using a liquid stable enzymatic colorimetric assay (Randox Laboratories, #BI3863) and analyzed by a Cobas Mira Plus 5600 Autoanalyzer (Roche, Indianapolis, IN).

Results

Overexpression of eNOS prevents diet induced obesity. To examine the role of eNOS in the regulation of systemic metabolism, mice overexpressing eNOS

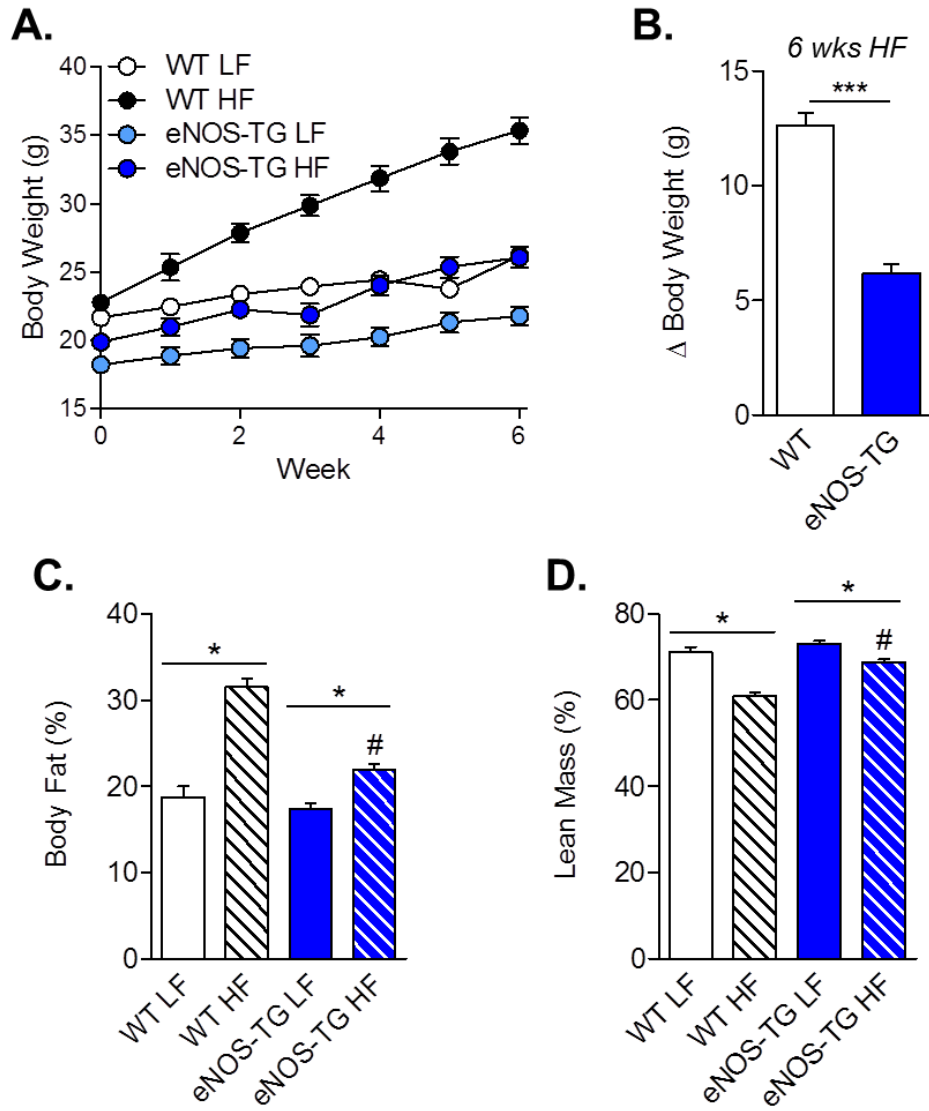
(eNOS-TG) and C57BL/6J (WT) mice were placed on a low fat diet (LFD) or high fat diet (HFD) for six weeks. In agreement with our previous results, high fat-fed eNOS-TG mice were protected against diet-induced obesity and gained 50% less weight than high fat-fed WT mice (Fig. 32B). Dexascan analysis confirmed that the body fat percentage of the eNOS-TG mice was significantly lower and lean mass was significantly higher compared with WT mice after high fat feeding (Fig. 32C,D).

Plasma metabolomic analysis. To understand how overexpression of eNOS prevents diet-induced obesity in mice in greater detail, we measured the relative abundance of circulating metabolites in the plasma of WT and eNOS-TG mice on low or high fat diets. This analysis led to the identification of 298 metabolites. Using levels of these metabolites and excluding the genotype and diet group for each animal (i.e., WT LFD), we performed a multivariate (PLS-DA) analysis of the data. We found that group separation distance was significantly different when groups were separated based on their given characteristic (genotype and diet) rather than a randomly assigned variable. This indicates that the individuals within each group are more similar to each other than if they were placed in any other randomly assembled group.

After PLS-DA confirmed that the experimental animal groups were distinct, we interrogated the differences in metabolite profiles between the groups. There were 34 metabolites that were significantly different between low fat- and high

Figure 32. Overexpression of eNOS prevents diet-induced obesity. Weight gain and adiposity measurements from WT and eNOS-TG mice fed a low fat (LFD) or high fat diet (HFD): **(A)** Body weights during 6 weeks of high or low fat feeding, n = 7 per group; **(B)** Summarized weight gain over the course of 6 weeks of HF feeding, n = 7 per group; **(C)** Body fat percentage and **(D)** lean mass percentage following 6 weeks of diet measured by Dexascan analysis. n = 7 per group; * $p < 0.05$ and *** $p < 0.001$ vs. indicated groups; # $p < 0.05$ vs. WT HFD.

Figure 32

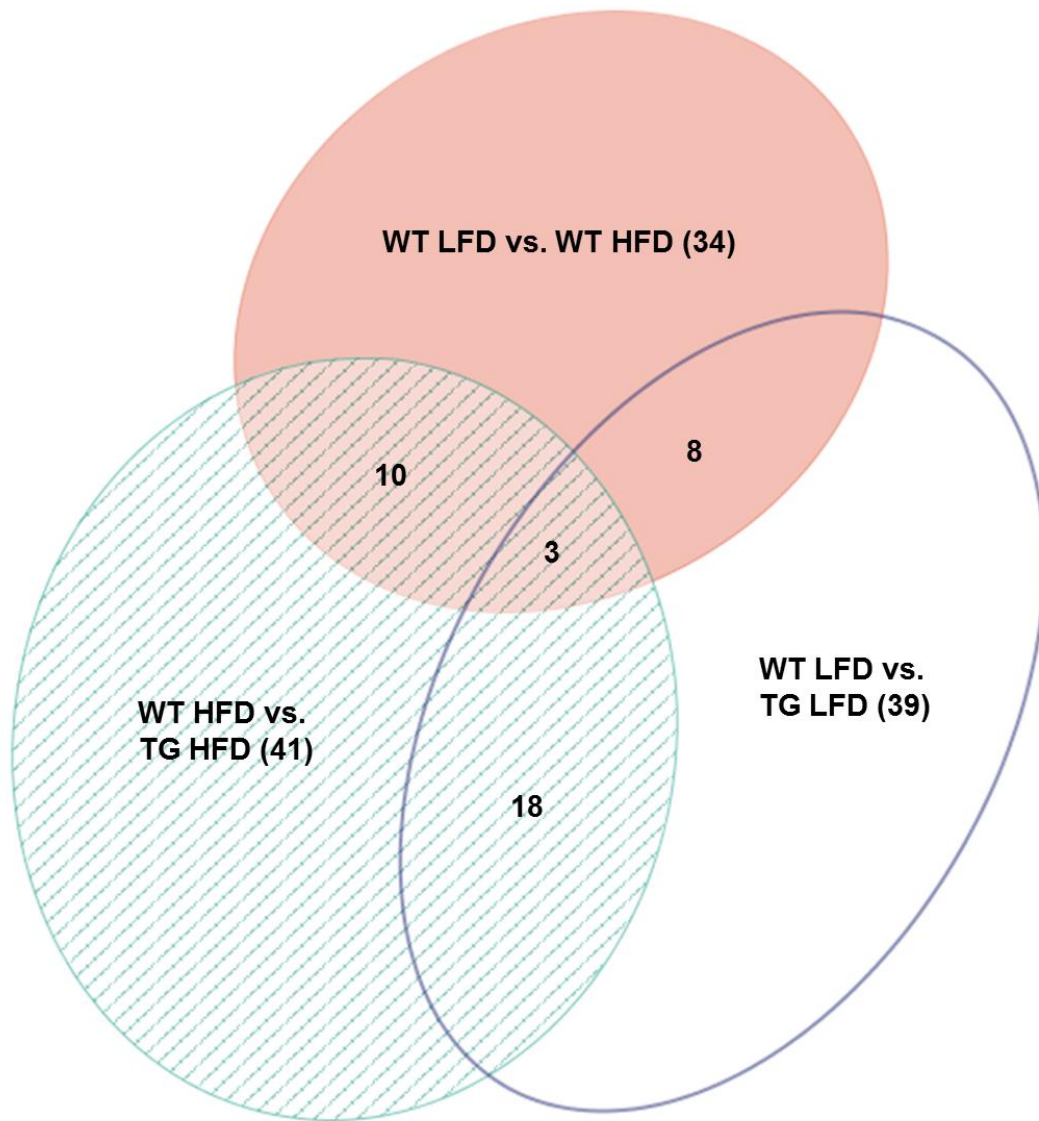


fat-fed WT mice, 39 between low fat-fed WT and low fat-fed eNOS-TG mice, and 41 between high fat-fed WT and high fat-fed eNOS-TG mice. However, each of these metabolites may not have been unique to only one comparison of animal groups. For instance, of the 34 metabolites that were significantly different between the low fat- and high fat-fed WT mice, 8 were also significantly different between the low fat-fed WT and low fat-fed eNOS-TG groups. Further, 10 of the 34 metabolites that were significantly different between low fat- and high fat-fed WT mice were also significantly different between the high fat-fed WT and eNOS-TG groups. Finally, 3 metabolites were significantly different in each comparison between the groups. This is illustrated by the Euler diagram in Figure 33 with each comparison between animal groups represented by a separate oval. The number of significantly different metabolites between these groups is in parentheses. In the regions where the ovals overlap, the number represents the number of metabolites that are shared between those comparisons of different animals.

Plasma metabolic changes due to diet. As stated above, of the 298 metabolites identified, 34 were significantly different between the low and high fat-fed WT mice. Volcano plot analysis showed that 12 of these metabolites were increased and 22 were decreased after high fat feeding (Fig. 34A). To delineate the biological relationships between metabolites that changed, we used the MetPA tool of Metaboanalyst 2.0 for pathway analysis. Pathways were calculated as the sum of the importance measures of the matched metabolites normalized

Figure 33. Changes in the plasma metabolome due to high fat feeding or eNOS overexpression. Euler diagram showing the set-theoretic relationships between WT and eNOS-TG mice fed a low fat (LFD) or high fat diet (HFD). Total number of significantly different metabolites between the groups is shown in parentheses. Number of significantly different metabolites shared between groups is in the overlapping region of the corresponding groups. Diagram constructed using Euler APE v3 software. n = 7 per group, total n = 21.

Figure 33



by the sum of the importance measures of all metabolites in each pathway²⁸⁸. The highest pathway impact value was related to branched chain amino acid (BCAA) biosynthesis (i.e., valine, leucine and isoleucine) while glycerophospholipid metabolism and glyoxalate and dicarboxylate metabolism were also elevated. The pathway with the highest statistical significance was primary bile acid synthesis (Fig. 34B).

A Z-score analysis was then performed and metabolites that were significantly changed by more than 60% were plotted (Fig. 35). Metabolites that were lower in the high fat-fed group were mostly lipids (lysolipids and long chain fatty acids). Dicarboxylic fatty acids (decanedioate, tetradecanedioate, hexadecanedioate and octadecanedioate) also were lower in high fat-fed mice. Additionally, 1,5-anhydroglucitol (a marker of glycemic control) and members of the bile acid metabolism pathway (β -muricholate, cholate, taurocholate) were reduced. Sphingolipids (palmitoyl sphingomyelin and stearoyl sphingomyelin) and markers of cysteine metabolism (S-methylcysteine and cystine) were among the metabolites that were increased.

Plasma metabolic changes due to genotype. To delineate the systemic metabolic changes that are induced by eNOS overexpression, similar analyses as described above were performed on the 39 metabolites that were significantly different between the low fat-fed WT and eNOS-TG mice. Volcano plot analysis identified that 13 metabolites were increased and 26 decreased in the eNOS-TG

Figure 34. Plasma metabolic changes due to diet. Metabolomic analyses of plasma from WT mice fed a low fat (LFD) or high fat diet (HFD) for 6 weeks: **(A)** Univariate analysis: Volcano plot of metabolites. Those metabolites that significantly increased are in the quadrant on the right side of the plot and those that significantly decreased are on the left ($p < 0.05$, t-test); **(D)** Metabolites found to be significantly different were subjected to pathway impact analysis using Metaboanalyst MetPA and the *Mus musculus* pathway library. Fisher's exact test was used for overrepresentation analysis, and relative betweenness centrality was used for pathway topology analysis. n = 14 animals: 7 WT LFD and 7 WT HFD

Figure 34

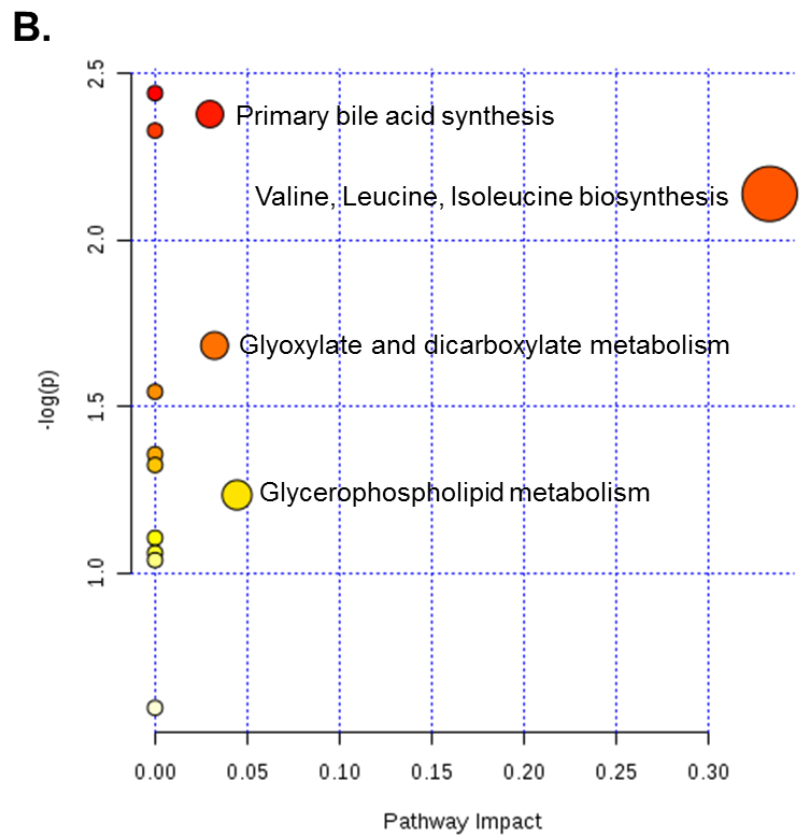
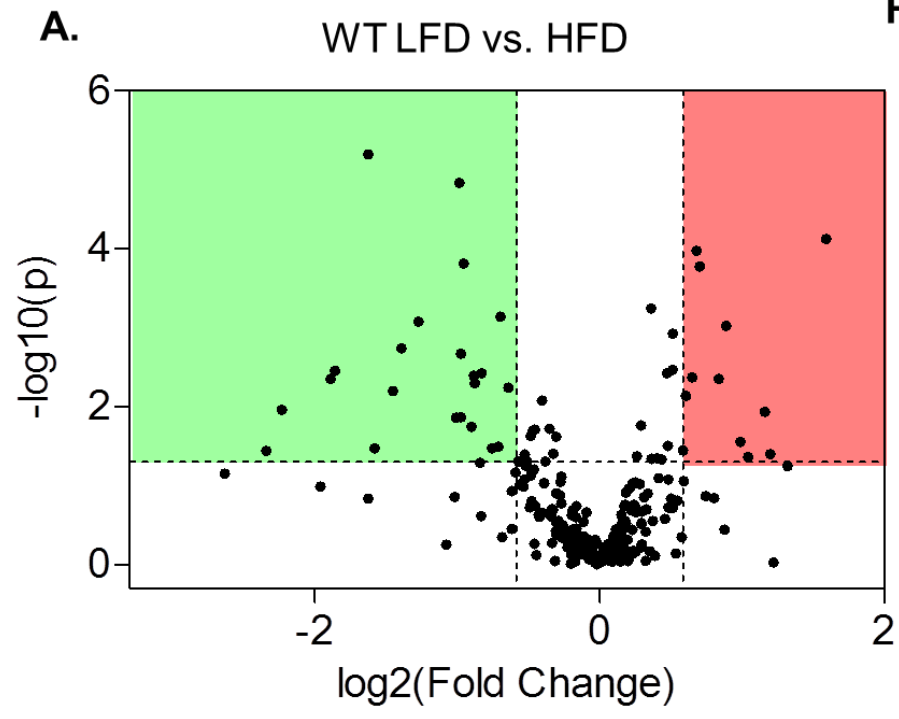
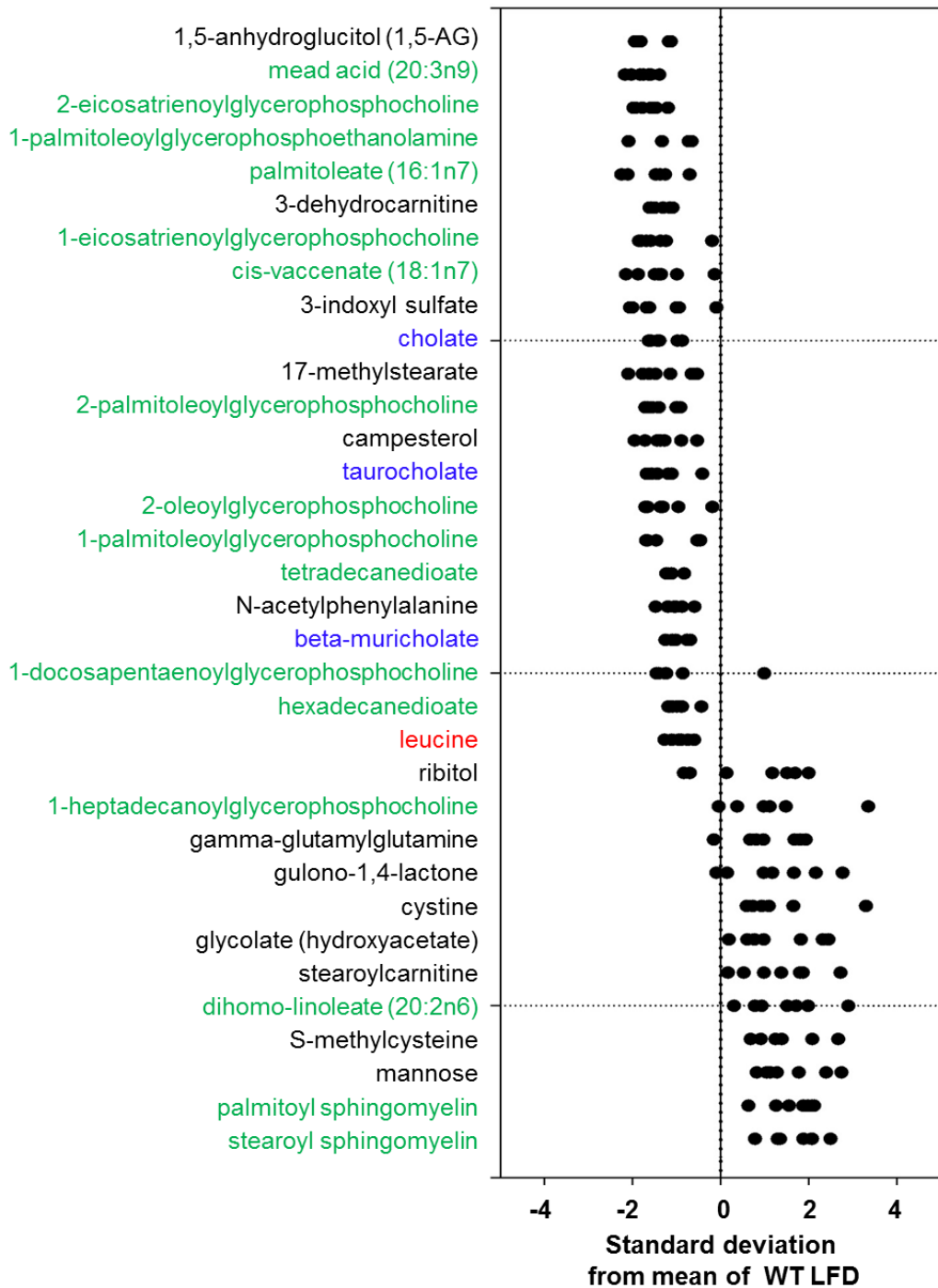


Figure 35. Z-score plot analysis of metabolite changes in plasma from low and high fat-fed mice. WT mice were fed a low fat (LFD) or high fat diet (HFD) for 6 weeks. Data are shown as standard deviations from the mean of LFD. Only metabolites that increased significantly and those that decreased by >60% are shown. Each point represents one metabolite in one sample. The color of metabolite indicates the superpathway to which it belongs: green - lipid metabolism; blue - bile acid metabolism; red - BCAA metabolism. n = 7 per group.

Figure 35

WT LFD vs. WT HFD



compared with the WT mice (Fig. 36A). Metabolic pathway analysis (Fig. 36B) showed that α -linolenic acid metabolism had a very high pathway impact value and was highly significant. Other significant pathways were BCAA metabolism, glycerophospholipid metabolism, pantothenate and CoA biosynthesis and lysine metabolism.

In the eNOS overexpressing mice several markers of BCAA metabolism (isovalerylcarnitine, propionylcarnitine, isobutyrylcarnitine, and 4-methyl-2-oxopentanoate) and bile acid metabolism (taurodeoxycholate, deoxycholate, and cholate) were significantly increased as shown in the Z-score plot (Fig. 37). Lysolipids and long chain fatty acids were decreased in the low fat-fed eNOS-TG compared with low fat-fed WT mice.

Metabolic changes in high fat-fed WT and eNOS-TG mice were also considered. Between groups there were 41 metabolites that were significantly different; as determined by volcano plot analysis, 28 were increased in the eNOS-TG mice while 13 decreased (Fig. 38A). After metabolic pathway analysis was performed (Fig. 38B) three pathways were found to have both high pathway impact values and significance: α -linolenic acid metabolism, BCAA biosynthesis, and ubiquinone and terpenoid biosynthesis. Other significant pathways were arginine and proline metabolism, bile acid biosynthesis, histidine metabolism and β -alanine metabolism.

Similar to the metabolic changes in low fat-fed eNOS-TG mice, markers of bile acid metabolism (β -muricholate, cholate, deoxycholate, taurocholate,

Figure 36. Plasma metabolic changes due to genotype. Metabolomic analyses of plasma from WT and eNOS-TG mice fed a low fat diet (LFD) for 6 weeks: **(A)** Univariate analysis: Volcano plot of metabolites. Those metabolites that significantly increased are in the quadrant on the right side of the plot and those that significantly decreased are on the left ($p < 0.05$, t-test); **(D)** The metabolites found to be significantly different were subjected to pathway impact analysis using Metaboanalyst MetPA and the *Mus musculus* pathway library. Fisher's exact test was used for overrepresentation analysis, and relative betweenness centrality was used for pathway topology analysis. n = 14 animals: 7 WT LFD and 7 eNOS-TG LFD

Figure 36

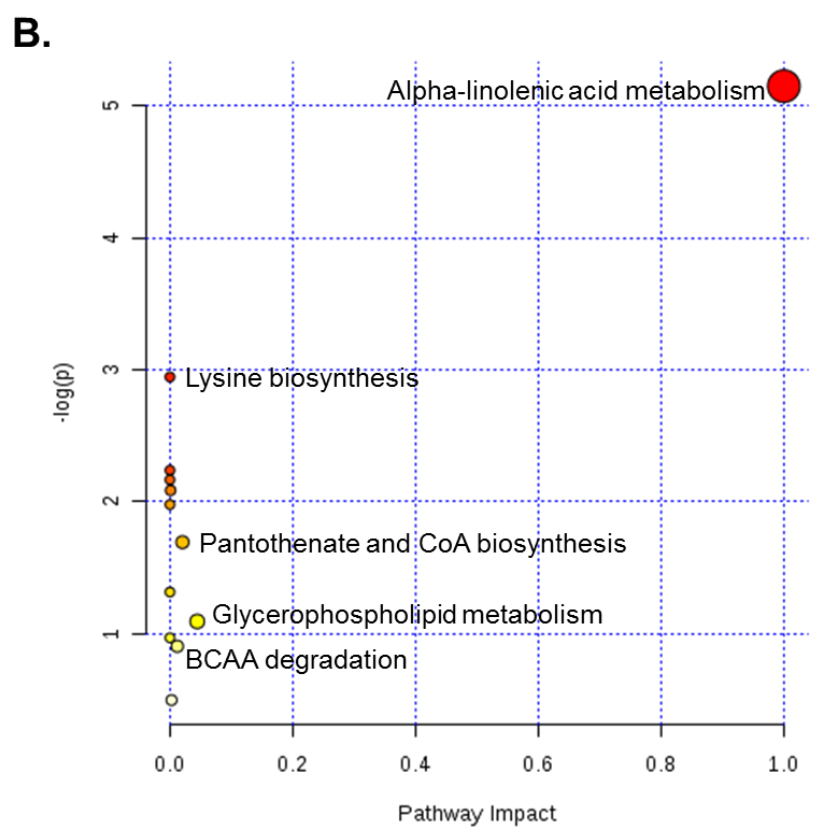
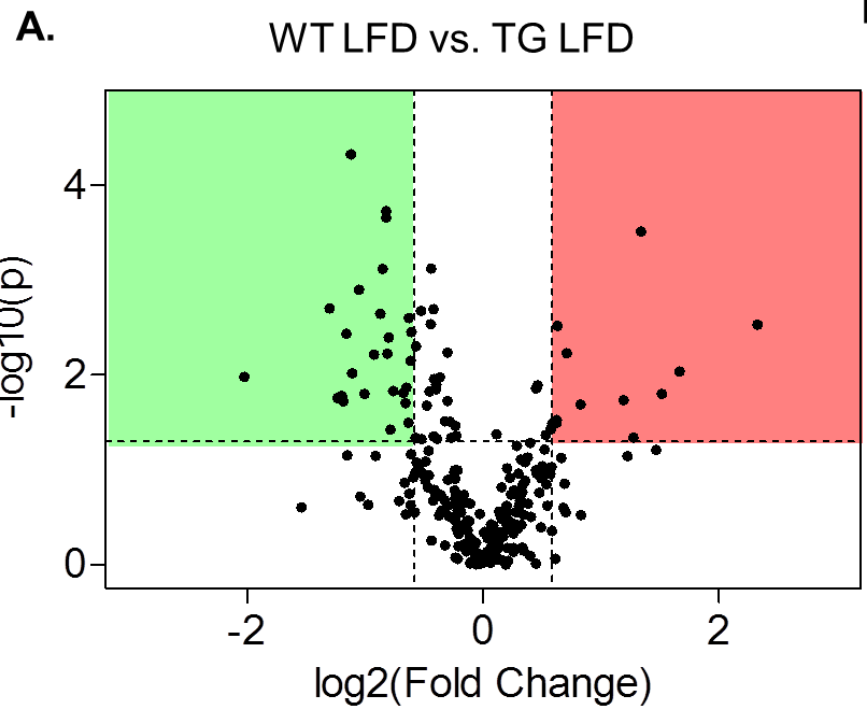


Figure 37. Z-score plot analysis of metabolite changes in plasma from low fat-fed WT and eNOS-TG mice. WT and eNOS-TG mice were fed a low fat diet (LFD) for 6 weeks. Data are shown as standard deviations from the mean of WT LFD. Only metabolites that increased significantly and those that decreased by >60% are shown. Each point represents one metabolite in one sample. The color of metabolite indicates the superpathway to which it belongs: green - lipid metabolism; blue - bile acid metabolism; red - BCAA metabolism. n = 7 per group.

Figure 37

WT LFD vs. eNOS-TG LFD

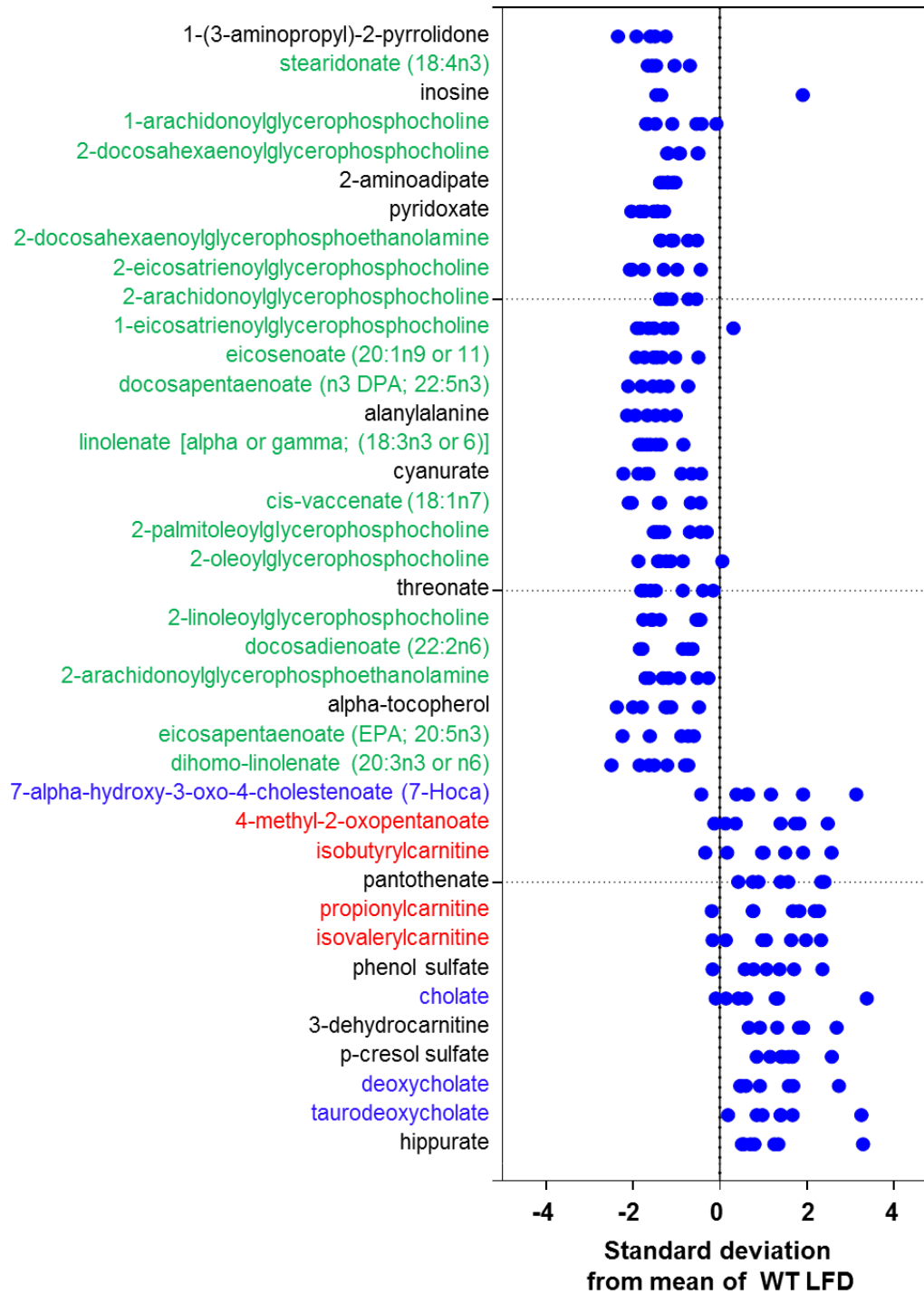
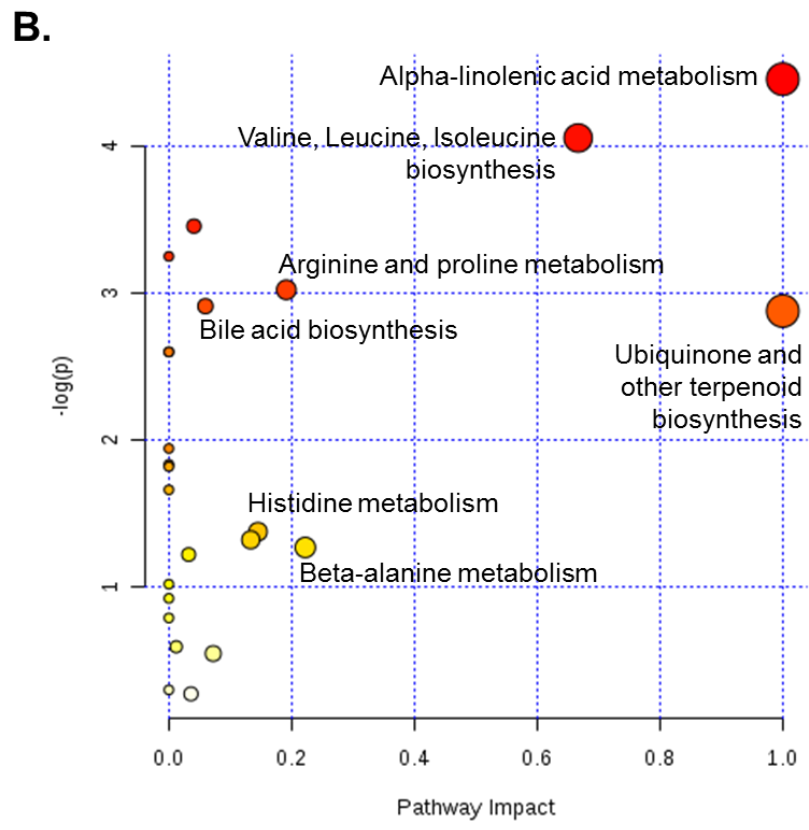
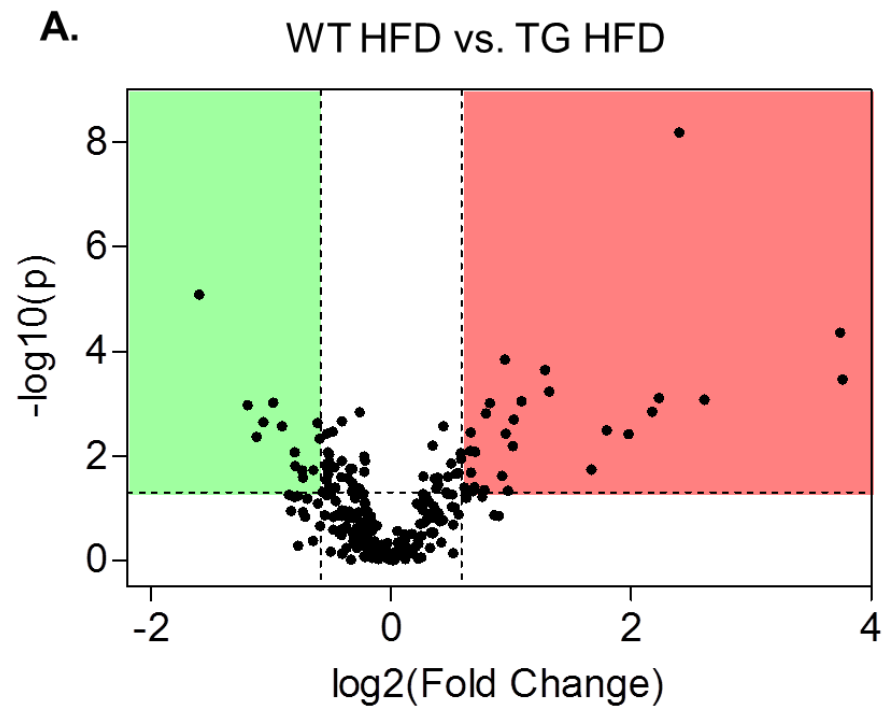


Figure 38. Plasma metabolic changes due to genotype in obesity.

Metabolomic analyses of plasma from WT and eNOS-TG mice fed a high fat diet (HFD) for 6 weeks: **(A)** Univariate analysis: Volcano plot of metabolites. Metabolites that significantly increased are in the quadrant on the right side of the plot and those that significantly decreased are on the left ($p < 0.05$, t-test); **(D)** Metabolites found to be significantly different were subjected to pathway impact analysis using Metaboanalyst MetPA and the *Mus musculus* pathway library. Fisher's exact test was used for overrepresentation analysis, and relative betweenness centrality was used for pathway topology analysis. n = 14 animals: 7 WT HFD and 7 eNOS-TG HFD.

Figure 38



taurodeoxycholate and taurochenodeoxycholate) and BCAA metabolism (isovalerylcarnitine, isobutyrylcarnitine, propionylcarnitine, N-acetyl-leucine, leucine and valine) were significantly elevated in eNOS-TG compared with WT mice on a high fat diet (Fig. 39). Phenylalanine and tyrosine metabolism and urea cycle intermediates were also significantly elevated. Levels of long chain fatty acids, lysolipids, and essential fatty acids were major metabolites that were lower in the high fat-fed eNOS-TG compared with WT mice.

Plasma metabolic changes due to diet and genotype. To visualize the metabolic changes more likely to be involved in eNOS-induced resistance to diet-induced obesity, we identified those metabolic changes occurring in HF-fed WT mice that were reversed by eNOS overexpression. For this we plotted the Z-scores of plasma metabolites found to be significantly different between WT LFD and WT HFD mice (as in Fig. 35) and then superimposed the Z-scores from eNOS-TG mice (Fig. 40). Although most metabolites were affected similarly by HFD in both genotypes, 3-dehydrocarnitine, 3-indoxyl sulfate, cholate, taurocholate, and leucine were significantly decreased by HFD in WT mice but were comparatively higher in high fat-fed eNOS-TG mice. This could indicate that the metabolic pathways to which they belong may be important in the mechanism by which eNOS overexpression protects from diet-induced obesity and adiposity.

Figure 39. Z-score plot analysis of metabolite changes in plasma from high fat-fed WT and eNOS-TG mice. WT and eNOS-TG mice were fed a high fat diet (HFD) for 6 weeks. Data are shown as standard deviations from the mean of WT HFD. Only metabolites that increased significantly and those that decreased by >60% are shown. Each point represents one metabolite in one sample. The color of metabolite indicates the superpathway to which it belongs: green - lipid metabolism; blue - bile acid metabolism; red - BCAA metabolism. n = 7 per group.

Figure 39

WT HFD vs. eNOS-TG HFD

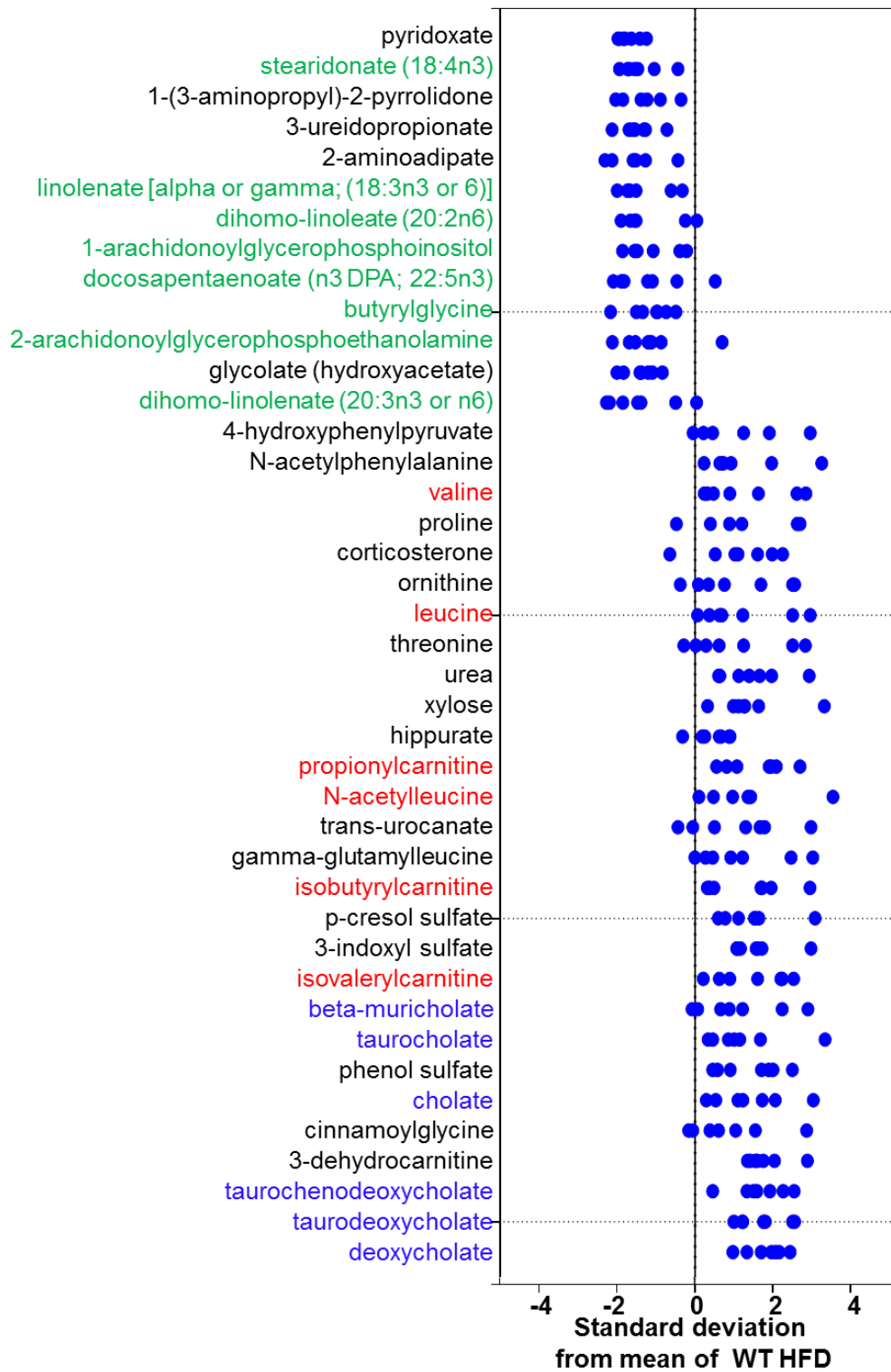
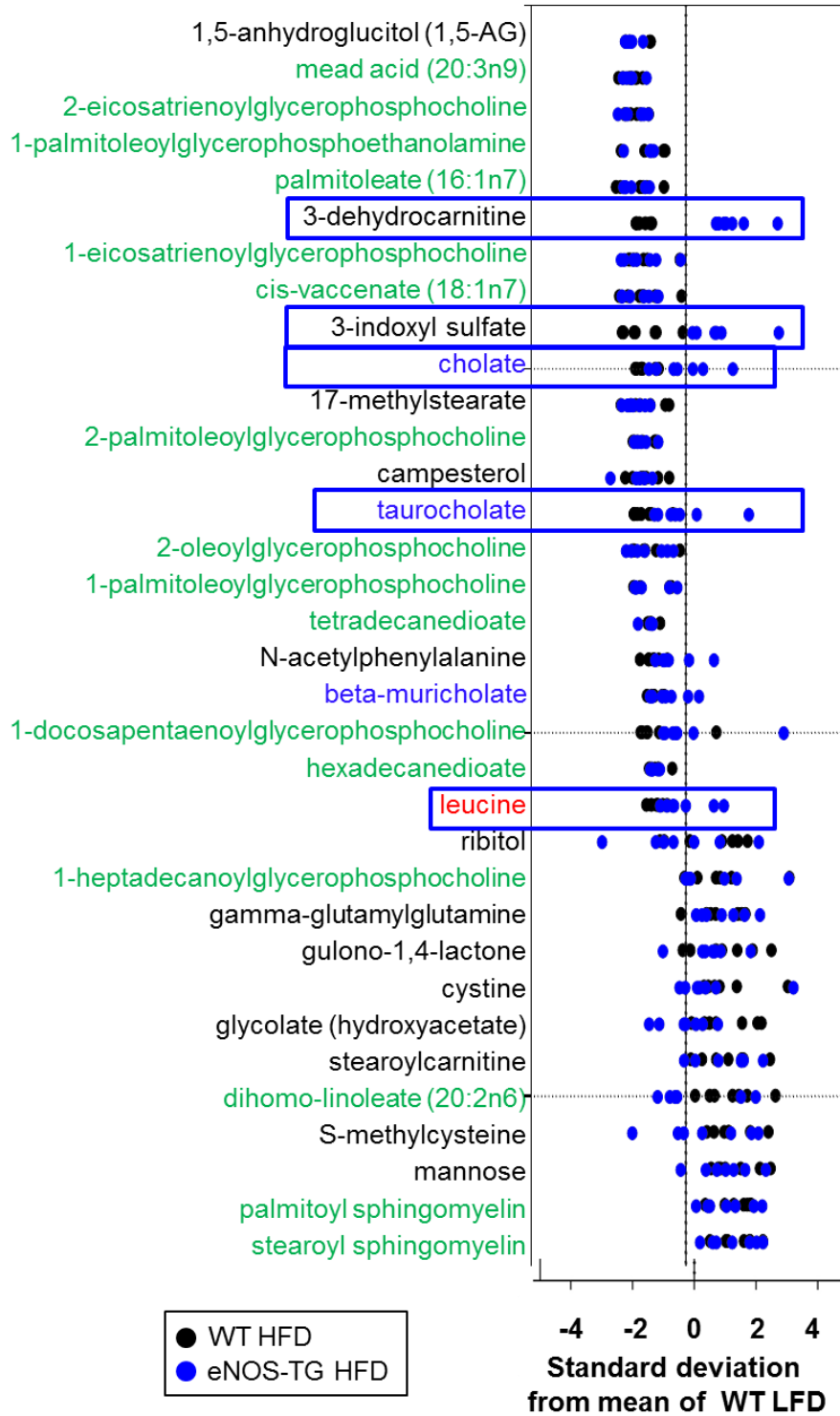


Figure 40. Modified Z-score plot analysis of metabolite changes in plasma from low fat-fed WT and both high fat-fed WT and eNOS-TG mice. WT mice were fed a low fat (LFD) or high fat diet (HFD) and eNOS-TG mice were fed a HFD for 6 weeks. Data are shown as standard deviations from the mean of WT LFD. Metabolites that increased significantly and those that decreased by >60% between the WT LFD and HFD (black circles) are shown. Levels of those metabolites were then compared between WT LFD and eNOS-TG HFD and plotted (blue circles). Each point represents one metabolite in one sample. n = 7 per group.

Figure 40

WT LFD vs. WT and eNOS-TG HFD

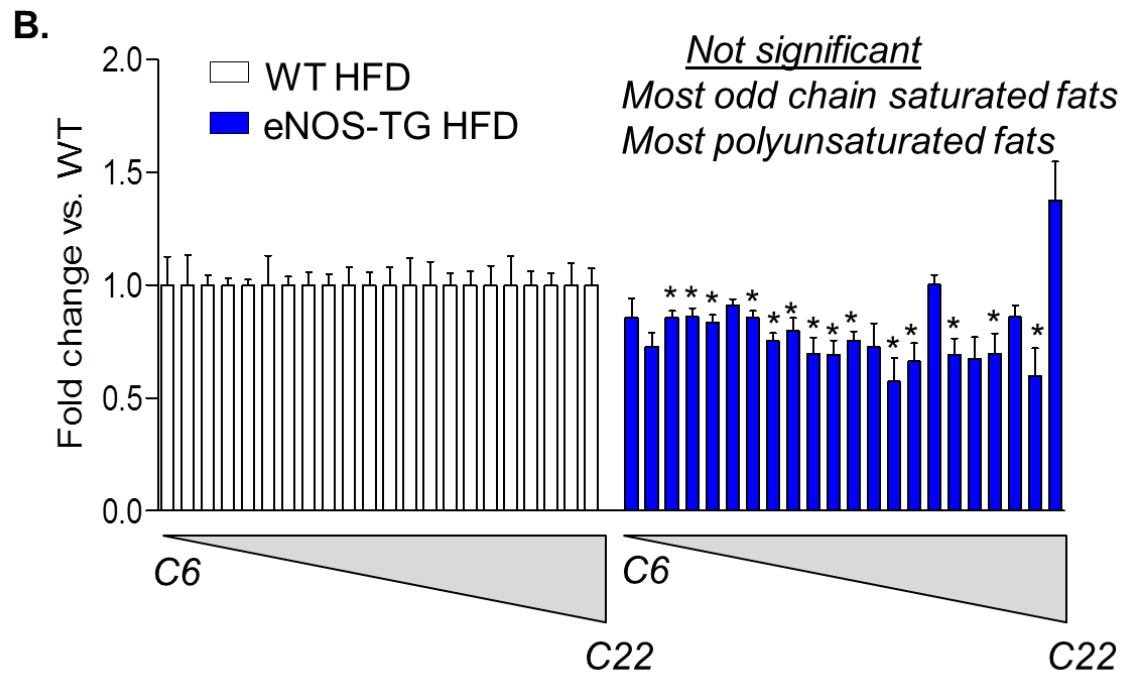
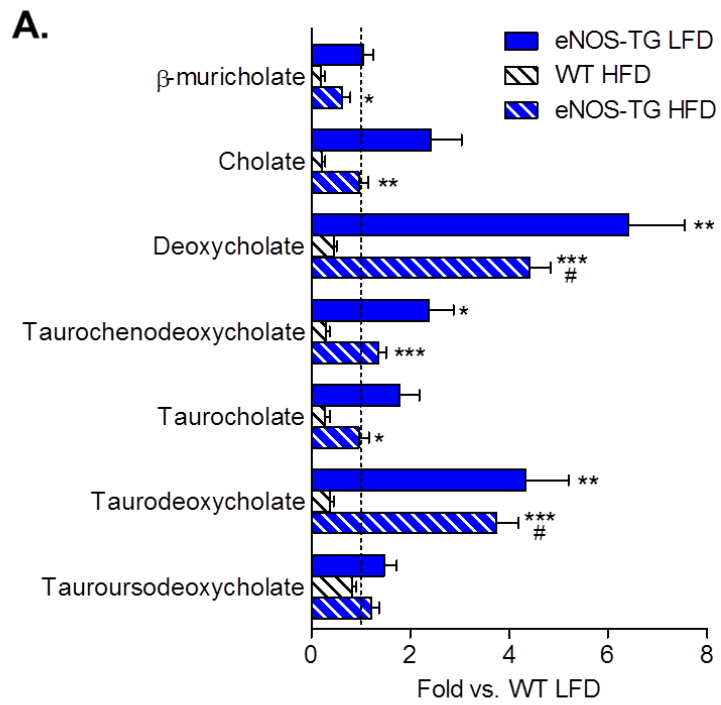


Changes in bile acids and fatty acids are induced by diet and eNOS overexpression. Analyses described above suggested that bile acid metabolism, which can regulate energy expenditure and obesity^{421, 422}, and carnitine metabolism, which is involved in regulating fatty acid oxidation, might be significant pathways contributing to eNOS-induced resistance to obesity. Therefore, to obtain additional insights into these metabolic changes, we plotted changes in bile acids and fatty acid metabolism. In WT mice, HFD significantly decreased 5 of the 7 bile acids compared with WT, low fat-fed mice (dotted line, Fig. 41A). In the context of LFD, eNOS overexpression was associated with higher levels of three of the bile acids compared with WT (Fig. 41A). On HFD, eNOS-TG mice had significantly higher levels of all but one bile acid compared with high fat-fed WT mice (Fig. 41A). When compared with WT LFD mice, levels of bile acids were not significantly different in eNOS-TG mice fed a HFD, with the marked exception of deoxycholate and taurodeoxycholate which were significantly elevated.

Bile acid signaling has been linked to increased fatty acid oxidation by increased PPAR α ⁴²³ and PDK-4⁴²⁴ expression in liver. Our previous metabolic pathway analyses showed that α -linolenic acid metabolism had the highest pathway impact and statistical significance of any pathway in eNOS-TG mice when compared to WT on both diets (Fig 36B and 38B). Together these results led us to investigate if levels of markers of fatty acid metabolism mirrored those of bile acids. Indeed, medium-chain, long-chain, and essential fatty acids were decreased in eNOS-TG mice when compared with WT on both LFD (data not

Figure 41. Changes in bile acid and fatty acid levels induced by diet and eNOS overexpression. Plasma levels of **(A)** bile acids obtained from metabolomics analyses from WT mice fed a high fat diet (HFD) (white hatched bars) or eNOS-TG mice fed a low fat diet (LFD) (blue bars) or HFD (blue hatched bars) for 6 weeks. n = 7 per group; * $p < 0.05$, ** $p < 0.01$ and *** $p < 0.001$ vs. WT of same diet; # $p < 0.001$ vs. WT LFD. **(B)** Plasma levels of fatty acids from HFD-fed WT (white bars) and eNOS-TG (blue bars) mice. Data are expressed as fold change vs. WT HFD. n = 7 per group, * $p < 0.05$ vs. WT HFD.

Figure 41

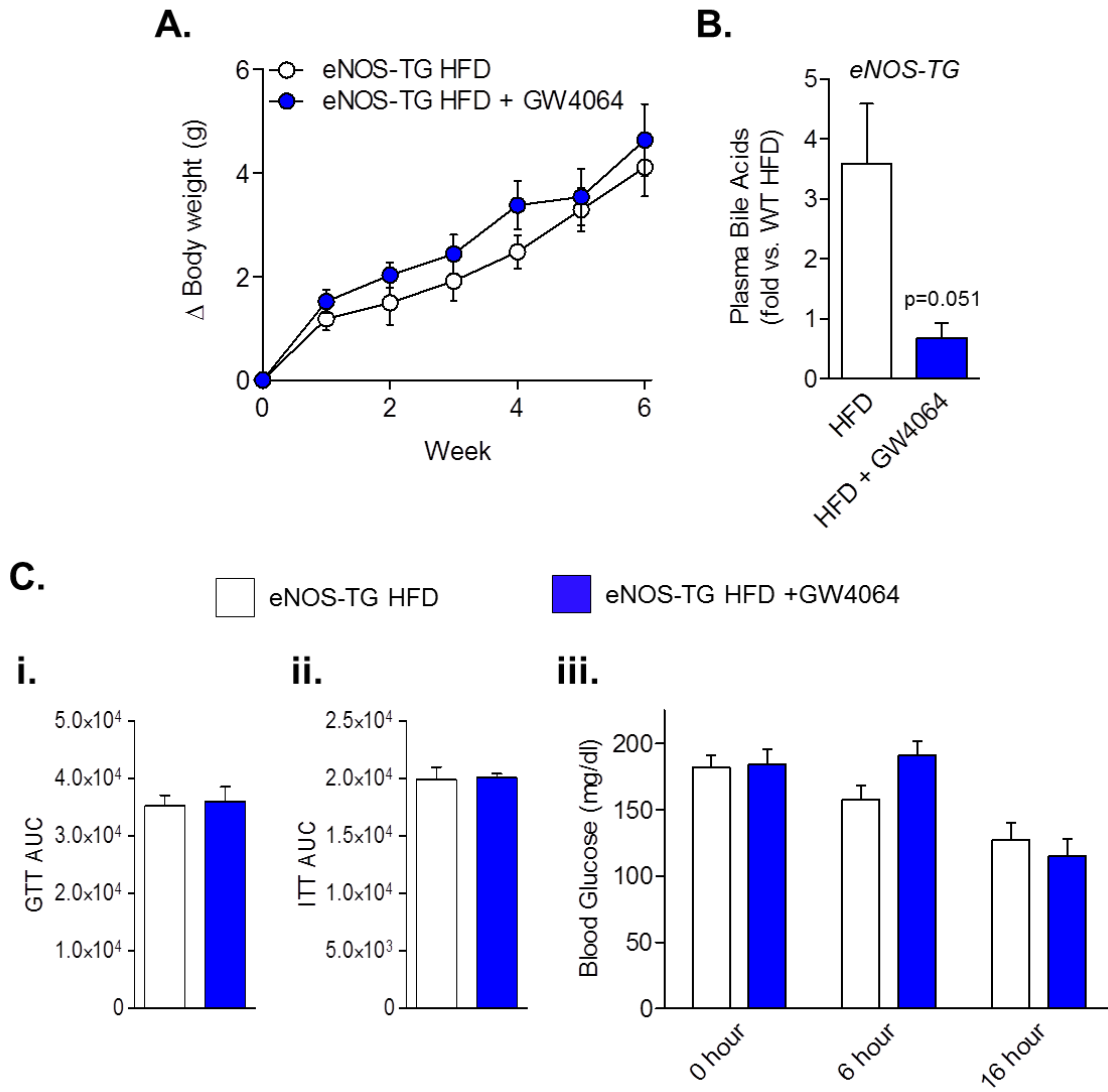


shown) and HFD (Fig. 41B). A majority of fatty acid species that were not significantly decreased were either saturated fats with an odd numbered chain length or polyunsaturated fats. These data suggest that eNOS overexpression increases bile acid synthesis, which could increase the oxidation of fatty acids and augment overall energy expenditure

Preventing bile acid synthesis does not prevent diet-induced obesity. To test whether the lean phenotype of eNOS-TG mice is due to eNOS-induced changes in bile acid metabolism, eNOS-TG mice were placed on a HFD for 6 weeks along with a synthetic inhibitor of bile acid synthesis, GW4064, which is a farnesoid X receptor (FXR) agonist that decreases bile acid biosynthesis and bile acid pool size in C57BL/6J mice ⁴²¹. We reasoned that if bile acids are responsible for the lean phenotype of eNOS-TG mice, decreasing their synthesis should increase weight gain. Treatment of eNOS-TG mice with the bile acid inhibitor showed a trend toward decreased levels of circulating bile acids (Fig. 42B), however there was no difference in weight gain compared with those fed HFD alone (Fig. 42A). Likewise, glucose tolerance, insulin sensitivity and fasting blood glucose levels were unaffected by the GW4064 supplementation (Fig. 42C-i-iii). These findings indicate that eNOS overexpression increases systemic energy expenditure by a bile acid-independent mechanism.

Figure 42. Preventing bile acid synthesis does not prevent diet-induced obesity. eNOS-TG mice were fed a high fat diet (HFD) with or without GW4064 for 6 weeks. Body weight gain, glucose tolerance and insulin sensitivity were examined: **(A)** Body weight gain by week of HFD. n = 5-6 per group; **(B)** Levels of plasma bile acids. n = 4-6 per group; **(C)** Glucose tolerance test (GTT) area under the curve (AUC), insulin tolerance test (ITT) AUC and fasting blood glucose levels are shown. n = 5-6 per group.

Figure 42



Discussion

The major goal of this study was to identify systemic metabolic changes that could underlie the lean phenotype induced by eNOS overexpression. During this analysis we considered that eNOS overexpression could either prevent a defect caused by high fat feeding or increase metabolic pathways that would otherwise promote resistance to obesity. Using metabolomics analysis, we identified several metabolic pathways that were significantly affected by high fat feeding or overexpression of eNOS. We found that, bile acid metabolites were significantly decreased by high fat feeding and significantly elevated due to eNOS overexpression. Additionally, after high fat feeding, bile acids remained significantly elevated in eNOS-TG compared to WT mice. This indicated that eNOS protects from a diet-induced suppression of bile acid metabolism and may play a role in the resistance to obesity observed in eNOS-TG mice. We also found evidence of significantly increased fatty acid metabolism in eNOS-TG mice. Therefore, we hypothesized that eNOS overexpression stimulates bile acid synthesis, which in turn increases both fatty acid oxidation and energy expenditure, providing intrinsic resistance to diet-induced obesity. If this were true, we reasoned that inhibiting bile acid synthesis would cause an accentuated weight gain in eNOS-TG mice on a HFD. Alternatively, bile acid-independent, eNOS-dependent changes in fatty acid metabolism could be important for the maintenance of a lean phenotype.

To understand how eNOS overexpression induces a lean phenotype during nutrient excess, we first investigated the systemic metabolic changes that

occur in WT mice on a HFD. Metabolomic analyses showed several metabolic pathways affected in obesity. Primarily, HFD altered fatty acid and lipid metabolism (mainly lysophospholipid and sphingolipids), bile acid metabolism, glucose and cholesterol metabolism and markers of oxidative stress.

Lysophospholipid metabolism and its role in the regulation of obesity and systemic metabolism are unclear. The term 'lysophospholipid' (LPL) refers to any phospholipid that is missing one of its two O-acyl chains. Thus, LPLs have a free alcohol at either the sn-1 or sn-2 position. The prefix 'lyso-' derives from the early observations that LPLs were hemolytic, however, it is now used to refer generally to phospholipids missing an acyl chain. Lysophosphatidylcholine (lysoPC) is found in small amounts in most tissues and is formed by hydrolysis of phosphatidylcholine by the enzyme phospholipase A2, as part of the de-acylation/re-acylation cycle that controls its overall molecular composition ⁴²⁵. In plasma, significant amounts of lysoPC are formed by a specific enzyme system, lecithin:cholesterol acyltransferase (LCAT), which is secreted from the liver ⁴²⁶. The enzyme catalyzes the transfer of the fatty acids of position sn-2 of phosphatidylcholine to the free cholesterol in plasma, with formation of cholesterol esters and lysoPC ⁴²⁷. LPLs play a key role in lipid signaling by binding to the LPL receptors (LPL-R) ⁴²⁸. LPL-Rs are members of the G protein-coupled receptor family of integral membrane proteins ⁴²⁹. LysoPCs are known to account for 5–20% of all phospholipids in the serum ⁴³⁰ and have been suggested to be closely associated with endothelial dysfunction, oxidative stress, inflammation, atherogenesis, and obesity ⁴³⁰.

Since lysoPCs have a relatively short half-life, they are thought to be metabolic intermediates that are produced during the formation or breakdown of other lipids. LysoPCs can have different combinations of fatty acids of varying lengths and saturation attached at the C-1 (sn-1) position. Fatty acids containing 16, 18 and 20 carbons are the most common. In our analysis, several species of lysoPC, including lysoPC 16:1 and 18:1 were decreased while one, lysoPC 17:0, was increased by HFD. These findings are in accordance with a previous study that showed decreased levels of lysoPC 16:1 and 18:1, as well as lysoPC 14:0, 15:0, 16:0, 17:1, 18:2, 19:0, 20:1 and 20:4 while lysoPC 17:0, 18:0 and 18:3 were increased in diet-induced obese mice ⁴³¹. Additional studies have shown decreased serum levels of lysoPC 18:1 and increased lysoPCs 14:0 and 18:0 in obese men ⁴³² as well as increased lysoPC 18:0 in high fat-fed pigs ⁴³³. While there was an association between specific lysoPC species and obesity, further study is needed to elucidate their role in regulation of body composition.

Decreased levels of lysoPCs measured in obesity could indicate a decrease in the activity of the enzymes responsible for their esterification. However, studies in mice lacking LCAT, the main generator of circulating lysoPCs, demonstrate a resistance to diet-induced obesity and insulin insensitivity ⁴³⁴. Further, LDLR/LCAT double knockout mice, in addition to remaining lean after high fat feeding, display ectopic depositions of brown adipocytes in skeletal muscle ⁴³⁴. Though phospholipids, generally, were decreased in these mice, the authors did not specify as to their species. Conversely, overexpression of LCAT in mice has been shown to increase plasma

HDL and markedly reduced VLDL, LDL and triglyceride levels, but offered no protection from the development of diet-induced atherosclerosis ⁴³⁵. While our analysis is suggestive of a decreased synthesis of circulating lysoPCs by LCAT, further examination of the activity and expression of the enzyme would be necessary to determine the mechanism underlying these changes.

As in our previous analysis of adipose tissue, we found that the plasma levels of sphingolipid metabolites were profoundly increased in obesity. Palmitoyl sphingomyelin and stearoyl sphingomyelin were the most significantly increased metabolites high and low fat-fed animals. As mentioned previously (Chapter II), the breakdown of sphingomyelin could yield significant amounts of ceramide, which is a potent inhibitor of insulin signaling. Plasma ceramide levels are elevated in obese individuals and correlate with the severity of insulin resistance ⁴³⁶.

Carbohydrate metabolism and glucose handling were also altered by HFD, specifically, glucose and mannose levels were elevated while 1,5-anhydroglucitol (1,5-AG), an important marker of glycemic control ⁴³⁷, was significantly decreased. This evidence of disrupted glucose metabolism is consistent with our previous data that six weeks of high fat feeding is sufficient to induce glucose and insulin intolerance (Chapter II, Fig. 4).

Bile acids have been shown to be potent regulators of metabolism. Synthesized from cholesterol in the liver, bile acids are secreted into the intestines to aid in digestion, primarily fat emulsion ⁴³⁸. Recently, new roles for

bile acids as important signaling molecules have also been described. Bile acid signaling has been shown to augment energy expenditure⁴³⁹, lipid and glucose homeostasis^{440, 441}, and body composition⁴²¹. Through its control of short heterodimer partner (SHP) expression, FXR has been shown to downregulate hepatic fatty acid and triglyceride synthesis⁴⁴⁰ while bile acid supplementation increased brown adipose tissue energy expenditure and prevented obesity and insulin resistance in mice⁴³⁹. Conversely, decreasing bile acid pool size worsened obesity and diabetes in high fat-fed mice⁴²¹. Further, there is evidence supporting an NO-induced increase of bile acid synthesis. Perfusion of livers with NO donors increased bile acid outflow^{442, 443} while inhibition of NOS reduced the biosynthesis of bile acids by inhibiting the activity of hepatic Cyp7A1⁴⁴⁴, the rate-limiting enzyme in bile acid production⁴⁴⁵. Bile acids can also increase mitochondrial biogenesis. Through the binding and activation of the G-coupled receptor, TGR-5, in brown adipose tissue and skeletal muscle, bile acids trigger a signaling cascade that activates PGC-1 α , a master regulator of mitochondrial biogenesis⁴³⁹. These data support the idea that increased bile acid synthesis in eNOS-TG mice could have a significant impact on body composition and energy expenditure.

The relationship of bile acids and triglyceride metabolism has been established for decades⁴⁴⁵. In clinical trials, dyslipidemic patients given bile acid-sequestering resins exhibited increased plasma triglyceride and VLDL levels^{446, 447}. Additionally, patients with deficiencies in *CYP7A1* are also characterized by increased plasma triglyceride concentrations⁴⁴⁸. In rodent models, FXR

activation has been linked to lower plasma triglycerides^{440, 449} by the induction of hepatic PPAR α expression⁴²³. In our analysis, overexpression of eNOS induced a broad decrease in plasma FFA levels, predominantly long chain fatty acids and essential fatty acids. Further, on HFD levels of the β -oxidation intermediates, 3-hydroxyoctanoate and 3-hydroxydecanoate, were decreased while the carnitine-conjugated end product, propionylcarnitine, was higher in eNOS-TG mice compared with WT mice. Taken together, these data suggest that eNOS overexpression increased β -oxidation and decreased fatty acid synthesis.

Studies in NO donor-treated rat hepatocytes showed similar results by increasing β -oxidation in a cGMP-dependent manner and decreasing lipid synthesis⁴⁵⁰. Additionally, inhibitors of NOS⁴⁵¹ and deletion of eNOS increased hepatic lipid synthesis⁴⁵². The eNOS KO mice also showed decreased expression of genes involved in β -oxidation and increased expression of neolipogenic genes in skeletal muscle³³⁷. Collectively, these data suggest that eNOS regulates lipid metabolism, possibly via a PPAR α -mediated mechanism⁴⁵³. As shown previously, PPAR α was elevated in the adipose tissue of eNOS-TG mice (Chapter III) which supports the hypothesis that eNOS overexpression increases fatty oxidation capacity.

Because the liver is the site of both bile acid synthesis and fatty acid metabolism, we hypothesized that eNOS overexpression increases bile acid synthesis, and, in doing so, might increase fat utilization, either directly by increasing PPAR α activity in the liver, or indirectly, by promoting increased thermogenesis in other peripheral tissues, such as brown adipose tissue.

Activation of FXR by the synthetic agonist GW4064 was shown previously to be sufficient to decrease bile acid levels and energy expenditure, thereby accentuating diet-induced weight gain and insulin resistance ⁴²¹. However, in our study, bile acid inhibition had no effect on weight gain, glucose handling or insulin sensitivity in eNOS-TG mice.

These data appear to indicate that eNOS overexpression increases fatty acid metabolism and systemic energy expenditure by a bile acid-independent mechanism. The increase in PPAR α expression measured in the adipose tissue of eNOS-TG mice may indicate that eNOS overexpression has a direct effect on PPAR α -mediated increased fatty acid oxidation in other tissues as well. To address this hypothesis, we plan to measure PPAR α -driven genes in liver and skeletal muscle. Should results suggest a role for PPAR α , future experiments would focus on pharmacological or genetic disruption of PPAR α in the eNOS overexpressing mice. For example, crossing PPAR α knockout mice with eNOS-TG mice and feeding a high fat diet could be an especially revealing experiment. If these mice were to become obese as a result of high fat feeding we would have strong evidence to support the claim that eNOS protects from obesity via a PPAR α -mediated mechanism. Additionally, activation of PPAR α in WT mice during high fat feeding could also be informative. Fibrates are a class of PPAR α agonists that have been used in combination with statins to lower plasma cholesterol and triglycerides ⁴⁵⁴ and have been shown to reduce micro- and macrovascular risk ⁴⁵⁵. Fibrate treatment during high fat feeding of WT mice

would provide additional insights into the role of PPAR α -induced fatty acid metabolism on the development of metabolic disease.

Fibrates have also been shown to promote the catabolism of BCAAs⁴⁵⁶. In our analysis, plasma levels of BCAAs and short-chain acyl carnitines were decreased in high fat-fed WT mice and increased in the eNOS-TG mice, similar to our previous findings in adipose tissue (Chapter III). It has been shown before that plasma BCAAs are increased in obese and diabetic humans and rodents^{66, 312}, but the significance of BCAAs in regulating adiposity or insulin resistance is unclear. BCAAs have also been shown to promote insulin resistance³¹². Despite lower levels of weight gain, rats fed a BCAA/HF diet remain insulin resistant. Sustained insulin resistance in these rats has been linked to mTOR activation³¹², which induces insulin resistance by phosphorylating IRS1^{457, 458}.

BCAA supplementation has been shown to have favorable effects on diet-induced metabolic disease. Feeding leucine prevented obesity in rodents^{459, 460}, and was associated with lower adiposity in humans⁴⁶¹, while isoleucine decreased tissue TG accumulation and adiposity and increased expression of PPAR α and UCPs in diet-induced obese mice⁴⁶². Additionally, increasing BCAA levels by deletion of BCATm, the enzyme that catalyzes the first step in BCAA metabolism, completely prevents HFD-induced insulin resistance and adiposity in mice³¹¹. Furthermore, BCAAs as well as 3C-acylcarnitines increase mitochondrial biogenesis and promote energy expenditure^{311, 354-356}. Therefore, it is possible that BCAA levels in high fat-fed eNOS-TG mice is due to increased protein degradation and synthesis, which dissipates excess energy.

Limitations of this study are inherent to the descriptive approach employed by metabolomics analyses. Metabolomics is a powerful analytical tool to interrogate wide-ranging changes in different experimental samples. However, metabolomics analysis is designed mainly to generate new hypotheses as opposed to test specific hypotheses. These analyses can be very useful in nutritional research and biomarker discovery, but they give only a “snapshot” of changes that are occurring at that moment. Furthermore, current libraries of known metabolites and metabolic pathway models are incomplete. Nevertheless, such approaches are indispensable for identifying novel pathways that might be important to health and disease.

In summary, this study identified significantly altered metabolic pathways due to high fat feeding and eNOS overexpression. Bile acid metabolism and fatty acid metabolism pathways were significantly decreased by nutrient excess in WT mice but were rescued by eNOS overexpression. Inhibiting bile acid synthesis did not produce an obese phenotype in eNOS-TG mice on HFD; however, eNOS shows a clear influence on fatty acid metabolism. Future studies will focus on the mechanism(s) by which increased eNOS activity regulates fatty acid metabolism and energy expenditure.

CHAPTER V

CONCLUDING DISCUSSION

We undertook the studies presented here were to develop a better understanding of how NO regulates metabolism. For this, we examined metabolic changes that accompany diet-induced obesity and insulin resistance and we assessed the impact of increasing NO during nutrient excess. **Our hypothesis was that increased NO derived from eNOS prevents diet-induced obesity by promoting adipose tissue browning and increasing systemic metabolism.** To address this hypothesis, we examined whether overexpression of eNOS was sufficient to promote metabolic alterations in WAT during high fat feeding that would prevent obesity and insulin resistance. To obtain a more comprehensive view, we investigated changes in systemic metabolism that were induced by eNOS.

As discussed in Chapter II, we first examined the metabolic and bioenergetic changes occurring in WAT with obesity. After six weeks of high fat feeding, metabolomic analyses showed marked changes in glycerolipid and amino acid metabolism, with most metabolites showing a decrease in WAT of obese mice. Levels of succinate, however, increased significantly in WAT from high fat-fed mice, suggesting changes in mitochondrial metabolism. Furthermore,

we found changes indicative of mitochondrial remodeling, decreased mitochondrial bioenergetic capacity and striking decreases in eNOS abundance. Collectively, these results revealed a range of coordinated changes in mitochondrial function that might be contributing to the “whitening” of adipose tissue in obesity.

To examine the significance of in eNOS downregulation in WAT, we investigated whether increasing eNOS expression would prevent obesity and its metabolic consequences. In Chapter III, we present data showing that endothelial-specific overexpression of eNOS prevents diet-induced obesity and reduces plasma levels of insulin, TGs and FFAs, without affecting systemic glucose intolerance. The eNOS-TG mice displayed a higher metabolic rate and reduced adipocyte hypertrophy in WAT. Metabolomic analyses indicated an increase in fatty acid oxidation in WAT that was reflected by an increase in the expression levels of PPAR- α and PPAR- γ genes, higher abundance of mitochondrial proteins and increased rate of mitochondrial oxygen consumption. These findings demonstrate that eNOS has anti-obesogenic effects that prevent high fat diet-induced obesity without affecting systemic insulin resistance, in part by stimulating metabolic activity in WAT.

Although effects of eNOS overexpression on WAT were quite profound, we questioned whether these effects could account fully for the increase in whole-body energy expenditure and the lean phenotype observed in eNOS-TG mice. Therefore, as discussed in Chapter IV, we studied effects of eNOS overexpression on systemic metabolism. Measurements of plasma metabolites in

eNOS-TG mice were consistent with increases in fatty acid, bile acid and BCAA metabolism. However, our experiments to decrease bile acids in eNOS-TG mice did not markedly affect on body composition and glucose or insulin handling suggesting that the metabolic effects of eNOS overexpression on fatty acid metabolism are not mediated by bile acids. From these findings we propose that eNOS increases BCAA metabolism thereby increasing PPAR α activity in the liver and possibly skeletal muscle leading to increased fat utilization. Further elucidation of the regulatory effects of eNOS on BCAA metabolism and its effects on fatty acid metabolism could help understand the mechanism by which eNOS increases systemic energy expenditure and prevents adiposity.

Nevertheless, data obtained from studies so far support a pivotal role of NO as a central regulator of energy metabolism and body composition. This regulation, however, is inherently complex and growing evidence demonstrates divergent effects of NO depending on its source and anatomic location. In the sections that follow, our findings are discussed in the context of the known interactions between NO, its sources of generation and obesity and insulin resistance.

Regulation of obesity and insulin resistance by NO

In one approach, pharmacological studies as well as gain-of-function and loss-of-function studies helped in elucidating the critical roles for NO in regulating obesity and insulin resistance. Previously, supplementation with the NOS

substrate, L-arginine, and inhibition of NOSs were the most common pharmacological approaches used to determine how NO regulates body composition and insulin sensitivity. Genetic approaches, utilizing mice in which components integral to the synthesis of NO have been deleted or overexpressed, have led to further development of a model by which NO regulates systemic metabolism. The model thus built is extensive in its complexity and integration and involves nearly all aspects thought to be important in regulating metabolic homeostasis.

Lessons from pharmacological interventions

Using primarily L-arginine and NOS inhibitors, early pharmacological studies showed that NO is a potent regulator of both energy intake and expenditure. Interestingly, both L-arginine and NOS inhibitors prevent obesity and insulin resistance, albeit by different mechanisms.

nNOS-derived NO increases food intake

In rodents, L-arginine was shown to increase, and NOS inhibitors to decrease, food intake^{193, 463-466}. These effects were due to NO activity in the brain, impinging on the leptin and serotonergic systems that regulate hunger. Leptin, given intracranially, was found to diminish diencephalic NOS activity and decrease food intake and body weight gain, and intracranial co-administration of L-arginine antagonized this effect⁴⁶⁷. Furthermore, intracerebroventricular injection of L-arginine, likely through stimulation of NOS activity, inhibited

serotonin-induced anorexia caused by IL-1 β ⁴⁶⁸. Studies with NOS inhibitors have further solidified our understanding of the central effects of NO on hunger. Systemic administration of the NOS inhibitor, NG-nitro-L-arginine, reduced food intake in obese rats and increased serotonin metabolism in the cortex, diencephalon, and medulla pons, thereby implicating the central serotonergic system in mediating the anorexic effect of NOS inhibitors ⁴⁶⁹. Other NOS inhibitors, such as L-NAME, promote weight loss and diminish food intake in *ob/ob* and *db/db* mice ⁴⁶⁵ and obese rats ⁴⁷⁰ and reduce adiposity and improve insulin sensitivity in high fat-fed mouse models ⁴⁷¹. Interestingly, intracerebroventricular administration of NG-monomethyl-L-arginine (L-NMMA) was shown also to regulate insulin secretion and peripheral insulin sensitivity ⁴⁷², suggesting that centrally derived NO has effects that extend to distal nodes of systemic metabolism. It is also possible that this effect contributes to the hyperphagic effects of NO, as insulin is well known to regulate hunger and satiety ⁴⁷³⁻⁴⁷⁷. Taken together with numerous other studies demonstrating a role for NO in the regulation of hunger ⁴⁷⁸⁻⁴⁸², it would appear that NO produced in the brain antagonizes anorectic signals and stimulates food intake.

Evidence supporting a role of NO in energy expenditure and glucose and lipid metabolism

Ostensibly, the reported anti-anorexic effects of NO might imply that by promoting food intake, increased levels of NO, e.g., that elicited by supplementation with L-arginine, should increase adiposity and insulin

resistance. However, human studies have shown repeatedly that L-arginine supplementation has favorable effects on body composition and insulin sensitivity⁴⁸³⁻⁴⁸⁹. Results from animal studies are in agreement: in rodents, L-arginine treatment has multimodal effects characterized by decreased fat mass, increased muscle mass, and improved insulin sensitivity. Despite promoting hyperphagia, L-arginine feeding reduced WAT mass, improved insulin sensitivity, and increased energy expenditure in mice⁴⁹⁰. In rats, not only has dietary L-arginine supplementation been shown to reduce fat mass, but it appears to increase skeletal muscle and brown fat mass and reduce serum concentrations of glucose, TGs, FFAs, homocysteine, dimethylarginines, and leptin as well^{491, 492}. Similar salubrious systemic effects of L-arginine have been demonstrated in pigs⁴⁹³. Overall, these collective data suggest that L-arginine, and by inference, NO, has the capacity to reduce fat mass by increasing mitochondrial biogenesis, regulating brown adipose tissue signaling, and increasing the expression of genes that promote oxidation of energy substrates⁴⁹⁴.

Chronic treatment with sildenafil, which prevents the degradation of cGMP and is commonly prescribed to improve penile erectile function, improved insulin action and diminished obesity in high fat-fed mice⁴⁹⁵. Shorter durations of sildenafil treatment have been shown to promote “browning” of white adipose tissue⁴⁹⁶. While there are no reports that type 5-phosphodiesterase inhibitors such as sildenafil regulate obesity in humans, they have been shown to increase mitochondrial biogenesis in human adipose tissue *ex vivo*⁴⁹⁷, suggesting at least the potential to increase energy expenditure.

Other drugs that affect NO production or function lend additional support to a role for NO in regulating insulin sensitivity. Beraprost (a stable prostaglandin analog) restores eNOS phosphorylation in endothelial-specific IRS-2 knockout mice and has been found to rescue capillary recruitment and to promote adequate insulin and glucose delivery to the skeletal muscle²¹⁷. Insulin, L-arginine, and sodium nitroprusside, by promoting S-nitro(sy)lation of key proteins, have been found to be particularly critical for regulating vascular endothelial insulin uptake and its transendothelial transport⁴⁹⁸. Hence, NO derived from eNOS appears play an important role in regulating systemic glucose metabolism and insulin delivery to peripheral tissues.

A characteristic feature of NO signaling is that effects of NO depend on its site of generation, concentration, and duration of application. Particularly interesting are the modes of action of NO in the liver, skeletal muscle, and pancreas. Although chronic treatment with NOS inhibitors promote weight loss and insulin sensitivity in animal models^{465, 470, 471}, acute application of these inhibitors causes systemic insulin resistance⁴⁹⁹. This is mediated in part by actions in the liver, which can regulate systemic responses to insulin⁵⁰⁰. Administration of BH₄, which is known to be oxidized to BH₂ in the diabetic state⁵⁰¹⁻⁵⁰³ and plays an important role in regulating coupled eNOS activity (see above), to STZ-induced diabetic mice lowered fasting blood glucose levels in an eNOS-dependent manner and improved glucose tolerance and insulin sensitivity in *ob/ob* mice⁵⁰⁴. This metabolic improvement was at least partially due to eNOS-mediated activation of AMPK in the liver, which suppressed hepatic

gluconeogenesis⁵⁰⁴. Hence, eNOS uncoupling in liver may be important for regulating systemic glucose metabolism.

Several studies demonstrate an important role of eNOS and nitrogen oxides in the liver. For example, intraportal administration of NOS inhibitors was shown to cause insulin resistance, which was rescued by intraportal delivery of the NO and superoxide donor, SIN-1^{505, 506}. Interestingly, when liver glutathione was first depleted by buthionine sulfoximine, the effects could not be rescued by sodium nitroprusside or SIN-1⁵⁰⁶. These results suggest that the formation of nitrosated glutathione (GSNO) in the liver might be important in mediating systemic responses to insulin. That intraportal delivery of glutathione methyl ester and SIN-1 enhances insulin sensitivity in rats would appear to support this view⁵⁰⁷.

The NO-HISS connection?

How does NO (and its oxidation products) in the liver mediate systemic responses to insulin? It has been suggested that the hepatic role of NO may relate to a hormone called 'hepatic insulin-sensitizing substance (HISS)'. This substance, for which there are only suggestive candidates (e.g., bone morphogenetic protein-9⁵⁰⁸), appears to account for 55% of the glucose disposal by insulin. Briefly, it is posited that post-prandial elevations in insulin results in release of a hormone, i.e., HISS, from the liver that acts on skeletal muscle to promote glucose uptake^{509, 510}. Intriguingly, one study suggests that HISS, not insulin action, regulates the peripheral vasodilation generally attributed to insulin

⁵¹¹. Atropine or hepatic surgical denervation inhibited the peripheral vascular actions of insulin, allegedly by blocking HISS release, whereas intraportal delivery of acetylcholine, which increases NOS activity, restored HISS release and insulin-mediated vasodilation ⁵¹¹. These findings are consistent with original studies showing that insulin-mediated vasodilation is dependent on NO ^{512, 513} and that insulin-mediated skeletal muscle vasodilation contributes to insulin sensitivity in humans ⁵¹⁴. Combined with other studies suggesting a role for NO in promoting the release of HISS ⁵¹⁵⁻⁵¹⁷, this suggests that the putative hormone could be an NO-regulated, liver-produced, endocrine mediator of classical EDRF crucial for glucose disposal. However, (in addition to the identity of HISS) it remains unclear how this distally engendered mode of vasoregulation integrates physiologically (and pathologically) with the local effects of insulin and NO in the vasculature ²¹⁴⁻²¹⁷.

Pancreatic effects of NO

Extremely important for maintaining metabolic homeostasis, the pancreas utilizes NO to regulate their function. The pancreas is comprised of two types of glands: (1) exocrine glands, which secrete the bicarbonate and digestive enzymes needed to neutralize the acidic gastric contents entering the small intestine and to complete digestion of food, respectively; and (2) endocrine glands, i.e., the islets of Langerhans, which contain several types of secretory cells, including α cells, β cells, δ cells, and F cells. Each of these cell types secretes multiple proteins, such as insulin (β cells), glucagon (α cells), and

somatostatin (δ cells). NO has been shown to affect both exocrine and endocrine functions of the pancreas ^{518, 519}.

With respect to insulin release, it appears that NO stimulates early, glucose-induced insulin release, while it is responsible for cytokine (e.g., IL-1 β)-mediated inhibition of insulin secretion. This dual role of NO in regulating insulin secretion has been a subject of controversy (e.g., ⁵²⁰), which may be, in part, due to the mechanistic complexity regulating pancreatic insulin secretion; compounded by the multiple actions of NO. The inhibitory actions of NO on insulin release appear to be due to iNOS-derived NO, which is implicated in the destruction of islet cells in type 1 diabetes ^{521, 522}. However, mechanisms regulating the insulin-stimulating effects of NO ⁵²³⁻⁵²⁶ have been more difficult to elucidate. NO has been suggested to stimulate islet cell insulin secretion by inducing calcium release from mitochondria ⁵²⁷, which may be due to NO-mediated inhibition of respiration and mitochondrial depolarization. Nevertheless, the stimulatory effects of NO on insulin secretion are relatively subtle ⁵²⁶, which might explain why some studies suggest that NO is not involved in the initiation of insulin secretion from pancreatic islets ^{528, 529}.

Lessons from human studies and genetic interventions

Considerable data suggests an association between genetic polymorphisms in NOS isoforms and insulin resistance. Notably, several studies have associated a T(-786)C variant of the eNOS gene with insulin resistance ⁵³⁰⁻⁵³². Several other genetic variants in the eNOS locus are associated with T2D ⁵³³, susceptibility for

insulin resistance, hypertriglyceridemia, and low HDL⁵³⁴, or worsened endothelial function in individuals prone to T2D⁵³⁵. Polymorphisms in the iNOS gene have been associated with higher plasma glucose and elevated waist/hip ratios⁵³⁶, and variants in the iNOS gene promoter are associated with T2D⁵³⁷.

Genetic deletion, manipulation, and overexpression of NOS isoforms in mice have allowed for interrogation of mechanisms by which NO regulates metabolic health and disease. In mice, it has been reported that deletion of eNOS causes insulin resistance, hyperlipidemia, and hypertension³³⁶. While full gene deletion mimics human “metabolic syndrome,” even partial gene deletion of eNOS results in exaggerated insulin resistance, glucose intolerance, and hypertension induced by a high fat diet^{538, 539}. Mice lacking all NOS isoforms, i.e., eNOS/nNOS/iNOS triple knockout mice, demonstrate increased visceral obesity, hypertension, hypertriglyceridemia, and impaired glucose tolerance, and, it is interesting to note, that this is one of the few mouse strains to date to have spontaneous myocardial infarctions, apparently due to unstable coronary arteriosclerotic lesions⁵⁴⁰. That NOS is important to insulin sensitivity was further shown by studies in mice in which overexpression of dimethylarginine dimethylaminohydrolase—an enzyme that catalyzes the breakdown of the endogenous inhibitor of NOS, ADMA—increased insulin sensitivity⁵⁴¹.

Anti-obesogenic effects of eNOS

It appears that the metabolic phenotype elicited by insufficient levels of eNOS-derived NO relates directly to defects in intermediary metabolism in key

peripheral tissues. Supporting evidence supplied by eNOS KO mice include a markedly lower energy expenditure and decreases in mitochondrial content and fatty acid oxidation in muscle compared with WT mice ³³⁷; and, as expected, eNOS KO mice demonstrate an impaired ability to exercise ⁵⁴². Gain-of-function studies show a remarkable ability of eNOS to regulate body composition and increase metabolism. Supplementation of eNOS KO mice with nitrate, which can be serially reduced to nitrite and NO, decreases not only blood pressure, but visceral fat and TGs as well, thus reversing features of metabolic syndrome ³⁶³. Furthermore, our studies show that mice overexpressing eNOS acquire an anti-obesogenic phenotype characterized by resistance to accumulation of white adipose tissue in response to a high fat diet, a higher metabolic rate, resistance to diet-induced hyperinsulinemia, and remarkably lower plasma levels of FFAs and TGs (Chapter III) ²⁸⁶. Our findings were supported by results from an investigation of an eNOS phosphomimetic point mutant mouse model that was published shortly after our study ^{543, 544}. Mutation of serine 1176 of eNOS to an aspartic acid resulted in increased endothelial NO production as well as resistance to diet-induced weight gain and hyperinsulinemia; mutation of the residue to an alanine, which cannot be phosphorylated, resulted in insulin resistance and features of metabolic syndrome ^{195, 544}.

How does eNOS regulate metabolism and body composition? Several possibilities exist. Consistent changes in plasma lipids insinuate a central role of eNOS in lipid oxidation or synthesis, e.g., eNOS KO mice have elevated plasma levels TGs and FFAs compared with WT mice ^{336, 539}, while eNOS transgenic

mice show diminished abundance of the lipids ¹⁶⁰. That these differences are due to modulation of fat oxidation are suggested by studies showing a direct effect of NO on the capacity to oxidize fat. Not only do eNOS KO mice show diminished fat oxidation capacity in skeletal muscle ³³⁷, but administration of a NOS inhibitor is sufficient to increase serum TGs and diminish hepatic fatty acid oxidation in rats ⁵⁴⁵, potentially by decreasing the activity of carnitine palmitoyl transferase ⁵⁴⁶. Similar, NOS inhibitor-dependent decreases in fat oxidation capacity have been found in heart ⁵⁴⁷. In isolated hepatocytes, treatment with NO donors was shown to increase fatty acid oxidation in a cGMP-dependent manner by inhibiting acetyl CoA carboxylase (thereby decreasing production of malonyl CoA) and stimulating carnitine palmitoyl transferase activity ⁴⁵⁰. Interestingly, NO also inhibits fatty acid synthesis in hepatocytes ⁴⁵⁰, which is consistent with studies showing that NOS inhibitors ⁴⁵¹ or genetic deletion of eNOS increases lipid synthesis in liver ⁴⁵². In skeletal muscle, genetic deletion of eNOS increases neolipogenic genes expression while downregulating genes involved in β -oxidation ³³⁷.

That genes involved in fatty acid oxidation are modulated by NO is consistent with data showing that overexpression of eNOS increases the expression of peroxisome proliferator activated receptor (PPAR)- α ¹⁶⁰, which is well known to regulate lipid metabolism ⁴⁵³. However, it is possible that NO regulates fat oxidation post-translationally as well. Recent studies show widespread S-nitrosation of multiple enzymes involved in intermediary metabolism. In particular, the liver enzyme, very long chain acyl-coA

dehydrogenase (VLCAD) was shown to be nitrosated at Cys238, which increased the catalytic efficiency of the enzyme, and this modification was absent in eNOS KO mice ⁵⁴⁸. Collectively, these studies suggest that the powerful anti-obesity effects of eNOS-derived NO could be due to simultaneous increases and decreases in fat oxidation and a decrease in fat synthesis.

iNOS promotes insulin resistance

The iNOS enzyme also regulates systemic metabolism, particularly insulin resistance. Although ablation of the iNOS gene has no effect on diet-induced obesity, its absence was shown to improve glucose tolerance, normalize insulin sensitivity, and prevent derangements in the PI3K/Akt signaling in response to insulin ⁵⁴⁹. Commonly, increases in iNOS expression in skeletal muscle of obese mice are associated with increased S-nitrosation of the insulin receptor (IR), IRS-1, and Akt, suggesting that nitrosative post-translational modifications of proteins in the insulin signaling pathway are responsible for iNOS-induced insulin resistance ^{550, 551}. The presence of iNOS appears to decrease the abundance of IRS-1 by promoting its proteasomal degradation ¹⁸⁶. Interestingly, an acute bout of exercise was sufficient to downregulate iNOS in high fat-fed rats as well as prevent S-nitrosation of proteins involved in insulin signaling, and administration of an inhibitor of iNOS (L-N6-(1-iminoethyl)lysine; L-NIL) pheno-copied these effects ⁵⁵². Also, aspirin—which is one of the oldest known treatments for diabetes ^{553, 554} and which improves blood glucose and insulin sensitivity in diabetic patients ⁵⁵⁵ and animal models of T2D ⁵⁵⁶—inhibited

iNOS-mediated S-nitrosation of IR, IRS-1, and Akt in skeletal muscle and improved insulin sensitivity⁵⁵⁷.

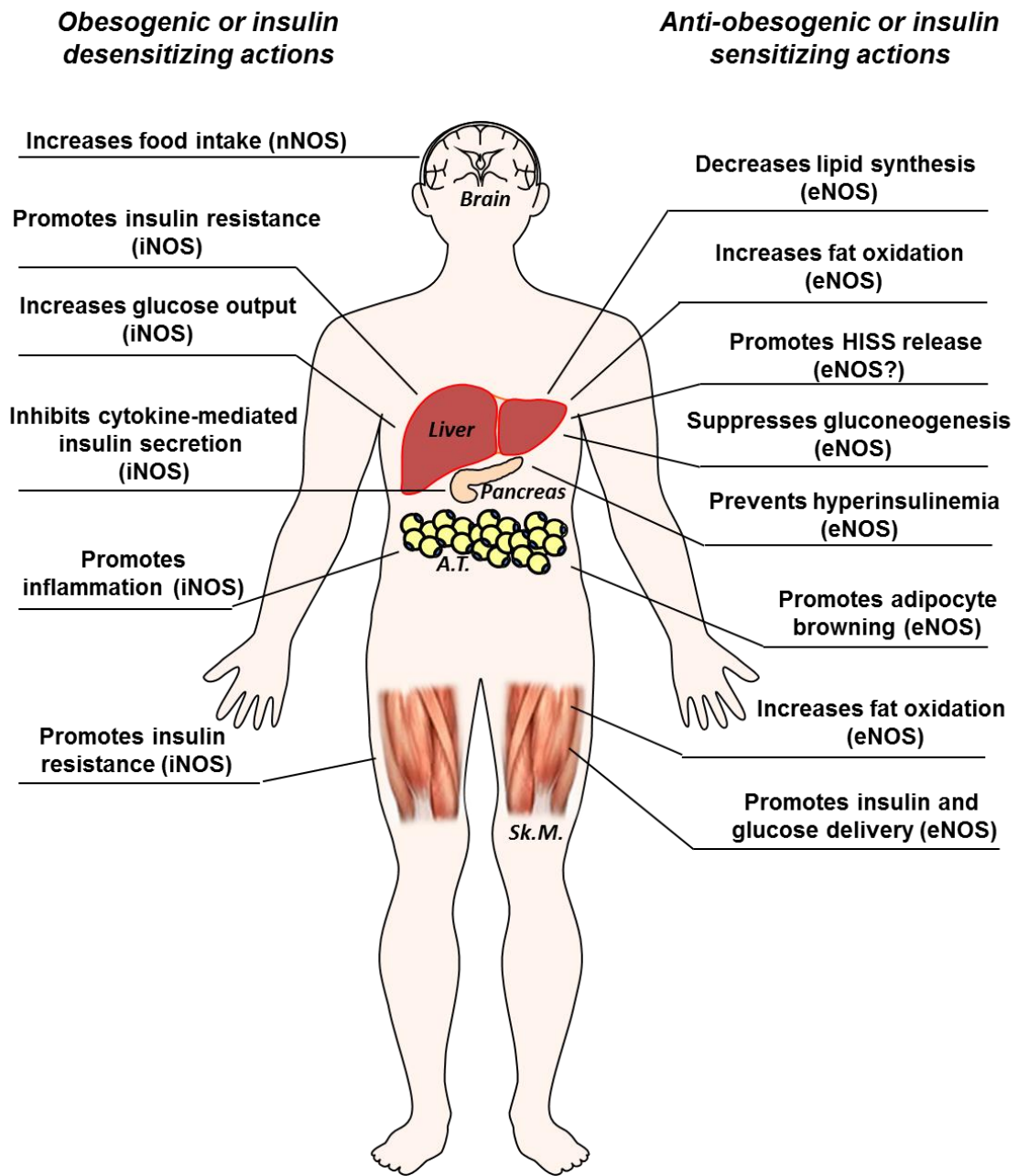
Expression of iNOS in peripheral tissues other than skeletal muscle is also important for regulating insulin sensitivity. Selective overexpression of iNOS in liver is sufficient to cause hepatic insulin resistance, hyperglycemia and hyperinsulinemia⁵⁵⁸, and the use of an iNOS-specific inhibitor (L-NIL) reversed hyperglycemia, hyperinsulinemia, and insulin resistance in *ob/ob* mice¹⁸⁸. In obesity, proinflammatory macrophages accumulating in adipose tissue are responsible for the majority of iNOS expression¹⁸⁹⁻¹⁹¹ and may propagate the inflammatory signaling implicated in insulin resistance¹⁶⁸. Importantly, the role of iNOS in adipose tissue appears to differ remarkably from the canonical NO-cGMP pathway, as high fat diet-induced increases in proinflammatory cytokines and macrophage recruitment were attenuated by the administration of sildenafil⁵⁵⁹. Interestingly, lack of iNOS does not prevent age-induced insulin resistance⁵⁶⁰, which suggests that not all insulin resistant states are created equal⁵⁶¹. In agreement with this view it has been shown that mice lacking the nNOS isoform are insulin resistant due to a sympathetic, alpha-adrenergic mechanism⁵⁶².

Integration of findings from these studies, and our own, helps to form a model illustrating the complex role of NO in regulating obesity and insulin resistance (Fig. 43). NO derived from eNOS appears to have both anti-obesogenic and insulin-sensitizing properties. Its anti-obesogenic role stems from its ability to increase fat oxidation in peripheral tissues such as skeletal muscle, liver, and adipose tissue. As mentioned above, there is evidence that NO

also decreases lipid synthesis in liver. The impact of eNOS on glucose metabolism and insulin sensitivity is supported by its capacity to increase the transport of insulin and glucose to key peripheral tissues such as skeletal muscle and to regulate gluconeogenesis. Additionally, there may be implications for eNOS-mediated HISS release, which enhances the vasodilatory properties of insulin. That eNOS prevents hyperinsulinemia in two separate genetic gain-of-function studies^{160, 544} suggests further that it could impact glucose metabolism directly by modulating insulin release. Other isoforms of NOS appear to promote deleterious changes in metabolism. In the brain, evidence suggests that nNOS-derived NO promotes hyperphagia. The iNOS isoform promotes insulin resistance in both liver and skeletal muscle and is critical in inflammatory responses in multiple tissues, most notably, the adipose organ. In contrast to eNOS, iNOS appears to promote gluconeogenesis, and iNOS has remarkable effects on cytokine-mediated insulin secretion. Collectively, it is apparent that NO is one of the most critical regulators of metabolism, body composition, and insulin sensitivity. Harnessing its beneficial metabolic actions is an exciting prospect for combatting metabolic disease in the future.

Figure 43. Working model of the systemic effects of NO on obesity and metabolism. Illustration of major organs and processes affected by NO and nitrogen oxides derived from eNOS, nNOS, and iNOS: The eNOS isoform shows anti-obesogenic and insulin sensitizing effects, which appears to be based in the ability of the enzyme to decrease lipid synthesis and promote fat oxidation in the liver and skeletal muscle. Additionally, eNOS may be implicated in the secretion of hepatic insulin sensitizing substance (HISS), which might support insulin sensitivity in peripheral tissues such as skeletal muscle. eNOS is important also for maximizing delivery of insulin and substrates to skeletal muscle, and this is likely critical in regulating insulin sensitivity and glucose tolerance. Through its actions in liver and pancreas, eNOS may also suppress gluconeogenesis and prevent hyperinsulinemia, respectively. Additionally, NO increases the abundance of mitochondria and stimulates substrate oxidation capacity in adipose tissue, effectively promoting “browning” of white adipocytes. Conversely, other isoforms of NOS appear to have a more malevolent role in metabolism. NO derived from nNOS promotes hyperphagia, and iNOS-derived nitrogen oxides can promote insulin resistance and inflammation in key peripheral tissues such as liver, skeletal muscle, and adipose tissue. In addition, iNOS may affect glucose homeostasis by increasing glucose output from the liver and by impairing the exocrine and endocrine activities of the pancreas.

Figure 43



REFERENCES

1. Ahima RS. Digging deeper into obesity. *J Clin Invest*. 2011;121:2076-2079
2. Ogden CL, Carroll MD, Kit BK, Flegal KM. Prevalence of obesity in the united states, 2009-2010. *NCHS Data Brief*. 2012:1-8
3. Ervin RB. Prevalence of metabolic syndrome among adults 20 years of age and over, by sex, age, race and ethnicity, and body mass index: United states, 2003-2006. *Natl Health Stat Report*. 2009:1-7
4. Roger VL, Go AS, Lloyd-Jones DM, Benjamin EJ, Berry JD, Borden WB, Bravata DM, Dai S, Ford ES, Fox CS, Fullerton HJ, Gillespie C, Hailpern SM, Heit JA, Howard VJ, Kissela BM, Kittner SJ, Lackland DT, Lichtman JH, Lisabeth LD, Makuc DM, Marcus GM, Marelli A, Matchar DB, Moy CS, Mozaffarian D, Mussolino ME, Nichol G, Paynter NP, Soliman EZ, Sorlie PD, Sotoodehnia N, Turan TN, Virani SS, Wong ND, Woo D, Turner MB. Heart disease and stroke statistics--2012 update: A report from the american heart association. *Circulation*. 2011
5. Calle EE, Thun MJ, Petrelli JM, Rodriguez C, Heath CW, Jr. Body-mass index and mortality in a prospective cohort of u.S. Adults. *N Engl J Med*. 1999;341:1097-1105
6. Zamosky L. The obesity epidemic. While america swallows \$147 billion in obesity-related healthcare costs, physicians called on to confront the crisis. *Medical economics*. 2013;90:14-17
7. Tseng YH, Cypess AM, Kahn CR. Cellular bioenergetics as a target for obesity therapy. *Nature reviews. Drug discovery*. 2010;9:465-482
8. Kant AK, Graubard BI. Eating out in america, 1987-2000: Trends and nutritional correlates. *Prev Med*. 2004;38:243-249
9. Nielsen SJ, Popkin BM. Patterns and trends in food portion sizes, 1977-1998. *JAMA*. 2003;289:450-453
10. Briefel RR, Johnson CL. Secular trends in dietary intake in the united states. *Annu Rev Nutr*. 2004;24:401-431
11. Hill JO, Peters JC. Environmental contributions to the obesity epidemic. *Science*. 1998;280:1371-1374
12. Jones OA, Maguire ML, Griffin JL. Environmental pollution and diabetes: A neglected association. *Lancet*. 2008;371:287-288
13. Smink A, Ribas-Fito N, Garcia R, Torrent M, Mendez MA, Grimalt JO, Sunyer J. Exposure to hexachlorobenzene during pregnancy increases the risk of overweight in children aged 6 years. *Acta paediatrica*. 2008;97:1465-1469
14. Sun Q, Yue P, Deiuliis JA, Lumeng CN, Kampfrath T, Mikolaj MB, Cai Y, Ostrowski MC, Lu B, Parthasarathy S, Brook RD, Moffatt-Bruce SD, Chen LC, Rajagopalan S. Ambient air pollution exaggerates adipose inflammation and insulin resistance in a mouse model of diet-induced obesity. *Circulation*. 2009;119:538-546
15. Schell LM, Burnitz KK, Lathrop PW. Pollution and human biology. *Annals of human biology*. 2010;37:347-366
16. Xu X, Yavar Z, Verdin M, Ying Z, Mihai G, Kampfrath T, Wang A, Zhong M, Lippmann M, Chen LC, Rajagopalan S, Sun Q. Effect of early particulate air pollution exposure on obesity in mice: Role of p47phox. *Arterioscler Thromb Vasc Biol*. 2010;30:2518-2527
17. Yan YH, Chou CC, Lee CT, Liu JY, Cheng TJ. Enhanced insulin resistance in diet-induced obese rats exposed to fine particles by instillation. *Inhalation toxicology*. 2011;23:507-519

18. Bolton JL, Smith SH, Huff NC, Gilmour MI, Foster WM, Auten RL, Bilbo SD. Prenatal air pollution exposure induces neuroinflammation and predisposes offspring to weight gain in adulthood in a sex-specific manner. *FASEB J*. 2012;26:4743-4754
19. Rundle A, Hoepner L, Hassoun A, Oberfield S, Freyer G, Holmes D, Reyes M, Quinn J, Camann D, Perera F, Whyatt R. Association of childhood obesity with maternal exposure to ambient air polycyclic aromatic hydrocarbons during pregnancy. *American journal of epidemiology*. 2012;175:1163-1172
20. Cupul-Uicab LA, Skjaerven R, Haug K, Melve KK, Engel SM, Longnecker MP. In utero exposure to maternal tobacco smoke and subsequent obesity, hypertension, and gestational diabetes among women in the moba cohort. *Environmental health perspectives*. 2012;120:355-360
21. Langer P, Ukropec J, Kocan A, Drobna B, Radikova Z, Huckova M, Imrich R, Gasperikova D, Klimes I, Trnovec T. Obesogenic and diabetogenic impact of high organochlorine levels (hcb, p,p'-dde, pcbs) on inhabitants in the highly polluted eastern slovakia. *Endocrine regulations*. 2014;48:17-24
22. Sallis JF, Floyd MF, Rodriguez DA, Saelens BE. Role of built environments in physical activity, obesity, and cardiovascular disease. *Circulation*. 2012;125:729-737
23. Ding D, Sallis JF, Kerr J, Lee S, Rosenberg DE. Neighborhood environment and physical activity among youth a review. *American journal of preventive medicine*. 2011;41:442-455
24. Durand CP, Andalib M, Dunton GF, Wolch J, Pentz MA. A systematic review of built environment factors related to physical activity and obesity risk: Implications for smart growth urban planning. *Obesity reviews : an official journal of the International Association for the Study of Obesity*. 2011;12:e173-182
25. Antunes LC, Levandovski R, Dantas G, Caumo W, Hidalgo MP. Obesity and shift work: Chronobiological aspects. *Nutrition research reviews*. 2010;23:155-168
26. Garaulet M, Ordovas JM, Madrid JA. The chronobiology, etiology and pathophysiology of obesity. *International journal of obesity*. 2010;34:1667-1683
27. Challet E. Circadian clocks, food intake, and metabolism. *Progress in molecular biology and translational science*. 2013;119:105-135
28. Widen E, Lehto M, Kanninen T, Walston J, Shuldiner AR, Groop LC. Association of a polymorphism in the beta 3-adrenergic-receptor gene with features of the insulin resistance syndrome in finns. *N Engl J Med*. 1995;333:348-351
29. Bouchard C, Tremblay A, Despres JP, Nadeau A, Lupien PJ, Theriault G, Dussault J, Moorjani S, Pinault S, Fournier G. The response to long-term overfeeding in identical twins. *N Engl J Med*. 1990;322:1477-1482
30. Bouchard C. The biological predisposition to obesity: Beyond the thrifty genotype scenario. *Int J Obes (Lond)*. 2007;31:1337-1339
31. Wells JC. Thrift: A guide to thrifty genes, thrifty phenotypes and thrifty norms. *Int J Obes (Lond)*. 2009;33:1331-1338
32. Redman LM, Heilbronn LK, Martin CK, de Jonge L, Williamson DA, Delany JP, Ravussin E. Metabolic and behavioral compensations in response to caloric restriction: Implications for the maintenance of weight loss. *PLoS One*. 2009;4:e4377
33. Leibel RL, Rosenbaum M, Hirsch J. Changes in energy expenditure resulting from altered body weight. *N Engl J Med*. 1995;332:621-628
34. Ford ES, Williamson DF, Liu S. Weight change and diabetes incidence: Findings from a national cohort of us adults. *Am J Epidemiol*. 1997;146:214-222
35. Resnick HE, Valsania P, Halter JB, Lin X. Relation of weight gain and weight loss on subsequent diabetes risk in overweight adults. *J Epidemiol Community Health*. 2000;54:596-602
36. Crawford AG, Cote C, Couto J, Daskiran M, Gunnarsson C, Haas K, Haas S, Nigam SC, Schuette R. Prevalence of obesity, type ii diabetes mellitus, hyperlipidemia, and hypertension in the united states: Findings from the ge centrality electronic medical record database. *Popul Health Manag*. 2010;13:151-161
37. Will JC, Williamson DF, Ford ES, Calle EE, Thun MJ. Intentional weight loss and 13-year diabetes incidence in overweight adults. *Am J Public Health*. 2002;92:1245-1248

38. Alberti KG, Zimmet PZ. Definition, diagnosis and classification of diabetes mellitus and its complications. Part 1: Diagnosis and classification of diabetes mellitus provisional report of a who consultation. *Diabet Med.* 1998;15:539-553
39. Spiegelman BM, Flier JS. Obesity and the regulation of energy balance. *Cell.* 2001;104:531-543
40. Ahima RS, Flier JS. Leptin. *Annu Rev Physiol.* 2000;62:413-437
41. Schwartz MW, Woods SC, Porte D, Jr., Seeley RJ, Baskin DG. Central nervous system control of food intake. *Nature.* 2000;404:661-671
42. Stanley BG, Kyrkouli SE, Lampert S, Leibowitz SF. Neuropeptide y chronically injected into the hypothalamus: A powerful neurochemical inducer of hyperphagia and obesity. *Peptides.* 1986;7:1189-1192
43. Billington CJ, Briggs JE, Harker S, Grace M, Levine AS. Neuropeptide y in hypothalamic paraventricular nucleus: A center coordinating energy metabolism. *Am J Physiol.* 1994;266:R1765-1770
44. Beck B, Pourie G. Ghrelin, neuropeptide y, and other feeding-regulatory peptides active in the hippocampus: Role in learning and memory. *Nutrition reviews.* 2013;71:541-561
45. Bray GA, Tartaglia LA. Medicinal strategies in the treatment of obesity. *Nature.* 2000;404:672-677
46. Baretic M. Obesity drug therapy. *Minerva endocrinologica.* 2013;38:245-254
47. Rueda-Clausen CF, Padwal RS, Sharma AM. New pharmacological approaches for obesity management. *Nature reviews. Endocrinology.* 2013;9:467-478
48. Harper ME, Green K, Brand MD. The efficiency of cellular energy transduction and its implications for obesity. *Annu Rev Nutr.* 2008;28:13-33
49. Cutting WC, Rytand DA, Tainter ML. Relationship between blood cholesterol and increased metabolism from dinitrophenol and thyroid. *J Clin Invest.* 1934;13:547-552
50. Tainter ML, Cutting WC, Stockton AB. Use of dinitrophenol in nutritional disorders : A critical survey of clinical results. *Am J Public Health Nations Health.* 1934;24:1045-1053
51. Colman E. Dinitrophenol and obesity: An early twentieth-century regulatory dilemma. *Regulatory toxicology and pharmacology : RTP.* 2007;48:115-117
52. Kopecky J, Rossmeisl M, Hodny Z, Syrový I, Horáková M, Kolarová P. Reduction of dietary obesity in ap2-ucp transgenic mice: Mechanism and adipose tissue morphology. *Am J Physiol.* 1996;270:E776-786
53. Li B, Nolte LA, Ju JS, Han DH, Coleman T, Holloszy JO, Semenkovich CF. Skeletal muscle respiratory uncoupling prevents diet-induced obesity and insulin resistance in mice. *Nat Med.* 2000;6:1115-1120
54. Befroy DE, Petersen KF, Dufour S, Mason GF, Rothman DL, Shulman GI. Increased substrate oxidation and mitochondrial uncoupling in skeletal muscle of endurance-trained individuals. *Proc Natl Acad Sci U S A.* 2008;105:16701-16706
55. Schrauwen-Hinderling VB, Hesselink MK, Moonen-Kornips E, Schaart G, Kooi ME, Saris WH, Schrauwen P. Short-term training is accompanied by a down regulation of acc2 mrna in skeletal muscle. *Int J Sports Med.* 2006;27:786-791
56. Schrauwen-Hinderling VB, Kooi ME, Hesselink MK, Moonen-Kornips E, Schaart G, Mustard KJ, Hardie DG, Saris WH, Nicolay K, Schrauwen P. Intramyocellular lipid content and molecular adaptations in response to a 1-week high-fat diet. *Obes Res.* 2005;13:2088-2094
57. Rothwell NJ, Stock MJ. Luxusconsumption, diet-induced thermogenesis and brown fat: The case in favour. *Clin Sci (Lond).* 1983;64:19-23
58. Lowell BB, Flier JS. Brown adipose tissue, beta 3-adrenergic receptors, and obesity. *Annu Rev Med.* 1997;48:307-316
59. Cypess AM, Lehman S, Williams G, Tal I, Rodman D, Goldfine AB, Kuo FC, Palmer EL, Tseng YH, Doria A, Kolodny GM, Kahn CR. Identification and importance of brown adipose tissue in adult humans. *N Engl J Med.* 2009;360:1509-1517
60. Virtanen KA, Lidell ME, Orava J, Heglind M, Westergren R, Niemi T, Taittonen M, Laine J, Savisto NJ, Enerback S, Nuutila P. Functional brown adipose tissue in healthy adults. *N Engl J Med.* 2009;360:1518-1525

61. Kozak LP, Harper ME. Mitochondrial uncoupling proteins in energy expenditure. *Annu Rev Nutr.* 2000;20:339-363
62. Vidal-Puig A, Solanes G, Grujic D, Flier JS, Lowell BB. Ucp3: An uncoupling protein homologue expressed preferentially and abundantly in skeletal muscle and brown adipose tissue. *Biochem Biophys Res Commun.* 1997;235:79-82
63. Kershaw EE, Flier JS. Adipose tissue as an endocrine organ. *J Clin Endocrinol Metab.* 2004;89:2548-2556
64. Rosen ED, Spiegelman BM. Adipocytes as regulators of energy balance and glucose homeostasis. *Nature.* 2006;444:847-853
65. Guilherme A, Virbasius JV, Puri V, Czech MP. Adipocyte dysfunctions linking obesity to insulin resistance and type 2 diabetes. *Nat Rev Mol Cell Biol.* 2008;9:367-377
66. Muoio DM, Newgard CB. Obesity-related derangements in metabolic regulation. *Annu Rev Biochem.* 2006;75:367-401
67. Qatanani M, Lazar MA. Mechanisms of obesity-associated insulin resistance: Many choices on the menu. *Genes Dev.* 2007;21:1443-1455
68. Rajala MW, Scherer PE. Minireview: The adipocyte--at the crossroads of energy homeostasis, inflammation, and atherosclerosis. *Endocrinology.* 2003;144:3765-3773
69. Sartipy P, Loskutoff DJ. Monocyte chemoattractant protein 1 in obesity and insulin resistance. *Proc Natl Acad Sci U S A.* 2003;100:7265-7270
70. Unger RH. Lipotoxicity in the pathogenesis of obesity-dependent niddm. Genetic and clinical implications. *Diabetes.* 1995;44:863-870
71. Unger RH. Lipotoxic diseases. *Annu Rev Med.* 2002;53:319-336
72. Boden G, Chen X. Effects of fat on glucose uptake and utilization in patients with non-insulin-dependent diabetes. *J Clin Invest.* 1995;96:1261-1268
73. Roden M, Price TB, Perseghin G, Petersen KF, Rothman DL, Cline GW, Shulman GI. Mechanism of free fatty acid-induced insulin resistance in humans. *J Clin Invest.* 1996;97:2859-2865
74. Dresner A, Laurent D, Marcucci M, Griffin ME, Dufour S, Cline GW, Slezak LA, Andersen DK, Hundal RS, Rothman DL, Petersen KF, Shulman GI. Effects of free fatty acids on glucose transport and irs-1-associated phosphatidylinositol 3-kinase activity. *J Clin Invest.* 1999;103:253-259
75. Griffin ME, Marcucci MJ, Cline GW, Bell K, Barucci N, Lee D, Goodyear LJ, Kraegen EW, White MF, Shulman GI. Free fatty acid-induced insulin resistance is associated with activation of protein kinase c theta and alterations in the insulin signaling cascade. *Diabetes.* 1999;48:1270-1274
76. Savage DB, Petersen KF, Shulman GI. Disordered lipid metabolism and the pathogenesis of insulin resistance. *Physiol Rev.* 2007;87:507-520
77. Boden G. Role of fatty acids in the pathogenesis of insulin resistance and niddm. *Diabetes.* 1997;46:3-10
78. Kelley DE, Mokan M, Simoneau JA, Mandarino LJ. Interaction between glucose and free fatty acid metabolism in human skeletal muscle. *J Clin Invest.* 1993;92:91-98
79. Lam TK, van de Werve G, Giacca A. Free fatty acids increase basal hepatic glucose production and induce hepatic insulin resistance at different sites. *Am J Physiol Endocrinol Metab.* 2003;284:E281-290
80. Boden G, Lebed B, Schatz M, Homko C, Lemieux S. Effects of acute changes of plasma free fatty acids on intramyocellular fat content and insulin resistance in healthy subjects. *Diabetes.* 2001;50:1612-1617
81. Perseghin G, Scifo P, De Cobelli F, Pagliato E, Battezzati A, Arcelloni C, Vanzulli A, Testolin G, Pozza G, Del Maschio A, Luzi L. Intramyocellular triglyceride content is a determinant of in vivo insulin resistance in humans: A 1h-13c nuclear magnetic resonance spectroscopy assessment in offspring of type 2 diabetic parents. *Diabetes.* 1999;48:1600-1606
82. Newgard CB, McGarry JD. Metabolic coupling factors in pancreatic beta-cell signal transduction. *Annu Rev Biochem.* 1995;64:689-719

83. Zhou YP, Grill VE. Long-term exposure of rat pancreatic islets to fatty acids inhibits glucose-induced insulin secretion and biosynthesis through a glucose fatty acid cycle. *J Clin Invest.* 1994;93:870-876
84. Kim JY, De Wall EV, Laplante M, Azzara A, Trujillo ME, Hofmann SM, Schraw T, Durand JL, Li H, Li G, Jelicks LA, Mehler MF, Hui DY, Deshaies Y, Shulman GI, Schwartz GJ, Scherer PE. Obesity-associated improvements in metabolic profile through expansion of adipose tissue. *Journal of Clinical Investigation.* 2007;117:2621-2637
85. Kim JK, Gavrilova O, Chen Y, Reitmann ML, Shulman GI. Mechanism of insulin resistance in a-*zip/f-1* fatless mice. *Journal of Biological Chemistry.* 2000;275:8456-8460
86. Shulman GI. Cellular mechanisms of insulin resistance. *Journal of Clinical Investigation.* 2000;106:171-176
87. Muoio DM, Neufer PD. Lipid-induced mitochondrial stress and insulin action in muscle. *Cell Metabolism.* 2012;15:595-605
88. De Pauw A, Tejerina S, Raes M, Keijer J, Arnould T. Mitochondrial (dys)function in adipocyte (de)differentiation and systemic metabolic alterations. *American Journal of Pathology.* 2009;175:927-939
89. Tormos KV, Anso E, Hamanaka RB, Eisenhart J, Joseph J, Kalyanaraman B, Chandel NS. Mitochondrial complex iii ros regulate adipocyte differentiation. *Cell Metabolism.* 2011;14:537-544
90. Lu RH, Ji H, Chang ZG, Su SS, Yang GS. Mitochondrial development and the influence of its dysfunction during rat adipocyte differentiation. *Mol Biol Rep.* 2010;37:2173-2182
91. Kusminski CM, Scherer PE. Mitochondrial dysfunction in white adipose tissue. *Trends Endocrinol Metab.* 2012;23:435-443
92. Nye C, Kim J, Kalhan SC, Hanson RW. Reassessing triglyceride synthesis in adipose tissue. *Trends Endocrinol Metab.* 2008;19:356-361
93. Choo HJ, Kim JH, Kwon OB, Lee CS, Mun JY, Han SS, Yoon YS, Yoon G, Choi KM, Ko YG. Mitochondria are impaired in the adipocytes of type 2 diabetic mice. *Diabetologia.* 2006;49:784-791
94. Keller MP, Attie AD. Physiological insights gained from gene expression analysis in obesity and diabetes. *Annu Rev Nutr.* 2010;30:341-364
95. Devarakonda S, Gupta K, Chalmers MJ, Hunt JF, Griffin PR, Van Duyne GD, Spiegelman BM. Disorder-to-order transition underlies the structural basis for the assembly of a transcriptionally active *pgc-1alpha/errgamma* complex. *Proc Natl Acad Sci U S A.* 2011;108:18678-18683
96. Krishnan J, Danzer C, Simka T, Ukropec J, Walter KM, Kumpf S, Mirtschink P, Ukropcova B, Gasperikova D, Pedrazzini T, Krek W. Dietary obesity-associated *hif1alpha* activation in adipocytes restricts fatty acid oxidation and energy expenditure via suppression of the *sirt2-nad+* system. *Genes Dev.* 2012;26:259-270
97. Bogacka I, Ukropcova B, McNeil M, Gimble JM, Smith SR. Structural and functional consequences of mitochondrial biogenesis in human adipocytes in vitro. *J Clin Endocrinol Metab.* 2005;90:6650-6656
98. Puigserver P, Wu Z, Park CW, Graves R, Wright M, Spiegelman BM. A cold-inducible coactivator of nuclear receptors linked to adaptive thermogenesis. *Cell.* 1998;92:829-839
99. Handschin C, Spiegelman BM. Peroxisome proliferator-activated receptor gamma coactivator 1 coactivators, energy homeostasis, and metabolism. *Endocr Rev.* 2006;27:728-735
100. Serra D, Mera P, Malandrino MI, Mir JF, Herrero L. Mitochondrial fatty acid oxidation in obesity. *Antioxid Redox Signal.* 2013;19:269-284
101. Bostrom P, Wu J, Jedrychowski MP, Korde A, Ye L, Lo JC, Rasbach KA, Bostrom EA, Choi JH, Long JZ, Kajimura S, Zingaretti MC, Vind BF, Tu H, Cinti S, Hojlund K, Gygi SP, Spiegelman BM. A *pgc1-alpha*-dependent myokine that drives brown-fat-like development of white fat and thermogenesis. *Nature.* 2012;481:463-468
102. Nisoli E, Clementi E, Paolucci C, Cozzi V, Tonello C, Sciorati C, Bracale R, Valerio A, Francolini M, Moncada S, Carruba MO. Mitochondrial biogenesis in mammals: The role of endogenous nitric oxide. *Science.* 2003;299:896-899

103. Nisoli E, Falcone S, Tonello C, Cozzi V, Palomba L, Fiorani M, Pisconti A, Brunelli S, Cardile A, Francolini M, Cantoni O, Carruba MO, Moncada S, Clementi E. Mitochondrial biogenesis by no yields functionally active mitochondria in mammals. *Proceedings of the National Academy of Sciences of the United States of America*. 2004;101:16507-16512
104. Clement E, Nisoli E. Nitric oxide and mitochondrial biogenesis: A key to long-term regulation of cellular metabolism. *Comparative Biochemistry and Physiology a-Molecular & Integrative Physiology*. 2005;142:102-110
105. Hill BG, Dranka BP, Bailey SM, Lancaster JR, Jr., Darley-Usmar VM. What part of no don't you understand? Some answers to the cardinal questions in nitric oxide biology. *J Biol Chem*. 2010;285:19699-19704
106. Sprigge JS. Sir humphry davy; his researches in respiratory physiology and his debt to antoine lavoisier. *Anaesthesia*. 2002;57:357-364
107. Alderton WK, Cooper CE, Knowles RG. Nitric oxide synthases: Structure, function and inhibition. *Biochem J*. 2001;357:593-615
108. Li H, Poulos TL. Structure-function studies on nitric oxide synthases. *J Inorg Biochem*. 2005;99:293-305
109. Dudzinski DM, Michel T. Life history of enos: Partners and pathways. *Cardiovasc Res*. 2007;75:247-260
110. Oess S, Icking A, Fulton D, Govers R, Muller-Esterl W. Subcellular targeting and trafficking of nitric oxide synthases. *Biochem J*. 2006;396:401-409
111. Sessa WC. Enos at a glance. *J Cell Sci*. 2004;117:2427-2429
112. Balligand JL, Feron O, Dessy C. Enos activation by physical forces: From short-term regulation of contraction to chronic remodeling of cardiovascular tissues. *Physiol Rev*. 2009;89:481-534
113. Kone BC, Kuncewicz T, Zhang W, Yu ZY. Protein interactions with nitric oxide synthases: Controlling the right time, the right place, and the right amount of nitric oxide. *Am J Physiol Renal Physiol*. 2003;285:F178-190
114. Kleinert H, Pautz A, Linker K, Schwarz PM. Regulation of the expression of inducible nitric oxide synthase. *Eur J Pharmacol*. 2004;500:255-266
115. Finocchietto PV, Franco MC, Holod S, Gonzalez AS, Converso DP, Arciuch VG, Serra MP, Poderoso JJ, Carreras MC. Mitochondrial nitric oxide synthase: A masterpiece of metabolic adaptation, cell growth, transformation, and death. *Exp Biol Med (Maywood)*. 2009;234:1020-1028
116. Kato K, Giulivi C. Critical overview of mitochondrial nitric-oxide synthase. *Front Biosci*. 2006;11:2725-2738
117. Vitturi DA, Patel RP. Current perspectives and challenges in understanding the role of nitrite as an integral player in nitric oxide biology and therapy. *Free Radic Biol Med*. 2011;51:805-812
118. Lundberg JO, Gladwin MT, Ahluwalia A, Benjamin N, Bryan NS, Butler A, Cabrales P, Fago A, Feelisch M, Ford PC, Freeman BA, Frenneaux M, Friedman J, Kelm M, Kevil CG, Kim-Shapiro DB, Kozlov AV, Lancaster JR, Jr., Lefer DJ, McColl K, McCurry K, Patel RP, Petersson J, Rassaf T, Reutov VP, Richter-Addo GB, Schechter A, Shiva S, Tsuchiya K, van Faassen EE, Webb AJ, Zuckerbraun BS, Zweier JL, Weitzberg E. Nitrate and nitrite in biology, nutrition and therapeutics. *Nature chemical biology*. 2009;5:865-869
119. Thomas DD, Liu X, Kantrow SP, Lancaster JR, Jr. The biological lifetime of nitric oxide: Implications for the perivascular dynamics of no and o2. *Proc Natl Acad Sci U S A*. 2001;98:355-360
120. Pacher P, Beckman JS, Liaudet L. Nitric oxide and peroxynitrite in health and disease. *Physiological reviews*. 2007;87:315-424
121. Trujillo M, Ferrer-Sueta G, Radi R. Peroxynitrite detoxification and its biologic implications. *Antioxid Redox Signal*. 2008;10:1607-1620
122. Szabo C, Ischiropoulos H, Radi R. Peroxynitrite: Biochemistry, pathophysiology and development of therapeutics. *Nat Rev Drug Discov*. 2007;6:662-680
123. Beckman JS. Understanding peroxynitrite biochemistry and its potential for treating human diseases. *Arch Biochem Biophys*. 2009;484:114-116

124. McAndrew J, Patel RP, Jo H, Cornwell T, Lincoln T, Moellering D, White CR, Matalon S, Darley-Usmar V. The interplay of nitric oxide and peroxynitrite with signal transduction pathways: Implications for disease. *Semin Perinatol.* 1997;21:351-366
125. Alvarez B, Radi R. Peroxynitrite reactivity with amino acids and proteins. *Amino Acids.* 2003;25:295-311
126. Xu S, Ying J, Jiang B, Guo W, Adachi T, Sharov V, Lazar H, Menzoian J, Knyushko TV, Bigelow D, Schoneich C, Cohen RA. Detection of sequence-specific tyrosine nitration of manganese sod and serca in cardiovascular disease and aging. *Am J Physiol Heart Circ Physiol.* 2006;290:H2220-2227
127. Koeck T, Stuehr DJ, Aulak KS. Mitochondria and regulated tyrosine nitration. *Biochem Soc Trans.* 2005;33:1399-1403
128. Aulak KS, Miyagi M, Yan L, West KA, Massillon D, Crabb JW, Stuehr DJ. Proteomic method identifies proteins nitrated in vivo during inflammatory challenge. *Proc Natl Acad Sci U S A.* 2001;98:12056-12061
129. Halliwell B, Gutteridge JMC. *Free radicals in biology and medicine.* Oxford: Oxford University Press; 1998.
130. Hogg N. The biochemistry and physiology of s-nitrosothiols. *Annu Rev Pharmacol Toxicol.* 2002;42:585-600
131. Hill BG, Bhatnagar A. Role of glutathiolation in preservation, restoration and regulation of protein function. *IUBMB life.* 2007;59:21-26
132. Forstermann U, Sessa WC. Nitric oxide synthases: Regulation and function. *Eur Heart J.* 2012;33:829-837, 837a-837d
133. Furchgott RF, Zawadzki JV. The obligatory role of endothelial cells in the relaxation of arterial smooth muscle by acetylcholine. *Nature.* 1980;288:373-376
134. Rapoport RM, Draznin MB, Murad F. Endothelium-dependent relaxation in rat aorta may be mediated through cyclic gmp-dependent protein phosphorylation. *Nature.* 1983;306:174-176
135. Rapoport RM, Murad F. Agonist-induced endothelium-dependent relaxation in rat thoracic aorta may be mediated through cgmp. *Circ Res.* 1983;52:352-357
136. Forstermann U, Mulch A, Bohme E, Busse R. Stimulation of soluble guanylate cyclase by an acetylcholine-induced endothelium-derived factor from rabbit and canine arteries. *Circ Res.* 1986;58:531-538
137. Rajfer J, Aronson WJ, Bush PA, Dorey FJ, Ignarro LJ. Nitric oxide as a mediator of relaxation of the corpus cavernosum in response to nonadrenergic, noncholinergic neurotransmission. *The New England journal of medicine.* 1992;326:90-94
138. Moncada S, Palmer RM, Gryglewski RJ. Mechanism of action of some inhibitors of endothelium-derived relaxing factor. *Proc Natl Acad Sci U S A.* 1986;83:9164-9168
139. Gryglewski RJ, Moncada S, Palmer RM. Bioassay of prostacyclin and endothelium-derived relaxing factor (edrf) from porcine aortic endothelial cells. *British journal of pharmacology.* 1986;87:685-694
140. Palmer RM, Ferrige AG, Moncada S. Nitric oxide release accounts for the biological activity of endothelium-derived relaxing factor. *Nature.* 1987;327:524-526
141. Melikian N, Seddon MD, Casadei B, Chowienczyk PJ, Shah AM. Neuronal nitric oxide synthase and human vascular regulation. *Trends in cardiovascular medicine.* 2009;19:256-262
142. Togashi H, Sakuma I, Yoshioka M, Kobayashi T, Yasuda H, Kitabatake A, Saito H, Gross SS, Levi R. A central nervous system action of nitric oxide in blood pressure regulation. *The Journal of pharmacology and experimental therapeutics.* 1992;262:343-347
143. Sakuma I, Togashi H, Yoshioka M, Saito H, Yanagida M, Tamura M, Kobayashi T, Yasuda H, Gross SS, Levi R. Ng-methyl-l-arginine, an inhibitor of l-arginine-derived nitric oxide synthesis, stimulates renal sympathetic nerve activity in vivo. A role for nitric oxide in the central regulation of sympathetic tone? *Circ Res.* 1992;70:607-611
144. el Karib AO, Sheng J, Betz AL, Malvin RL. The central effects of a nitric oxide synthase inhibitor (n omega-nitro-l-arginine) on blood pressure and plasma renin. *Clinical and experimental hypertension.* 1993;15:819-832

145. Toda N, Ayajiki K, Okamura T. Control of systemic and pulmonary blood pressure by nitric oxide formed through neuronal nitric oxide synthase. *Journal of hypertension*. 2009;27:1929-1940
146. Kim N, Azadzi KM, Goldstein I, Saenz de Tejada I. A nitric oxide-like factor mediates nonadrenergic-noncholinergic neurogenic relaxation of penile corpus cavernosum smooth muscle. *J Clin Invest*. 1991;88:112-118
147. Shiva S, Oh JY, Landar AL, Ulasova E, Venkatraman A, Bailey SM, Darley-Usmar VM. Nitroxia: The pathological consequence of dysfunction in the nitric oxide-cytochrome c oxidase signaling pathway. *Free Radic Biol Med*. 2005;38:297-306
148. Cooper CE, Giulivi C. Nitric oxide regulation of mitochondrial oxygen consumption ii: Molecular mechanism and tissue physiology. *Am J Physiol Cell Physiol*. 2007;292:C1993-2003
149. Wolzt M, MacAllister RJ, Davis D, Feelisch M, Moncada S, Vallance P, Hobbs AJ. Biochemical characterization of s-nitrosohemoglobin. Mechanisms underlying synthesis, no release, and biological activity. *J Biol Chem*. 1999;274:28983-28990
150. Patel RP, Hogg N, Spencer NY, Kalyanaraman B, Matalon S, Darley-Usmar VM. Biochemical characterization of human s-nitrosohemoglobin. Effects on oxygen binding and transnitrosation. *J Biol Chem*. 1999;274:15487-15492
151. Kelly DP, Scarpulla RC. Transcriptional regulatory circuits controlling mitochondrial biogenesis and function. *Genes Dev*. 2004;18:357-368
152. Nisoli E, Clementi E, Paolucci C, Cozzi V, Tonello C, Sciorati C, Bracale R, Valerio A, Francolini M, Moncada S, Carruba MO. Mitochondrial biogenesis in mammals: The role of endogenous nitric oxide. *Science*. 2003;299:896-899
153. Nisoli E, Falcone S, Tonello C, Cozzi V, Palomba L, Fiorani M, Pisconti A, Brunelli S, Cardile A, Francolini M, Cantoni O, Carruba MO, Moncada S, Clementi E. Mitochondrial biogenesis by no yields functionally active mitochondria in mammals. *Proc Natl Acad Sci U S A*. 2004;101:16507-16512
154. Bender SB, Herrick EK, Lott ND, Klabunde RE. Diet-induced obesity and diabetes reduce coronary responses to nitric oxide due to reduced bioavailability in isolated mouse hearts. *Diabetes Obes Metab*. 2007;9:688-696
155. Kim F, Pham M, Maloney E, Rizzo NO, Morton GJ, Wisse BE, Kirk EA, Chait A, Schwartz MW. Vascular inflammation, insulin resistance, and reduced nitric oxide production precede the onset of peripheral insulin resistance. *Arterioscler Thromb Vasc Biol*. 2008;28:1982-1988
156. Higashi Y, Sasaki S, Nakagawa K, Matsuura H, Chayama K, Oshima T. Effect of obesity on endothelium-dependent, nitric oxide-mediated vasodilation in normotensive individuals and patients with essential hypertension. *Am J Hypertens*. 2001;14:1038-1045
157. Gruber HJ, Mayer C, Mangge H, Fauler G, Grandits N, Wilders-Truschning M. Obesity reduces the bioavailability of nitric oxide in juveniles. *Int J Obes (Lond)*. 2008;32:826-831
158. Georgescu A, Popov D, Constantin A, Nemezc M, Alexandru N, Cochior D, Tudor A. Dysfunction of human subcutaneous fat arterioles in obesity alone or obesity associated with type 2 diabetes. *Clinical science*. 2011;120:463-472
159. Perez-Matute P, Neville MJ, Tan GD, Frayn KN, Karpe F. Transcriptional control of human adipose tissue blood flow. *Obesity (Silver Spring)*. 2009;17:681-688
160. Sansbury BE, Cummins TD, Tang Y, Hellmann J, Holden CR, Harbeson MA, Chen Y, Patel RP, Spite M, Bhatnagar A, Hill BG. Overexpression of endothelial nitric oxide synthase prevents diet-induced obesity and regulates adipocyte phenotype. *Circulation Research*. 2012;111:1176-1189
161. Valerio A, Cardile A, Cozzi V, Bracale R, Tedesco L, Pisconti A, Palomba L, Cantoni O, Clementi E, Moncada S, Carruba MO, Nisoli E. Tnf-alpha downregulates enos expression and mitochondrial biogenesis in fat and muscle of obese rodents. *J Clin Invest*. 2006;116:2791-2798
162. Kraus RM, Houmard JA, Kraus WE, Tanner CJ, Pierce JR, Choi MD, Hickner RC. Obesity, insulin resistance, and skeletal muscle nitric oxide synthase. *J Appl Physiol (1985)*. 2012;113:758-765

163. Awolesi MA, Sessa WC, Sumpio BE. Cyclic strain upregulates nitric oxide synthase in cultured bovine aortic endothelial cells. *J Clin Invest.* 1995;96:1449-1454
164. Zembowicz A, Tang JL, Wu KK. Transcriptional induction of endothelial nitric oxide synthase type iii by lysophosphatidylcholine. *J Biol Chem.* 1995;270:17006-17010
165. Hirata K, Miki N, Kuroda Y, Sakoda T, Kawashima S, Yokoyama M. Low concentration of oxidized low-density lipoprotein and lysophosphatidylcholine upregulate constitutive nitric oxide synthase mrna expression in bovine aortic endothelial cells. *Circ Res.* 1995;76:958-962
166. Zeng G, Nystrom FH, Ravichandran LV, Cong LN, Kirby M, Mostowski H, Quon MJ. Roles for insulin receptor, pi3-kinase, and akt in insulin-signaling pathways related to production of nitric oxide in human vascular endothelial cells. *Circulation.* 2000;101:1539-1545
167. Hambrecht R, Wolf A, Gielen S, Linke A, Hofer J, Erbs S, Schoene N, Schuler G. Effect of exercise on coronary endothelial function in patients with coronary artery disease. *The New England journal of medicine.* 2000;342:454-460
168. Hotamisligil GS, Shargill NS, Spiegelman BM. Adipose expression of tumor necrosis factor-alpha: Direct role in obesity-linked insulin resistance. *Science.* 1993;259:87-91
169. Michel T, Lamas S. Molecular cloning of constitutive endothelial nitric oxide synthase: Evidence for a family of related genes. *Journal of cardiovascular pharmacology.* 1992;20 Suppl 12:S45-49
170. Lai PF, Mohamed F, Monge JC, Stewart DJ. Downregulation of enos mrna expression by tnfa: Identification and functional characterization of rna-protein interactions in the 3'utr. *Cardiovascular research.* 2003;59:160-168
171. Neumann P, Gertzberg N, Johnson A. Tnf-alpha induces a decrease in enos promoter activity. *American journal of physiology. Lung cellular and molecular physiology.* 2004;286:L452-459
172. Anderson HD, Rahmutula D, Gardner DG. Tumor necrosis factor-alpha inhibits endothelial nitric-oxide synthase gene promoter activity in bovine aortic endothelial cells. *J Biol Chem.* 2004;279:963-969
173. Alonso J, Sanchez de Miguel L, Monton M, Casado S, Lopez-Farre A. Endothelial cytosolic proteins bind to the 3' untranslated region of endothelial nitric oxide synthase mrna: Regulation by tumor necrosis factor alpha. *Mol Cell Biol.* 1997;17:5719-5726
174. Sanchez de Miguel L, Alonso J, Gonzalez-Fernandez F, de la Osada J, Monton M, Rodriguez-Feo JA, Guerra JI, Arriero MM, Rico L, Casado S, Lopez-Farre A. Evidence that an endothelial cytosolic protein binds to the 3'-untranslated region of endothelial nitric oxide synthase mrna. *Journal of vascular research.* 1999;36:201-208
175. Yoshizumi M, Perrella MA, Burnett JC, Jr., Lee ME. Tumor necrosis factor downregulates an endothelial nitric oxide synthase mrna by shortening its half-life. *Circ Res.* 1993;73:205-209
176. Yan G, You B, Chen SP, Liao JK, Sun J. Tumor necrosis factor-alpha downregulates endothelial nitric oxide synthase mrna stability via translation elongation factor 1-alpha 1. *Circ Res.* 2008;103:591-597
177. Bulotta S, Barsacchi R, Rotiroti D, Borgese N, Clementi E. Activation of the endothelial nitric-oxide synthase by tumor necrosis factor-alpha. A novel feedback mechanism regulating cell death. *J Biol Chem.* 2001;276:6529-6536
178. Kawanaka H, Jones MK, Szabo IL, Baatar D, Pai R, Tsugawa K, Sugimachi K, Sarfeh IJ, Tarnawski AS. Activation of enos in rat portal hypertensive gastric mucosa is mediated by tnf-alpha via the pi 3-kinase-akt signaling pathway. *Hepatology.* 2002;35:393-402
179. Barsacchi R, Perrotta C, Bulotta S, Moncada S, Borgese N, Clementi E. Activation of endothelial nitric-oxide synthase by tumor necrosis factor-alpha: A novel pathway involving sequential activation of neutral sphingomyelinase, phosphatidylinositol-3' kinase, and akt. *Molecular pharmacology.* 2003;63:886-895
180. De Palma C, Meacci E, Perrotta C, Bruni P, Clementi E. Endothelial nitric oxide synthase activation by tumor necrosis factor alpha through neutral sphingomyelinase 2, sphingosine kinase 1, and sphingosine 1 phosphate receptors: A novel pathway relevant to the pathophysiology of endothelium. *Arterioscler Thromb Vasc Biol.* 2006;26:99-105

181. Vaziri ND, Wang XQ. Cgmp-mediated negative-feedback regulation of endothelial nitric oxide synthase expression by nitric oxide. *Hypertension*. 1999;34:1237-1241
182. Grumbach IM, Chen W, Mertens SA, Harrison DG. A negative feedback mechanism involving nitric oxide and nuclear factor kappa-b modulates endothelial nitric oxide synthase transcription. *J Mol Cell Cardiol*. 2005;39:595-603
183. Zhang MX, Ou H, Shen YH, Wang J, Wang J, Coselli J, Wang XL. Regulation of endothelial nitric oxide synthase by small rna. *Proc Natl Acad Sci U S A*. 2005;102:16967-16972
184. Shimabukuro M, Ohneda M, Lee Y, Unger RH. Role of nitric oxide in obesity-induced beta cell disease. *J Clin Invest*. 1997;100:290-295
185. Noronha BT, Li JM, Wheatcroft SB, Shah AM, Kearney MT. Inducible nitric oxide synthase has divergent effects on vascular and metabolic function in obesity. *Diabetes*. 2005;54:1082-1089
186. Sugita H, Fujimoto M, Yasukawa T, Shimizu N, Sugita M, Yasuhara S, Martyn JA, Kaneki M. Inducible nitric-oxide synthase and no donor induce insulin receptor substrate-1 degradation in skeletal muscle cells. *J Biol Chem*. 2005;280:14203-14211
187. Mantena SK, Vaughn DP, Andringa KK, Eccleston HB, King AL, Abrams GA, Doeller JE, Kraus DW, Darley-Usmar VM, Bailey SM. High fat diet induces dysregulation of hepatic oxygen gradients and mitochondrial function in vivo. *Biochem J*. 2009;417:183-193
188. Fujimoto M, Shimizu N, Kunii K, Martyn JA, Ueki K, Kaneki M. A role for inos in fasting hyperglycemia and impaired insulin signaling in the liver of obese diabetic mice. *Diabetes*. 2005;54:1340-1348
189. Weisberg SP, McCann D, Desai M, Rosenbaum M, Leibel RL, Ferrante AW, Jr. Obesity is associated with macrophage accumulation in adipose tissue. *J Clin Invest*. 2003;112:1796-1808
190. Lumeng CN, Bodzin JL, Saltiel AR. Obesity induces a phenotypic switch in adipose tissue macrophage polarization. *J Clin Invest*. 2007;117:175-184
191. Lumeng CN, Deyoung SM, Bodzin JL, Saltiel AR. Increased inflammatory properties of adipose tissue macrophages recruited during diet-induced obesity. *Diabetes*. 2007;56:16-23
192. Merial C, Bouloumie A, Trocheris V, Lafontan M, Galitzky J. Nitric oxide-dependent downregulation of adipocyte ucp-2 expression by tumor necrosis factor-alpha. *American journal of physiology. Cell physiology*. 2000;279:C1100-1106
193. Sadler CJ, Wilding JP. Reduced ventromedial hypothalamic neuronal nitric oxide synthase and increased sensitivity to nos inhibition in dietary obese rats: Further evidence of a role for nitric oxide in the regulation of energy balance. *Brain research*. 2004;1016:222-228
194. Benkhoff S, Loot AE, Pierson I, Sturza A, Kohlstedt K, Fleming I, Shimokawa H, Grisk O, Brandes RP, Schroder K. Leptin potentiates endothelium-dependent relaxation by inducing endothelial expression of neuronal no synthase. *Arterioscler Thromb Vasc Biol*. 2012;32:1605-1612
195. Huang PL. Enos, metabolic syndrome and cardiovascular disease. *Trends in endocrinology and metabolism: TEM*. 2009;20:295-302
196. Rafikov R, Fonseca FV, Kumar S, Pardo D, Darragh C, Elms S, Fulton D, Black SM. Enos activation and no function: Structural motifs responsible for the posttranslational control of endothelial nitric oxide synthase activity. *The Journal of endocrinology*. 2011;210:271-284
197. Ju H, Zou R, Venema VJ, Venema RC. Direct interaction of endothelial nitric-oxide synthase and caveolin-1 inhibits synthase activity. *J Biol Chem*. 1997;272:18522-18525
198. Michel JB, Feron O, Sacks D, Michel T. Reciprocal regulation of endothelial nitric-oxide synthase by ca2+-calmodulin and caveolin. *J Biol Chem*. 1997;272:15583-15586
199. Yang N, Ying C, Xu M, Zuo X, Ye X, Liu L, Nara Y, Sun X. High-fat diet up-regulates caveolin-1 expression in aorta of diet-induced obese but not in diet-resistant rats. *Cardiovascular research*. 2007;76:167-174
200. Bikman BT, Summers SA. Ceramides as modulators of cellular and whole-body metabolism. *J Clin Invest*. 2011;121:4222-4230

201. Zhang QJ, Holland WL, Wilson L, Tanner JM, Kearns D, Cahoon JM, Pettey D, Losee J, Duncan B, Gale D, Kowalski CA, Deeter N, Nichols A, Deesing M, Arrant C, Ruan T, Boehme C, McCamey DR, Rou J, Ambal K, Narra KK, Summers SA, Abel ED, Symons JD. Ceramide mediates vascular dysfunction in diet-induced obesity by pp2a-mediated dephosphorylation of the enos-akt complex. *Diabetes*. 2012;61:1848-1859
202. Gratton JP, Fontana J, O'Connor DS, Garcia-Cardena G, McCabe TJ, Sessa WC. Reconstitution of an endothelial nitric-oxide synthase (enos), hsp90, and caveolin-1 complex in vitro. Evidence that hsp90 facilitates calmodulin stimulated displacement of enos from caveolin-1. *J Biol Chem*. 2000;275:22268-22272
203. McCabe TJ, Fulton D, Roman LJ, Sessa WC. Enhanced electron flux and reduced calmodulin dissociation may explain "calcium-independent" enos activation by phosphorylation. *J Biol Chem*. 2000;275:6123-6128
204. Elrod JW, Duranski MR, Langston W, Greer JJ, Tao L, Dugas TR, Kevil CG, Champion HC, Lefer DJ. Enos gene therapy exacerbates hepatic ischemia-reperfusion injury in diabetes: A role for enos uncoupling. *Circ Res*. 2006;99:78-85
205. Zhong JC, Yu XY, Huang Y, Yung LM, Lau CW, Lin SG. Apelin modulates aortic vascular tone via endothelial nitric oxide synthase phosphorylation pathway in diabetic mice. *Cardiovascular research*. 2007;74:388-395
206. Li Q, Atochin D, Kashiwagi S, Earle J, Wang A, Mandeville E, Hayakawa K, d'Uscio LV, Lo EH, Katusic Z, Sessa W, Huang PL. Deficient enos phosphorylation is a mechanism for diabetic vascular dysfunction contributing to increased stroke size. *Stroke*. 2013;44:3183-3188
207. Taguchi K, Kobayashi T, Matsumoto T, Kamata K. Dysfunction of endothelium-dependent relaxation to insulin via pkc-mediated grk2/akt activation in aortas of ob/ob mice. *Am J Physiol Heart Circ Physiol*. 2011;301:H571-583
208. Kim F, Pham M, Luttrell I, Bannerman DD, Tupper J, Thaler J, Hawn TR, Raines EW, Schwartz MW. Toll-like receptor-4 mediates vascular inflammation and insulin resistance in diet-induced obesity. *Circ Res*. 2007;100:1589-1596
209. Symons JD, McMillin SL, Riehle C, Tanner J, Palionyte M, Hillas E, Jones D, Cooksey RC, Birnbaum MJ, McClain DA, Zhang QJ, Gale D, Wilson LJ, Abel ED. Contribution of insulin and akt1 signaling to endothelial nitric oxide synthase in the regulation of endothelial function and blood pressure. *Circ Res*. 2009;104:1085-1094
210. Naruse K, Rask-Madsen C, Takahara N, Ha SW, Suzuma K, Way KJ, Jacobs JR, Clermont AC, Ueki K, Ohshiro Y, Zhang J, Goldfine AB, King GL. Activation of vascular protein kinase c-beta inhibits akt-dependent endothelial nitric oxide synthase function in obesity-associated insulin resistance. *Diabetes*. 2006;55:691-698
211. Zecchin HG, Priviero FB, Souza CT, Zecchin KG, Prada PO, Carvalheira JB, Velloso LA, Antunes E, Saad MJ. Defective insulin and acetylcholine induction of endothelial cell-nitric oxide synthase through insulin receptor substrate/akt signaling pathway in aorta of obese rats. *Diabetes*. 2007;56:1014-1024
212. Park K, Li Q, Rask-Madsen C, Mima A, Mizutani K, Winnay J, Maeda Y, D'Aquino K, White MF, Feener EP, King GL. Serine phosphorylation sites on irs2 activated by angiotensin ii and protein kinase c to induce selective insulin resistance in endothelial cells. *Mol Cell Biol*. 2013;33:3227-3241
213. Low Wang CC, Lu L, Leitner JW, Sarraf M, Gianani R, Draznin B, Greyson CR, Reusch JE, Schwartz GG. Arterial insulin resistance in yucatan micropigs with diet-induced obesity and metabolic syndrome. *Journal of diabetes and its complications*. 2013;27:307-315
214. Dimmeler S, Fleming I, Fisslthaler B, Hermann C, Busse R, Zeiher AM. Activation of nitric oxide synthase in endothelial cells by akt-dependent phosphorylation. *Nature*. 1999;399:601-605
215. Hermann C, Assmus B, Urbich C, Zeiher AM, Dimmeler S. Insulin-mediated stimulation of protein kinase akt: A potent survival signaling cascade for endothelial cells. *Arterioscler Thromb Vasc Biol*. 2000;20:402-409

216. Duncan ER, Crossey PA, Walker S, Anilkumar N, Poston L, Douglas G, Ezzat VA, Wheatcroft SB, Shah AM, Kearney MT. Effect of endothelium-specific insulin resistance on endothelial function in vivo. *Diabetes*. 2008;57:3307-3314
217. Kubota T, Kubota N, Kumagai H, Yamaguchi S, Kozono H, Takahashi T, Inoue M, Itoh S, Takamoto I, Sasako T, Kumagai K, Kawai T, Hashimoto S, Kobayashi T, Sato M, Tokuyama K, Nishimura S, Tsunoda M, Ide T, Murakami K, Yamazaki T, Ezaki O, Kawamura K, Masuda H, Moroi M, Sugi K, Oike Y, Shimokawa H, Yanagihara N, Tsutsui M, Terauchi Y, Tobe K, Nagai R, Kamata K, Inoue K, Kodama T, Ueki K, Kadowaki T. Impaired insulin signaling in endothelial cells reduces insulin-induced glucose uptake by skeletal muscle. *Cell Metab*. 2011;13:294-307
218. Kim F, Tysseling KA, Rice J, Pham M, Haji L, Gallis BM, Baas AS, Paramsothy P, Giachelli CM, Corson MA, Raines EW. Free fatty acid impairment of nitric oxide production in endothelial cells is mediated by ikkbeta. *Arterioscler Thromb Vasc Biol*. 2005;25:989-994
219. Edirisinghe I, McCormick Hallam K, Kappagoda CT. Effect of fatty acids on endothelium-dependent relaxation in the rabbit aorta. *Clin Sci (Lond)*. 2006;111:145-151
220. Du X, Edelstein D, Obici S, Higham N, Zou MH, Brownlee M. Insulin resistance reduces arterial prostacyclin synthase and eNOS activities by increasing endothelial fatty acid oxidation. *J Clin Invest*. 2006;116:1071-1080
221. Steinberg HO, Paradisi G, Hook G, Crowder K, Cronin J, Baron AD. Free fatty acid elevation impairs insulin-mediated vasodilation and nitric oxide production. *Diabetes*. 2000;49:1231-1238
222. Steinberg HO, Tarshoby M, Monestel R, Hook G, Cronin J, Johnson A, Bayazeed B, Baron AD. Elevated circulating free fatty acid levels impair endothelium-dependent vasodilation. *J Clin Invest*. 1997;100:1230-1239
223. Jang HJ, Kim HS, Hwang DH, Quon MJ, Kim JA. Toll-like receptor 2 mediates high-fat diet-induced impairment of vasodilator actions of insulin. *Am J Physiol Endocrinol Metab*. 2013;304:E1077-1088
224. Du XL, Edelstein D, Dimmeler S, Ju Q, Sui C, Brownlee M. Hyperglycemia inhibits endothelial nitric oxide synthase activity by posttranslational modification at the akt site. *J Clin Invest*. 2001;108:1341-1348
225. Rodriguez-Crespo I, Gerber NC, Ortiz de Montellano PR. Endothelial nitric-oxide synthase. Expression in escherichia coli, spectroscopic characterization, and role of tetrahydrobiopterin in dimer formation. *J Biol Chem*. 1996;271:11462-11467
226. Rodriguez-Crespo I, Ortiz de Montellano PR. Human endothelial nitric oxide synthase: Expression in escherichia coli, coexpression with calmodulin, and characterization. *Archives of biochemistry and biophysics*. 1996;336:151-156
227. Alp NJ, Channon KM. Regulation of endothelial nitric oxide synthase by tetrahydrobiopterin in vascular disease. *Arterioscler Thromb Vasc Biol*. 2004;24:413-420
228. Li H, Forstermann U. Uncoupling of endothelial nitric oxide synthase in atherosclerosis and vascular disease. *Current opinion in pharmacology*. 2013;13:161-167
229. Zweier JL, Chen CA, Druhan LJ. S-glutathionylation reshapes our understanding of endothelial nitric oxide synthase uncoupling and nitric oxide/reactive oxygen species-mediated signaling. *Antioxidants & redox signaling*. 2011;14:1769-1775
230. Channon KM. Tetrahydrobiopterin: A vascular redox target to improve endothelial function. *Current vascular pharmacology*. 2012;10:705-708
231. Ding H, Triggle CR. Endothelial dysfunction in diabetes: Multiple targets for treatment. *Pflugers Archiv : European journal of physiology*. 2010;459:977-994
232. Chander PN, Gealekman O, Brodsky SV, Elitok S, Tojo A, Crabtree M, Gross SS, Goligorsky MS. Nephropathy in Zucker diabetic fat rat is associated with oxidative and nitrosative stress: Prevention by chronic therapy with a peroxynitrite scavenger ebselen. *Journal of the American Society of Nephrology : JASN*. 2004;15:2391-2403
233. Shinozaki K, Kashiwagi A, Nishio Y, Okamura T, Yoshida Y, Masada M, Toda N, Kikkawa R. Abnormal biopterin metabolism is a major cause of impaired endothelium-dependent relaxation through nitric oxide/o₂- imbalance in insulin-resistant rat aorta. *Diabetes*. 1999;48:2437-2445

234. Pannirselvam M, Verma S, Anderson TJ, Triggle CR. Cellular basis of endothelial dysfunction in small mesenteric arteries from spontaneously diabetic (db/db *-/-*) mice: Role of decreased tetrahydrobiopterin bioavailability. *British journal of pharmacology*. 2002;136:255-263
235. Cai S, Khoo J, Channon KM. Augmented bh4 by gene transfer restores nitric oxide synthase function in hyperglycemic human endothelial cells. *Cardiovascular research*. 2005;65:823-831
236. Crabtree MJ, Smith CL, Lam G, Goligorsky MS, Gross SS. Ratio of 5,6,7,8-tetrahydrobiopterin to 7,8-dihydrobiopterin in endothelial cells determines glucose-elicited changes in no vs. Superoxide production by enos. *Am J Physiol Heart Circ Physiol*. 2008;294:H1530-1540
237. Forstermann U, Li H. Therapeutic effect of enhancing endothelial nitric oxide synthase (enos) expression and preventing enos uncoupling. *British journal of pharmacology*. 2011;164:213-223
238. Kietadisorn R, Juni RP, Moens AL. Tackling endothelial dysfunction by modulating nos uncoupling: New insights into its pathogenesis and therapeutic possibilities. *Am J Physiol Endocrinol Metab*. 2012;302:E481-495
239. Crabtree MJ, Channon KM. Synthesis and recycling of tetrahydrobiopterin in endothelial function and vascular disease. *Nitric oxide : biology and chemistry / official journal of the Nitric Oxide Society*. 2011;25:81-88
240. Sanchez A, Contreras C, Martinez MP, Climent B, Benedito S, Garcia-Sacristan A, Hernandez M, Prieto D. Role of neural no synthase (nnos) uncoupling in the dysfunctional nitregeric vasorelaxation of penile arteries from insulin-resistant obese zucker rats. *PLoS One*. 2012;7:e36027
241. Molnar J, Yu S, Mzhavia N, Pau C, Chereshnev I, Dansky HM. Diabetes induces endothelial dysfunction but does not increase neointimal formation in high-fat diet fed c57bl/6j mice. *Circ Res*. 2005;96:1178-1184
242. Brodsky SV, Gealekman O, Chen J, Zhang F, Togashi N, Crabtree M, Gross SS, Nasjletti A, Goligorsky MS. Prevention and reversal of premature endothelial cell senescence and vasculopathy in obesity-induced diabetes by ebselen. *Circ Res*. 2004;94:377-384
243. Cassuto J, Dou H, Czikora I, Szabo A, Patel VS, Kamath V, Belin de Chantemele E, Feher A, Romero MJ, Bagi Z. Peroxynitrite disrupts endothelial caveolae leading to enos uncoupling and diminished flow-mediated dilation in coronary arterioles of diabetic patients. *Diabetes*. 2013
244. Landmesser U, Dikalov S, Price SR, McCann L, Fukai T, Holland SM, Mitch WE, Harrison DG. Oxidation of tetrahydrobiopterin leads to uncoupling of endothelial cell nitric oxide synthase in hypertension. *J Clin Invest*. 2003;111:1201-1209
245. Satoh M, Fujimoto S, Haruna Y, Arakawa S, Horike H, Komai N, Sasaki T, Tsujioka K, Makino H, Kashihara N. Nad(p)h oxidase and uncoupled nitric oxide synthase are major sources of glomerular superoxide in rats with experimental diabetic nephropathy. *American journal of physiology. Renal physiology*. 2005;288:F1144-1152
246. Bitar MS, Wahid S, Mustafa S, Al-Saleh E, Dhaunsi GS, Al-Mulla F. Nitric oxide dynamics and endothelial dysfunction in type ii model of genetic diabetes. *European journal of pharmacology*. 2005;511:53-64
247. Xu J, Xie Z, Reece R, Pimental D, Zou MH. Uncoupling of endothelial nitric oxidase synthase by hypochlorous acid: Role of nad(p)h oxidase-derived superoxide and peroxynitrite. *Arterioscler Thromb Vasc Biol*. 2006;26:2688-2695
248. Dikalova AE, Gongora MC, Harrison DG, Lambeth JD, Dikalov S, Griendling KK. Upregulation of nox1 in vascular smooth muscle leads to impaired endothelium-dependent relaxation via enos uncoupling. *Am J Physiol Heart Circ Physiol*. 2010;299:H673-679
249. Zhang Q, Malik P, Pandey D, Gupta S, Jagnandan D, Belin de Chantemele E, Banfi B, Marrero MB, Rudic RD, Stepp DW, Fulton DJ. Paradoxical activation of endothelial nitric oxide synthase by nadph oxidase. *Arterioscler Thromb Vasc Biol*. 2008;28:1627-1633
250. Koppenol WH. 100 years of peroxynitrite chemistry and 11 years of peroxynitrite biochemistry. *Redox report : communications in free radical research*. 2001;6:339-341

251. Toutouzas K, Riga M, Stefanadi E, Stefanadis C. Asymmetric dimethylarginine (adma) and other endogenous nitric oxide synthase (nos) inhibitors as an important cause of vascular insulin resistance. *Hormone and metabolic research = Hormon- und Stoffwechselforschung = Hormones et metabolisme*. 2008;40:655-659
252. Risbano MG, Gladwin MT. Therapeutics targeting of dysregulated redox equilibrium and endothelial dysfunction. *Handb Exp Pharmacol*. 2013;218:315-349
253. Chen CA, Wang TY, Varadharaj S, Reyes LA, Hemann C, Talukder MA, Chen YR, Druhan LJ, Zweier JL. S-glutathionylation uncouples enos and regulates its cellular and vascular function. *Nature*. 2010;468:1115-1118
254. Lei H, Luo S, Qin H, Xia Y. Molecular mechanisms of endothelial no synthase uncoupling. *Current pharmaceutical design*. 2013
255. Williams IL, Wheatcroft SB, Shah AM, Kearney MT. Obesity, atherosclerosis and the vascular endothelium: Mechanisms of reduced nitric oxide bioavailability in obese humans. *Int J Obes Relat Metab Disord*. 2002;26:754-764
256. Steinberg HO, Chaker H, Leaming R, Johnson A, Brechtel G, Baron AD. Obesity/insulin resistance is associated with endothelial dysfunction. Implications for the syndrome of insulin resistance. *J Clin Invest*. 1996;97:2601-2610
257. Laine H, Yki-Jarvinen H, Kirvela O, Tolvanen T, Raitakari M, Solin O, Haaparanta M, Knuuti J, Nuutila P. Insulin resistance of glucose uptake in skeletal muscle cannot be ameliorated by enhancing endothelium-dependent blood flow in obesity. *J Clin Invest*. 1998;101:1156-1162
258. Van Guilder GP, Stauffer BL, Greiner JJ, Desouza CA. Impaired endothelium-dependent vasodilation in overweight and obese adult humans is not limited to muscarinic receptor agonists. *Am J Physiol Heart Circ Physiol*. 2008;294:H1685-1692
259. Arcaro G, Zamboni M, Rossi L, Turcato E, Covi G, Armellini F, Bosello O, Lechi A. Body fat distribution predicts the degree of endothelial dysfunction in uncomplicated obesity. *International journal of obesity and related metabolic disorders : journal of the International Association for the Study of Obesity*. 1999;23:936-942
260. Tack CJ, Ong MK, Lutterman JA, Smits P. Insulin-induced vasodilatation and endothelial function in obesity/insulin resistance. Effects of troglitazone. *Diabetologia*. 1998;41:569-576
261. Westerbacka J, Vehkavaara S, Bergholm R, Wilkinson I, Cockcroft J, Yki-Jarvinen H. Marked resistance of the ability of insulin to decrease arterial stiffness characterizes human obesity. *Diabetes*. 1999;48:821-827
262. Sturm W, Sandhofer A, Engl J, Laimer M, Molnar C, Kaser S, Weiss H, Tilg H, Ebenbichler CF, Patsch JR. Influence of visceral obesity and liver fat on vascular structure and function in obese subjects. *Obesity*. 2009;17:1783-1788
263. Parikh NI, Keyes MJ, Larson MG, Pou KM, Hamburg NM, Vita JA, O'Donnell CJ, Vasan RS, Mitchell GF, Hoffmann U, Fox CS, Benjamin EJ. Visceral and subcutaneous adiposity and brachial artery vasodilator function. *Obesity*. 2009;17:2054-2059
264. Gupta AK, Cornelissen G, Greenway FL, Dhoopati V, Halberg F, Johnson WD. Abnormalities in circadian blood pressure variability and endothelial function: Pragmatic markers for adverse cardiometabolic profiles in asymptomatic obese adults. *Cardiovascular diabetology*. 2010;9:58
265. Grassi G, Seravalle G, Scopelliti F, Dell'Oro R, Fattori L, Quarti-Trevano F, Brambilla G, Schiffrin EL, Mancia G. Structural and functional alterations of subcutaneous small resistance arteries in severe human obesity. *Obesity*. 2010;18:92-98
266. Weil BR, Westby CM, Van Guilder GP, Greiner JJ, Stauffer BL, DeSouza CA. Enhanced endothelin-1 system activity with overweight and obesity. *Am J Physiol Heart Circ Physiol*. 2011;301:H689-695
267. Lambert E, Sari CI, Dawood T, Nguyen J, McGrane M, Eikelis N, Chopra R, Wong C, Chatzivlastou K, Head G, Straznicki N, Esler M, Schlaich M, Lambert G. Sympathetic nervous system activity is associated with obesity-induced subclinical organ damage in young adults. *Hypertension*. 2010;56:351-358

268. Han KA, Patel Y, Lteif AA, Chisholm R, Mather KJ. Contributions of dysglycaemia, obesity, and insulin resistance to impaired endothelium-dependent vasodilation in humans. *Diabetes/metabolism research and reviews*. 2011;27:354-361
269. Andersson J, Sjoström LG, Karlsson M, Wiklund U, Hultin M, Karpe F, Olsson T. Dysregulation of subcutaneous adipose tissue blood flow in overweight postmenopausal women. *Menopause*. 2010;17:365-371
270. Miadi-Messaoud H, Chouchane A, Abderrazek E, Debbabi H, Zaouali-Ajina M, Tabka Z, Ben-Jebria A. Obesity-induced impairment of endothelium-dependent vasodilation in Tunisian women. *International journal of obesity*. 2010;34:273-279
271. Mahmud FH, Hill DJ, Cuerden MS, Clarson CL. Impaired vascular function in obese adolescents with insulin resistance. *J Pediatr*. 2009;155:678-682
272. Bhattacharjee R, Alotaibi WH, Kheirandish-Gozal L, Capdevila OS, Gozal D. Endothelial dysfunction in obese non-hypertensive children without evidence of sleep-disordered breathing. *BMC pediatrics*. 2010;10:8
273. Bhattacharjee R, Kim J, Alotaibi WH, Kheirandish-Gozal L, Capdevila OS, Gozal D. Endothelial dysfunction in children without hypertension: Potential contributions of obesity and obstructive sleep apnea. *Chest*. 2012;141:682-691
274. El Assar M, Ruiz de Adana JC, Angulo J, Pindado Martinez ML, Hernandez Matias A, Rodriguez-Manas L. Preserved endothelial function in human obesity in the absence of insulin resistance. *Journal of translational medicine*. 2013;11:263
275. Biasucci LM, Graziani F, Rizzello V, Liuzzo G, Guidone C, De Caterina AR, Brugaletta S, Mingrone G, Crea F. Paradoxical preservation of vascular function in severe obesity. *The American journal of medicine*. 2010;123:727-734
276. Czernichow S, Greenfield JR, Galan P, Bastard JP, Charnaux N, Samaras K, Safar ME, Blacher J, Hercberg S, Levy BI. Microvascular dysfunction in healthy insulin-sensitive overweight individuals. *Journal of hypertension*. 2010;28:325-332
277. Flegal KM, Carroll MD, Ogden CL, Curtin LR. Prevalence and trends in obesity among US adults, 1999-2008. *JAMA*. 2010;303:235-241
278. Haslam DW, James WP. Obesity. *Lancet*. 2005;366:1197-1209
279. Hu FB, Li TY, Colditz GA, Willett WC, Manson JE. Television watching and other sedentary behaviors in relation to risk of obesity and type 2 diabetes mellitus in women. *JAMA*. 2003;289:1785-1791
280. Robinson TN. Reducing children's television viewing to prevent obesity: A randomized controlled trial. *JAMA*. 1999;282:1561-1567
281. Wang YC, Bleich SN, Gortmaker SL. Increasing caloric contribution from sugar-sweetened beverages and 100% fruit juices among US children and adolescents, 1988-2004. *Pediatrics*. 2008;121:e1604-1614
282. Smorlesi A, Frontini A, Giordano A, Cinti S. The adipose organ: White-brown adipocyte plasticity and metabolic inflammation. *Obes Rev*. 2012;13 Suppl 2:83-96
283. Sutherland LN, Capozzi LC, Turchinsky NJ, Bell RC, Wright DC. Time course of high-fat diet-induced reductions in adipose tissue mitochondrial proteins: Potential mechanisms and the relationship to glucose intolerance. *Am J Physiol Endocrinol Metab*. 2008;295:E1076-1083
284. Bogacka I, Xie H, Bray GA, Smith SR. Pioglitazone induces mitochondrial biogenesis in human subcutaneous adipose tissue in vivo. *Diabetes*. 2005;54:1392-1399
285. Wilson-Fritch L, Nicoloso S, Chouinard M, Lazar MA, Chui PC, Leszyk J, Straubhaar J, Czech MP, Corvera S. Mitochondrial remodeling in adipose tissue associated with obesity and treatment with rosiglitazone. *J Clin Invest*. 2004;114:1281-1289
286. Sansbury BE, Cummins TD, Tang Y, Hellmann J, Holden CR, Harbeson MA, Chen Y, Patel RP, Spite M, Bhatnagar A, Hill BG. Overexpression of endothelial nitric oxide synthase prevents diet-induced obesity and regulates adipocyte phenotype. *Circ Res*. 2012;111:1176-1189
287. Hellmann J, Tang Y, Kosuri M, Bhatnagar A, Spite M. Resolvin D1 decreases adipose tissue macrophage accumulation and improves insulin sensitivity in obese-diabetic mice. *FASEB J*. 2011;25:2399-2407

288. Xia J, Wishart DS. Web-based inference of biological patterns, functions and pathways from metabolomic data using metaboanalyst. *Nat Protoc.* 2011;6:743-760
289. Horrillo R, Gonzalez-Periz A, Martinez-Clemente M, Lopez-Parra M, Ferre N, Titos E, Moran-Salvador E, Deulofeu R, Arroyo V, Claria J. 5-lipoxygenase activating protein signals adipose tissue inflammation and lipid dysfunction in experimental obesity. *J Immunol.* 2010;184:3978-3987
290. Villena JA, Hock MB, Chang WY, Barcas JE, Giguere V, Kralli A. Orphan nuclear receptor estrogen-related receptor alpha is essential for adaptive thermogenesis. *Proc Natl Acad Sci U S A.* 2007;104:1418-1423
291. Hotamisligil GS, Arner P, Caro JF, Atkinson RL, Spiegelman BM. Increased adipose tissue expression of tumor necrosis factor-alpha in human obesity and insulin resistance. *J Clin Invest.* 1995;95:2409-2415
292. Sewter CP, Digby JE, Blows F, Prins J, O'Rahilly S. Regulation of tumour necrosis factor-alpha release from human adipose tissue in vitro. *J Endocrinol.* 1999;163:33-38
293. Hill BG, Benavides GA, Lancaster JR, Ballinger S, Dell'italia L, Zhang J, Darley-USmar VM. Integration of cellular bioenergetics with mitochondrial quality control and autophagy. *Biol Chem.* 2012;393:1485-1512
294. Spite M, Hellmann J, Tang Y, Mathis SP, Kosuri M, Bhatnagar A, Jala VR, Haribabu B. Deficiency of the leukotriene b4 receptor, blt-1, protects against systemic insulin resistance in diet-induced obesity. *J Immunol.* 2011;187:1942-1949
295. Nishimura S, Manabe I, Nagasaki M, Eto K, Yamashita H, Ohsugi M, Otsu M, Hara K, Ueki K, Sugiura S, Yoshimura K, Kadowaki T, Nagai R. Cd8+ effector t cells contribute to macrophage recruitment and adipose tissue inflammation in obesity. *Nat Med.* 2009;15:914-920
296. Adams DO, Hamilton TA. The cell biology of macrophage activation. *Annu Rev Immunol.* 1984;2:283-318
297. Yanaka N. Mammalian glycerophosphodiester phosphodiesterases. *Biosci Biotechnol Biochem.* 2007;71:1811-1818
298. Prentki M, Madiraju SR. Glycerolipid metabolism and signaling in health and disease. *Endocr Rev.* 2008;29:647-676
299. Cadoudal T, Distel E, Durant S, Fouque F, Blouin JM, Collinet M, Bortoli S, Forest C, Benelli C. Pyruvate dehydrogenase kinase 4: Regulation by thiazolidinediones and implication in glyceroneogenesis in adipose tissue. *Diabetes.* 2008;57:2272-2279
300. Owen OE, Kalhan SC, Hanson RW. The key role of anaplerosis and cataplerosis for citric acid cycle function. *J Biol Chem.* 2002;277:30409-30412
301. Yamanouchi T, Ogata N, Tagaya T, Kawasaki T, Sekino N, Funato H, Akaoka L, Miyashita H. Clinical usefulness of serum 1,5-anhydroglucitol in monitoring glycaemic control. *Lancet.* 1996;347:1514-1518
302. Stickle D, Turk J. A kinetic mass balance model for 1,5-anhydroglucitol: Applications to monitoring of glycemic control. *Am J Physiol.* 1997;273:E821-830
303. Mitsutake S, Zama K, Yokota H, Yoshida T, Tanaka M, Mitsui M, Ikawa M, Okabe M, Tanaka Y, Yamashita T, Takemoto H, Okazaki T, Watanabe K, Igarashi Y. Dynamic modification of sphingomyelin in lipid microdomains controls development of obesity, fatty liver, and type 2 diabetes. *J Biol Chem.* 2011;286:28544-28555
304. Li Z, Zhang H, Liu J, Liang CP, Li Y, Teitelman G, Beyer T, Bui HH, Peake DA, Zhang Y, Sanders PE, Kuo MS, Park TS, Cao G, Jiang XC. Reducing plasma membrane sphingomyelin increases insulin sensitivity. *Mol Cell Biol.* 2011;31:4205-4218
305. Chavez JA, Summers SA. A ceramide-centric view of insulin resistance. *Cell Metab.* 2012;15:585-594
306. Shah C, Yang G, Lee I, Bielawski J, Hannun YA, Samad F. Protection from high fat diet-induced increase in ceramide in mice lacking plasminogen activator inhibitor 1. *J Biol Chem.* 2008;283:13538-13548
307. Schmitz-Peiffer C. Targeting ceramide synthesis to reverse insulin resistance. *Diabetes.* 2010;59:2351-2353

308. Ussher JR, Koves TR, Cadete VJ, Zhang L, Jaswal JS, Swyrd SJ, Lopaschuk DG, Proctor SD, Keung W, Muoio DM, Lopaschuk GD. Inhibition of de novo ceramide synthesis reverses diet-induced insulin resistance and enhances whole-body oxygen consumption. *Diabetes*. 2010;59:2453-2464
309. Adams SH. Emerging perspectives on essential amino acid metabolism in obesity and the insulin-resistant state. *Adv Nutr*. 2011;2:445-456
310. Cheng S, Rhee EP, Larson MG, Lewis GD, McCabe EL, Shen D, Palma MJ, Roberts LD, Dejam A, Souza AL, Deik AA, Magnusson M, Fox CS, O'Donnell CJ, Vasan RS, Melander O, Clish CB, Gerszten RE, Wang TJ. Metabolite profiling identifies pathways associated with metabolic risk in humans. *Circulation*. 2012;125:2222-2231
311. She P, Reid TM, Bronson SK, Vary TC, Hajnal A, Lynch CJ, Hutson SM. Disruption of bcatm in mice leads to increased energy expenditure associated with the activation of a futile protein turnover cycle. *Cell Metab*. 2007;6:181-194
312. Newgard CB, An J, Bain JR, Muehlbauer MJ, Stevens RD, Lien LF, Haqq AM, Shah SH, Arlotto M, Slentz CA, Rochon J, Gallup D, Ilkayeva O, Wenner BR, Yancy WS, Jr., Eisenson H, Musante G, Surwit RS, Millington DS, Butler MD, Svetkey LP. A branched-chain amino acid-related metabolic signature that differentiates obese and lean humans and contributes to insulin resistance. *Cell Metab*. 2009;9:311-326
313. Herman MA, She P, Peroni OD, Lynch CJ, Kahn BB. Adipose tissue branched chain amino acid (bcaa) metabolism modulates circulating bcaa levels. *J Biol Chem*. 2010;285:11348-11356
314. Chacko BK, Kramer PA, Ravi S, Johnson MS, Hardy RW, Ballinger SW, Darley-USmar VM. Methods for defining distinct bioenergetic profiles in platelets, lymphocytes, monocytes, and neutrophils, and the oxidative burst from human blood. *Laboratory investigation; a journal of technical methods and pathology*. 2013;93:690-700
315. Hill BG, Benavides GA, Lancaster JR, Jr., Ballinger S, Dell'Italia L, Jianhua Z, Darley-USmar VM. Integration of cellular bioenergetics with mitochondrial quality control and autophagy. *Biol Chem*. 2012;393:1485-1512
316. Furukawa S, Fujita T, Shimabukuro M, Iwaki M, Yamada Y, Nakajima Y, Nakayama O, Makishima M, Matsuda M, Shimomura I. Increased oxidative stress in obesity and its impact on metabolic syndrome. *J Clin Invest*. 2004;114:1752-1761
317. Matsuzawa-Nagata N, Takamura T, Ando H, Nakamura S, Kurita S, Misu H, Ota T, Yokoyama M, Honda M, Miyamoto K, Kaneko S. Increased oxidative stress precedes the onset of high-fat diet-induced insulin resistance and obesity. *Metabolism*. 2008;57:1071-1077
318. Okada S, Kozuka C, Masuzaki H, Yasue S, Ishii-Yonemoto T, Tanaka T, Yamamoto Y, Noguchi M, Kusakabe T, Tomita T, Fujikura J, Ebihara K, Hosoda K, Sakaue H, Kobori H, Ham M, Lee YS, Kim JB, Saito Y, Nakao K. Adipose tissue-specific dysregulation of angiotensinogen by oxidative stress in obesity. *Metabolism*. 2010;59:1241-1251
319. Curtis JM, Grimsrud PA, Wright WS, Xu X, Foncea RE, Graham DW, Brestoff JR, Wiczer BM, Ilkayeva O, Cianflone K, Muoio DE, Arriaga EA, Bernlohr DA. Downregulation of adipose glutathione s-transferase a4 leads to increased protein carbonylation, oxidative stress, and mitochondrial dysfunction. *Diabetes*. 2010;59:1132-1142
320. Long EK, Olson DM, Bernlohr DA. High-fat diet induces changes in adipose tissue trans-4-oxo-2-nonenal and trans-4-hydroxy-2-nonenal levels in a depot-specific manner. *Free Radic Biol Med*. 2013;63:390-398
321. Asano H, Yamada T, Hashimoto O, Umemoto T, Sato R, Ohwatari S, Kanamori Y, Terachi T, Funaba M, Matsui T. Diet-induced changes in ucp1 expression in bovine adipose tissues. *Gen Comp Endocrinol*. 2013;184:87-92
322. Yin X, Lanza IR, Swain JM, Sarr MG, Nair KS, Jensen MD. Adipocyte mitochondrial function is reduced in human obesity independent of fat cell size. *The Journal of clinical endocrinology and metabolism*. 2014;99:E209-216
323. Bjorkoy G, Lamark T, Pankiv S, Overvatn A, Brech A, Johansen T. Monitoring autophagic degradation of p62/sqstm1. *Methods in enzymology*. 2009;452:181-197

324. Singh R, Xiang Y, Wang Y, Baikati K, Cuervo AM, Luu YK, Tang Y, Pessin JE, Schwartz GJ, Czaja MJ. Autophagy regulates adipose mass and differentiation in mice. *J Clin Invest*. 2009;119:3329-3339
325. Zhang Y, Goldman S, Baerga R, Zhao Y, Komatsu M, Jin S. Adipose-specific deletion of autophagy-related gene 7 (atg7) in mice reveals a role in adipogenesis. *Proc Natl Acad Sci U S A*. 2009;106:19860-19865
326. Ost A, Svensson K, Ruishalme I, Brannmark C, Franck N, Krook H, Sandstrom P, Kjolhede P, Stralfors P. Attenuated mtor signaling and enhanced autophagy in adipocytes from obese patients with type 2 diabetes. *Molecular medicine*. 2010;16:235-246
327. Kovsan J, Bluher M, Tarnovscki T, Kloting N, Kirshtein B, Madar L, Shai I, Golan R, Harman-Boehm I, Schon MR, Greenberg AS, Elazar Z, Bashan N, Rudich A. Altered autophagy in human adipose tissues in obesity. *The Journal of clinical endocrinology and metabolism*. 2011;96:E268-277
328. Jansen HJ, van Essen P, Koenen T, Joosten LA, Netea MG, Tack CJ, Stienstra R. Autophagy activity is up-regulated in adipose tissue of obese individuals and modulates proinflammatory cytokine expression. *Endocrinology*. 2012;153:5866-5874
329. Kim KY, Stevens MV, Akter MH, Rusk SE, Huang RJ, Cohen A, Noguchi A, Springer D, Bocharov AV, Eggerman TL, Suen DF, Youle RJ, Amar M, Remaley AT, Sack MN. Parkin is a lipid-responsive regulator of fat uptake in mice and mutant human cells. *J Clin Invest*. 2011;121:3701-3712
330. Vincow ES, Merrihew G, Thomas RE, Shulman NJ, Beyer RP, Maccoss MJ, Pallanck LJ. The pink1-parkin pathway promotes both mitophagy and selective respiratory chain turnover in vivo. *Proc Natl Acad Sci U S A*. 2013
331. Williamson DF, Madans J, Anda RF, Kleinman JC, Kahn HS, Byers T. Recreational physical activity and ten-year weight change in a us national cohort. *Int J Obes Relat Metab Disord*. 1993;17:279-286
332. Gesta S, Tseng YH, Kahn CR. Developmental origin of fat: Tracking obesity to its source. *Cell*. 2007;131:242-256
333. Lehrke M, Lazar MA. The many faces of ppargamma. *Cell*. 2005;123:993-999
334. Baron AD, Steinberg HO. Endothelial function, insulin sensitivity, and hypertension. *Circulation*. 1997;96:725-726
335. Shankar RR, Wu Y, Shen HQ, Zhu JS, Baron AD. Mice with gene disruption of both endothelial and neuronal nitric oxide synthase exhibit insulin resistance. *Diabetes*. 2000;49:684-687
336. Duplain H, Burcelin R, Sartori C, Cook S, Egli M, Lepori M, Vollenweider P, Pedrazzini T, Nicod P, Thorens B, Scherrer U. Insulin resistance, hyperlipidemia, and hypertension in mice lacking endothelial nitric oxide synthase. *Circulation*. 2001;104:342-345
337. Le Gouill E, Jimenez M, Binnert C, Jayet PY, Thalmann S, Nicod P, Scherrer U, Vollenweider P. Endothelial nitric oxide synthase (enos) knockout mice have defective mitochondrial beta-oxidation. *Diabetes*. 2007;56:2690-2696
338. Ohashi Y, Kawashima S, Hirata K, Yamashita T, Ishida T, Inoue N, Sakoda T, Kurihara H, Yazaki Y, Yokoyama M. Hypotension and reduced nitric oxide-elicited vasorelaxation in transgenic mice overexpressing endothelial nitric oxide synthase. *J Clin Invest*. 1998;102:2061-2071
339. McGuinness OP, Ayala JE, Laughlin MR, Wasserman DH. Nih experiment in centralized mouse phenotyping: The vanderbilt experience and recommendations for evaluating glucose homeostasis in the mouse. *Am J Physiol Endocrinol Metab*. 2009;297:E849-855
340. Taniguchi CM, Kondo T, Sajan M, Luo J, Bronson R, Asano T, Farese R, Cantley LC, Kahn CR. Divergent regulation of hepatic glucose and lipid metabolism by phosphoinositide 3-kinase via akt and pkclambda/zeta. *Cell Metab*. 2006;3:343-353
341. Kelpke SS, Chen B, Bradley KM, Teng X, Chumley P, Brandon A, Yancey B, Moore B, Head H, Viera L, Thompson JA, Crossman DK, Bray MS, Eckhoff DE, Agarwal A, Patel RP. Sodium nitrite protects against kidney injury induced by brain death and improves post-transplant function. *Kidney Int*. 2012

342. Xue Y, Lim S, Brakenhielm E, Cao Y. Adipose angiogenesis: Quantitative methods to study microvessel growth, regression and remodeling in vivo. *Nat Protoc.* 2010;5:912-920
343. Xia J, Wishart DS. Metabolomic data processing, analysis, and interpretation using metaboanalyst. *Curr Protoc Bioinformatics.* 2011;Chapter 14:Unit 14 10
344. Cox JE, Powley TL. Development of obesity in diabetic mice pair-fed with lean siblings. *J Comp Physiol Psychol.* 1977;91:347-358
345. Jones SP, Greer JJ, Kakkar AK, Ware PD, Turnage RH, Hicks M, van Haperen R, de Crom R, Kawashima S, Yokoyama M, Lefer DJ. Endothelial nitric oxide synthase overexpression attenuates myocardial reperfusion injury. *Am J Physiol Heart Circ Physiol.* 2004;286:H276-282
346. Duranski MR, Elrod JW, Calvert JW, Bryan NS, Feelisch M, Lefer DJ. Genetic overexpression of enos attenuates hepatic ischemia-reperfusion injury. *Am J Physiol Heart Circ Physiol.* 2006;291:H2980-2986
347. Takenaka K, Nishimura Y, Nishiuma T, Sakashita A, Yamashita T, Kobayashi K, Satouchi M, Ishida T, Kawashima S, Yokoyama M. Ventilator-induced lung injury is reduced in transgenic mice that overexpress endothelial nitric oxide synthase. *Am J Physiol Lung Cell Mol Physiol.* 2006;290:L1078-1086
348. Kawashima S, Yamashita T, Ozaki M, Ohashi Y, Azumi H, Inoue N, Hirata K, Hayashi Y, Itoh H, Yokoyama M. Endothelial no synthase overexpression inhibits lesion formation in mouse model of vascular remodeling. *Arterioscler Thromb Vasc Biol.* 2001;21:201-207
349. Yamashita T, Kawashima S, Ohashi Y, Ozaki M, Ueyama T, Ishida T, Inoue N, Hirata K, Akita H, Yokoyama M. Resistance to endotoxin shock in transgenic mice overexpressing endothelial nitric oxide synthase. *Circulation.* 2000;101:931-937
350. Harats D, Kurihara H, Belloni P, Oakley H, Ziober A, Ackley D, Cain G, Kurihara Y, Lawn R, Sigal E. Targeting gene expression to the vascular wall in transgenic mice using the murine preproendothelin-1 promoter. *J Clin Invest.* 1995;95:1335-1344
351. Schenk S, Saberi M, Olefsky JM. Insulin sensitivity: Modulation by nutrients and inflammation. *J Clin Invest.* 2008;118:2992-3002
352. Zhang H, Wang Y, Zhang J, Potter BJ, Sowers JR, Zhang C. Bariatric surgery reduces visceral adipose inflammation and improves endothelial function in type 2 diabetic mice. *Arterioscler Thromb Vasc Biol.* 2011;31:2063-2069
353. Heusch G. Obesity and inflammatory vasculopathy: A surgical solution as ultima ratio? *Arterioscler Thromb Vasc Biol.* 2011;31:1953-1954
354. Siliprandi N, Siliprandi D, Ciman M. Stimulation of oxidation of mitochondrial fatty acids and of acetate by acetylcarnitine. *Biochem J.* 1965;96:777-780
355. Sayed-Ahmed MM, Shouman SA, Rezk BM, Khalifa MH, Osman AM, El-Merzabani MM. Propionyl-L-carnitine as potential protective agent against adriamycin-induced impairment of fatty acid beta-oxidation in isolated heart mitochondria. *Pharmacol Res.* 2000;41:143-150
356. D'Antona G, Ragni M, Cardile A, Tedesco L, Dossena M, Bruttini F, Caliaro F, Corsetti G, Bottinelli R, Carruba MO, Valerio A, Nisoli E. Branched-chain amino acid supplementation promotes survival and supports cardiac and skeletal muscle mitochondrial biogenesis in middle-aged mice. *Cell Metab.* 2010;12:362-372
357. Nisoli E, Tonello C, Cardile A, Cozzi V, Bracale R, Tedesco L, Falcone S, Valerio A, Cantoni O, Clementi E, Moncada S, Carruba MO. Calorie restriction promotes mitochondrial biogenesis by inducing the expression of enos. *Science.* 2005;310:314-317
358. Wu Z, Puigserver P, Andersson U, Zhang C, Adelmant G, Mootha V, Troy A, Cinti S, Lowell B, Scarpulla RC, Spiegelman BM. Mechanisms controlling mitochondrial biogenesis and respiration through the thermogenic coactivator pgc-1. *Cell.* 1999;98:115-124
359. Li P, Zhu Z, Lu Y, Granneman JG. Metabolic and cellular plasticity in white adipose tissue ii: Role of peroxisome proliferator-activated receptor-alpha. *Am J Physiol Endocrinol Metab.* 2005;289:E617-626

360. Rong JX, Qiu Y, Hansen MK, Zhu L, Zhang V, Xie M, Okamoto Y, Mattie MD, Higashiyama H, Asano S, Strum JC, Ryan TE. Adipose mitochondrial biogenesis is suppressed in db/db and high-fat diet-fed mice and improved by rosiglitazone. *Diabetes*. 2007;56:1751-1760
361. Koh YJ, Park BH, Park JH, Han J, Lee IK, Park JW, Koh GY. Activation of ppar gamma induces profound multilocularization of adipocytes in adult mouse white adipose tissues. *Exp Mol Med*. 2009;41:880-895
362. Kong X, Wang R, Xue Y, Liu X, Zhang H, Chen Y, Fang F, Chang Y. Sirtuin 3, a new target of pgc-1alpha, plays an important role in the suppression of ros and mitochondrial biogenesis. *PLoS One*. 2010;5:e11707
363. Carlstrom M, Larsen FJ, Nystrom T, Hezel M, Borniquel S, Weitzberg E, Lundberg JO. Dietary inorganic nitrate reverses features of metabolic syndrome in endothelial nitric oxide synthase-deficient mice. *Proc Natl Acad Sci U S A*. 2010;107:17716-17720
364. Boo YC, Sorescu G, Boyd N, Shiojima I, Walsh K, Du J, Jo H. Shear stress stimulates phosphorylation of endothelial nitric-oxide synthase at ser1179 by akt-independent mechanisms: Role of protein kinase a. *J Biol Chem*. 2002;277:3388-3396
365. Goirand F, Solar M, Athea Y, Viollet B, Mateo P, Fortin D, Leclerc J, Hoerter J, Ventura-Clapier R, Garnier A. Activation of amp kinase alpha1 subunit induces aortic vasorelaxation in mice. *J Physiol*. 2007;581:1163-1171
366. Mingorance C, Gonzalez del Pozo M, Dolores Herrera M, Alvarez de Sotomayor M. Oral supplementation of propionyl-L-carnitine reduces body weight and hyperinsulinaemia in obese zucker rats. *Br J Nutr*. 2009;102:1145-1153
367. Hirschey MD, Shimazu T, Goetzman E, Jing E, Schwer B, Lombard DB, Grueter CA, Harris C, Biddinger S, Ilkayeva OR, Stevens RD, Li Y, Saha AK, Ruderman NB, Bain JR, Newgard CB, Farese RV, Jr., Alt FW, Kahn CR, Verdin E. Sirt3 regulates mitochondrial fatty-acid oxidation by reversible enzyme deacetylation. *Nature*. 2010;464:121-125
368. Hallows WC, Yu W, Smith BC, Devries MK, Ellinger JJ, Someya S, Shortreed MR, Prolla T, Markley JL, Smith LM, Zhao S, Guan KL, Denu JM. Sirt3 promotes the urea cycle and fatty acid oxidation during dietary restriction. *Mol Cell*. 2011;41:139-149
369. Moncada S, Higgs EA. The discovery of nitric oxide and its role in vascular biology. *Br J Pharmacol*. 2006;147 Suppl 1:S193-201
370. Victor VM, Nunez C, D'Ocon P, Taylor CT, Esplugues JV, Moncada S. Regulation of oxygen distribution in tissues by endothelial nitric oxide. *Circ Res*. 2009;104:1178-1183
371. Murohara T, Asahara T, Silver M, Bauters C, Masuda H, Kalka C, Kearney M, Chen D, Symes JF, Fishman MC, Huang PL, Isner JM. Nitric oxide synthase modulates angiogenesis in response to tissue ischemia. *J Clin Invest*. 1998;101:2567-2578
372. Petersen KF, Shulman GI. Pathogenesis of skeletal muscle insulin resistance in type 2 diabetes mellitus. *Am J Cardiol*. 2002;90:11G-18G
373. Cederberg A, Gronning LM, Ahren B, Tasken K, Carlsson P, Enerback S. Foxc2 is a winged helix gene that counteracts obesity, hypertriglyceridemia, and diet-induced insulin resistance. *Cell*. 2001;106:563-573
374. Polak P, Cybulski N, Feige JN, Auwerx J, Ruegg MA, Hall MN. Adipose-specific knockout of raptor results in lean mice with enhanced mitochondrial respiration. *Cell Metab*. 2008;8:399-410
375. Seale P, Conroe HM, Estall J, Kajimura S, Frontini A, Ishibashi J, Cohen P, Cinti S, Spiegelman BM. Prdm16 determines the thermogenic program of subcutaneous white adipose tissue in mice. *J Clin Invest*. 2011;121:96-105
376. Kim JY, van de Wall E, Laplante M, Azzara A, Trujillo ME, Hofmann SM, Schraw T, Durand JL, Li H, Li G, Jelicks LA, Mehler MF, Hui DY, Deshaies Y, Shulman GI, Schwartz GJ, Scherer PE. Obesity-associated improvements in metabolic profile through expansion of adipose tissue. *J Clin Invest*. 2007;117:2621-2637
377. Yuan M, Konstantopoulos N, Lee J, Hansen L, Li ZW, Karin M, Shoelson SE. Reversal of obesity- and diet-induced insulin resistance with salicylates or targeted disruption of ikkbeta. *Science*. 2001;293:1673-1677

378. Patsouris D, Li PP, Thapar D, Chapman J, Olefsky JM, Neels JG. Ablation of cd11c-positive cells normalizes insulin sensitivity in obese insulin resistant animals. *Cell Metab.* 2008;8:301-309
379. Kanda H, Tateya S, Tamori Y, Kotani K, Hiasa K, Kitazawa R, Kitazawa S, Miyachi H, Maeda S, Egashira K, Kasuga M. Mcp-1 contributes to macrophage infiltration into adipose tissue, insulin resistance, and hepatic steatosis in obesity. *J Clin Invest.* 2006;116:1494-1505
380. Wood IS, de Heredia FP, Wang B, Trayhurn P. Cellular hypoxia and adipose tissue dysfunction in obesity. *Proc Nutr Soc.* 2009;68:370-377
381. Ye J. Emerging role of adipose tissue hypoxia in obesity and insulin resistance. *Int J Obes (Lond).* 2009;33:54-66
382. Apovian CM, Bigornia S, Mott M, Meyers MR, Ulloor J, Gagua M, McDonnell M, Hess D, Joseph L, Gokce N. Adipose macrophage infiltration is associated with insulin resistance and vascular endothelial dysfunction in obese subjects. *Arterioscler Thromb Vasc Biol.* 2008;28:1654-1659
383. Lumeng CN, Deyoung SM, Saltiel AR. Macrophages block insulin action in adipocytes by altering expression of signaling and glucose transport proteins. *Am J Physiol Endocrinol Metab.* 2007;292:E166-174
384. Garg A. Acquired and inherited lipodystrophies. *N Engl J Med.* 2004;350:1220-1234
385. Cortes VA, Curtis DE, Sukumaran S, Shao X, Parameswara V, Rashid S, Smith AR, Ren J, Esser V, Hammer RE, Agarwal AK, Horton JD, Garg A. Molecular mechanisms of hepatic steatosis and insulin resistance in the agpat2-deficient mouse model of congenital generalized lipodystrophy. *Cell Metab.* 2009;9:165-176
386. Cui X, Wang Y, Tang Y, Liu Y, Zhao L, Deng J, Xu G, Peng X, Ju S, Liu G, Yang H. Seipin ablation in mice results in severe generalized lipodystrophy. *Hum Mol Genet.* 2011;20:3022-3030
387. Fleming I, Busse R. Molecular mechanisms involved in the regulation of the endothelial nitric oxide synthase. *Am J Physiol Regul Integr Comp Physiol.* 2003;284:R1-12
388. Musicki B, Kramer MF, Becker RE, Burnett AL. Inactivation of phosphorylated endothelial nitric oxide synthase (ser-1177) by o-glcnac in diabetes-associated erectile dysfunction. *Proc Natl Acad Sci U S A.* 2005;102:11870-11875
389. Shaul PW, Smart EJ, Robinson LJ, German Z, Yuhanna IS, Ying Y, Anderson RG, Michel T. Acylation targets endothelial nitric-oxide synthase to plasmalemmal caveolae. *J Biol Chem.* 1996;271:6518-6522
390. Garcia-Cardena G, Oh P, Liu J, Schnitzer JE, Sessa WC. Targeting of nitric oxide synthase to endothelial cell caveolae via palmitoylation: Implications for nitric oxide signaling. *Proc Natl Acad Sci U S A.* 1996;93:6448-6453
391. Fabbrini E, Sullivan S, Klein S. Obesity and nonalcoholic fatty liver disease: Biochemical, metabolic, and clinical implications. *Hepatology.* 2010;51:679-689
392. Rolfe DF, Brown GC. Cellular energy utilization and molecular origin of standard metabolic rate in mammals. *Physiol Rev.* 1997;77:731-758
393. Rolfe DFS, Brown GC. Cellular energy utilization and molecular origin of standard metabolic rate in mammals. *Physiological Reviews.* 1997;77:731-758
394. Kelley DE, He J, Menshikova EV, Ritov VB. Dysfunction of mitochondria in human skeletal muscle in type 2 diabetes. *Diabetes.* 2002;51:2944-2950
395. Kim JA, Wei Y, Sowers JR. Role of mitochondrial dysfunction in insulin resistance. *Circ Res.* 2008;102:401-414
396. Ritz P, Berrut G. Mitochondrial function, energy expenditure, aging and insulin resistance. *Diabetes Metab.* 2005;31 Spec No 2:5S67-65S73
397. Sparks LM, Xie H, Koza RA, Mynatt R, Hulver MW, Bray GA, Smith SR. A high-fat diet coordinately downregulates genes required for mitochondrial oxidative phosphorylation in skeletal muscle. *Diabetes.* 2005;54:1926-1933
398. Mavrelis PG, Ammon HV, Gleysteen JJ, Komorowski RA, Charaf UK. Hepatic free fatty acids in alcoholic liver disease and morbid obesity. *Hepatology.* 1983;3:226-231
399. Yen TT, Allan JA, Yu PL, Acton MA, Pearson DV. Triacylglycerol contents and in vivo lipogenesis of ob/ob, db/db and avy/a mice. *Biochim Biophys Acta.* 1976;441:213-220

400. Griglio S, Malewiak MI. Hepatic triglyceride storage and ketonemia in rats fed high fat diets. *Nutr Metab.* 1975;19:131-144
401. Perez-Carreras M, Del Hoyo P, Martin MA, Rubio JC, Martin A, Castellano G, Colina F, Arenas J, Solis-Herruzo JA. Defective hepatic mitochondrial respiratory chain in patients with nonalcoholic steatohepatitis. *Hepatology.* 2003;38:999-1007
402. Pessayre D, Fromenty B. Nash: A mitochondrial disease. *J Hepatol.* 2005;42:928-940
403. Xu A, Wang Y, Keshaw H, Xu LY, Lam KS, Cooper GJ. The fat-derived hormone adiponectin alleviates alcoholic and nonalcoholic fatty liver diseases in mice. *J Clin Invest.* 2003;112:91-100
404. Seo YS, Kim JH, Jo NY, Choi KM, Baik SH, Park JJ, Kim JS, Byun KS, Bak YT, Lee CH, Kim A, Yeon JE. Ppar agonists treatment is effective in a nonalcoholic fatty liver disease animal model by modulating fatty-acid metabolic enzymes. *J Gastroenterol Hepatol.* 2008;23:102-109
405. Stefanovic-Racic M, Perdomo G, Mantell BS, Sipula IJ, Brown NF, O'Doherty RM. A moderate increase in carnitine palmitoyltransferase 1a activity is sufficient to substantially reduce hepatic triglyceride levels. *Am J Physiol Endocrinol Metab.* 2008;294:E969-977
406. Savage DB, Choi CS, Samuel VT, Liu ZX, Zhang D, Wang A, Zhang XM, Cline GW, Yu XX, Geisler JG, Bhanot S, Monia BP, Shulman GI. Reversal of diet-induced hepatic steatosis and hepatic insulin resistance by antisense oligonucleotide inhibitors of acetyl-coa carboxylases 1 and 2. *J Clin Invest.* 2006;116:817-824
407. Mihalik SJ, Goodpaster BH, Kelley DE, Chace DH, Vockley J, Toledo FG, DeLany JP. Increased levels of plasma acylcarnitines in obesity and type 2 diabetes and identification of a marker of glucolipotoxicity. *Obesity (Silver Spring).* 2010;18:1695-1700
408. Koves TR, Ussher JR, Noland RC, Slentz D, Mosedale M, Ilkayeva O, Bain J, Stevens R, Dyck JR, Newgard CB, Lopaschuk GD, Muoio DM. Mitochondrial overload and incomplete fatty acid oxidation contribute to skeletal muscle insulin resistance. *Cell Metab.* 2008;7:45-56
409. Reaven GM, Hollenbeck C, Jeng CY, Wu MS, Chen YD. Measurement of plasma glucose, free fatty acid, lactate, and insulin for 24 h in patients with niddm. *Diabetes.* 1988;37:1020-1024
410. Golay A, Swislocki AL, Chen YD, Jaspan JB, Reaven GM. Effect of obesity on ambient plasma glucose, free fatty acid, insulin, growth hormone, and glucagon concentrations. *J Clin Endocrinol Metab.* 1986;63:481-484
411. Frazee E, Donner CC, Swislocki AL, Chiou YA, Chen YD, Reaven GM. Ambient plasma free fatty acid concentrations in noninsulin-dependent diabetes mellitus: Evidence for insulin resistance. *J Clin Endocrinol Metab.* 1985;61:807-811
412. Boden G, Shulman GI. Free fatty acids in obesity and type 2 diabetes: Defining their role in the development of insulin resistance and beta-cell dysfunction. *Eur J Clin Invest.* 2002;32 Suppl 3:14-23
413. Wang TJ, Larson MG, Vasan RS, Cheng S, Rhee EP, McCabe E, Lewis GD, Fox CS, Jacques PF, Fernandez C, O'Donnell CJ, Carr SA, Mootha VK, Florez JC, Souza A, Melander O, Clish CB, Gerszten RE. Metabolite profiles and the risk of developing diabetes. *Nat Med.* 2011;17:448-453
414. Nicholson JK, Lindon JC. Systems biology: Metabonomics. *Nature.* 2008;455:1054-1056
415. Xie B, Waters MJ, Schirra HJ. Investigating potential mechanisms of obesity by metabolomics. *J Biomed Biotechnol.* 2012;2012:805683
416. Zhao X, Fritsche J, Wang J, Chen J, Rittig K, Schmitt-Kopplin P, Fritsche A, Haring HU, Schleicher ED, Xu G, Lehmann R. Metabonomic fingerprints of fasting plasma and spot urine reveal human pre-diabetic metabolic traits. *Metabolomics.* 2010;6:362-374
417. Manna SK, Patterson AD, Yang Q, Krausz KW, Idle JR, Fornace AJ, Gonzalez FJ. Uplc-ms-based urine metabolomics reveals indole-3-lactic acid and phenyllactic acid as conserved biomarkers for alcohol-induced liver disease in the ppara-null mouse model. *J Proteome Res.* 2011;10:4120-4133

418. Wang X, Zhang A, Han Y, Wang P, Sun H, Song G, Dong T, Yuan Y, Yuan X, Zhang M, Xie N, Zhang H, Dong H, Dong W. Urine metabolomics analysis for biomarker discovery and detection of jaundice syndrome in patients with liver disease. *Mol Cell Proteomics*. 2012;11:370-380
419. Wang C, Kong H, Guan Y, Yang J, Gu J, Yang S, Xu G. Plasma phospholipid metabolic profiling and biomarkers of type 2 diabetes mellitus based on high-performance liquid chromatography/electrospray mass spectrometry and multivariate statistical analysis. *Anal Chem*. 2005;77:4108-4116
420. Nicholson JK, Wilson ID. Opinion: Understanding 'global' systems biology: Metabonomics and the continuum of metabolism. *Nat Rev Drug Discov*. 2003;2:668-676
421. Watanabe M, Horai Y, Houten SM, Morimoto K, Sugizaki T, Arita E, Mataka C, Sato H, Tanigawara Y, Schoonjans K, Itoh H, Auwerx J. Lowering bile acid pool size with a synthetic farnesoid x receptor (fxr) agonist induces obesity and diabetes through reduced energy expenditure. *J Biol Chem*. 2011;286:26913-26920
422. Cariou B, van Harmelen K, Duran-Sandoval D, van Dijk TH, Grefhorst A, Abdelkarim M, Caron S, Torpier G, Fruchart JC, Gonzalez FJ, Kuipers F, Staels B. The farnesoid x receptor modulates adiposity and peripheral insulin sensitivity in mice. *J Biol Chem*. 2006;281:11039-11049
423. Pineda Torra I, Claudel T, Duval C, Kosykh V, Fruchart JC, Staels B. Bile acids induce the expression of the human peroxisome proliferator-activated receptor alpha gene via activation of the farnesoid x receptor. *Mol Endocrinol*. 2003;17:259-272
424. Savkur RS, Bramlett KS, Michael LF, Burris TP. Regulation of pyruvate dehydrogenase kinase expression by the farnesoid x receptor. *Biochem Biophys Res Commun*. 2005;329:391-396
425. Hooks SB, Cummings BS. Role of ca²⁺-independent phospholipase a₂ in cell growth and signaling. *Biochem Pharmacol*. 2008;76:1059-1067
426. Glomset JA. The plasma lecithins:Cholesterol acyltransferase reaction. *J Lipid Res*. 1968;9:155-167
427. Ng DS. The role of lecithin:Cholesterol acyltransferase in the modulation of cardiometabolic risks - a clinical update and emerging insights from animal models. *Biochim Biophys Acta*. 2012;1821:654-659
428. Fukushima N, Ishii I, Contos JJ, Weiner JA, Chun J. Lysophospholipid receptors. *Annu Rev Pharmacol Toxicol*. 2001;41:507-534
429. Ishii I, Fukushima N, Ye X, Chun J. Lysophospholipid receptors: Signaling and biology. *Annu Rev Biochem*. 2004;73:321-354
430. Kim MJ, Yang HJ, Kim JH, Ahn CW, Lee JH, Kim KS, Kwon DY. Obesity-related metabolomic analysis of human subjects in black soybean peptide intervention study by ultraperformance liquid chromatography and quadrupole-time-of-flight mass spectrometry. *J Obes*. 2013;2013:874981
431. Kim HJ, Kim JH, Noh S, Hur HJ, Sung MJ, Hwang JT, Park JH, Yang HJ, Kim MS, Kwon DY, Yoon SH. Metabolomic analysis of livers and serum from high-fat diet induced obese mice. *Journal of Proteome Research*. 2011;10:722-731
432. Kim JY, Park JY, Kim OY, Ham BM, Kim HJ, Kwon DY, Jang Y, Lee JH. Metabolic profiling of plasma in overweight/obese and lean men using ultra performance liquid chromatography and q-tof mass spectrometry (uplc-q-tof ms). *Journal of Proteome Research*. 2010;9:4368-4375
433. Galili O, Versari D, Sattler KJ, Olson ML, Mannheim D, McConnell JP, Chade AR, Lerman LO, Lerman A. Early experimental obesity is associated with coronary endothelial dysfunction and oxidative stress. *American Journal of Physiology-Heart and Circulatory Physiology*. 2007;292:H904-H911
434. Li LX, Hossain MA, Sadat S, Hager L, Liu L, Tam L, Schroer S, Huogen L, Fantus IG, Connelly PW, Woo M, Ng DS. Lecithin cholesterol acyltransferase null mice are protected from diet-induced obesity and insulin resistance in a gender-specific manner through multiple pathways. *Journal of Biological Chemistry*. 2011;286:17809-17820

435. Mehlum A, Muri M, Hagve TA, Solberg LA, Prydz H. Mice overexpressing human lecithin: Cholesterol acyltransferase are not protected against diet-induced atherosclerosis. *APMIS*. 1997;105:861-868
436. Haus JM, Kashyap SR, Kasumov T, Zhang R, Kelly KR, Defronzo RA, Kirwan JP. Plasma ceramides are elevated in obese subjects with type 2 diabetes and correlate with the severity of insulin resistance. *Diabetes*. 2009;58:337-343
437. Kim WJ, Park CY. 1,5-anhydroglucitol in diabetes mellitus. *Endocrine*. 2013;43:33-40
438. Thomas C, Pellicciari R, Pruzanski M, Auwerx J, Schoonjans K. Targeting bile-acid signalling for metabolic diseases. *Nat Rev Drug Discov*. 2008;7:678-693
439. Watanabe M, Houten SM, Matakai C, Christoffolete MA, Kim BW, Sato H, Messaddeq N, Harney JW, Ezaki O, Kodama T, Schoonjans K, Bianco AC, Auwerx J. Bile acids induce energy expenditure by promoting intracellular thyroid hormone activation. *Nature*. 2006;439:484-489
440. Watanabe M, Houten SM, Wang L, Moschetta A, Mangelsdorf DJ, Heyman RA, Moore DD, Auwerx J. Bile acids lower triglyceride levels via a pathway involving fxr, shp, and srebp-1c. *J Clin Invest*. 2004;113:1408-1418
441. Zhang Y, Lee FY, Barrera G, Lee H, Vales C, Gonzalez FJ, Willson TM, Edwards PA. Activation of the nuclear receptor fxr improves hyperglycemia and hyperlipidemia in diabetic mice. *Proc Natl Acad Sci U S A*. 2006;103:1006-1011
442. Trauner M, Nathanson MH, Mennone A, Rydberg SA, Boyer JL. Nitric oxide donors stimulate bile flow and glutathione disulfide excretion independent of guanosine 3',5'-cyclic [corrected] monophosphate in the isolated perfused rat liver. *Hepatology*. 1997;25:263-269
443. Trauner M, Mennone A, Gigliozzi A, Fraioli F, Boyer JL. Nitric oxide and guanosine 3',5'-cyclic monophosphate stimulate bile secretion in isolated rat hepatocyte couplets, but not in isolated bile duct units. *Hepatology*. 1998;28:1621-1628
444. Khedara A, Goto T, Kayashita J, Kato N. Hypercholesterolemic effect in rats of a dietary addition of the nitric oxide synthase inhibitor, l-n omega nitroarginine, by less synthesis of bile acids. *Biosci Biotechnol Biochem*. 1998;62:773-777
445. Lefebvre P, Cariou B, Lien F, Kuipers F, Staels B. Role of bile acids and bile acid receptors in metabolic regulation. *Physiol Rev*. 2009;89:147-191
446. Angelin B, Hershon KS, Brunzell JD. Bile acid metabolism in hereditary forms of hypertriglyceridemia: Evidence for an increased synthesis rate in monogenic familial hypertriglyceridemia. *Proc Natl Acad Sci U S A*. 1987;84:5434-5438
447. Crouse JR, 3rd. Hypertriglyceridemia: A contraindication to the use of bile acid binding resins. *Am J Med*. 1987;83:243-248
448. Pullinger CR, Eng C, Salen G, Shefer S, Batta AK, Erickson SK, Verhagen A, Rivera CR, Mulvihill SJ, Malloy MJ, Kane JP. Human cholesterol 7alpha-hydroxylase (cyp7a1) deficiency has a hypercholesterolemic phenotype. *J Clin Invest*. 2002;110:109-117
449. Sinal CJ, Tohkin M, Miyata M, Ward JM, Lambert G, Gonzalez FJ. Targeted disruption of the nuclear receptor fxr/bar impairs bile acid and lipid homeostasis. *Cell*. 2000;102:731-744
450. Garcia-Villafranca J, Guillen A, Castro J. Involvement of nitric oxide/cyclic gmp signaling pathway in the regulation of fatty acid metabolism in rat hepatocytes. *Biochem Pharmacol*. 2003;65:807-812
451. Goto T, Ohnami S, Khedara A, Kato N, Ogawa H, Yanagita T. Feeding the nitric oxide synthase inhibitor l-n(omega)nitroarginine elevates serum very low density lipoprotein and hepatic triglyceride synthesis in rats. *J Nutr Biochem*. 1999;10:274-278
452. Schild L, Dombrowski F, Lendeckel U, Schulz C, Gardemann A, Keilhoff G. Impairment of endothelial nitric oxide synthase causes abnormal fat and glycogen deposition in liver. *Biochim Biophys Acta*. 2008;1782:180-187
453. Lefebvre P, Chinetti G, Fruchart JC, Staels B. Sorting out the roles of ppar alpha in energy metabolism and vascular homeostasis. *J Clin Invest*. 2006;116:571-580
454. Barnett J, Viljoen A, Wierzbicki AS. The need for combination drug therapies in patients with complex dyslipidemia. *Curr Cardiol Rep*. 2013;15:391

455. Fruchart JC. Selective peroxisome proliferator-activated receptor alpha modulators (spparmalpha): The next generation of peroxisome proliferator-activated receptor alpha-agonists. *Cardiovasc Diabetol.* 2013;12:82
456. Kobayashi R, Murakami T, Obayashi M, Nakai N, Jaskiewicz J, Fujiwara Y, Shimomura Y, Harris RA. Clofibrin acid stimulates branched-chain amino acid catabolism by three mechanisms. *Arch Biochem Biophys.* 2002;407:231-240
457. Ozes ON, Akca H, Mayo LD, Gustin JA, Maehama T, Dixon JE, Donner DB. A phosphatidylinositol 3-kinase/akt/mTOR pathway mediates and pten antagonizes tumor necrosis factor inhibition of insulin signaling through insulin receptor substrate-1. *Proc Natl Acad Sci U S A.* 2001;98:4640-4645
458. Tremblay F, Krebs M, Dombrowski L, Brehm A, Bernroider E, Roth E, Nowotny P, Waldhausl W, Marette A, Roden M. Overactivation of s6 kinase 1 as a cause of human insulin resistance during increased amino acid availability. *Diabetes.* 2005;54:2674-2684
459. Zhang Y, Guo K, LeBlanc RE, Loh D, Schwartz GJ, Yu YH. Increasing dietary leucine intake reduces diet-induced obesity and improves glucose and cholesterol metabolism in mice via multimechanisms. *Diabetes.* 2007;56:1647-1654
460. Vianna D, Resende GF, Torres-Leal FL, Pantaleao LC, Donato J, Jr., Tirapegui J. Long-term leucine supplementation reduces fat mass gain without changing body protein status of aging rats. *Nutrition.* 2012;28:182-189
461. Qin LQ, Xun P, Bujnowski D, Daviglius ML, Van Horn L, Stamler J, He K. Higher branched-chain amino acid intake is associated with a lower prevalence of being overweight or obese in middle-aged east asian and western adults. *J Nutr.* 2011;141:249-254
462. Nishimura J, Masaki T, Arakawa M, Seike M, Yoshimatsu H. Isoleucine prevents the accumulation of tissue triglycerides and upregulates the expression of pparalpha and uncoupling protein in diet-induced obese mice. *J Nutr.* 2010;140:496-500
463. Morley JE, Flood JF. Evidence that nitric oxide modulates food intake in mice. *Life sciences.* 1991;49:707-711
464. Morley JE, Flood JF. Competitive antagonism of nitric oxide synthetase causes weight loss in mice. *Life sciences.* 1992;51:1285-1289
465. Morley JE, Flood JF. Effect of competitive antagonism of NO synthetase on weight and food intake in obese and diabetic mice. *The American journal of physiology.* 1994;266:R164-168
466. Squadrito F, Calapai G, Cucinotta D, Altavilla D, Zingarelli B, Ioculano M, Urna G, Sardella A, Campo GM, Caputi AP. Anorectic activity of ng-nitro-L-arginine, an inhibitor of brain nitric oxide synthase, in obese Zucker rats. *European journal of pharmacology.* 1993;230:125-128
467. Calapai G, Corica F, Allegra A, Corsonello A, Sautebin L, De Gregorio T, Di Rosa M, Costantino G, Buemi M, Caputi AP. Effects of intracerebroventricular leptin administration on food intake, body weight gain and diencephalic nitric oxide synthase activity in the mouse. *British journal of pharmacology.* 1998;125:798-802
468. Iuras A, Telles MM, Bertocini CR, Ko GM, de Andrade IS, Silveira VL, Ribeiro EB. Central administration of a nitric oxide precursor abolishes both the hypothalamic serotonin release and the hypophagia induced by interleukin-1beta in obese Zucker rats. *Regulatory peptides.* 2005;124:145-150
469. Squadrito F, Calapai G, Altavilla D, Cucinotta D, Zingarelli B, Arcoraci V, Campo GM, Caputi AP. Central serotonergic system involvement in the anorexia induced by ng-nitro-L-arginine, an inhibitor of nitric oxide synthase. *European journal of pharmacology.* 1994;255:51-55
470. Stricker-Krongrad A, Beck B, Burlet C. Nitric oxide mediates hyperphagia of obese Zucker rats: Relation to specific changes in the microstructure of feeding behavior. *Life sciences.* 1996;58:PL9-15
471. Tsuchiya K, Sakai H, Suzuki N, Iwashima F, Yoshimoto T, Shichiri M, Hirata Y. Chronic blockade of nitric oxide synthesis reduces adiposity and improves insulin resistance in high fat-induced obese mice. *Endocrinology.* 2007;148:4548-4556

472. Shankar R, Zhu JS, Ladd B, Henry D, Shen HQ, Baron AD. Central nervous system nitric oxide synthase activity regulates insulin secretion and insulin action. *J Clin Invest.* 1998;102:1403-1412
473. Rodin J. Insulin levels, hunger, and food intake: An example of feedback loops in body weight regulation. *Health psychology : official journal of the Division of Health Psychology, American Psychological Association.* 1985;4:1-24
474. Rodin J, Wack J, Ferrannini E, DeFronzo RA. Effect of insulin and glucose on feeding behavior. *Metabolism.* 1985;34:826-831
475. Louis-Sylvestre J. Meal size: Role of reflexly induced insulin release. *Journal of the autonomic nervous system.* 1984;10:317-324
476. Woods SC, Gibbs J. The regulation of food intake by peptides. *Annals of the New York Academy of Sciences.* 1989;575:236-243
477. Pliquett RU, Fuhrer D, Falk S, Zysset S, von Cramon DY, Stumvoll M. The effects of insulin on the central nervous system--focus on appetite regulation. *Hormone and metabolic research = Hormon- und Stoffwechselforschung = Hormones et metabolisme.* 2006;38:442-446
478. Yamada J, Sugimoto Y, Yoshikawa T, Horisaka K. Effects of a nitric oxide synthase inhibitor on 5-ht1a receptor agonist 8-oh-dpat-induced hyperphagia in rats. *European journal of pharmacology.* 1996;316:23-26
479. Sugimoto Y, Yamada J, Yoshikawa T. A neuronal nitric oxide synthase inhibitor 7-nitroindazole reduces the 5-ht1a receptor against 8-oh-dpat-elicited hyperphagia in rats. *European journal of pharmacology.* 1999;376:1-5
480. Sugimoto Y, Yoshikawa T, Yamada J. Involvement of nitric oxide in the 5-ht1a autoreceptor-mediated hyperphagia in rats. *Advances in experimental medicine and biology.* 1999;467:109-111
481. Czech DA, Kazel MR, Harris J. A nitric oxide synthase inhibitor, n(g)-nitro-l-arginine methyl ester, attenuates lipoprivic feeding in mice. *Physiol Behav.* 2003;80:75-79
482. Li M, Vizzard MA, Jaworski DM, Galbraith RA. The weight loss elicited by cobalt protoporphyrin is related to decreased activity of nitric oxide synthase in the hypothalamus. *J Appl Physiol (1985).* 2006;100:1983-1991
483. Wascher TC, Graier WF, Dittrich P, Hussain MA, Bahadori B, Wallner S, Toplak H. Effects of low-dose l-arginine on insulin-mediated vasodilatation and insulin sensitivity. *European journal of clinical investigation.* 1997;27:690-695
484. Lucotti P, Setola E, Monti LD, Galluccio E, Costa S, Sandoli EP, Fermo I, Rabaiotti G, Gatti R, Piatti P. Beneficial effects of a long-term oral l-arginine treatment added to a hypocaloric diet and exercise training program in obese, insulin-resistant type 2 diabetic patients. *Am J Physiol Endocrinol Metab.* 2006;291:E906-912
485. Alizadeh M, Safaeiyan A, Ostadrahimi A, Estakhri R, Daneghian S, Ghaffari A, Gargari BP. Effect of l-arginine and selenium added to a hypocaloric diet enriched with legumes on cardiovascular disease risk factors in women with central obesity: A randomized, double-blind, placebo-controlled trial. *Annals of nutrition & metabolism.* 2012;60:157-168
486. Bogdanski P, Suliburska J, Grabanska K, Musialik K, Cieslewicz A, Skoluda A, Jablecka A. Effect of 3-month l-arginine supplementation on insulin resistance and tumor necrosis factor activity in patients with visceral obesity. *European review for medical and pharmacological sciences.* 2012;16:816-823
487. Bogdanski P, Szulinska M, Suliburska J, Pupek-Musialik D, Jablecka A, Witmanowski H. Supplementation with l-arginine favorably influences plasminogen activator inhibitor type 1 concentration in obese patients. A randomized, double blind trial. *Journal of endocrinological investigation.* 2013;36:221-226
488. Suliburska J, Bogdanski P, Szulinska M, Pupek-Musialik D, Jablecka A. Changes in mineral status are associated with improvements in insulin sensitivity in obese patients following l-arginine supplementation. *European journal of nutrition.* 2014;53:387-393
489. Monti LD, Casiraghi MC, Setola E, Galluccio E, Pagani MA, Quaglia L, Bosi E, Piatti P. L-arginine enriched biscuits improve endothelial function and glucose metabolism: A pilot study in healthy subjects and a cross-over study in subjects with impaired glucose tolerance and metabolic syndrome. *Metabolism.* 2013;62:255-264

490. Clemmensen C, Madsen AN, Smajilovic S, Holst B, Brauner-Osborne H. L-arginine improves multiple physiological parameters in mice exposed to diet-induced metabolic disturbances. *Amino Acids*. 2012;43:1265-1275
491. Fu WJ, Haynes TE, Kohli R, Hu J, Shi W, Spencer TE, Carroll RJ, Meininger CJ, Wu G. Dietary l-arginine supplementation reduces fat mass in Zucker diabetic fatty rats. *J Nutr*. 2005;135:714-721
492. Jobgen W, Meininger CJ, Jobgen SC, Li P, Lee MJ, Smith SB, Spencer TE, Fried SK, Wu G. Dietary l-arginine supplementation reduces white fat gain and enhances skeletal muscle and brown fat masses in diet-induced obese rats. *J Nutr*. 2009;139:230-237
493. Tan B, Yin Y, Liu Z, Li X, Xu H, Kong X, Huang R, Tang W, Shinzato I, Smith SB, Wu G. Dietary l-arginine supplementation increases muscle gain and reduces body fat mass in growing-finishing pigs. *Amino Acids*. 2009;37:169-175
494. McKnight JR, Satterfield MC, Jobgen WS, Smith SB, Spencer TE, Meininger CJ, McNeal CJ, Wu G. Beneficial effects of l-arginine on reducing obesity: Potential mechanisms and important implications for human health. *Amino Acids*. 2010;39:349-357
495. Ayala JE, Bracy DP, Julien BM, Rottman JN, Fueger PT, Wasserman DH. Chronic treatment with sildenafil improves energy balance and insulin action in high fat-fed conscious mice. *Diabetes*. 2007;56:1025-1033
496. Mitschke MM, Hoffmann LS, Gnad T, Scholz D, Kruthoff K, Mayer P, Haas B, Sassmann A, Pfeifer A, Kilic A. Increased cGMP promotes healthy expansion and browning of white adipose tissue. *FASEB J*. 2013;27:1621-1630
497. De Toni L, Strapazon G, Gianesello L, Caretta N, Pilon C, Bruttocao A, Foresta C. Effects of type 5-phosphodiesterase inhibition on energy metabolism and mitochondrial biogenesis in human adipose tissue ex vivo. *Journal of endocrinological investigation*. 2011;34:738-741
498. Wang H, Wang AX, Aylor K, Barrett EJ. Nitric oxide directly promotes vascular endothelial insulin transport. *Diabetes*. 2013;62:4030-4042
499. Baron AD, Zhu JS, Marshall S, Irsula O, Brechtel G, Keech C. Insulin resistance after hypertension induced by the nitric oxide synthesis inhibitor l-nmMA in rats. *The American journal of physiology*. 1995;269:E709-715
500. Meshkani R, Adeli K. Hepatic insulin resistance, metabolic syndrome and cardiovascular disease. *Clinical biochemistry*. 2009;42:1331-1346
501. Meininger CJ, Marinos RS, Hatakeyama K, Martinez-Zaguilan R, Rojas JD, Kelly KA, Wu G. Impaired nitric oxide production in coronary endothelial cells of the spontaneously diabetic BB rat is due to tetrahydrobiopterin deficiency. *Biochem J*. 2000;349:353-356
502. Xu J, Wu Y, Song P, Zhang M, Wang S, Zou MH. Proteasome-dependent degradation of guanosine 5'-triphosphate cyclohydrolase I causes tetrahydrobiopterin deficiency in diabetes mellitus. *Circulation*. 2007;116:944-953
503. Meininger CJ, Cai S, Parker JL, Channon KM, Kelly KA, Becker EJ, Wood MK, Wade LA, Wu G. GTP cyclohydrolase I gene transfer reverses tetrahydrobiopterin deficiency and increases nitric oxide synthesis in endothelial cells and isolated vessels from diabetic rats. *FASEB J*. 2004;18:1900-1902
504. Abudukadier A, Fujita Y, Obara A, Ohashi A, Fukushima T, Sato Y, Ogura M, Nakamura Y, Fujimoto S, Hosokawa M, Hasegawa H, Inagaki N. Tetrahydrobiopterin has a glucose-lowering effect by suppressing hepatic gluconeogenesis in an endothelial nitric oxide synthase-dependent manner in diabetic mice. *Diabetes*. 2013;62:3033-3043
505. Sadri P, Lauth WW. Blockade of hepatic nitric oxide synthase causes insulin resistance. *The American journal of physiology*. 1999;277:G101-108
506. Guarino MP, Afonso RA, Raimundo N, Raposo JF, Macedo MP. Hepatic glutathione and nitric oxide are critical for hepatic insulin-sensitizing substance action. *American journal of physiology. Gastrointestinal and liver physiology*. 2003;284:G588-594
507. Guarino MP, Macedo MP. Co-administration of glutathione and nitric oxide enhances insulin sensitivity in Wistar rats. *British journal of pharmacology*. 2006;147:959-965

508. Sosa I, Cvijanovic O, Celic T, Cuculic D, Crncevic-Orlic Z, Vukelic L, Zoricic Cvek S, Dudaric L, Bosnar A, Bobinac D. Hepatoregenerative role of bone morphogenetic protein-9. *Medical science monitor : international medical journal of experimental and clinical research*. 2011;17:HY33-35
509. Lutt WW. A new paradigm for diabetes and obesity: The hepatic insulin sensitizing substance (hiss) hypothesis. *Journal of pharmacological sciences*. 2004;95:9-17
510. Lutt WW. Insulin sensitivity in skeletal muscle regulated by a hepatic hormone, hiss. *Canadian journal of applied physiology = Revue canadienne de physiologie appliquee*. 2005;30:304-312
511. Ming Z, Lutt WW. Hiss, not insulin, causes vasodilation in response to administered insulin. *J Appl Physiol (1985)*. 2011;110:60-68
512. Steinberg HO, Brechtel G, Johnson A, Fineberg N, Baron AD. Insulin-mediated skeletal muscle vasodilation is nitric oxide dependent. A novel action of insulin to increase nitric oxide release. *J Clin Invest*. 1994;94:1172-1179
513. Scherrer U, Randin D, Vollenweider P, Vollenweider L, Nicod P. Nitric oxide release accounts for insulin's vascular effects in humans. *J Clin Invest*. 1994;94:2511-2515
514. Baron AD. Hemodynamic actions of insulin. *The American journal of physiology*. 1994;267:E187-202
515. Guarino MP, Correia NC, Lutt WW, Macedo MP. Insulin sensitivity is mediated by the activation of the ach/no/cgmp pathway in rat liver. *American journal of physiology. Gastrointestinal and liver physiology*. 2004;287:G527-532
516. Guarino MP, Correia NC, Raposo J, Macedo MP. Nitric oxide synthase inhibition decreases output of hepatic insulin sensitizing substance (hiss), which is reversed by sin-1 but not by nitroprusside. *Proceedings of the Western Pharmacology Society*. 2001;44:25-26
517. Lutt WW, Macedo MP, Sadri P, Takayama S, Duarte Ramos F, Legare DJ. Hepatic parasympathetic (hiss) control of insulin sensitivity determined by feeding and fasting. *American journal of physiology. Gastrointestinal and liver physiology*. 2001;281:G29-36
518. Barreto SG, Carati CJ, Toouli J, Saccone GT. The islet-acinar axis of the pancreas: More than just insulin. *American journal of physiology. Gastrointestinal and liver physiology*. 2010;299:G10-22
519. Chey WY, Chang T. Neural hormonal regulation of exocrine pancreatic secretion. *Pancreatology : official journal of the International Association of Pancreatology*. 2001;1:320-335
520. Vincent SR. Nitric oxide and arginine-evoked insulin secretion. *Science*. 1992;258:1376-1378
521. Broniowska KA, Oleson BJ, Corbett JA. Beta-cell responses to nitric oxide. *Vitamins and hormones*. 2014;95:299-322
522. Takamura T, Kato I, Kimura N, Nakazawa T, Yonekura H, Takasawa S, Okamoto H. Transgenic mice overexpressing type 2 nitric-oxide synthase in pancreatic beta cells develop insulin-dependent diabetes without insulinitis. *J Biol Chem*. 1998;273:2493-2496
523. Laychock SG, Modica ME, Cavanaugh CT. L-arginine stimulates cyclic guanosine 3',5'-monophosphate formation in rat islets of langerhans and rim5f insulinoma cells: Evidence for l-arginine:nitric oxide synthase. *Endocrinology*. 1991;129:3043-3052
524. Schmidt HH, Warner TD, Ishii K, Sheng H, Murad F. Insulin secretion from pancreatic b cells caused by l-arginine-derived nitrogen oxides. *Science*. 1992;255:721-723
525. Spinass GA, Laffranchi R, Francoys I, David I, Richter C, Reinecke M. The early phase of glucose-stimulated insulin secretion requires nitric oxide. *Diabetologia*. 1998;41:292-299
526. Spinass GA. The dual role of nitric oxide in islet beta-cells. *News in physiological sciences : an international journal of physiology produced jointly by the International Union of Physiological Sciences and the American Physiological Society*. 1999;14:49-54
527. Laffranchi R, Gogvadze V, Richter C, Spinass GA. Nitric oxide (nitrogen monoxide, no) stimulates insulin secretion by inducing calcium release from mitochondria. *Biochemical and biophysical research communications*. 1995;217:584-591

528. Jones PM, Persaud SJ, Bjaaland T, Pearson JD, Howell SL. Nitric oxide is not involved in the initiation of insulin secretion from rat islets of langerhans. *Diabetologia*. 1992;35:1020-1027
529. Weigert N, Dollinger M, Schmid R, Schusdziarra V. Contribution of neural intrapancreatic non-cholinergic non-adrenergic mechanisms to glucose-induced insulin release in the isolated rat pancreas. *Diabetologia*. 1992;35:1133-1139
530. Ohtoshi K, Yamasaki Y, Gorogawa S, Hayaishi-Okano R, Node K, Matsuhisa M, Kajimoto Y, Hori M. Association of (-)786t-c mutation of endothelial nitric oxide synthase gene with insulin resistance. *Diabetologia*. 2002;45:1594-1601
531. Yoshimura T, Hisatomi A, Kajihara S, Yasutake T, Ogawa Y, Mizuta T, Ozaki I, Utsunomiyai T, Yamamoto K. The relationship between insulin resistance and polymorphisms of the endothelial nitric oxide synthase gene in patients with coronary artery disease. *Journal of atherosclerosis and thrombosis*. 2003;10:43-47
532. Vecoli C, Andreassi MG, Liga R, Colombo MG, Coceani M, Carpeggiani C, L'Abbate A, Neglia D. T(-786)-->c polymorphism of the endothelial nitric oxide synthase gene is associated with insulin resistance in patients with ischemic or non ischemic cardiomyopathy. *BMC medical genetics*. 2012;13:92
533. Monti LD, Barlassina C, Citterio L, Galluccio E, Berzuini C, Setola E, Valsecchi G, Lucotti P, Pozza G, Bernardinelli L, Casari G, Piatti P. Endothelial nitric oxide synthase polymorphisms are associated with type 2 diabetes and the insulin resistance syndrome. *Diabetes*. 2003;52:1270-1275
534. Gonzalez-Sanchez JL, Martinez-Larrad MT, Saez ME, Zabena C, Martinez-Calatrava MJ, Serrano-Rios M. Endothelial nitric oxide synthase haplotypes are associated with features of metabolic syndrome. *Clinical chemistry*. 2007;53:91-97
535. Rittig K, Holder K, Stock J, Tschritter O, Peter A, Stefan N, Fritsche A, Machicao F, Haring HU, Balletshofer B. Endothelial no-synthase intron 4 polymorphism is associated with disturbed in vivo nitric oxide production in individuals prone to type 2 diabetes. *Hormone and metabolic research = Hormon- und Stoffwechselforschung = Hormones et metabolisme*. 2008;40:13-17
536. Morris BJ, Glenn CL, Wilcken DE, Wang XL. Influence of an inducible nitric oxide synthase promoter variant on clinical variables in patients with coronary artery disease. *Clinical science*. 2001;100:551-556
537. Bagarolli RA, Saad MJ, Saad ST. Toll-like receptor 4 and inducible nitric oxide synthase gene polymorphisms are associated with type 2 diabetes. *Journal of diabetes and its complications*. 2010;24:192-198
538. Cook S, Hugli O, Egli M, Menard B, Thalmann S, Sartori C, Perrin C, Nicod P, Thorens B, Vollenweider P, Scherrer U, Burcelin R. Partial gene deletion of endothelial nitric oxide synthase predisposes to exaggerated high-fat diet-induced insulin resistance and arterial hypertension. *Diabetes*. 2004;53:2067-2072
539. Cook S, Hugli O, Egli M, Vollenweider P, Burcelin R, Nicod P, Thorens B, Scherrer U. Clustering of cardiovascular risk factors mimicking the human metabolic syndrome x in enos null mice. *Swiss medical weekly*. 2003;133:360-363
540. Nakata S, Tsutsui M, Shimokawa H, Suda O, Morishita T, Shibata K, Yatera Y, Sabanai K, Tanimoto A, Nagasaki M, Tasaki H, Sasaguri Y, Nakashima Y, Otsuji Y, Yanagihara N. Spontaneous myocardial infarction in mice lacking all nitric oxide synthase isoforms. *Circulation*. 2008;117:2211-2223
541. Sydow K, Mondon CE, Schrader J, Konishi H, Cooke JP. Dimethylarginine dimethylaminohydrolase overexpression enhances insulin sensitivity. *Arterioscler Thromb Vasc Biol*. 2008;28:692-697
542. Lee-Young RS, Ayala JE, Hunley CF, James FD, Bracy DP, Kang L, Wasserman DH. Endothelial nitric oxide synthase is central to skeletal muscle metabolic regulation and enzymatic signaling during exercise in vivo. *American journal of physiology. Regulatory, integrative and comparative physiology*. 2010;298:R1399-1408
543. Atochin DN, Huang PL. Endothelial nitric oxide synthase transgenic models of endothelial dysfunction. *Pflugers Archiv : European journal of physiology*. 2010;460:965-974

544. Kashiwagi S, Atochin DN, Li Q, Schleicher M, Pong T, Sessa WC, Huang PL. Enos phosphorylation on serine 1176 affects insulin sensitivity and adiposity. *Biochem Biophys Res Commun.* 2013;431:284-290
545. Khedara A, Kawai Y, Kayashita J, Kato N. Feeding rats the nitric oxide synthase inhibitor, l-n(omega)nitroarginine, elevates serum triglyceride and cholesterol and lowers hepatic fatty acid oxidation. *J Nutr.* 1996;126:2563-2567
546. Khedara A, Goto T, Morishima M, Kayashita J, Kato N. Elevated body fat in rats by the dietary nitric oxide synthase inhibitor, l-n omega nitroarginine. *Bioscience, biotechnology, and biochemistry.* 1999;63:698-702
547. Recchia FA, Osorio JC, Chandler MP, Xu X, Panchal AR, Lopaschuk GD, Hintze TH, Stanley WC. Reduced synthesis of no causes marked alterations in myocardial substrate metabolism in conscious dogs. *Am J Physiol Endocrinol Metab.* 2002;282:E197-206
548. Gould N, Doulias PT, Tenopoulou M, Raju K, Ischiropoulos H. Regulation of protein function and signaling by reversible cysteine s-nitrosylation. *J Biol Chem.* 2013;288:26473-26479
549. Perreault M, Marette A. Targeted disruption of inducible nitric oxide synthase protects against obesity-linked insulin resistance in muscle. *Nat Med.* 2001;7:1138-1143
550. Carvalho-Filho MA, Ueno M, Hirabara SM, Seabra AB, Carvalheira JB, de Oliveira MG, Velloso LA, Curi R, Saad MJ. S-nitrosation of the insulin receptor, insulin receptor substrate 1, and protein kinase b/akt: A novel mechanism of insulin resistance. *Diabetes.* 2005;54:959-967
551. Carvalho-Filho MA, Ueno M, Carvalheira JB, Velloso LA, Saad MJ. Targeted disruption of inos prevents lps-induced s-nitrosation of irbeta/irs-1 and akt and insulin resistance in muscle of mice. *Am J Physiol Endocrinol Metab.* 2006;291:E476-482
552. Pauli JR, Ropelle ER, Cintra DE, Carvalho-Filho MA, Moraes JC, De Souza CT, Velloso LA, Carvalheira JB, Saad MJ. Acute physical exercise reverses s-nitrosation of the insulin receptor, insulin receptor substrate 1 and protein kinase b/akt in diet-induced obese wistar rats. *The Journal of physiology.* 2008;586:659-671
553. Williamson RT. On the treatment of glycosuria and diabetes mellitus with sodium salicylate. *British medical journal.* 1901;1:760-762
554. Smith MJ, Meade BW. The effect of salicylate on glycosuria, blood glucose and liver glycogen of the alloxan-diabetic rat. *Biochem J.* 1952;51:18-20
555. Hundal RS, Petersen KF, Mayerson AB, Randhawa PS, Inzucchi S, Shoelson SE, Shulman GI. Mechanism by which high-dose aspirin improves glucose metabolism in type 2 diabetes. *J Clin Invest.* 2002;109:1321-1326
556. Kim JK, Kim YJ, Fillmore JJ, Chen Y, Moore I, Lee J, Yuan M, Li ZW, Karin M, Perret P, Shoelson SE, Shulman GI. Prevention of fat-induced insulin resistance by salicylate. *J Clin Invest.* 2001;108:437-446
557. Carvalho-Filho MA, Ropelle ER, Pauli RJ, Cintra DE, Tsukumo DM, Silveira LR, Curi R, Carvalheira JB, Velloso LA, Saad MJ. Aspirin attenuates insulin resistance in muscle of diet-induced obese rats by inhibiting inducible nitric oxide synthase production and s-nitrosylation of irbeta/irs-1 and akt. *Diabetologia.* 2009;52:2425-2434
558. Shinozaki S, Choi CS, Shimizu N, Yamada M, Kim M, Zhang T, Shiota G, Dong HH, Kim YB, Kaneki M. Liver-specific inducible nitric-oxide synthase expression is sufficient to cause hepatic insulin resistance and mild hyperglycemia in mice. *J Biol Chem.* 2011;286:34959-34975
559. Handa P, Tateya S, Rizzo NO, Cheng AM, Morgan-Stevenson V, Han CY, Clowes AW, Daum G, O'Brien KD, Schwartz MW, Chait A, Kim F. Reduced vascular nitric oxide-cgmp signaling contributes to adipose tissue inflammation during high-fat feeding. *Arterioscler Thromb Vasc Biol.* 2011;31:2827-2835
560. Cha HN, Kim YW, Kim JY, Kim YD, Song IH, Min KN, Park SY. Lack of inducible nitric oxide synthase does not prevent aging-associated insulin resistance. *Experimental gerontology.* 2010;45:711-718
561. Taniguchi CM, Emanuelli B, Kahn CR. Critical nodes in signalling pathways: Insights into insulin action. *Nature reviews. Molecular cell biology.* 2006;7:85-96

562. Turini P, Thalmann S, Jayet PY, Cook S, Mathieu C, Burcelin R, Nicod P, Vollenweider P, Sartori C, Scherrer U. Insulin resistance in mice lacking neuronal nitric oxide synthase is related to an alpha-adrenergic mechanism. *Swiss medical weekly*. 2007;137:700-704

CURRICULUM VITAE

NAME: Brian E. Sansbury

May 2014

PRESENT PRIMARY POSITION AND ADDRESS:

Doctoral Graduate Student
Department of Physiology and Biophysics
School of Medicine
Diabetes and Obesity Center
University of Louisville
580 South Preston St.
Delia Baxter Building, Rm 407
Louisville, KY 40202
Phone: (502) 852-1029
Email: brian.sansbury@louisville.edu

BIOGRAPHICAL

DATE & PLACE OF BIRTH: July 7, 1985 – Louisville, KY USA

HOME ADDRESS: 609 Merwin Ave.
Louisville, KY 40217

EDUCATION

<u>Institution</u>	<u>Date</u>	<u>Degree</u>	<u>Subject</u>
Miami University Oxford, OH	2007	BA	Zoology
University of Louisville Louisville, KY	2008	MS	Physiology and Biophysics
University of Louisville Louisville, KY	2014	PhD	Physiology and Biophysics

SPECIAL TRAINING

2010 Seahorse Bioscience: Training in the non-invasive measurement of cellular bioenergetics using the Seahorse Extracellular Flux analyzer – Billerica, MA

PAST PROFESSIONAL EXPERIENCE

2009–2011 Research Technologist II Center for Diabetes and Obesity Research
University of Louisville

2011-2012 Graduate Student Tutor Dept. of Physiology and Biophysics
University of Louisville

SERVICE

2011-2014 Student Representative School of Medicine Graduate Faculty Council
University of Louisville

2012-2014 Graduate Student Ambassador School of Interdisciplinary and Graduate Studies
University of Louisville

2012-2013 Graduate Student Panelist and Volunteer IPIBS New Student Orientation
University of Louisville

MEMBERSHIP IN SCIENTIFIC SOCIETIES

2011-Present Student/Trainee Member, American Heart Association (Council on Basic Cardiovascular Sciences)

2011-Present Student/Trainee Member, Society for Free Radical Biology and Medicine (SFRBM)

2012-Present Student/Trainee Member, Kentucky Academy of Science (KAS)

AWARDS, HONORS and INVITED PRESENTATIONS

2010	Research!Louisville: Second Place Research Staff Award
2011	Research!Louisville: First Place Masters Basic Science Graduate Student Award
2011	University of Louisville Institute of Molecular Cardiology Outstanding Student of the Year
2011	SFRBM: Opening General Session Oral Presentation and Travel Award
2011	AHA Scientific Sessions: Extended Panel Discussion Oral Presentation; ATVB Travel Award for Young Investigators; Seahorse Bioscience Travel Award
2011	Southeast Regional IDeA Meeting: Oral and Poster Presentation
2011	Barnstable Brown Obesity and Diabetes Research Day: Poster Presentation
2012	Research!Louisville: Second Place Doctoral Basic Science Graduate Student Award
2012	SFRBM: Oral Presentation
2014	Graduate Dean's Citation

RESEARCH ACTIVITIES

Active areas of interest:

- Adipose Tissue Physiology
- Regulation of Metabolism in Diabetes and Obesity
- Role of Nitric Oxide in Metabolic Disease
- Mitochondrial Biology and Bioenergetics

RESEARCH SUPPORT

1P20RR024489-01A1

09/26/08–06/30/13

Bhatnagar A. (Program Director)

NIH/NCRR

Hill BG (PI: Project 3)

Title: *Center of Excellence in Diabetes and Obesity Research*

The primary objective and the central focus of the Center are to enable, promote, and support scientific research related to the cardiovascular causes and consequences of diabetes and obesity.

Role: Graduate Student

PUBLICATIONS

1. **Sansbury BE**, Riggs DW, Salabei JK, Jones SP, and Hill BG. Responses of hypertrophied myocytes to stress: Implications for glycolysis and electrophile metabolism. *Biochem J.* 435:519–528, 2011.
2. **Sansbury BE**, Jones SP, Riggs DW, Darley-Usmar VM and Hill BG. Bioenergetic function in cardiovascular cells: the importance of the reserve capacity and its biological regulation. *Chem Biol Interact.* 191:288-295, 2011.
3. **Sansbury BE**, Cummins TD, Tang Y, Hellman J, Holden CR, Harbeson M, Chen T, Patel RP, Spite M, Bhatnagar A, and Hill BG. Overexpression of endothelial nitric oxide synthase prevents diet-induced obesity and regulates adipose tissue phenotype. *Circ Res.* 111: 1176-1189, 2012.
4. **Sansbury BE**, De Martino AM, Xie Z, Brooks AC, Brainard RE, Watson LJ, DeFilippis AP, Cummins TD, Harbeson MA, Brittan KR, Prabhu SD, Bhatnagar A, Jones SP, and Hill BG. Metabolomic analysis of pressure-overloaded and infarcted mouse hearts. *Circ - Heart Fail (In press)*.
5. Cummins TD, Holden CR, **Sansbury BE**, Zafar N, Tang Y, Hellmann J, Spite M, Bhatnagar A, and Hill BG. Metabolomic remodeling of white adipose tissue in obesity. *AJP-Endo and Metabolism (In revision)*.
6. Hill BG, Riggs DW, **Sansbury BE**, Harbeson M, Fine ES, Srivastava S, Jones SP, and Darley-Usmar VM. Dynamic control of mitochondrial protein modifications by respiratory state. *FASEB J (In revision)*.

REVIEWS

1. **Sansbury BE** and Hill BG. Regulation of obesity and insulin resistance by nitric oxide. *FRBM. (Invited; In review)*.
2. **Sansbury BE** and Hill BG. Nitric oxide, mitochondria and metabolism/diabetes. *Frontiers in Mitochondrial Research (Invited; In preparation)*.

BOOK CHAPTERS

1. **Sansbury BE** and Hill BG. Anti-obesogenic role of endothelial nitric oxide synthase. In Nitric Oxide. *(Submitted)*.

ABSTRACTS

1. Zhou G, Keskey AL, Goel M, Hamid T, Guo SZ, Clair HB, Brittian KR, **Sansbury BE**, Hill BG, Prabhu SD. Endoplasmic Reticulum (ER) Stress is Critical for the Development of Diabetic Cardiomyopathy. *Circulation* 122: supplement 21, 2010.
2. Falkner KC, Hill BG, **Sansbury BE**, McClain CJ, Cave MC. Mitochondrial toxicity of chloroacetaldehyde in HepG2 cells. *Hepatology* 52: supplement 1, 2010.
3. Hill BG, **Sansbury BE**, McCracken J, Li Q, Bolli R, Jones SP and Bhatnagar A. Unique energetic profile of cardiac progenitor cells. Experimental Biology meeting, Abstract 735.3, April 2011.
4. Hill BG, Riggs DW, **Sansbury BE**, Jones SP, and Darley-Usmar VM. Dynamic control of mitochondrial protein modifications by respiratory state. Experimental Biology meeting, Abstract 832.4, April 2011.
5. Brooks AC, **Sansbury BE**, Xie Z, Brainard RE, Watson LJ, Brittian KR, Prabhu SD, Jones SP, and Hill BG. Metabolomic analysis of the early and late hypertrophic heart. *Circ Res* 109, Issue 12 supplement, AP137, 2011.
6. **Sansbury BE**, Hellman J, Tang Y, Spite M, Bhatnagar A, and Hill BG. Endothelial Nitric Oxide Synthase Promotes a Shift in Adipocyte Phenotype in Diet-Induced Obesity. *Circulation* 124: supplement 21, 2011.
7. **Sansbury BE**, Hellman J, Tang Y, Spite M, Bhatnagar A, and Hill BG. Nitric oxide prevents diet-induced obesity by regulating adipose tissue phenotype. *Free Rad Biol Med*. 51: supplement 1, S65, 2011.
8. Cummins TD, **Sansbury BE**, Holden CR, Bhatnagar A, and Hill BG. Metabolic remodeling of white adipose tissue in obesity. *Free Radic Biol Med*. 2012.
9. **Sansbury BE**, Cummins TD, Holden CR, Bhatnagar A, and Hill BG. Endothelial nitric oxide synthase prevents obesity by promoting futile protein turnover. *Free Radic Biol Med*. 2012

SCIENTIFIC MEETINGS ATTENDED

1. Barnstable Brown Obesity and Diabetes Research Day. Lexington, KY, May 2011. *Poster Presentation*
2. Southeast Regional IDeA Meeting. New Orleans, LA, September 2011. *Oral and Poster Presentation*

3. American Heart Association Scientific Sessions. Orlando, FL, November 2011. *Oral and Poster Presentation*
4. Society for Free Radical Biology and Medicine. Atlanta, GA, November 2011. *Oral Presentation*
5. Society for Free Radical Biology and Medicine. San Diego, CA. November 2012. *Oral Presentation*